Report Documentation Page	**1. Report No.** DE - FC 21 - 92MC29077	**2.**	**3. Recipient's Accession No.**

4. Title and Subtitle Fracturing Fluid Characterization Facility	**5. Report Date** August 31, 2000
	6.
7. Author(s) The University of Oklahoma	**8. Performing Organization Rept. No.**
9. Performing Organization Name and Address The University of Oklahoma Sarkeys Energy Center T301 100 E Boyd St Norman, OK 73019	**10. Project/Task/Work Unit No.**
	11. Contract (C) or Grant (G) No. DOE:DE FC21 92 MC29077
12. Sponsoring Organization Name and Address US Dept of Energy - FETL 3610 Collins Ferry Road Morgantown, WV 26505	**13. Type of Report & Period Covered** Final Report 09 30 92 – 03 31 00
	14.

15. Supplementary Notes
Several technical papers were prepared and presented at various Society of Petroleum Engineers Conferences and US Department of Energy Conferences. Aggressive efforts were also made to effectively transfer the past research results to the industry

16. Abstract (limit 200 words)
Hydraulic fracturing technology has been successfully applied for well stimulation of low and high permeability reservoirs for numerous years. Treatment optimization and improved economics have always been the key to the success and it is more so when the reservoirs under consideration are marginal. Fluids are widely used for the stimulation of wells. The Fracturing Fluid Characterization Facility (FFCF) has been established to provide the accurate prediction of the behavior of complex fracturing fluids under downhole conditions. The primary focus of the facility is to provide valuable insight into the various mechanisms that govern the flow of fracturing fluids and slurries through hydraulically created fractures.

During the time between September 30, 1992, and March 31, 2000, the research efforts were devoted to the areas of fluid rheology, proppant transport, proppant flowback, dynamic fluid loss, perforation pressure losses, and frictional pressure losses. In this regard, a unique above-the-ground fracture simulator was designed and constructed at the FFCF, labeled "The High Pressure Simulator" (HPS).

The FFCF is now available to industry for characterizing and understanding the behavior of complex fluid systems. To better reflect and encompass the broad spectrum of the petroleum industry, the FFCF now operates under a new name of "The Well Construction Technology Center" (WCTC).

This report documents the summary of the activities performed during 1992 – 2000 at the FFCF

17. Document Analysis a. Description
Oil and Gas Industry, Natural Gas Production, Hydraulic Fracturing, Reservoir Characterization

b. Identifiers/Open-Ended Terms
Hydraulic Fracturing, Proppant Transport, Proppant Flowback, Fluid Rheology, Fluid Leak-Off, Fluid characterization, Slurries, Non-Neutonian Fluids

c. COSATI Field/Group

18. Availability Statement	**19. Security Class (This Report)**	**21. No. of Pages**
Release Unlimited	**20. Security Class (This Page)**	**22. Price**

FRACTURING FLUID CHARACTERIZATION FACILITY

FINAL REPORT

September 30, 1992 - March 31, 2000

SUBMITTED BY

The University of Oklahoma
Mewbourne School of Petroleum and Geological Engineering
Energy Center, T 301
100 East Boyd
Norman, Oklahoma 73019-0628

for

UNITED STATES DEPARTMENT OF ENERGY
Federal Energy Technology Center
3610 Collins Ferry Road
Morgantown, WV 26505

Cooperative Agreement No. DE-FC21-92MC29077
DOE Manager: Anthony Zammerilli

August 2000

DEPARTMENT OF ENERGY DISCLAIMER

This report was prepared by **The University of Oklahoma (OU)** as an account of work sponsored, in part, by **U.S. Department of Energy (DOE)** , Financial Assistance Award DE-FC21-92MC29077. Such support does not constitute an endorsement by DOE of the information contained in this report.

UNIVERSITY OF OKLHAOMA DISCLAIMER

"LEGAL NOTICE"

This report was prepared by The University of Oklahoma as an account of work sponsored by the U.S. Department of Energy (DOE). Neither DOE members of DOE, The Board of Regents of The University of Oklahoma, nor any person acting on behalf of the aforementioned;

(a) makes any warranty or representation, express or implied, with respect to the accuracy, completeness, or usefulness of the information contained in this report, or that the use of any information, apparatus, method, or process disclosed in this report may not infringe privately owned rights; or,

(b) assumes any liability with respect to the use of, or for damages resulting form the use of any information, apparatus, method, or process disclosed in this report.

CONTRIBUTORS

The following authors have contributed to the preparation of the Fracturing Fluid Characterization Facility (FFCF) Annual Report:

Hyun Cho
Naval Goel
Sudhakar Khade
Max Mefford
Ameet Raichukar
Naim Saddiq
Subhash Shah
Yunxu Zhou

ACKNOWLEDGEMENTS

The FFCF Research Team at The University of Oklahoma wish to thank the U.S. Department of Energy for their continued support of this project.

TABLE OF CONTENTS

LIST OF FIGURES

LIST OF TABLES

Executive Summary

This document is the Final Report from the University of Oklahoma (OU) to the United States Department of Energy (DOE) as part of the Contract No. DE-FC21-92MC29077. It briefly summarizes the findings of research and development work performed by OU over the contract period from January 1, 1991 through March 31, 2000.

On April 5,1990, Gas Research Institute's (GRI) Natural Gas Supply Department issued RFP No. 90-211-0367 entitled "Fracturing Fluid Characterization." The purpose of this RFP was to solicit proposals from various qualified industry organizations with the objective of quantifying the behavior and effects of fracturing fluids and slurries, in the wellbore and in the fracture, during and after the hydraulic fracturing process. Following a thorough review, GRI selected the proposal submitted by OU as the most qualified from the several proposals submitted by industry organizations and research entities. During 1992 the Department of Energy executed Cooperative Agreement No. DE-FC21-92MC29077 and became a project co-sponsor and continued to be a major contributor to the program until the contract end on March 31, 2000.

During the contract period, based on consultation received from the Project Advisory Group (PAG) and the Technical Advisory Group (TAG), DOE/GRI periodically modified the statement of work to steer the project toward its goals and objectives. The statement of work was also modified occasionally to reflect changes in overall project direction as determined by DOE/GRI and its advisory groups.

Each year the progress of the project was presented to TAG and PAG at the semi-annual meetings. Furthermore, each year an Annual Report describing in detail the activities performed with the research results and implications was also submitted to DOE/GRI. The GRI contract was fulfilled on September 30, 1998 and the Final Report was submitted. The continuation of the project beyond this time (i.e. from September 30, 1998 through March 31, 2000) was made possible because of the DOE funds. This Final Report provides the summary of all previous reports and describes the major activities and research results and implications. For more detailed information the readers are referred to the published annual reports.

The major goals of the project were to develop a fracture simulator that provides an accurate rheological characterization of hydraulic fracturing fluids under field conditions and to provide a permanent facility that could be used by the industry for testing purposes. The University of Oklahoma has successfully accomplished both of these goals. The "Fracturing Fluid Characterization Facility (FFCF)" was established with total commitment from OU. The primary objective of this facility is to provide the oil and gas industry with a comprehensive, research-based organization, whose mission is to provide valuable insight into the various mechanisms that govern the flow of fracturing fluids and slurries through a hydraulically created fracture.

In this regard, a unique above-the-ground fracture simulator was designed and constructed at the FFCF, labeled "The High Pressure Simulator (HPS)." The HPS is a vertical, variable-width, parallel plate flow apparatus capable of operating at high temperatures (up to 250^{o}F) and pressures (up to 1200 psi). The HPS is the most advanced fracture simulator currently available to the industry. A state-of-the-art fiber optic-based "vision system" was developed for the HPS to facilitate the visualization and accurate measurement of flow behavior of fracturing fluids with and without proppant. Some of its key experimental research areas include fracturing fluid characterization, wall slippage phenomena, dynamic fluid loss, perforation pressure loss, proppant convection and encapsulation, and proppant flowback for a variety of fracturing fluids, slurries, and foams. In order to duplicate actual field conditions, field methods and equipment for mixing, pumping, and fluid preconditioning were developed. A state-of-the-art laboratory where fracturing fluid characterization can be performed was also established.

Joint industry consortia, such as the Coiled Tubing Consortium, were established and a technical program was developed to make the facility available to the industry in the form of third-party testing. Since 1996, the industry has utilized the FFCF testing facility to perform fluids-related research.

Specifically, this Final Report includes:

- Broad view of the project direction from initial issue of the RFP to project close
- Design and development of High Pressure Fracture Simulator (HPS)
- Fluid mixing and pumping equipment
- Instrumentation
- Data acquisition
- Laboratory rheological instruments
- Research results and implications
- Coiled tubing consortium
- Technology dissemination
- Commercialization of FFCF

Some of the numerical simulators used today for simulating hydraulic fracturing treatments have incorporated the data developed by the FFCF. The research and development work thus far accomplished at FFCF will not only serve as the foundation for future research but has also provided the industry with valuable insight into some of the more fundamental aspects of fluid flow in a hydraulic fracture. FFCF has investigated many of the fluid processes and visually demonstrated the impact on the overall efficiency of a fracturing treatment. Because hydraulic fracturing is so widely applied, small incremental improvements have the potential to produce an enormous impact on the overall economics of gas recovery.

Chapter 1 INTRODUCTION AND BACKGROUND

1.1 Summary

This chapter provides a broad view of the direction taken by the project from initial issue of the RFP (request for proposal) on April 5, 1990 to project close on March 31, 2000. It describes the rationale used by the Gas Research Institute (GRI) to formulate the RFP and the technological advancements expected from pursuit of the research effort outlined in the RFP. It also describes actions taken by the primary contractor and sub-contractors in response to the statement of work defined by the U.S. Department of Energy (DOE) and GRI. Based on consultation received from Project Advisory Group (PAG) and Technical Advisory Group (TAG), DOE/GRI periodically modified the statement of work to steer the project toward its goals and objectives. The statement of work was also modified occasionally to reflect changes in overall project direction as determined by DOE/GRI and their advisory groups.

1.2 Contractor Proposal

On April 5, 1990, GRI's Natural Gas Supply Department issued RFP No. 90-211-0367 entitled "Fracturing Fluid Characterization." The purpose of this RFP was to solicit proposals from various qualified industry organizations with the objective of quantifying the behavior and effects of fracturing fluids and slurries, in the wellbore and in the fracture, during and after the hydraulic fracturing process. Operational control of the fracturing process was considered critical to the development of optimized fracture treatments and lower completion costs.

In the RFP, GRI cited its experience with three Staged Field Experiments (SFE's) as evidence that it is not possible to perform an accurately controlled fracturing experiment, monitoring all processes involved, and obtain a unique interpretation of fracture growth. Improving industry knowledge of fracturing fluid behavior was considered to be a key factor in the effort to gain operational control of the fracturing process. Therefore, GRI issued RFP 90-211-0367 to sponsor the physical modeling of fluid and slurry flow processes that occur during a hydraulic fracturing treatment. The RFP recommended that an effort should be made to duplicate the actual scale of field equipment, and expected flow geometries to insure experimental observations can be related directly to field operations.

The primary benefit to be derived from this GRI sponsored research was expected to relate directly to a reduction in the cost of fracture treatments and increased reservoir deliverability as the result of improved stimulation design and implementation. It was GRI's desire that the information, hardware, and analytical tools that evolve from this research project would allow the industry to lower stimulation costs by reducing fluid volumes, horsepower requirements, and fluid additive costs. These results could also lead to an improvement in fracturing treatment data interpretation and therefore allow better estimates of fracture geometry and reservoir performance to be made.

Several proposals were received from various organizations and research entities by the May 25, 1990 deadline set by GRI. Following a thorough review, GRI selected the proposal submitted by the University of Oklahoma as being the most qualified based on criteria contained in the RFP. The University of Oklahoma proposed approaching the overall task with a multidisciplinary team supported by industry leading sub-contractors (MTS Systems Corporation, Minneapolis, Minnesota; Halliburton Services, Duncan, Oklahoma; RE/SPEC Inc., Rapid City, South Dakota). MTS Systems Corporation was chosen because of their expertise in the design and fabrication of servo-controlled test equipment and their expertise in the development of state-of-the-art test facilities. Halliburton Services was selected to support the facility because of their expertise in fracturing fluid formulation and evaluation and their expertise in field-scale equipment for mixing and pumping hydraulic fracturing fluids. RE/SPEC Inc. was chosen to support the facility because of their expertise in rock mechanics testing and quality assurance.

The multidisciplinary team from the University of Oklahoma and their team of sub-contractors proposed constructing a Fracturing Fluid Characterization Facility (FFCF) where large-scale physical models could be deployed and used for testing. They envisioned that industry could use these large-scale physical models to validate numerical models if certain criteria were met. These criteria include equipment design that allows accurate control of boundary conditions, knowledge of material properties and behavior, and the development of sophisticated measurement techniques. If validation of numerical models became possible at the facility, it would be a major step towards the ultimate goal of attaining operational control of the fracturing process and hence, optimization of stimulation treatments. To fulfill this vision, the contractor team proposed that a feasibility study be undertaken which includes the design and fabrication of a prototype fracture simulator. The goal of this feasibility study was to evaluate various alternatives, to delineate limitations, to access currently available technologies, and to ultimately provide GRI with an improved cost estimate. Those desiring additional details concerning the contractor proposal should refer to the original document submitted by the University of Oklahoma to GRI on May 21,1990.

1.3 Contractor/Subcontractor Team Approach

In the contract executed with The University of Oklahoma, Contract No. 5091-211-2114, GRI established January 1, 1991 as the effective start date for work on the project. The University of Oklahoma in concert with its subcontractors began the feasibility study that had been planned for the first year. Four teams were established, respectively, to cover the Mechanical, Rheological, Measurement/Control, and QA/QC/Environmental facets of the feasibility study. Each team provided input to formulation of the document entitled “Simulator Functional Requirements.” This enabling document allowed MTS to complete the design and begin construction of the prototype simulator prior to the end of the first year.

The inaugural meeting of the TAG occurred on June 3-4, 1991 in Chicago, Illinois. Mr. Steve Millett, Manager of Forecasting and Strategic Planning Studies at Battelle, was invited to conduct an exercise based on the nominal group technique. The TAG was asked, “What do we need to know to improve the effectiveness of fracturing

fluids in hydraulic fracturing of tight sands gas wells in order to increase production from these wells at least 10% by the year 2001?" Mr. Millett further clarified the question by commenting that the increase would be above that achievable with our current knowledge of the performance of fracturing fluids. The group was allowed 15 minutes to develop individual responses to the question. Their ideas were recorded in an around-the-table format until there were no new ideas coming forth. The 39 issues raised were reduced to 27 by eliminating redundancy and overlap between the topics. Each individual was then requested to select and rank the top eight issues from this list. Mr. Millett then tabulated the scores and listed the top five:

1. Identification of fluid properties that predict proppant transport, including characterization of proppant transport and settlement
2. Change in fluid properties along the fracture, including the effects of fluid loss
3. Slurry rheology, including characterization of fluid friction and behavior in the wellbore
4. Ways of reducing residual fracture conductivity damage
5. Behavior of nonuniform slurry flow in complex channels, including characterization of nonhomogeneous flow, velocity profiles (with possible fingering), and effects of fracture tortuosity and roughness.

The TAG also addressed the issue of building a prototype simulator at this meeting. The need for a prototype simulator was based on the desire to test the mechanical design, facings, controls, instrumentation, safety, and other aspects of the design concept before committing to the construction of a much larger simulator. The consensus of the TAG was that a prototype should be built to verify design concepts and to address safety issues. They also wanted prototype testing to provide meaningful data related to fracturing fluid properties when possible. These recommendations were presented to the PAG and approval for construction of a prototype was obtained. In this same time frame, the United States Department of Energy (DOE) executed Cooperative Agreement No. DE-FC21-92MC29077 and became a project co-sponsor and has continued to be a major contributor to the program.

During July 1992, the 37.5-ton prototype fracture simulator was installed in an aircraft hangar bay at 1928 Goddard Avenue on the North Campus of the University of Oklahoma. The hangar provided temporary housing for the simulator until the University constructed a permanent facility during 1996. The prototype simulator was a vertical, variable width, parallel-plate flow cell that was 7 feet high and 9-1/3 feet long. Further details concerning the design and construction of this simulator are found in Chapter 2. Following installation, a series of verification tests were undertaken to evaluate the ability of the simulator and associated instrumentation to perform according to design. However, the prototype simulator was quickly recognized by industry to be a considerable advancement in the technology available for evaluating fracturing fluids. Therefore, in addition to proof-of-concept testing for development of a large-scale simulator, a research plan was developed to investigate fluid rheology, proppant transport, and fluid loss with the prototype during 1993 and early 1994. The prototype verification and research testing conducted during this time period gave an indication of how the project was going to advance technology in fluid characterization. This testing

supported some industry assumptions about fluid behavior while contradicting others. However, a major limitation of the prototype installation at this time was that it did not have any type of fluid preconditioning capability. Knowledge gained from fabrication and operation of the prototype made it clear that a larger-scale version based on the same design concept could not be implemented within the budgetary constraints of the project. A large-scale, low-pressure simulator without fluid loss capability was also considered and found to be outside funding limits for the project. As a consequence of these findings, the prototype simulator was re-designated the high-pressure simulator (HPS) and became the foundation for future research at the facility.

During 1994, project scope was redefined to concentrate on using the advanced capabilities of the HPS to perform near-term research and development activities. The revised plan included research in the four major areas of Rheology, Proppant Transport, Perforation Pressure Loss, and Dynamic Fluid loss which encompass all of the TAG preferred topics with the exception of fracture conductivity measurements. In addition to the five preferred topics, the industry based Technical Advisory Group (TAG) also provided guidance during formulation of an R&D plan consisting of three phases. Phases I (October 1, 1994 – March 31, 1996) and II (April 1,1996 – September 30, 1997) were each 18 months in duration while Phase III (October 1, 1997 – September 30, 1998) was to extend for a period of 12 months. During the first phase of activity, a preconditioning loop was fabricated for simulating shear and temperature histories experienced by a fluid as it is injected down the wellbore and into the fracture. The fluid-preconditioning loop, low and high-pressure pumps, and other fluid mixing and handling equipment are described more fully in Chapter 3. Other equipment and instrumentation needed to provide a complete characterization of fracturing fluid behavior were also either fabricated or acquired during this time. Data acquisition hardware, software, and associated instrumentation were a major consideration and the rationale for their selection is described in Chapters 4 and 5. Acquisitions included a Nordman viscometer (rotational viscometer similar to the industry standard Model 50 Fann Viscometer) and a Bohlin rheometer. These instruments were acquired to measure material properties such as viscosity, normal forces, and oscillatory elastic response as a function of time, temperature, and pressure. Chapter 6 provides an in-depth discussion of these viscometers and other rheological instrumentation. Initial tests performed during the R&D effort were designed to confirm the satisfactory operation of newly acquired equipment and instrumentation. However, prior to the start of Phase II, the concept of a "Shared Vision" among the project sponsors was developed to guide future work on the project. Using the Shared Vision concept, project activities were subdivided into the following six categories:

1. Research and Development Program
2. Innovative Testing
3. Testing for Clients
4. Industry Consortia
5. Field Verification
6. Technology Transfer

The GRI Natural Gas Supply Project Advisors at their November 1996 meeting expressed concern about the project and the direction in which it was going. A major concern expressed by the TAG and PAG was the perception that the unique capabilities of the FFCF were not being completely utilized. The high pressure and temperature features of the HPS coupled with the vision system were noted to be important in view of their application to the potentially high-impact research area of proppant transport. Hence, in the revised Project Plan developed during early 1997, refinement of the vision system was moved to a very high priority. Development of the vision system and other instrumentation used by the facility to accomplish its mission are described in Chapter 4. The revised project plan was divided into the following areas:

1. Verification and Transfer of Past Research Results
2. Instrumentation Status
3. Research Focus
4. Consortium Funded Research
5. Testing for Clients
6. Field Verification
7. Technology Transfer

The Phase II of the revised project plan was successfully completed in March 1998. The scope of Phase III activities were then revised to focus on the following activities:

1. Proppant Transport and Proppant Flowback Research
2. Technology Transfer
3. Commercialization

The above activities were totally funded by the U. S. Department of Energy and GRI was still involved technically. The project period for the revised Phase III was from April 1998 through March 2000. The contract with GRI was fulfilled at the end of September 1998 by submission of the final report to GRI. The activities conducted during the period from September 1998 through March 2000 were solely from the DOE funds. The results obtained from the proppant transport and proppant flowback areas are included in Chapter 7. The technology transfer activities and comments on further commercialization of the FFCF and plans for its future expansion as a center for Well Construction Technology are documented in Chapters 9 and 10 respectively.

In addition to finalizing the planned research focus, the FFCF also successfully established an industry funded consortium and completed several tests for industry clients. The Coiled Tubing Consortium is in its third year of operation with good industry participation.

1.4 Gas Industry Benefits

Details concerning the R&D results obtained during Phases I to III and their implications for improved fracturing operations are covered in Chapter 7 of this report. Hydraulic fracturing is the key element of a strategy that is often applied during completion of gas

wells to obtain maximum rate of return on investment. Capabilities developed at the FFCF allow the complex chemical, physical, and fluid flow processes that occur during hydraulic fracturing to be simulated for the first time on a scale comparable to that found in field operations. Using these capabilities, the FFCF has experimentally investigated many of these processes to increase industry knowledge concerning how they impact the overall efficiency of a fracturing treatment. Because hydraulic fracturing is so widely applied, small incremental improvements have the potential to produce an enormous impact on the overall economics of gas recovery.

Chapter 2 HIGH PRESSURE FRACTURE SIMULATOR

2.1 Introduction

The major goals of the project were to design and develop a fracture simulator that provides an accurate rheological characterization of hydraulic fracturing fluids under field conditions and to provide a permanent facility that could be used for testing purposes. To accomplish these tasks, RFP No. 90-211-0367 entitled " Fracturing Fluid Characterization" (see Chapter 1 for further details) recommended that every effort should be made to duplicate the scale of field mixing and pumping equipment while preparing and handling of test fluids and slurries. The proposal submitted in response to the above referenced RFP envisioned essentially a full-scale simulation of all aspects of the fracturing process. Fracturing fluids with and without proppant would be mixed and blended in field equipment. A field scale high-pressure triplex pump would be used to inject fluids and/or slurries through substantial lengths of high-pressure tubing to simulate the wellbore. Tubular and fracture dimensions were also to be duplicated to the maximum extent possible to insure experimental observations at the facility can be directly related to field conditions without the need for scale-up. Varying the injection rate and length of tubing would approximate fluid shear history, which is an important consideration when evaluating crosslinked gels. Fluids and slurries exiting the wellbore simulator would be injected through perforations prior to entering a variable-width fracture simulator. These perforations would be capable of being sized to different dimensions and would be used to study erosion processes with slurries. A variable-width slot, which would be as large as practical based on operational and budgetary considerations, would be fabricated and used to investigate flow processes in a hydraulic fracture. Moreover, this chapter provides an overview of the evolution in design and development that occurred during fabrication of the fracture simulator, High Pressure Simulator (HPS), which is currently being used by the FFCF.

2.2 Design of Fracture Simulator

Four teams were established during the feasibility study to address the Mechanical, Rheological, Measurement/Control, and QA/QC/Environmental aspects of the project. Each team provided input individually and collectively to the formulation of a document entitled “Simulator Functional Requirements.” Maximum operating pressure and temperature, gap-width range, height, length, and other requirements for the simulator were based on industry experience and the practical limits posed by mechanical design constraints.

A fracture simulator approximately 100-ft long, 16-ft high, and having an adjustable gap width from 1/8 to 1 ¼-inch was recommended primarily for the purpose of investigating proppant transport. Maximum operating pressure and temperature were specified as 1200 psi and 250 ^{0}F, respectively. Using these specifications, MTS has developed a mechanical design concept based on having a fixed side and a movable side that would allow the simulator to have a variable gap width. The movable side would be

composed of a 7 by 43 array of hydraulically actuated platens. Each of the 28-inch square platens and the fixed side would be designed to accept a thin sheet of synthetic rock (facings) with permeability in the range of 0.01 to 0.1 md. The project team recommended that a prototype simulator be fabricated to test the mechanical design, facings, controls, instrumentation, safety, and other aspects of the design concept before committing to the construction of the much larger simulator. Technical and Project Advisory Groups (TAG and PAG) approved this recommendation and the design and construction of the prototype were well underway by the end of 1991.

2.3 Design and Construction of High Pressure Simulator

As discussed in section 2.2, the development of a fracture simulator started with the design and construction of a prototype. Originally, the high-pressure simulator was developed as a "prototype" simulator to eventually build a large-scale variable-width simulator capable of coupling slurry flow and fluid loss phenomena in a high temperature and pressure environment. Experience gained during the construction and operation of the prototype in 1993 suggested that budgetary constraints would not allow the large-scale fracture simulator to be built based on the operating principles originally proposed. Consequently, the former prototype was re-designated as the High Pressure Simulator, which is a vertical, variable-width parallel plate flow cell capable of operating at elevated temperature and pressure.

A comprehensive view of the HPS is shown in Fig. 2.1. The internal dimensions of the slot are 7-ft (2.13 m) high and 9.3-ft (2.84 m) long and the fluid enters and exits the slot through perforation manifolds representative of a wellbore. The operational pressure and temperature limits of the HPS are 1200 psi and 250 ^{0}F respectively. Slot width can be adjusted dynamically over the range of 0 to 1.25 in. by a system of 12 hydraulically actuated platens. One wall of the narrow flow channel (slot) was formed by 12 separate, movable steel platens which are 28 by 28 inch square and are laid out in a 3 by 4 matrix. The opposite wall is a stationary, continuous 6-inch thick steel slab. The gap between each movable platen and the stationary wall can be adjusted by means of a hydraulic actuator. Platen movement allows the gap width to be set to a selected value and is used to compensate for deformation of the supporting structure under high pressure and temperature. A 1-inch thick facing material covers each of the movable steel platens to create one wall of the simulated fracture. The opposite stationary wall is covered by a matching 3 by 4 matrix of facings that are also 1-inch thick and 28 by 28 inch square. These replaceable facings are used to simulate the rock surfaces of a hydraulic fracture. They can be prepared from either a synthetic resin-sand composite material or a natural rock slab. In one application, instrumentation such as a fiber-optic vision system, temperature sensors, and a LDV viewing port were cast into an impermeable resin facing material. By changing the facings, different properties, such as permeability and surface roughness, could be investigated for their effect on fluid loss, fluid flow, and proppant transport. During fluid loss tests, a series of channels behind the permeable facings provide a route for filtrate to exit the apparatus to a measurement point.

The prototype design consisted of a 3 by 4 array of the same hydraulically actuated platens that would be used in the large-scale simulator. With this design

approach, critical mechanical components of the simulator would be evaluated full-scale rather than in some miniaturized form as the term prototype often conveys. There was also the additional thought that some benefit might be derived from having prototype components interchangeable with the full-scale simulator. Other unique features of the HPS include the vision system for flow visualization of proppant-laden fluids and Laser Doppler Velocimeters (LDV) for accurate rheological characterization of various fluids. During July 1992, the 75,000-lb prototype simulator was installed in a remodeled aircraft hangar bay at 1928 Goddard Avenue on the North Campus of the University of Oklahoma.

Figure 2.1-High Pressure Fracture Simulator

Figure 2.2 shows the perforation and platen layout in the high Pressure Simulator. The inlet and exit manifolds (2.75 in. in diameter) are equipped with 22 equally spaced cylindrical openings. These openings are ¾-in. diameter, 3-in. long and spaced on 4-in. centers. The perforations whose configuration and size can be easily changed using a series of blank and sized inserts. These inserts allow the openings to be either plugged or converted to ¼-, 3/8-, or ½-in. diameters. A wide variety of perforation patterns and sizes can be simulated using these inserts. An access port, located on the backside of the inlet manifold, is provided for installation and removal of these inserts.

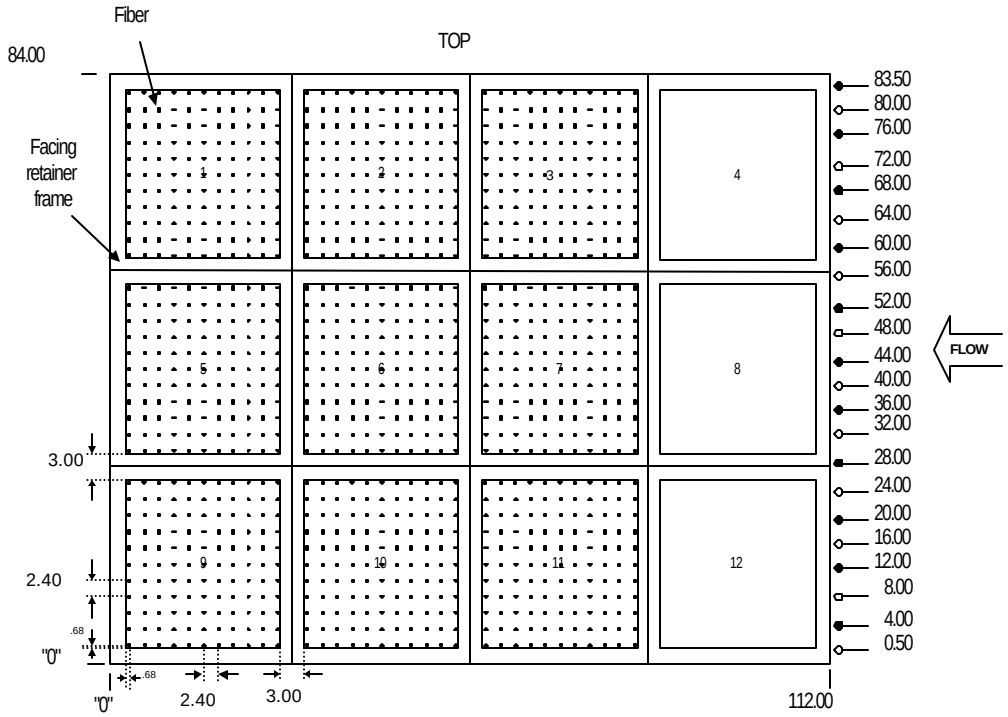

Figure 2.2-Perforation and Platen Layout in the HPS

2.4 Verification of Testing and Acceptance

The simulator was subjected to a series of verification tests to insure its compliance with design specifications. A research plan was also developed for using the High Pressure Simulator to conduct limited investigations of fluid characterization, proppant transport, proppant flowback, and dynamic fluid loss behavior of fracturing fluids both linear and crosslinked. These investigations were conducted to provide useful data for the industry and to gain operating experience with the mechanical and instrumentation systems planned for the large-scale simulator. Fabrication of the prototype and the experience gained during its operation in1993 indicated that a large-scale simulator built on these same principles would be too complex and costly. As a consequence, MTS developed new mechanical design concepts for a large-scale, low-pressure simulator (LPS) that would be simpler to operate and more economical to implement. The proposed simulator would have a variable width slot 15 ft high by 40 ft long and would be capable of operating at elevated temperatures and 300 psi. However the LPS was also found to be outside the funding guidelines established for joint sponsorship of the project by DOE and GRI.

Therefore, since 1994 the prototype was designed as the high-pressure simulator (HPS), and it is being utilized to perform near-term research and development activities in various hydraulic fracturing areas rather than large-scale hardware development. The HPS was moved to its current facility in August 1996 and has been continually improved through mechanical, instrumentation, and software modifications.

Chapter 3 FFCF CAPABILITIES

3.1 Summary

This chapter discusses the capabilities of the Fracturing Fluid Characterization Facility (FFCF) at the University of Oklahoma. The FFCF provides oil and gas industry with innovative technology to improve efficiency and economic viability of drilling, completion and production operations. Services provided and research areas of the FFCF (now called Well Construction Technology Center WCTC) fall into following six main categories:

- Fluid rheology and characterization applications using High Pressure Simulator
- Coiled tubing applications as industry joint project (Coiled Tubing Consortium - CTC)
- Drilling simulation using field scale Drilling Rig Simulator
- Development of cooperative projects with Sandia National Laboratories
- Training courses for the petroleum industry (Network of Excellence in Training NExT)
- Providing third-party tests

Each category of the FFCF activities is discussed in the following section in detail. These categories along with equipment and facilities describe the commitment of the FFCF to provide a world class research facility to the industry.

3.2 FFCF Research Capabilities

3.2.1 Fluid Rheology and Characterization Applications

The High Pressure Simulator (HPS) and its associated field scale mixing, pumping and preconditioning equipment as well as highly skilled personnel allows the WCTC to concentrate on the following research areas:

- Dynamic fluid loss
- Perforation pressure loss
- Proppant transport
- Proppant flowback

The HPS replicates all conditions experienced by a fracturing fluid from its formation to its leakage into a rock matrix. The HPS is a large, articulated, servo-controlled, parallel-plate flow cell designed to measure fluid properties at temperatures as high as 250^{o}F and pressures up to 1200 psi. Also integral to the facility is auxiliary equipment such as field apparatus for blending the fluid, mixing in the proppant and pumping the fluid through a simulated wellbore and the simulator's computerized data acquisition and control system. The FFCF's HPS is the world's only above-ground fracture simulator for fracturing fluid characterization. The HPS allows FFCF to perform unique research with field methods and equipment:

- Simulation under operating conditions of up to 1200 psi and 250^{o}F
- Simulation with a dynamically variable gap width

- Dynamic leak off test
- Fluid and proppant flow visualization
- LDV measurements/point velocities and velocity profiles of the fluid

The preconditioning facility, consisting of different lengths of coiled tubing and related equipment provides a shear history simulation for the fluid and thus, brings its viscosity closer to fluid flowing under actual downhole conditions.

3.2.2 Coiled Tubing Applications

One of the hottest issues in the oil industry is the application of coiled tubing and development of its relevant technology. The applications of coiled tubing are exploded from conventional application to new applications such as wellbore cleanout, coiled tubing drilling, etc. In order to meet industry's need for development of basic technologies, the FFCF teamed up with a number of industry service providers as a consortium.

The FFCF with the consortium (CTC) focused on gathering frictional pressure loss data for drilling, completion, and stimulation fluids; developing engineering and design correlations; and evaluating rheology fluids and foams as a function of shear rate and temeprature. The FFCF performs the study of flow behavior of commonly used fluids in coiled tubing, which takes into account the effects of curvature and seam. The field scale experimental facilities, which are discussed in the next section, allow the FFCF to currently undergo the following research:

- Drag reduction
- Wellbore cleanout
- Coiled tubing fracturing
- Field data comparison/confirmation

3.2.3 Drilling Simulations

The FFCF has a Drilling Rig Simulator housed at the former BP-Amoco Tulsa Technology Center in Tulsa. This simulator was donated by BP-Amoco to the OU's School of Petroleum and Geological Engineering in 1999. The field scale Drilling Rig Simulator is composed of five major systems; weight-on-bit system, which can produce 70,000 lbs, circulating system, rotary system, the back-pressure system and computer system. The detailed specifications of the simulator are described in the next section. The use of the Drilling Rig Simulator allows FFCF to perform research to develop new bit design, quality control checks, and evaluate new tools and products. The Drilling Rig Simulator is also used to perform high-quality and conclusive work to test and develop various downhole tools and systems. These include:

- Bit models: roller-cone, natural diamond, PDC
- Anti-whirl drill and core bits
- Hydraulic studies, bit balling characteristics
- Mud effects: ROP enhancers, shale stabilizing agents, lubricants

- Downhole tools: reamers, shock subs, motors, casing and sidetrack mills, casing shoes, stabilizers, jet nozzles
- Tubulars: quality control
- Pipe dope studies

3.2.4 Cooperative Project with Sandia National Laboratories

The FFCF is managed by the School of Petroleum and Geological Engineering at the University of Oklahoma, which has a record of success in science and technology development for the exploration and production of oil and gas. By signing a MOU (Memorandum of Understanding) with the Sandia National Laboratories, which has been DOE's leading laboratory for drilling technology for the past 20 years, the FFCF can get the advantages of sharing a variety of technologies developed by Sandia National Laboratories. These include modeling and simulation using high-performance computers, advanced sensing and information systems, robotics, and micro-machine technology.

Advanced technology research and development work, which cover the wide range of topics related to well construction and advanced drilling, will be done cooperatively with some projects done at each institution.

3.2.5 Third-Party Tests

The FFCF has made significant progress in the area of third-party testing. Several third party tests have been successfully performed in the areas of fluid rheology, proppant transport and coiled tubing applications. The previous tests brought very encouraging response from the customers. The clients expressed their satisfaction with the services provided by the FFCF.

Combining the resources available in the FFCF as well as other department at the University of Oklahoma, the FFCF can offer a unique range of services to assist the oil industry. The FFCF has in-depth knowledge, good experience in performing the various ranges of experimental work, unique facility and personnel who know how to design and carry out the tests on behalf of clients. A brief listing of third-party tests available in the FFCF is presented below.

- Fluid rheology (drilling, completion, foam, cross-linked slurry, etc.)
- Proppant transport
- Proppant flow back
- Perforation pressure loss
- Coiled tubing applications
- Wellbore cleanout
- Mathematical simulation
- Drag reduction

3.2.6 Network of Excellence in Training (NExT)

Heriot-Watt University, Texas A&M University, the University of Oklahoma and Schlumberger established a Network of Excellence in Training (NExT). The NExT is dedicated to conduct training courses for the petroleum industry that combine academic

excellence with professional expertise. The objectives of the NExT program are to keep the knowledge transferred up to date and fit-for-purpose, and to use technology to optimize delivery and assessment methods.

NExT offers the petroleum industry a network of intellectual capital in research, expertise and practical application-delivering solutions through industry training and technology transfer relationships worldwide. Program features include a master's degree program in addition to University certification for NExT courses and university credit for counting education units. Course delivery methods will vary from traditional classroom work at the universities and training centers to mentor-supported distance learning via on-line or CD-ROM self-study programs. NExT also designs the customized programs, providing on-site training at client locations worldwide.

The FFCF as a representative of the University of Oklahoma has special responsibilities for offering courses related to well construction, operation and petrophysics. The role of the FFCF in NExT is that of a technology transfer provider to the petroleum industry and provider of main training center of excellence for this project.

3.3 Equipment and Facilities

The research capabilities of the FFCF have been enhanced to a greater extent through various improvements in combination of facilities newly augmented in the institute. This chapter provides a detailed overview of equipment currently used for research activity, and testing capabilities available at the FFCF. This equipment and facilities fall into the following seven categories:

- Rheology Measuring System
- High Pressure Simulator
- Coiled Tubing Facility
- Drilling Rig Simulator
- Fluid Supply and Preconditioning System
- Data Acquisition and Control System
- Additional Equipment

These classifications are discussed in detail in the following sections.

3.3.1 Rheology Measuring System

There are several fluid rheology-measuring instruments available at the facility. They include the HPS (field scale), two Model 35 Fann Viscometers, a Nordman Rheometer and a Bohlin Rheometer for characterizing the viscosity of the fluids. The laboratory rheology data are necessary for quality control of the test fluid to insure reproducible large scale testing data. The Nordman Rheometer is a fully automated high-temperature (500°F), high-pressure (1000 psi) rheometer. It is equipped with a quick-disconnect fitting on the bottom of the sample cup to provide dynamic filling to avoid any period of no shear to the fluid. The Bohlin Controlled-Stress rheometer (CS-50) is also used to provide the viscoelastic properties of the fluids under investigation. It can supply steady-

shear as well as oscillatory-shear data at elevated pressures and temperatures. It is also capable of providing the fluid's normal stress measurement. The HPS can be utilized to measure the rheology of crosslinked fluids.

3.3.2 High Pressure Simulator

The workhorse of the FFCF is the high-pressure simulator (HPS) which is a vertical, variable-width parallel plate flow cell capable of operating at elevated temperature and pressure. The resin facings are smooth and impermeable, while the synthetic and natural rock facings have more texture and are permeable. Examples of instrumentation on the impermeable facings are fiber optics for vision system, sight glass for Laser Doppler Velocimetry (LDV), differential pressure tube, and thermocouple lead. The details are described in Chapter 2.

3.3.2 Coiled Tubing Facility

The FFCF is equipped with coiled tubing system consisting of various spools of coiled tubing connected in series which allows to study different energy input levels on fluid properties at various levels of shear. The shear history conditioning system is comprised of 1500 ft.1-inch coiled tubing system, which allows usage of 500 ft., 1000 ft., or 1500 ft. tubing lengths. The second system is comprised of 5000 ft. of 1 1/2-inch coiled tubing system, which allows usage of 1000 ft., 2000 ft., 3000 ft., 4000 ft., or 5000 ft. tubing lengths. The third system is comprised of 3000 ft. of 2 3/8-inch coiled tubing system, which allows usage of 1000 ft., 2000 ft., or 3000 ft. tubing lengths.

Figure 3.1 shows the coiled tubing systems. These coiled tubing systems are used for fluid friction loss tests. There are two annular sections, one fully concentric and the other fully eccentric. The outside tubing is 3 ½" nominal and the inside tubing is 2 3/8" nominal. This equipment is utilized for CTC research.

3.3.4 Drilling Rig Simulator

The drilling simulator is composed of five major systems; weight-on-bit system, circulating system, rotary system, the back-pressure system and the computer system. The detailed specifications of the simulator are described in the following sub-section.

Weight-On-Bit (WOB) System. The WOB system is controlled with a large hydraulic ram, which applies the WOB and also picks up the drillstring assembly. It is controlled by a servo valve and is, therefore, very precise. The maximum WOB that can be produced is 70,000 lbs.

The WOB can be run in two modes: (1) in weight control mode the system is operated to maintain a constant force on the load measuring sensor independent of the bit position and (2) Position control mode maintains a set bit position independent of the force applied to the bit.

Fig. 3.1 Coiled Tubing System

The Mud Pump System. The mud pump system provides the means of circulating the mud from the mud tank through the plumbing system, bit, pressure control system, and back into the tank. The primary mud pump is a Halliburton HT-400 triplex cementing pump. It is powered by a 600 HP DC motor that is connected to the pump through a 2 speed gear box. The gear box allows the pump to be directly connected to the pump input shaft or to be geared down with a 2:1 gear ratio to provide a higher torque (pressure) capability. In high gear, the maximum flowrate available is 590 gpm at 1,500 psi. In low gear, the flow rate is 300 gpm with a maximum pressure of 3,000 psi.

The secondary pump is a Dowell PG03 frac pump driven with an 850 HP Gulf Electroequip DC motor. This motor is directly connected to the pump input shaft. It is capable of pumping 190 gpm at 5,000 psi with the existing liner size. (The system pressure is currently limited to 3,000 psi due to the stand pipe and swivel pressure ratings.)

Combining both pumps allows for a maximum pressure of 3,000 psi at 490 gpm, and a maximum flow rate of 780 gpm at 1,500 psi. The pump system is fed through a centrifugal charge pump to provide a positive pressure to prevent cavitation while drilling and to facilitate mud mixing.

The closed loop mud system is complete with a high-speed shale shaker, a 100 bbl active system, a 100 bbl storage tank and a 90 bbl mixing tank.

The Rotary System. The low speed rotary system is capable of rotating the drillstring in the range of 30 to 215 rpm. A standard rotary table drives a square kelly. It is powered by a fixed displacement Sunstrand hydraulic motor. The motor is powered with a 400 HP

Sunstrand Series 27 variable displacement (9 piston) hydraulic pump. This pump is driven by a 400 HP AC motor and is used to drive a constant displacement hydraulic motor. A maximum torque of 6,500 ft-lbs. can be produced independent of the rotational speed. Figure 3.2 shows Rig floor of Drilling Rig Simulator located at the Tulsa Technology Center.

The high-speed rotary system is used for rotating the bit at speeds ranging from 300 to 1,500 rpm. This system is powered by the same 400 HP pump and control system as the low speed system. The hydraulic drive motor for this system is identical to the bit drive shaft with no gear reduction. This provides a maximum torque capability of 1,300 ft-lbs.

Fig. 3.2 Rig Floor of the Drilling Rig Simulator

The Back Pressure System. The back-pressure system is used to control the ambient pressure in the drilling vessel, which simulates hydrostatic head of the drilling fluid in a wellbore. It is composed of a coarse filter, a fixed choke, and a variable choke to produce the desired pressure. The fluid flows through the filter to remove any material that is large enough to plug the fixed choke and then flows through the variable choke system. The fixed choke unit contains carbide sliding plates and a diffuser. The objective of this fixed choke system is to control the pressure within 400 psi of the desired value. The variable choke is an ABC valve, which can further adjust the pressure to the desired value.

The Computer System. The rig can be operated in either a manual or computer controlled mode. The manual control system is used to control the rig during set up of a test and for rig control during some specialized testing. Critical electronic sensors are mounted on the rig to measure approximately 30 associated drilling parameters. There are 31 analog and 8 digital signals available. A current in-house PC software program is used to monitor, collect and store the data from the lab test. Data is sent to a printer, an 8-pen strip chart recorder, a reel-to-reel tape drive for long-term storage, and a spectrum analyzer to investigate frequencies of vibrations. This system will be updated soon. Control room for the Drilling Rig Simulator is shown in Fig. 3.3.

Fig. 3.3 Control Room for the Drilling Rig Simulator

3.3.5 Fluid Mixing and Preconditioning System

The FFCF Mixing and Pumping System is subdivided into two categories; namely, low pressure equipment and high pressure equipment. The low-pressure pumping equipment consists of a Moyno pump (6P10) and a Deming centrifugal pump (5M). The upper limit of operation of the Moyno pump is approximately 140 gpm at 600 psi. The centrifugal pump serves to impart additional mechanical energy to the fluid in order to achieve higher flow rates. The eye of the centrifugal pump is also used as a point for the injection of crosslinker for the preparation of crosslinked fluids and slurries. Fluid is stored in a 1000 gal polyethylene tank, and a 200 gal ribbon blender along with a 55 gal stainless steel tank equipped with three-bladed Lightning mixer are available for batch mixing slurries.

The high-pressure equipment consists of a triplex plunger pump (Fig. 3.4) capable of achieving flow rates in excess of 200 gpm at 1200 psi. A Galigher centrifugal pump is used in tandem with the triplex pump to impart additional energy at higher flow rates and as an injection point for the crosslinker and/or additives. Two 50 bbl storage tanks provided with agitators are used to prepare 100 bbls of test fluid with constant mixing. Sand is conveyed pneumatically (for preparation of slurries) to the storage tanks from two 330 sack storage tanks. Two ISCO syringe pumps insure constant injection of crosslinker at the eye of the centrifugal pumps (both low and high pressure systems) at flow rates of up to 1500 ml/min. A disposal tank of 150 bbl capacity is available for storage of the used test fluid.

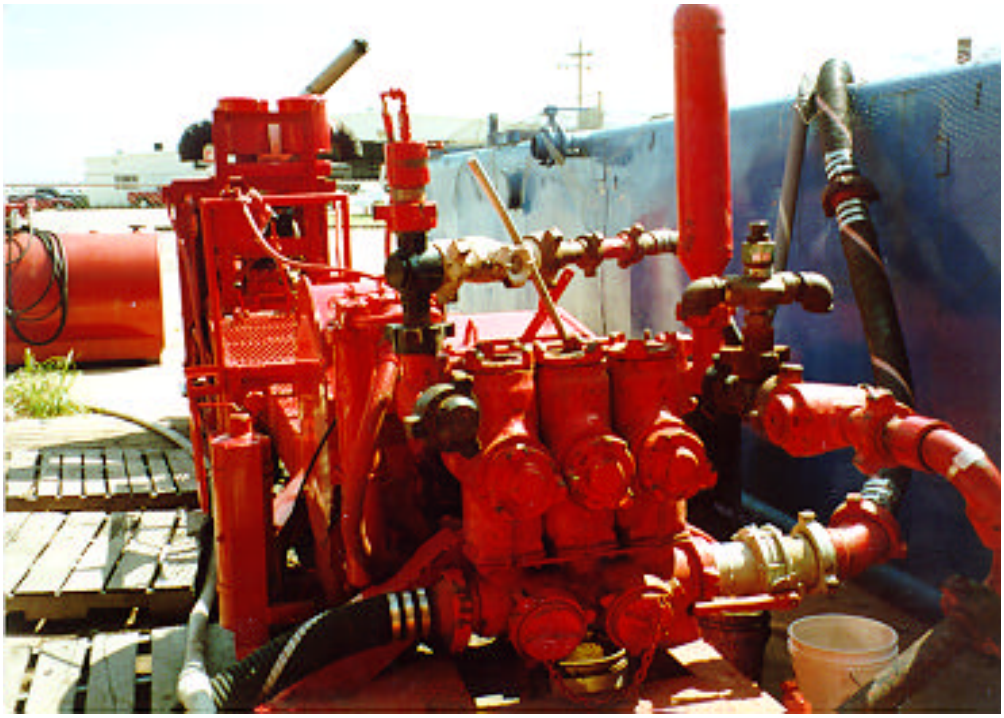

Fig. 3.4 Triplex Plunger Pump

The fluid preconditioning system at the FFCF is designed to provide both shear as well as thermal preconditioning. Coiled tubing reels provide shear preconditioning of the fluids representative of the flow of fluids down the wellbore. Further, the coiled tubing reels are also equipped with differential pressure transducers for quantification of shear effects. In order to provide thermal preconditioning, the FFCF is equipped with a low shear heat exchanger (Fig. 3.5) used in conjunction with the coiled tubing to simulate the effects of temperature gradient existing down a wellbore. The double pipe heat exchanger consists of a 2 inch tube (tube side) inside a 3 inch tube (shell side) with a total length of 500 feet. The heat exchanger is capable of heating crosslinked gels and slurries at 60 gpm up to 250 °F using 300 °F water at 40 gpm on the shell side. The temperature effects on the fluid can be monitored by means of thermocouples placed along the length of the heat exchanger.

Fig. 3.5 Double Pipe Heat Exchanger

3.3.6 Data Acquisition and Control System

The Data Acquisition and Control system constitutes the Vision System, the Laser Doppler Velocimeters (LDV), Pressure, Temperature and Flow Measurements.

With the improved vision system it is possible to monitor and quantify the proppant concentration during proppant transport and proppant flow back experiments in the HPS. For pressure, temperature and flow measurement a wireless fluke hydra system is used which is capable of receiving 40 data instructions every five seconds and transferring them to a PC where they can be saved for analysis. In order to illustrate the proppant transport and proppant flow back procedure and measurements, the details are described in Chapter 5 Data Acquisition.

3.3.7 Additional Equipment

Equipment now ready for use not included in the above categories are the foam flow loop, the clear plastic wellbore cleanout test bench, and Laser Doppler Velocimetry (LDV) to measure and analyze fluid velocity profile.

The clear plastic wellbore cleanout model is a 18 ft long and 4 in. diameter clear plastic pipe with tubing attachment at each end and a 2 in. diameter plastic tubing inside (Fig. 3.6). It is mounted on a steel frame that can be adjusted to any angle from horizontal to vertical.

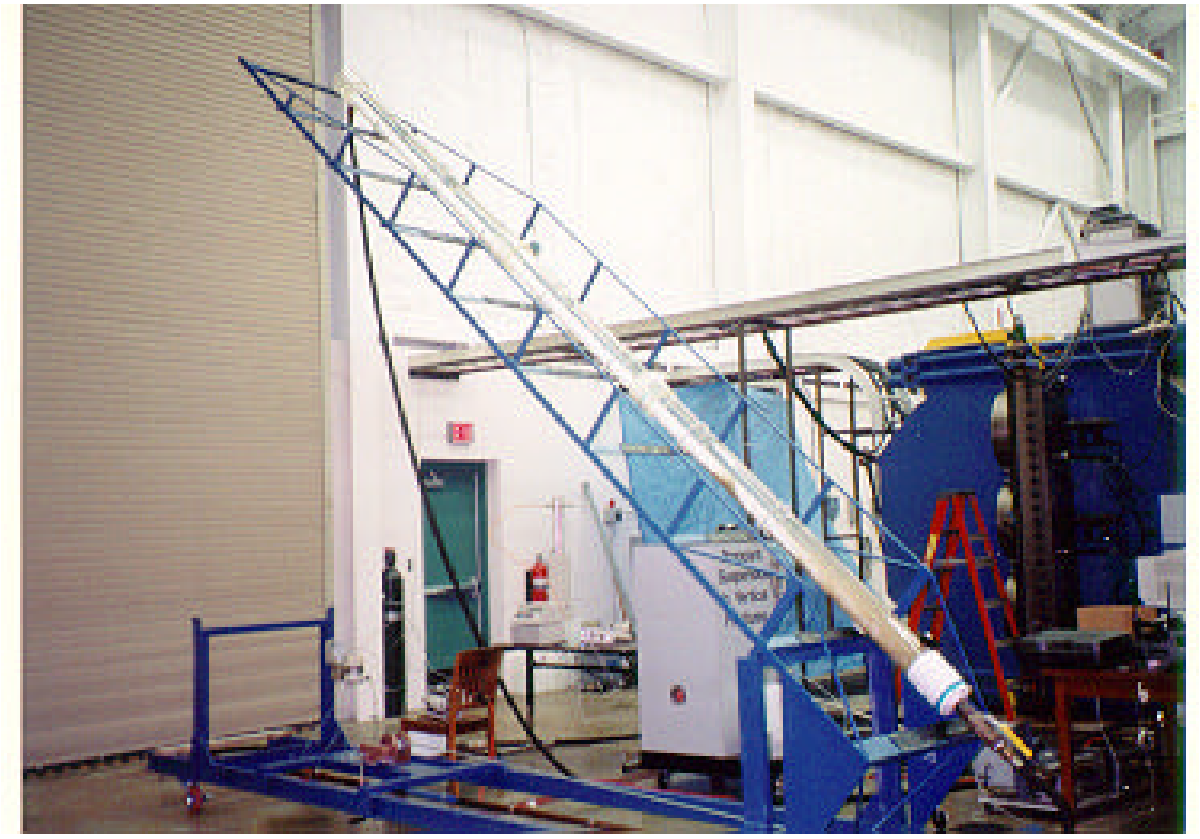

Fig. 3.6 Wellbore Simulator at a Deviated Angle of 45^{o}

The foam flow loop consists of three tubing sizes, ¼", 3/8", and ½" with a Honeywell differential pressure transducer which is applied across a 10' span of each of these, a Little Giant Triplex loading pump, an ISCO 500D pump and controller for crosslinker injection, a Micromotion flow meter, a Sprague pump, a Penberthy flow cell, a static mixer, and heat tape and controller. This system is capable of 1000 psi and 250 °F and is described in detail in Chapter 6.

Laser Doppler Velocimetry (LDV) does not suffer from the complications inherent in more typical methods of point-velocity measurement. The LDV is being used to characterize rheological properties of the complex fluids used in the Petroleum industry (fracturing gels, proppant-laden fluids etc). The LDV system is described in detail in Chapter 4 with results obtained using the system being presented in Chapter 7.

Chapter 4 INSTRUMENTATION

4.1 Introduction

Instruments are the most important part of an experimental set up and satisfactory performance of instruments is key to acquire quality data. The set up of FFCF is highly competitive and instruments are conFig.d with the set up as per demand at hand. In other words, each setup requires that the instruments be conFig.d for specific application of the FFCF. This means that each instrument is designed, developed, modified and mastered at the facility itself.

There are several instruments available at the FFCF. These instruments include vision and laser doppler velocimetry (LDV) system devices, HPS control tools, differential pressure transducers, and fluid flow measuring apparatus. These instruments are described in the following sections.

4.2 Vision System

The vision system provides a means to view inside the steel-walled high pressure simulator (HPS). To accomplish this task, a fiber optics lit vision system was used initially. Later on, the fiber light array was replaced with a light emitting diode source to provide light inside the HPS. In the fiber optics system, an array of light guides was cast into the synthetic rock facings on both walls of the HPS. One wall contained fibers that acted as light sources and other wall contained fibers that acted as light receivers. Both sets of fibers were positionally matched across the slot gap. The light source fibers were powered from outside the HPS through a piped setup.

The vision system works on the principle that the light generated on one wall is shadowed by the fluid flowing through the slot, and so an image is seen by the fibers on the opposite wall. These receiver fibers can, then, transfer the image to a camera. With a set of nine cameras installed on the HPS, a complete picture of the flow behavior inside the slot can be obtained. The fiber optics light source had many limitations that affected the performance of the vision system. These shortcomings arose due to many bends introduced into the fiber optic bundles. These bends increased the light attenuation in the transmitting fibers and restricted the light intensity generated by the fiber source. To overcome these shortcomings, a light emitting diode (LED) system replaced the fiber-source vision system.

The LED system enhances the light intensity inside the HPS and improves the illumination through the fluid; thus, it produces a more uniform image of the entire fluid flow in the slot. The better illumination is obtained due to larger light umbra produced by the LEDs than the fibers. In addition to the enhancements in the images, the new LED array provides cheaper light transmitting facing and utilizes a lower voltage to power the slot. This low voltage system decreases electric hazards associated with the operation of the HPS. The LED system uses a total of 121 discrete HP-2000 light emitting diodes on each synthetic facing of the slot. The LEDs are installed prior to preparing the facing. First, the facing mold is wired with a bus into a grid to which the LEDs are soldered.

Next, the mold is filled with facing material around the LEDs. Once the facing is set, the LED leads are insulated to prevent electric shocks. With an array of 121 LEDs on each facing and nine facing on one wall, 1089 LEDs illuminate one face of the slot. Each LED is aligned with a receiving fiber giving a total of 1089 fibers to capture the flow image on the opposite wall of the slot. This geometric array of LEDs and fibers is shown in Fig. 4.1.

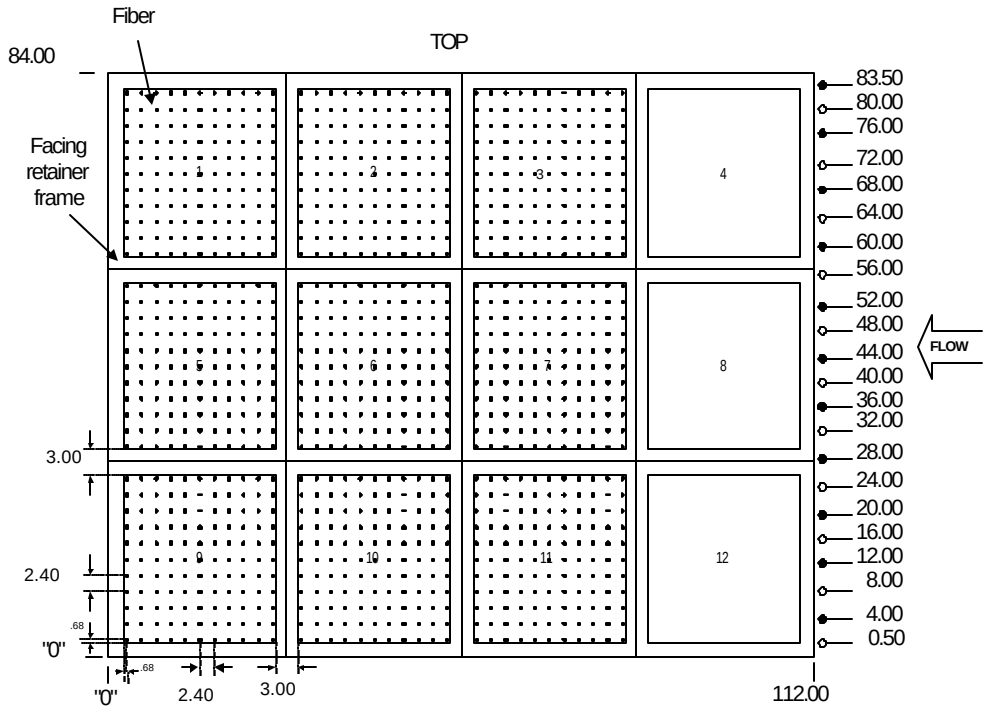

Fig. 4.1-An Array of LEDs and Fibers Installed on the HPS

The flow image captured on the fiber is to be conveyed to camera for display and processing. This task is accomplished by grouping the fibers. For each image-receiving facing of the slot, 121 fibers are grouped together to form 11 by 11 square bundle of fibers. This bundle, shown in Fig. 4.2, has one inch long sides and is constructed in similar spatial order as the fiber in the facing. The bundle conveys the image from the fracture wall to a window outside the HPS. From the window, the image is captured with a black and white video camera. Thus, from the nine facings, nine video cameras acquire the complete dynamic fluid image from the slot. An example of an image obtained from the vision system is shown in Fig. 4.3.

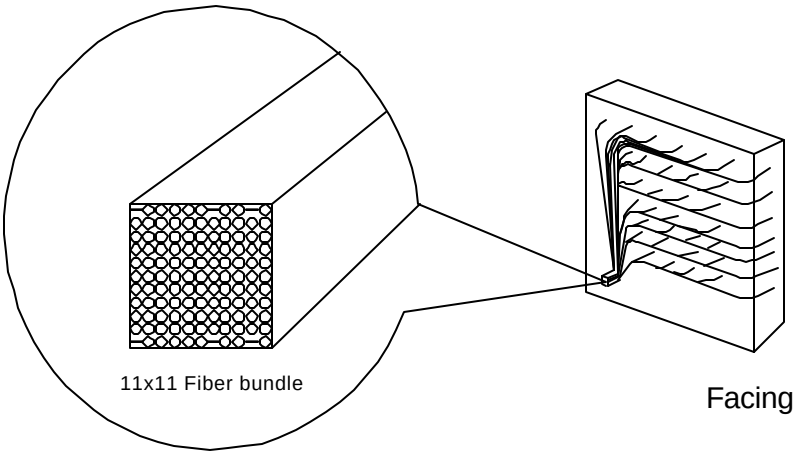

Fig. 4.2-The 11x11 Fiber Bundle to Capture Fluid Flow Image across the Platen

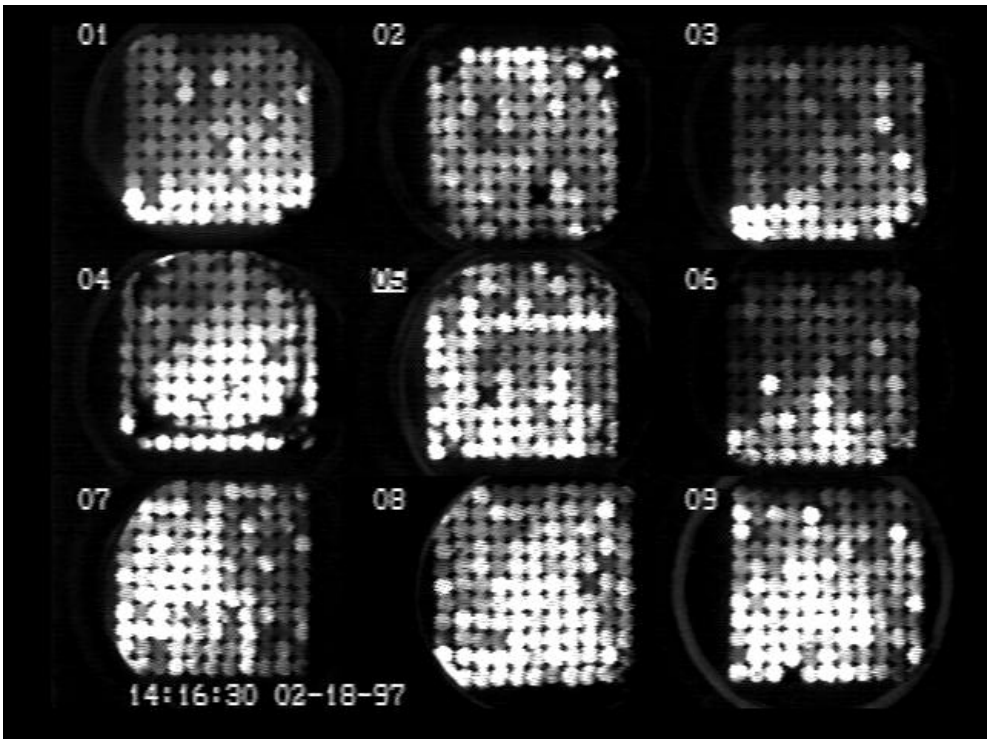

Fig. 4.3-Raw Fluid Flow Image Obtained with the Vision System

4.3 Laser Doppler Velocimetry (LDV)

The following characteristics of LDV make it especially advantageous for difficult flow experiments.

- It is non-invasive.
- It is immune to temperature effects.
- It is free from mechanical damage due to particulate abrasion.
- It has rapid response to velocity changes.
- It is ideal for fluid experiments which involve complex fluids like proppant-carrying fluids, mixtures and special fluids etc.
- Data can be acquired in real time
- The laser light can be focused into a very small volume and therefore spatial resolution obtained is far superior to any other technique.

The LDV system has been used for two types of slots:

1. High Pressure Simulator (HPS)
2. Plexiglas Slot

LDV probes are mounted on the HPS at each of the nine platens. It looks at the fluid through a glass window tuned to the LDV wavelength. The LDV measuring system uses a semiconductor diode laser that operates at a wavelength of 780 nm. This diode laser provides a compact measuring head and allows better penetration into the fluids. The measuring head contains the diode laser source whose output is collimated and then split into two equal intensity beams to provide dual beam LDV system. The beams are crossed by a focussing lens and are collected back after scattering from the measuring volume by a receiving lens. The receiving lens focuses the collected light beams onto an avalanche photodiode (APD) which transmits a Doppler signal on beat frequency to a signal processor. The processor analyzes the doppler signal and generates the fluid velocity profile.

Of the nine LDVs installed on the HPS, three have rotational and translational capabilities. These three stations can be moved easily to study velocity profiles at any location on the HPS. The nine-point velocities are used to spot-check flow uniformity and the three automated stations are used to provide flow cross-section at the spot-check point. Thus, the LDVs provide detailed information on the flow profiles, which can be compared to the theoretical profiles.

In addition to understanding the velocity profile across the slot width, knowledge of the fluid velocity in the near wall region is of great interest to rheologists. The near-wall velocity determines the velocity gradient, which is used to calculate nominal shear rate at the wall and thus, rheologically characterizes non-Newtonian fluids. Moreover, the near-wall velocity measurements are useful to investigate wall slippage and drag reduction characteristics of the fracturing fluids.

The LDV system available at the FFCF has the following specifications:

1. Focal length = 138.8mm
2. Fringe Spacing = 2.2283 micron
3. Peak Power = 650-780nm
4. Half angle = 9.57 degrees
5. Beam Spacing =50.0 mm
6. Transnational and rotational motion available
7. Single Head Probe with back-scattering mechanism

4.3.1 LDV Data Processing System and Software Setup

When particle passes through the measuring volume, the back scattering signal is collected with a 2.50-inch diameter-collecting lens and the back-scattered light is converted into electrical signal. This signal is then transmitted to the signal processor (Model TSI IFA-550), which is also called Intelligent Flow Analyzer.

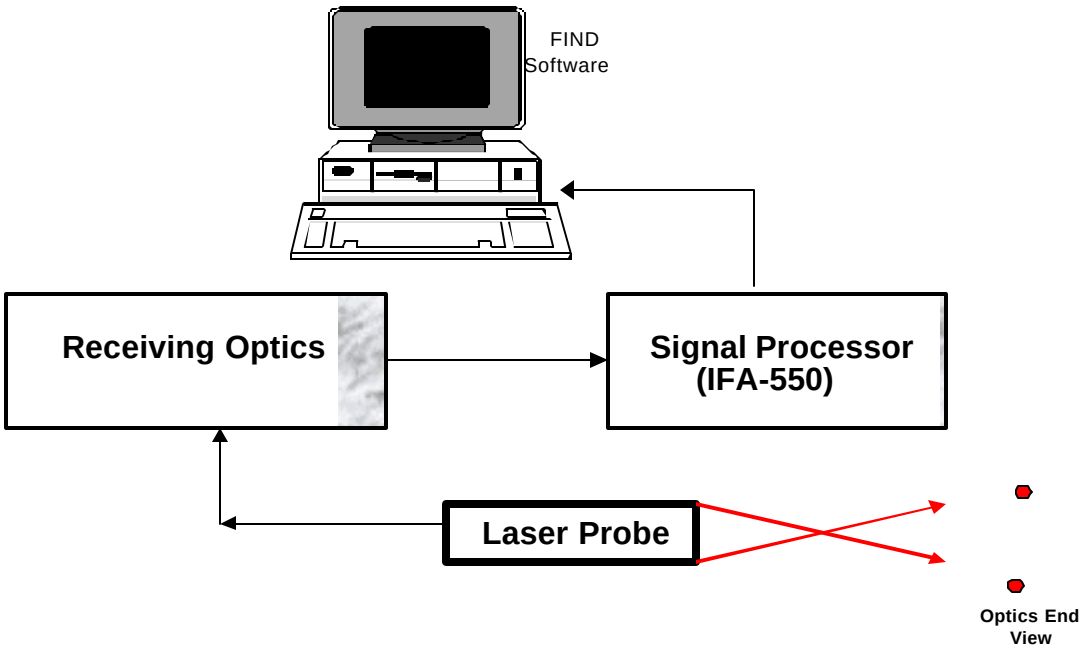

Figure 4.4: LDV Data Acquisition

This Intelligent Flow Analyzer is connected to a personal computer via parallel communication port. A flow analysis software (called Flow Information Display or FIND) then gathers and presents the velocity data. The software has facilities for calculating real time mean velocity and turbulent density values, along with data validation and histogram graphs of the velocity values obtained.

The data rate displayed by the (FIND) software is actually a measurement of the number of scattering particles passing through the measuring volume per second. The higher the data rate observed implies higher accuracy as greater number of particle velocities are averaged in the measuring volume.

4.4 HPS Control System

The most important instrument at the FFCF is the high pressure simulator, so it is necessary that the simulator is operated with state-of-the-art instruments.

The instruments on the HPS provide input to a five-mode control system that allows smooth and remote location running of the simulator. The five modes and their respective instruments are described below.

1) Position control uses linear voltage displacement transducers (LVDTs) in each actuator to measure the displacement of piston. This controller mode works when the HPS is opened or closed.

2) Slot width control uses LVDTs installed in the slot to maintain a parallel and constant gap width in the slot. This controller mode works only when the simulator is closed.

3) Slot pressure control uses a slot pressure transducer to adjust the slot width to compensate for structural variation in the simulator. This mode requires that the HPS is closed and filled with fluid.

4) Compliance control uses two user-specified parameters to make the simulator compliant to the changing pressures in the slot. The first specified variable is pressure that allows the system to become compliant, and the second variable is position movement per unit change in the pressure. This mode operates when the HPS is closed.

5) Actuator pressure control uses hydraulic oil in the actuators to apply constant pressure on the fluid or sand pack inside the HPS. This mode works only when the HPS is closed.

4.5 Differential Pressure Transducers

Differential pressure is a very important parameter for the fluid characterization studies. The differential pressure when combined with slot gap width measurements determines the wall shear stress on the fluid. The shear stress along with nominal wall shear rate describes the rheological properties of the fracturing fluid in a fracture. In addition to the rheological characterization studies, the differential pressure measurements are useful to predict friction pressure losses.

4.6 Rheological Characterization (Instruments and Capabilities)

4.6.1 Model 35 Fann Viscometer

Two Fann viscometers, one with a #1 spring and the other with a # 1/5 spring are available at FFCF to measure the rheological characteristics of fluids.

The fluid viscosities are calculated at several shear rates by varying the rotational rates of the bob in the fluid. With these viscosities, rheograms are developed for the test fluids. The measured data are fit with appropriate rheological models to describe fluid behavior and predict the fluid viscosities at the shear rates of interest to the industry.

The Fann viscometer is a very rugged and robust instrument. It is very helpful to provide a quick check on the fluid behavior and to compare the fluid viscosities with other measuring devices. The Fann viscometer is frequently calibrated and serviced to maintain its accuracy to measure the fluid viscosities.

A detailed description of the Fann viscometers is provided in chapter 6.

4.6.2 Bohlin Rheometer

Bohlin rheometer is a unique instrument available at the FFCF. This rheometer is different from the Fann and Nordman viscometers. Unlike the two controlled rate viscometers, Bohlin rheometer is a controlled stress instrument in which a shear stress is applied and resultant shear rate is measured. The Bohlin rheometer is capable of utilizing different measuring geometries and measure viscosity as well as viscoelastic characteristics of the fluid, whereas the two viscometers only use concentric cylinder geometry and measure fluid viscosity only.

The Bohlin rheometer works with a unique drag cup motor that applies torque to the fluid sample. This torque is transmitted through the measurement geometry to the fluid sample with the help of a frictionless air bearing. The applied torque induces shearing into the sample and the resultant displacement is measured with a highly sensitive optical angular position transducer. The state-of-the-art instrumentation on the Bohlin rheometer makes it a very accurate and versatile equipment.

The Bohlin rheometer is equipped with three measuring geometries: concentric cylinder, parallel plate, and cone and plate. The concentric cylinders are available in two bob diameters, 14 and 25 mm, and are respectively denoted as C14 and C25. The bobs are used in cups so that cup to bob radius ratios is similar at 1.1. The other two measuring devices, parallel plate and cone and plate, are different from the concentric cylinders because of their different geometric configurations. Both of these plates have same fixed bottom plate of 60 mm diameter but a dissimilar upper rotating plate of 40 mm diameter. The parallel plate has a flat upper rotating plate and is denoted by PP40. The cone/plate has a conical upper rotating plate with a cone angle of 4^{o} and is denoted by CP4/40.

In addition to the above-described measuring devices, Bohlin rheometer is equipped with a visual cell and normal force measurement device. The visual cell is a C25 device with transparent bob and cup to conduct flow visualization, light scattering and proppant transport studies. The normal force device is a cone and plate cell in which the lower plate is attached to a load measuring device. The normal cell has maximum axial load capability of 1000 gm and maximum torque capacity of 1000 gm-cm.

The Bohlin rheometer has a separate temperature bath for fluid characterization at different temperatures. This bath is capable of heating as well as cooling the fluid samples with circulating oil. The bath is electronically attached to the rheometer computer controls and is programmed for three temperature control modes: manual, constant and step. These modes provide very delicate control of the fluid temperature during the rheological characterization. In addition to the bath for controlling the temperature, the fluid environment is maintained with a thermal enclosure, which prevents evaporation of the fluid. The Bohlin rheometer is equipped with a special closed cell to measure the fluid rheology at very high temperatures and pressures. This cell is known as high pressure cell (HPC) and is capable of rheology measurement upto 284 ^{o}F temperature and 600 psi pressure.

4.6.3 Foam Flow Loop (Pipe Viscometer)

In addition to the rotational rheometers, FFCF has a pipe viscometer that consists of flow loops of different size pipes. This viscometer is designed to characterize several fluids that include liquids as well as foams under various pressure and temperature conditions. A schematic of equipment setup used to measure fluid viscosities with the flow loop is shown in Fig. 4.5.

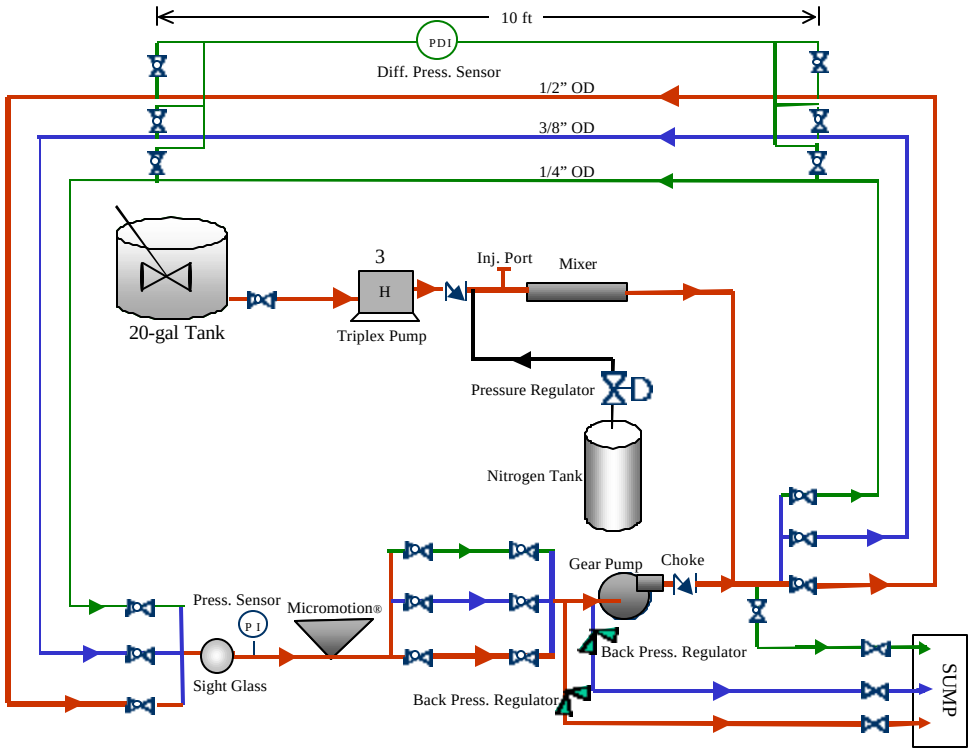

Fig. 4.5-Equipment Setup for Foam Rheology Measurements

The flow loop comprises of three pipes of nominal diameters 0.25, 0.375, and 0.5 inch. The loop draws fluid from a 20 gallon tank with the help of triplex and centrifugal pumps. These pumps are variable speed devices that can provide different fluid flow rates through the pipes. The flow rate is measured with a Micromotion mass flow meter, which also measures the fluid density and temperature. The Micromotion measured fluid temperature is fed to a temperature controller that regulates electric current supply to heating-tapes wrapped around the flow loop pipes. These tapes maintain fluid temperature, which is a very crucial parameter in the rheological characterization of the fluid. The Micromotion also measures the fluid density from which foam quality is calculated.

The fluid flow parameters provide nominal shear rates at the wall. The shear stress is calculated by measuring fluid pressure drop across various pipe diameters. The pressure drop is measured with a differential pressure sensor installed across 10 ft section of the pipes.

The flow loop is provided with a pressure transducer to measure fluid pressure, which is extremely important for characterization of the foam fluids. The fluid pressure is controlled with two backpressure regulators to maintain uniform pressure during the rheology study. The flow loop also contains a sight glass for visual inspection of the circulating fluid. The flow loop has additional provisions for introducing gaseous phase and crosslinker into the liquid stream. The experimental data gathered from the flow loop is transmitted with a wireless logger to a data acquisition system where the data are displayed and stored into electronics files.

Chapter 5 DATA ACQUISITION

5.1 Introduction

An effort is being made at the WCTC to simulate field conditions at the laboratory level. These conditions allow realistic characterization; the large-scale environment, however, make the experiments very expensive. Thus, in order to minimize costs, it is imperative that maximum information is acquired from a minimum number of tests. This requires that a very reliable data acquisition system be available at the WCTC. The system must satisfy bounded response time constraints to acquire real time data.

The data acquisition system is categorized as soft real time and hard real time system. The soft real time system means that system failure to meet response time constraints will degrade the performance of the data but will not destroy the experiment. An example of the soft system is graphical visualization of the data. The hard real time system, on the other hand, means that the system failure leads to complete failure of the data acquisition system and to void the experiment. Thus, the hard real system failure results in loss of money and in wastage of valuable time. The data acquisition system at the FFCF complies with the hard real time categorization. The system has the computational power to support analysis, logging, and display of full real time data.

The diverse operations performed at the facility require separate data acquisition systems for data logging, flow visualization studies and velocimetric measurements. The Data Acquisition and Control system constitutes the Vision System, the Laser Doppler Velocimeters (LDV), Pressure, Temperature and Flow Measurements.

These various systems are briefly described in the following sections. The description also includes discussion on the processing tools used for effective display of the acquired data.

5.2 Data Logger System

Initially, a dual architecture was used for logging experimental data. In this system, Masscomp was used to acquire data and IBM RISC was used to perform data reduction, logging, control and display. The data was collected on three IBM personal computers through different software packages. The data was then transferred through three RS 232 serial lines to an IBM RS/6000, which monitored each data through different software programs. The programs received data, recorded time, and wrote data to file or saved them on disks. This system performance, however, was unsatisfactory as three computers had different data acquisition rates making it impossible to synchronize the three sets of measurements.

The poor performance of the dual architecture provided a case to establish a new data acquisition system using Fluke Hydras. The new system improved the display and logging of the data. The Hydra system is tied to a personal computer reducing the cost of data acquisition.

The Hydra system consists of two high speed Flukes which are capable of monitoring individual test parameters. The Hydras have very high common mode

rejection and they are unaffected by ground loops or shorts that might occur in the HPS electrical system. The new system digitizes the signals close to its acquisition location. This allows much shorter signal lines and thereby, improves the signal to noise ratio on all experimental parameters.

The two Hydras provide a common time stamp on all data and thus allow very easy data matching and immediate data processing following the experiments. The Hydra system along with the personal computer provide better display of the data through various graphical and tabulation techniques. A detailed specification sheet of the Fluke Hydra system is given in Table 5.1.

The data acquisition system is housed in a user-friendly operating environment that can be readily integrated with spreadsheet programs. This allows fast and efficient processing of the data at the completion of an experiment.

Table 5.1- Fluke Hydra System Specifications

Channels	40 Analog inputs
Alarms	4 TTL
Digital Input/output	8 TTL
Telemetry	RS 232 at 19.2 kbaud; 8 data bits, no parity bit, one stop bit
Sample Rate	Up to 10 samples/second
Calibration	User controlled Mx +B User Controlled Gain and Offset
Dynamic Range	3 mV to 300 volts AC or DC 4-20 mAmp current loop

5.3 Vision System

With the improved vision system it is possible to monitor and quantify the proppant concentration during proppant transport and proppant flow back experiments in the HPS. In order to illustrate the proppant transport and proppant flow back procedure and measurements, a brief description of the vision system is essential at this stage.

The vision system is divided into two subsystems: the fiber optic system and the vision acquisition system. The fiber optic system is constructed of a 33 x 33 fiber matrix while the optic system is placed on the nine platens oriented toward the HPS outlet. Each platen contains 121 (11 x 11) fibers equally spaced (refer to Fig. 5.1).

The measurements can be performed at any of the 1089 points of the fiber optic system (Fig. 5.2). Precise measurement of the light intensity, which is present at each of the 1089 fibers, is not required for proppant monitoring. However, the measurement that detects the presence of sand is necessary.

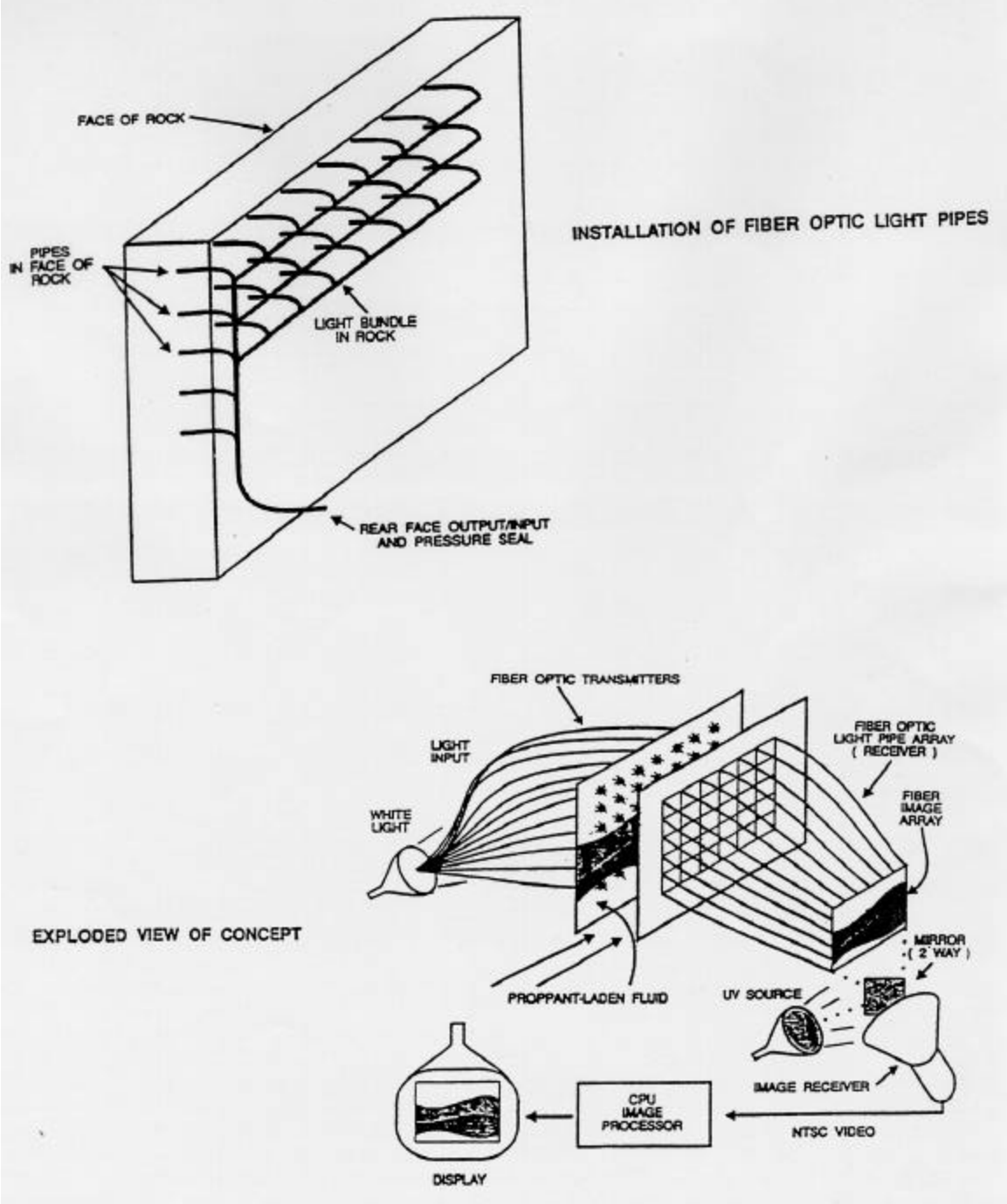

Fig. 5.1 The Vision System

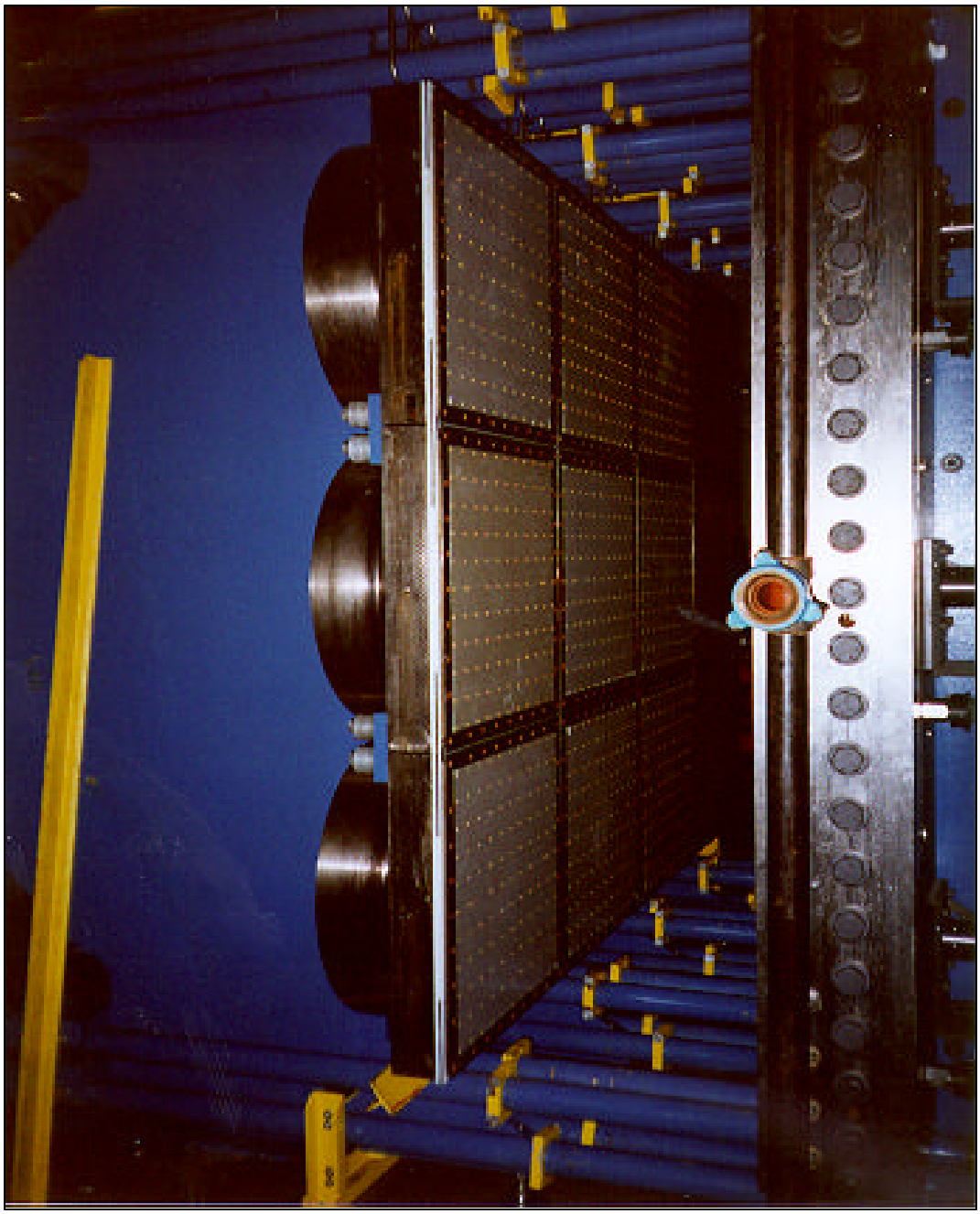

Fig. 5.2 Fiber Optic Outlets in the HPS

To accomplish the task of proppant monitoring, the raw videotape images acquired during a test are enhanced into fine images with the help of software developed within the facility.

The data acquisition system for the vision system comprises black and white charged coupled device (CCD) cameras, digital signal processing (DSP) frame grabber, enhanced display board (EDB), and frame accurate video recorders. These instruments

help to digitize, quantify, map, display, and store video data during experiments performed with the HPS. A schematic of the data acquisition system is shown in Fig. 5.3.

The slot image is acquired using nine cameras which output the images in National Television System Committee (NTSC) video signals at a rate of 30 frames per second. The video signals are driven by a nine channel gain controller device through cables to the data acquisition room. The individual image from the nine cameras is incorporated into a composite image signal using a video multiplexer, which generates 2.7 frames per second. The composite image is named as raw image and is simultaneously displayed on monitor and recorded on a Hi 8 mm video tape for future reference. An example of the raw image generated from the slot is shown in Fig. 5.4.

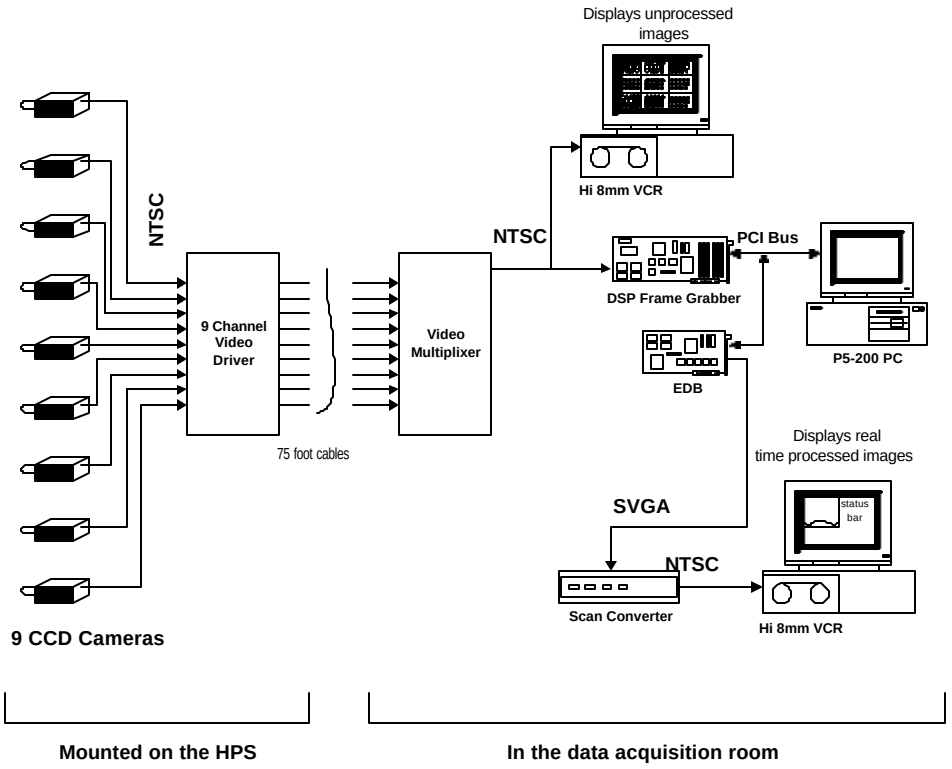

Fig. 5.3-A Schematic of Data Acquisition System for Vision System

The raw image is digitized by the DSP frame grabber and displayed by the EDB. The DSP allows the system to process one image as it grabs another, and the EDB displays the processed image in real time. Both the DSP and EDB boards are hosted in a personal computer on the PCI bus.

The digitized image is processed to obtain light intensities which are then converted to sand concentration using models developed at the FFCF. The real time processing of the image is performed with the help of a computer program written in C++ and TMS 32C40 assembly language. The program flowchart is enclosed in Fig. 5.5. The program generates base light intensity array, and processes and displays the fluid flow images in real time.

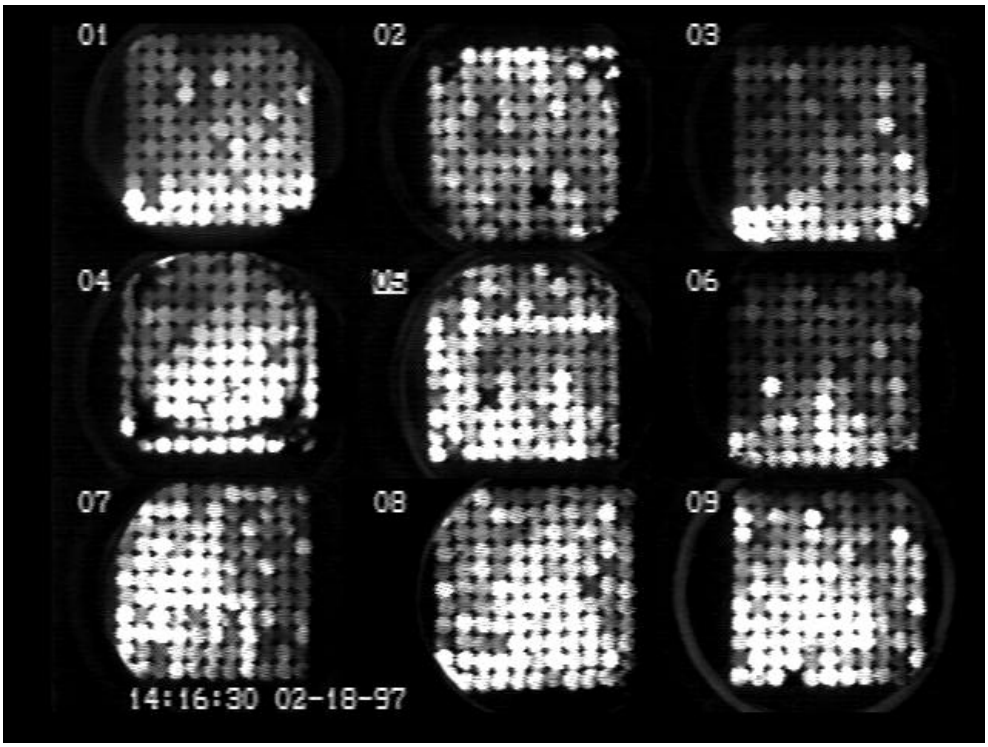

Fig. 5.4-Raw Image of Slot Acquired by the Vision System

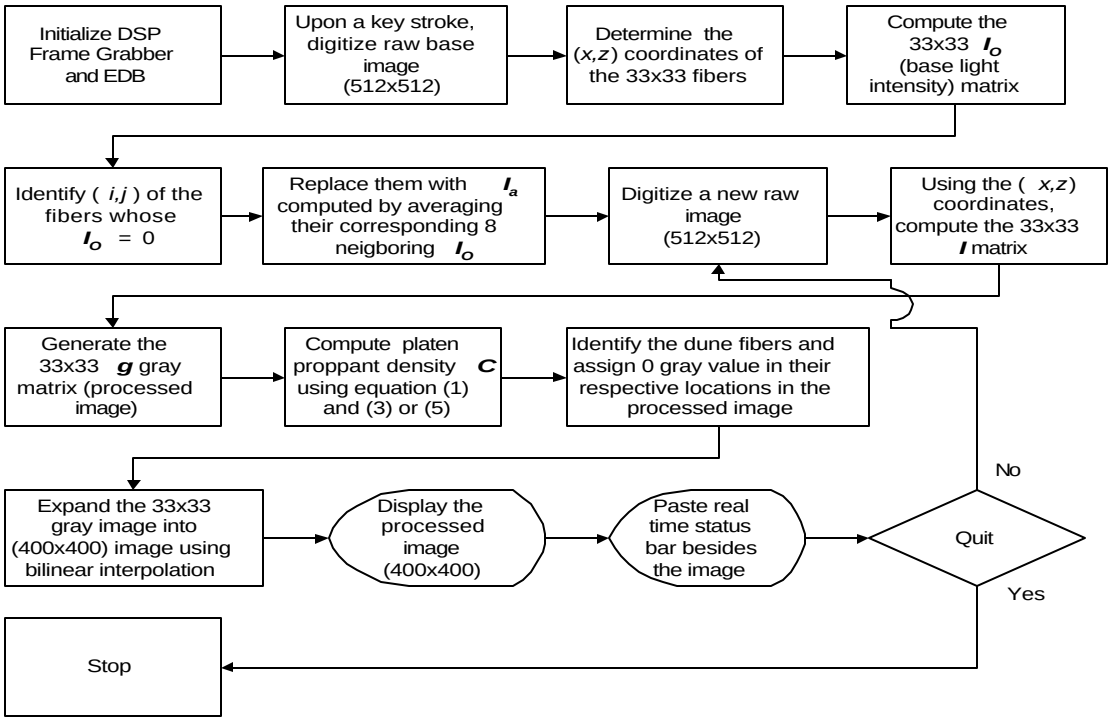

Fig. 5.5-Algorithm Flow Chart to Process Raw Image

The processed image is also available in NTSC format. It is displayed on a monitor and recorded on Hi 8 mm video tape. The processed image is shown in Fig. 5.6.

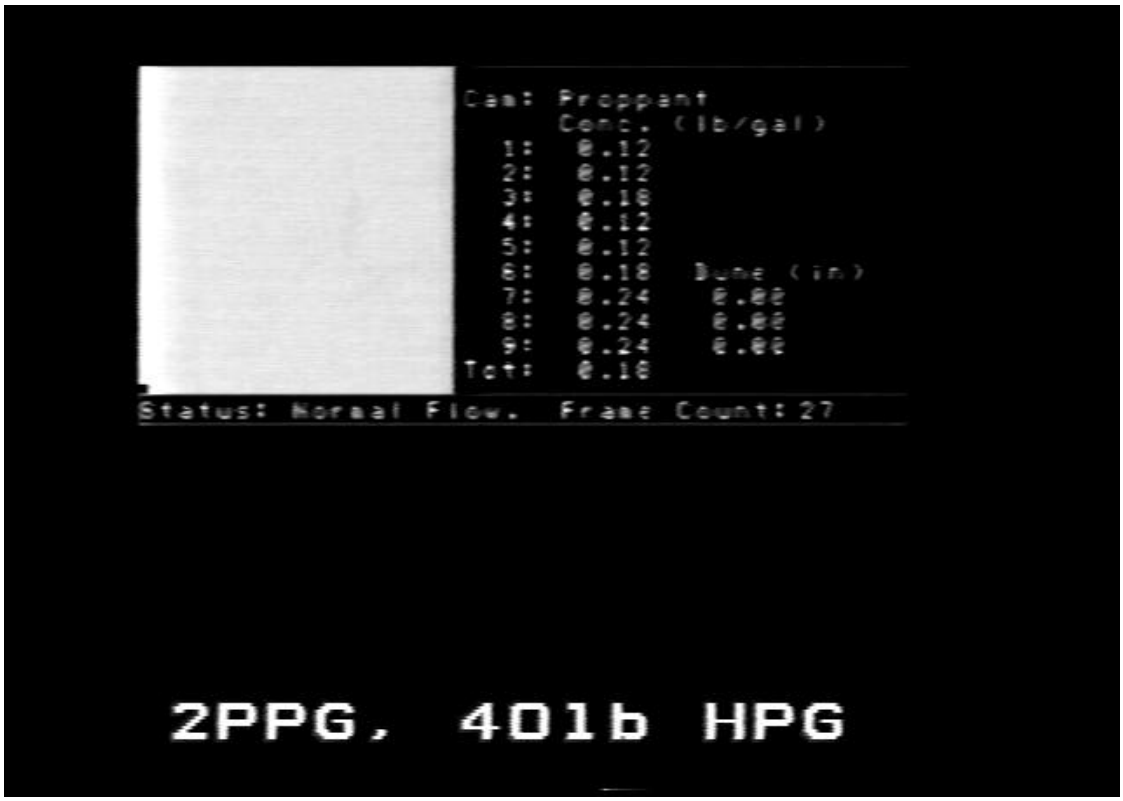

Fig. 5.6-Processed Image of Fig. 5.2

5.4 Laser Doppler Velocimetry (LDV) System

The data acquisition system for the LDV system were evaluated and reevaluated to improve its accuracy and effectiveness in the velocimetric measurements. Based on these evaluations, a number of improvements were made in the LDV system. These changes included installation of a new software called Flow Information Display (FIND^{TM}), updating the methodology used to locate fracture wall at the beginning of the test, and utilization of sensitive filtering methods to decrease the signal to noise ratio.

FIND provides detailed data analysis and storage, automated probe traversing and display of results. The new methodology comprises of locating the far-wall with the LDV and then, systematically traversing the gap width to obtain a velocity profile. The far-wall is located by monitoring and observing noise in the signal with an oscilloscope.

The velocity data is acquired with the probe in a horizontal position to measure horizontal velocity. The probe is then rotated to an angle of 45^{o} above and below the horizontal position. The velocity measured in the rotated position is resolved into vertical and horizontal components. The horizontal component is called indirect measurements. It is compared with the velocity measured directly with the probe in the horizontal

position. This comparison provides a good check on the velocities measured with the LDV system.

A comparison between the velocities measured directly and indirectly is shown in Fig. 5.7 for a HPG polymer solution flowing through a 0.25" slot gap. The figure shows excellent agreement between the two sets of measurements.

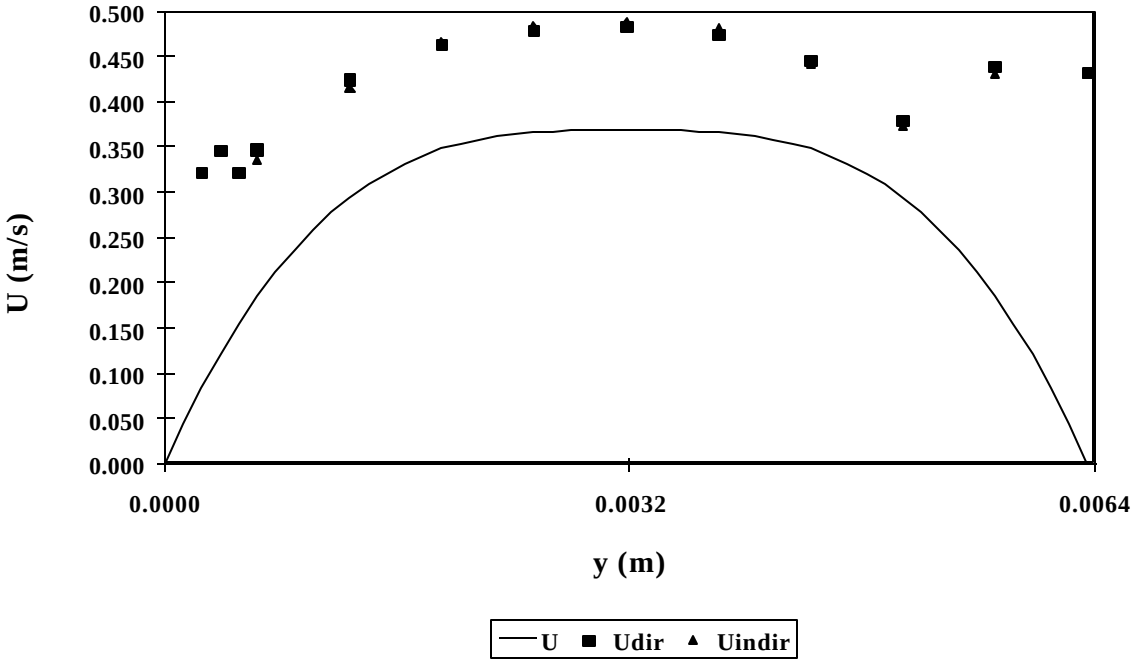

Fig. 5.7-Velocity Profile for Flow of Linear HPG solution through a Gap of 0.25"

Chapter 6 LABORATORY RHEOLOGY INSTRUMENTS

6.1 Introduction

Rheological characterization of a fluid is extremely important to understand their behavior during drilling and completion of a well. With the known characteristics, the fluid can be optimized and designed before their use in the reservoir.

The fluid characterization is best performed with viscometers, which are simple devices that provide the flexibility to study the fluid behavior under several shear rates, flow geometries, and pressure-temperature conditions. When the viscometric measurements are combined with a field-representative sample preparation and loading method, the fluid characterization resembles the real reservoir environment.

FFCF has several rheological instruments, which include rotational, pipe and slot viscometers. These instruments are described in the following section. The description provides the instruments dimensions, operation principles and capabilities. It also discusses the modifications made in these instruments to enhance their capabilities for specific fluid applications. Some instruments were bought from the manufacturers and modified; others were designed and developed at the FFCF itself.

6.2 Model 35 Fann Viscometer

Fann viscometer is a rotational type instrument that works as a controlled strain device. It uses concentric cylinder geometry to measure the fluid properties.

The viscometer comprises of an outer cylinder, known as rotor, and an inner cylinder, called a bob. The annular space between the two cylinders contains the fluid to be characterized. The rotor is driven at a predetermined rotational rate in the fluid sample; the cylinder rotation induces movement in the fluid, and exerts viscous drag on the inner bob. The drag on the bob is balanced by a helically wound spring and is read as deflection on a calibrated dial available on the viscometer. From the rotational rate and dial reading, shear rate and shear stress are calculated. These values are, then, used to determine apparent viscosity of the fluid.

The rotor has an inner radius of 1.8415 cm and bob has an outer radius of 1.7245 cm. The bob has a length of 3.8 cm and it provides a very large surface area for accurate measurements of fluid drag. The sensitivity of the instrument is further improved by using two separate springs No. 1 and $1/5^{th}$. The number $1/5^{th}$ spring is very useful for measuring viscosities of thin fluids.

The fluid viscosities are calculated at several shear rates by varying the rotational rates of the rotor in the fluid. With these viscosities, rheograms are developed for the test fluids. The measured data are fit with appropriate rheological model to describe fluid behavior and to predict the fluid viscosities at the shear rates of interest to the industry.

The Fann viscometer is a very rugged and robust instrument. It is very helpful to provide a quick check on the fluid behavior and to compare the fluid viscosities with other measuring devices. The Fann viscometer is frequently calibrated and serviced to maintain its accuracy to measure the fluid viscosities.

6.3 Nordman Rheometer

Like the Fann viscometer, Nordman rheometer is also a controlled rate instrument with concentric cylinder geometry. Here also, the shear rate is applied on the cup through the rotor motion and the viscous drag is measured on the bob. Unlike Fann, Nordman viscometer has a closed rotating sleeve as the sample cup. Nordman rheometer is the most widely used instrument to characterize crosslinked fracturing fluids.

The Nordman rheometer has more features than those in Fann 35 viscometer. The rheometer is completely computerized and is capable of measuring fluid properties upto 1000 psig pressure and 500^{o}F temperature. The instrument can heat the fluid sample with an external oil bath while simultaneously measuring the fluid viscosities. The instrument also has provision to apply pressure on the fluid sample and to offset any increase in fluid vapor pressure at higher temperatures. A photograph of the Nordman rheometer is shown in Figure 6.1.

Figure 6.1- Nordman Rheometer

The Nordman rheometer is capable of measuring the fluid viscosities with different size bobs. The rheometer, available at the FFCF, has three bobs: B1, B2x and B5x. The B1 bob has an outer radius of 1.7245 cm and is 7.62 cm high, the B2x has an outer radius of 1.2308 cm and is 8.529 cm high, and the B5x has an outer radius of 1.5987 cm and is 9.19 cm high. The rotating cup is similar for the three bobs, and is of 1.8415 cm inner radius.

The Nordman rheometer is programmed to perform several types of test. The program allows to perform standard as well as specific tests like API, custom, one-rate and calibration tests. The API and one rate tests are designed from API recommended standard procedures to evaluate fluid viscosities, whereas, the custom test is designed by the FFCF laboratory requirements. The calibration test is performed to evaluate the performance of the viscometer with the help of standard oils; in this test, the oil viscosity is programmed into the Nordman software, and the instrument adjusts the rheometer parameters to the calibration oil specifications.

The fluid samples are loaded into the Nordman rheometer by pouring the sample into the measuring cup. In addition to the manual loading, the sample can be transferred into the cup using a snap-on coupling assembly available at the bottom of the cup. This arrangement permits simultaneous loading and shearing of the fluid. The bottom-loading provision is very helpful for the characterization of time-dependent drilling and fracturing fluids. Because of the significance of this method, a dynamic loading system was designed to enhance the rheometer capability for online measurements of the fluid viscosities. A schematic of the designed experimental set up is shown in Figure 6.2.

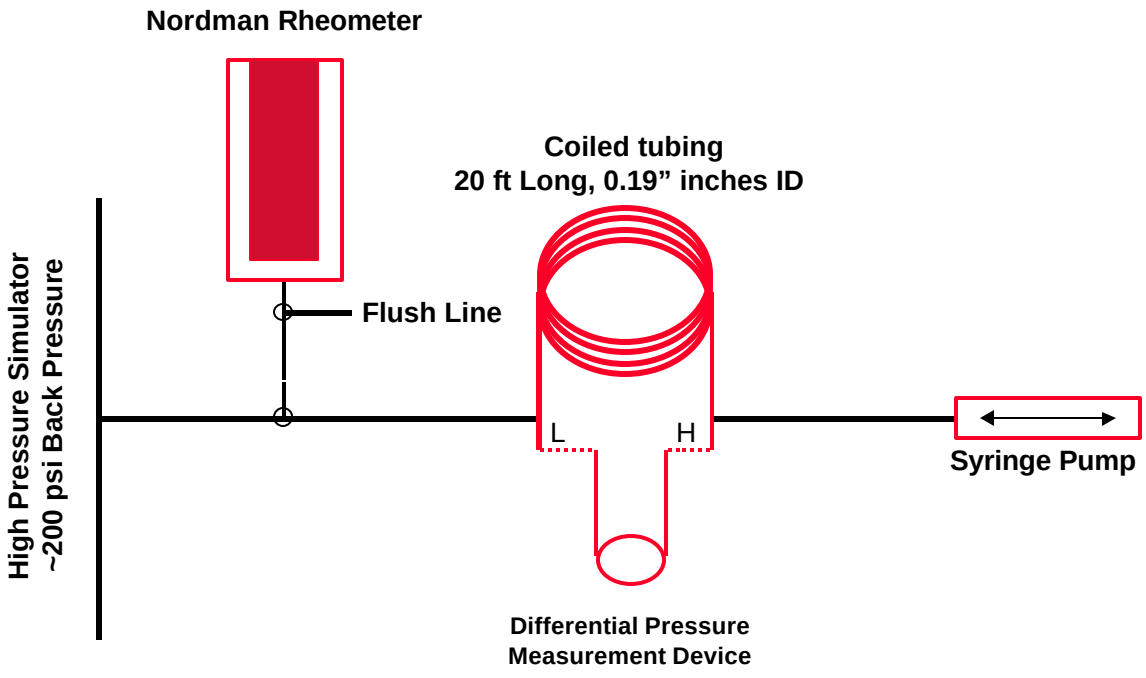

Figure 6.2- Dynamic Loading System Designed for the Nordman Rheometer

Figure 6.2 shows that the dynamic loading system as attached to the High Pressure Simulator (HPS), from where the fluid sample is drawn. A three-way valve is used to isolate the loading system from the HPS. The fluid is withdrawn from the HPS into a 20 ft long coiled tubing. The amount of fluid drawn into the coiled tubing depends on the volumetric capacity of the bob-cup geometry used in the measurement. Once a sufficient volume of the sample is drawn into the tubing, the three-way valve is adjusted to divert the fluid from the tubing to the rheometer. The fluid flow rate is carefully controlled so that the sample is subjected to identical shear rate in HPS, coiled tubing and the rheometer. The dynamic loading system has been successfully used to characterize and to generate reproducible rheology data for crosslinked fracturing fluids.

6.4 Bohlin Rheometer

Bohlin rheometer is a unique instrument available at the FFCF. This rheometer is different from the Fann and Nordman viscometers. Unlike the two controlled rate viscometers, Bohlin rheometer is a controlled stress instrument in which a shear stress is applied and resultant shear rate is measured. The Bohlin rheometer is capable of utilizing different measuring geometries and measuring viscosity as well as viscoelastic characteristics of the fluid, whereas the two viscometers only use concentric cylinder geometry and measure fluid viscosity only. A photograph of the Bohlin rheometer is shown in Figure 6.3.

Figure 6.3- Bohlin Rheometer

The Bohlin rheometer works with a unique drag cup motor that applies torque to the fluid sample. This torque is transmitted through the measurement geometry to the fluid sample with the help of a frictionless air bearing. The applied torque induces shearing into the sample and the resultant displacement is measured with a highly sensitive optical angular position transducer. The state-of-the-art instrumentation on the Bohlin rheometer makes it a very accurate and versatile equipment.

The Bohlin rheometer is equipped with three measuring geometries: concentric cylinder, parallel plate, and cone and plate. The concentric cylinders are available in two bob diameters, 14 and 25 mm, and are respectively denoted as C14 and C25. The bobs are used in cups so that cup to bob radius ratios is similar at 1.1. The other two measuring devices, parallel plate and cone and plate, are different from the concentric cylinders because of their different geometric configurations. Both of these plates have same fixed bottom plate of 60 mm diameter but a dissimilar upper rotating plate of 40 mm diameter. The parallel plate has a flat upper rotating plate and is denoted by PP40. The cone/plate has a conical upper rotating plate with a cone angle of 4^o and is denoted by CP4/40.

In addition to the above-described measuring devices, Bohlin rheometer is equipped with a visual cell and normal force measurement device. The visual cell is a C25 device with transparent bob and cup to conduct flow visualization, light scattering and proppant transport studies. The normal force device is a cone and plate cell in which the lower plate is attached to a load measuring device. The normal cell has maximum axial load capability of 1000 gm and maximum torque capacity of 1000 gm-cm.

The Bohlin rheometer has a separate temperature bath for fluid characterization at different temperatures. This bath is capable of heating as well as cooling the fluid samples with circulating oil. The bath is electronically attached to the rheometer computer controls and is programmed for three temperature control modes: manual, constant and step. These modes provide very delicate control of the fluid temperature during the rheological characterization. In addition to the bath for controlling the temperature, the fluid environment is maintained with a thermal enclosure, which prevents evaporation of the fluid.

The Bohlin rheometer is equipped with a special closed cell to measure the fluid rheology at very high temperatures and pressures. This cell is known as high pressure cell (HPC) and is capable of rheology measurement upto 284 ^{o}F temperature and 600 psi pressure.

The HPC is made up of two receptacles to fit the rheometer socket, hold fluid sample and apply torque on the fluid. The HPC is also a concentric cylinder geometry in which the torque applied by the motor is magnetically transferred from an outer coupling to an inner rotor bob. The bob, then, apply the desired shear on the fluid. The HPC can be filled by either pouring the fluid into the open cell or by injecting the sample through a side valve in the closed cell. A schematic of the HPC is shown in Figure 6.4.

The HPC was supplied separately as a specially designed geometry. It had some inherent operational drawbacks as it had no provision to directly measure fluid temperature; a thermocouple installed in the oil bath is used to monitor and maintain the test fluid temperature. This indirect measurement caused the rheometer to make rheology measurements on the fluid sample which was not representative of the test conditions. The second shortcoming of the HPC is due to manual loading of the fluid sample. While

the fluid is transferred into the HPC, a quiescent period is introduced into the sample when there is no shear on the fluid. This no-flow period alters the characteristics of the time-dependent fluid sample and provides inaccurate viscosity measurements. These drawbacks were overcome by making innovative modifications to the HPC at the FFCF. A schematic of the modified cell is shown in Figure 6.5. In the new setup, the inlet valve of the HPC was removed and a new assembly was installed. The new inlet manifold comprises of an inlet valve, a pressure relief valve and a high-pressure connector. The connector couples the present metric threads of the HPC with a nominal pipe thread (NPT) system. The pressure relief valve provides a primary safety mechanism on the new set-up, and it complies with the API recommended code of practice for the safety of a high-pressure vessel. The inlet valve controls the flow of fluid sample into the measuring cup and provides a direct connection to either a shear history simulator or a fluid-mixing device.

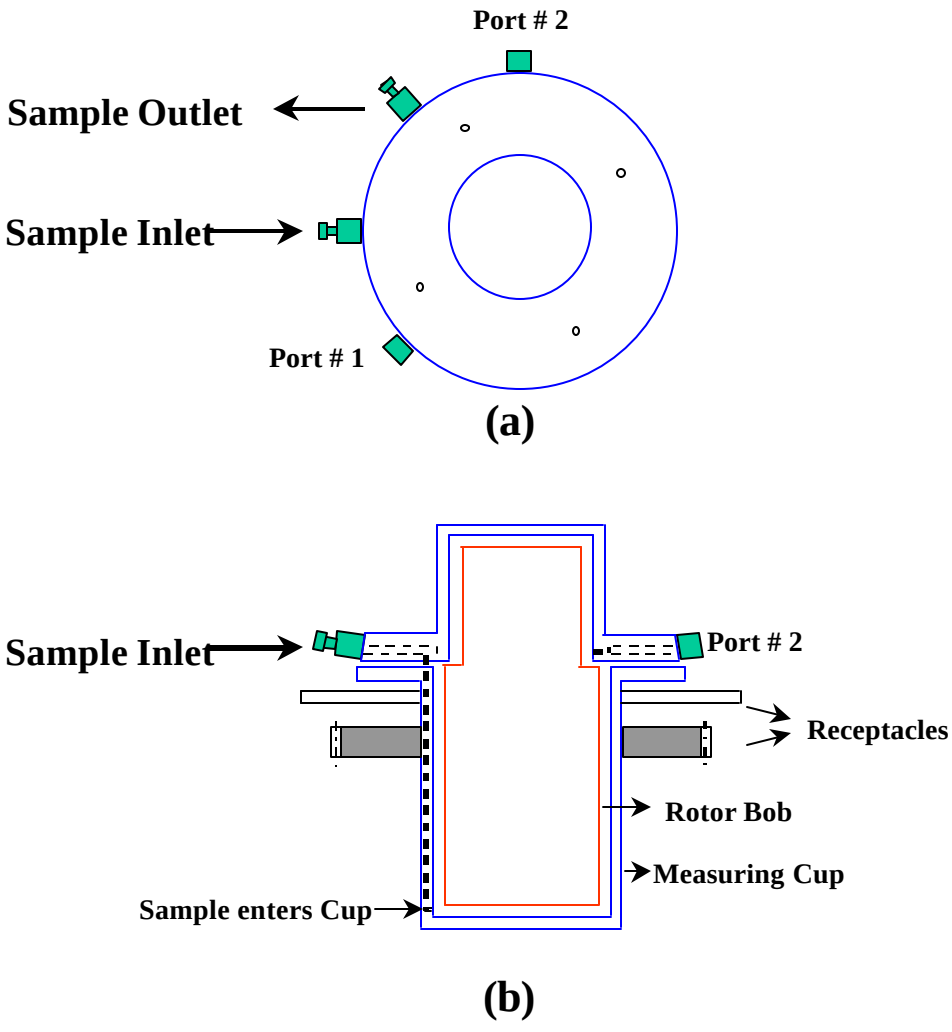

Figure 6.4-Schematic of High Pressure Cell

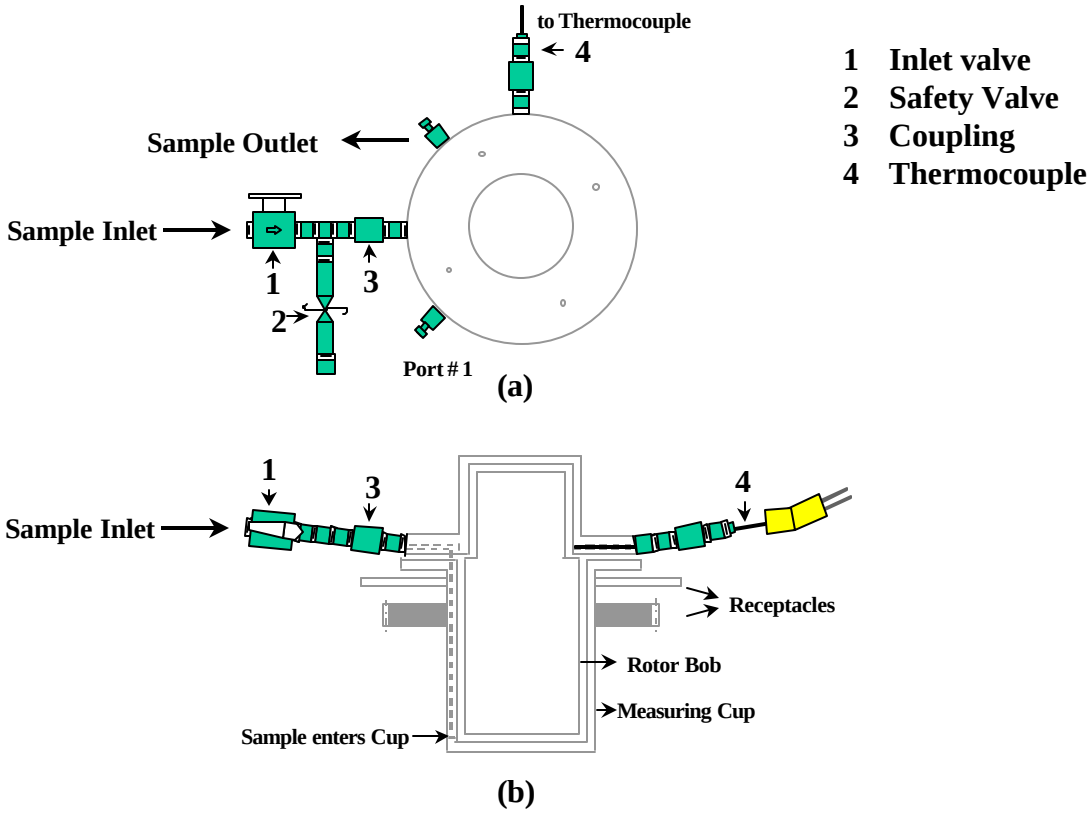

Figure 6.5-Modified HPC with Dynamic Sample Loading Capability

The new setup also avoids the problems associated with the fluid temperature. Now, the temperature can be measured with an external thermocouple installed in a port of the HPC. The thermocouple tip goes all the way to the fluid sample and monitors actual fluid temperature during the rheology measurements. The new inlet valve setup, thermocouple and the HPC were hydraulically tested to an operating pressure of 400 psig at ambient temperature.

The new setup provides a unique dynamic loading capability to the HPC. It maintains a fluid continuum for the rheological characterization of the fracturing fluids. This setup always maintains shearing conditions on a crosslinked fluid and thus, it eliminates any quiescent period prior to the viscometric measurements, and allows more accurate fluid characterization. Moreover, the new setup allows fluid circulation through the HPC; this ensures that sufficient quantity of fluid is sampled in the viscometer without measuring the quantity. Hence, the new setup can also be used as an online device to monitor fluid properties while performing an actual hydraulic fracturing treatment.

6.5 Foam Flow Loop

In addition to the rotational rheometers, FFCF has a pipe viscometer that consists of flow loops of different size pipes. This viscometer is designed to characterize several fluids

that include liquids as well as foams under various pressure and temperature conditions. A photograph of the foam flow loop is shown in Figure 6.6, and a schematic of equipment setup used to measure fluid viscosities with the flow loop is shown in Figure 6.7.

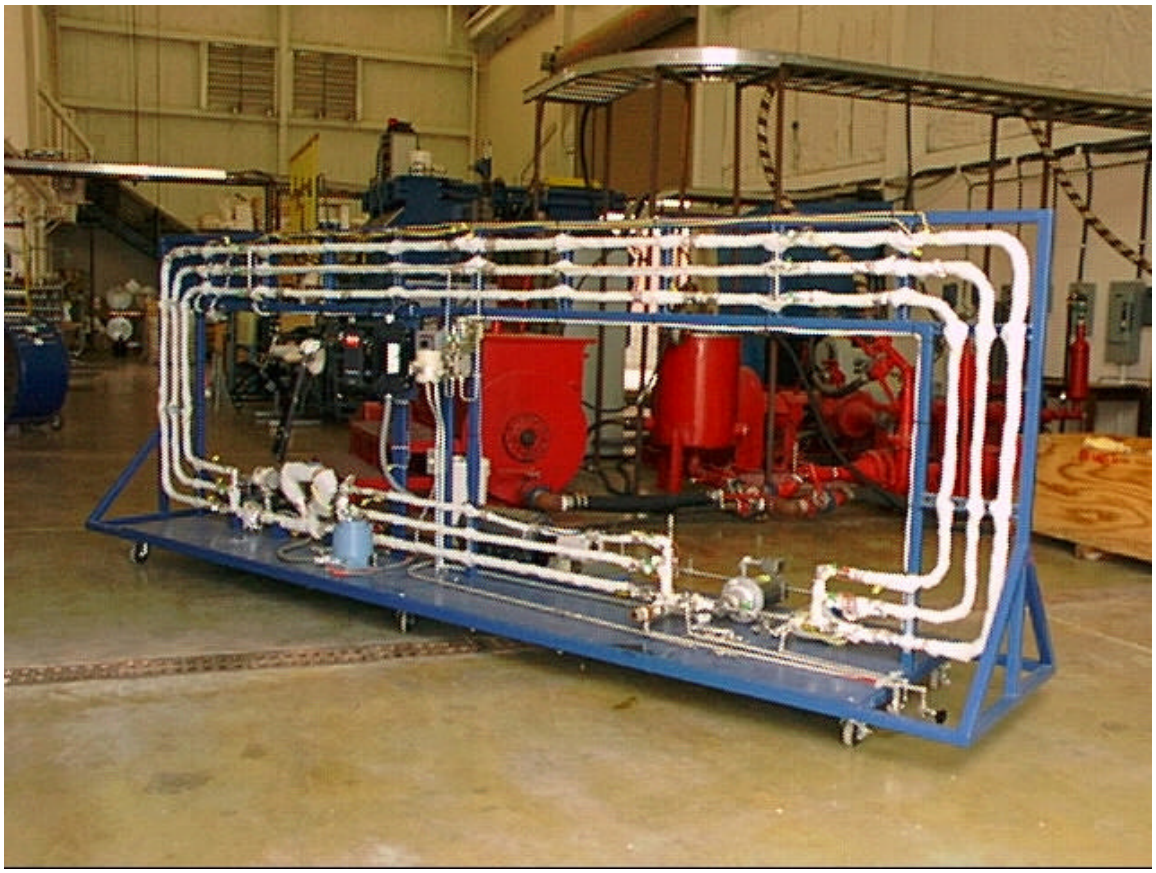

Figure 6.6-Foam Flow Loop

The flow loop comprises of three pipes of nominal diameters 0.25, 0.375, and 0.5 inch. The loop draws fluid from a 20 gallon tank with the help of triplex and centrifugal pumps. These pumps are variable speed devices that can provide different fluid flow rates through the pipes. The flow rate is measured with a Micromotion mass flow meter, which also measures the fluid density and temperature. The Micromotion measured fluid temperature is fed to a temperature controller that regulates electric current supply to heating-tapes wrapped around the flow loop pipes. These tapes maintain fluid temperature, which is a very crucial parameter in the rheological characterization of the fluid. The Micromotion also measures the fluid density from which foam quality is calculated.

The fluid flow parameters provide nominal shear rates at the wall. The shear stress is calculated by measuring fluid pressure drop across various pipe diameters. The pressure drop is measured with a differential pressure sensor installed across 10 ft section of the pipes.

The flow loop is provided with a pressure transducer to measure fluid pressure, which is extremely important for characterization of the foam fluids. The fluid pressure is controlled with two backpressure regulators to maintain uniform pressure during the rheology study. The flow loop also contains a sight glass for visual inspection of the circulating fluid. The flow loop has additional provisions for introducing gaseous phase and crosslinkers into the liquid stream.

The experimental data gathered from the flow loop is transmitted with a wireless logger to a data acquisition system where the data are displayed and stored into electronic files.

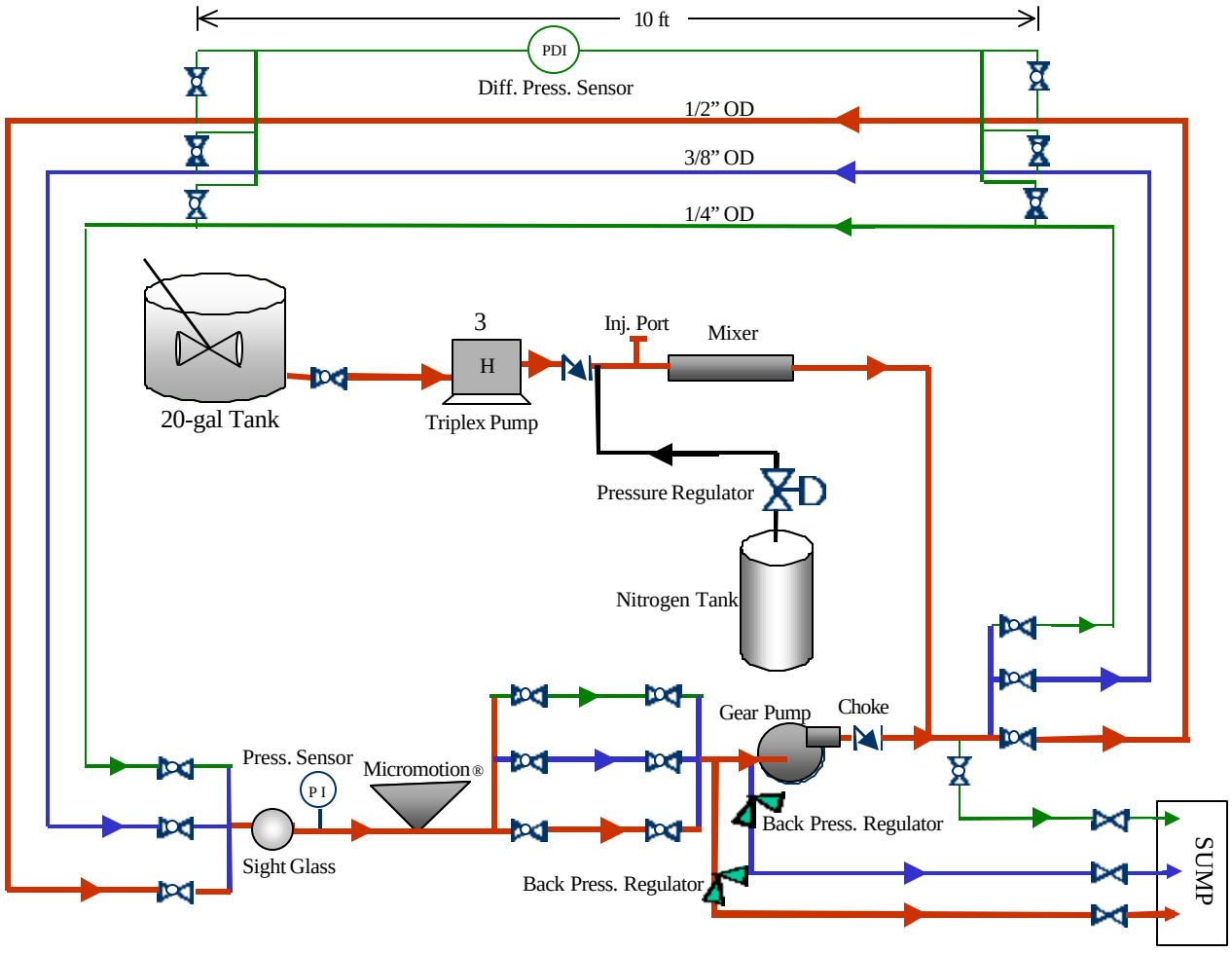

Figure 6.7-Equipment Setup for Foam Rheology Measurements

6.6 Plexiglass Parallel Plate Slot

As a fracture is represented by parallel plate, slot provides a better geometry to characterize fracturing fluids than either pipe or rotational viscometer. Therefore, a

mobile plexiglass parallel plate slot is available at the FFCF to measure fluid viscosity. The slot is 1 ft high and 4 ft long and is set for single gap width of 0.25 inch. The slot contains two ports in the inlet and outlet section to simulate perforations. The slot is made from plexiglass sheets to make visual observations during the rheological characterization.

In addition to the viscosity measurements, the slot has been used to capture images and observe particle movement in a fracture. The slot has also been used to calibrate Laser Doppler Velocimetry, cameras and vision system installed on the High Pressure Simulator. The slot has been used to determine length where entrance effects are significant in parallel plate geometry, and to study jet entry effects and penetration lengths where turbulent effects cease and uniform flow begin. These studies were very helpful to design the HPS as no data were available for the fluid flow through parallel plate device.

Chapter 7 RESEARCH RESULTS AND IMPLICATIONS

7.1 Introduction

During the lifetime of the FFCF project, the research efforts were focused on eight different aspects of the hydraulic fracturing stimulation. These research areas included proppant transport, fluid rheology, heat transfer, proppant flowback, foam fluid rheology, dynamic fluid loss, perforation pressure loss and tubular friction loss. These research areas are briefly described in the present chapter.

The chapter is subdivided in several sections. Each section contains the objectives of the individual research area, a brief introduction or significance of the study, the procedure used to perform experimental investigation, and the discussions of the major results obtained for the respective research. In addition to the above mentioned sections, two sections are included at the end to list the references and nomenclatures used in the chapter.

7.2 Correlating Proppant Transport with Fluid Rheology

Objective: The objective of this study is to better understand the correlation between a crosslinked gel rheology and its proppant transport capabilities, and to identify a rheological property to predict proppant transport through a fracture.

Introduction: The guar-based fracturing fluids are viscoelastic fluids and are characterized by both elastic and viscous components. Among these two parameters, fluid viscosity is more extensively evaluated and is being used to describe fracturing fluid behavior.[1-2] However, the viscosity does not correlate well with proppant transport in a fracture. Hannah and Harrington,[3] and Clark and Quadir[4] found that the experimentally observed settling velocities in an uncrosslinked or a crosslinked fluid are very different from the values calculated with viscosity-based correlations. Because of these differences, Power approached the proppant settling problem from a gel point criterion.[5] He correlated sand settling under static conditions with the fluid gel point, which is described with a maximum in the loss modulus of crosslinked fluids.[6,7] Similarly, Acharya,[8] de Kruijf et al.,[9] and Jin and Penney[10] studied fluid elasticity or storage modulus to understand particle suspension in fractures. de Kruijf et al. even proposed an elastic modulus criterion for predicting proppant transport in a fracture, which was supported only with sand settling studies carried out in static fluid conditions. None of these studies confirmed its results under slurry flow conditions.[5-10] Because fluid viscosity does not describe proppant settling, and fluid elasticity has not been confirmed with large scale testing, there is a great need to better correlate proppant transport capabilities with crosslinked guar gel rheology.

Procedure: A guar concentration of 35 lb/Mgal was used to understand the correlation between the proppant transport and fluid rheology. This concentration was selected because of its wide use in the fracturing treatments. The guar solution pH was adjusted

to 9, 10, and 11 respectively with sodium hydroxide and muriatic acid. These pH-adjusted solutions were then crosslinked at different crosslinker quantities of a borate-crosslinking solution. The crosslinker concentration was varied from nil to values where the borate-crosslinked gels exhibit phase separation. The formulated fluids were the analyzed in the laboratory for their viscoelastic properties and for their sand suspension capacities. From the laboratory characterization results, a crosslinker concentration was selected at each pH to prepare borate-crosslinked guar gel to further evaluate it for its proppant transport capabilities using two large size slot models, which simulate flow of fluids through fracture. A schematic of the large scale testing is shown in Figure 7.2.1.

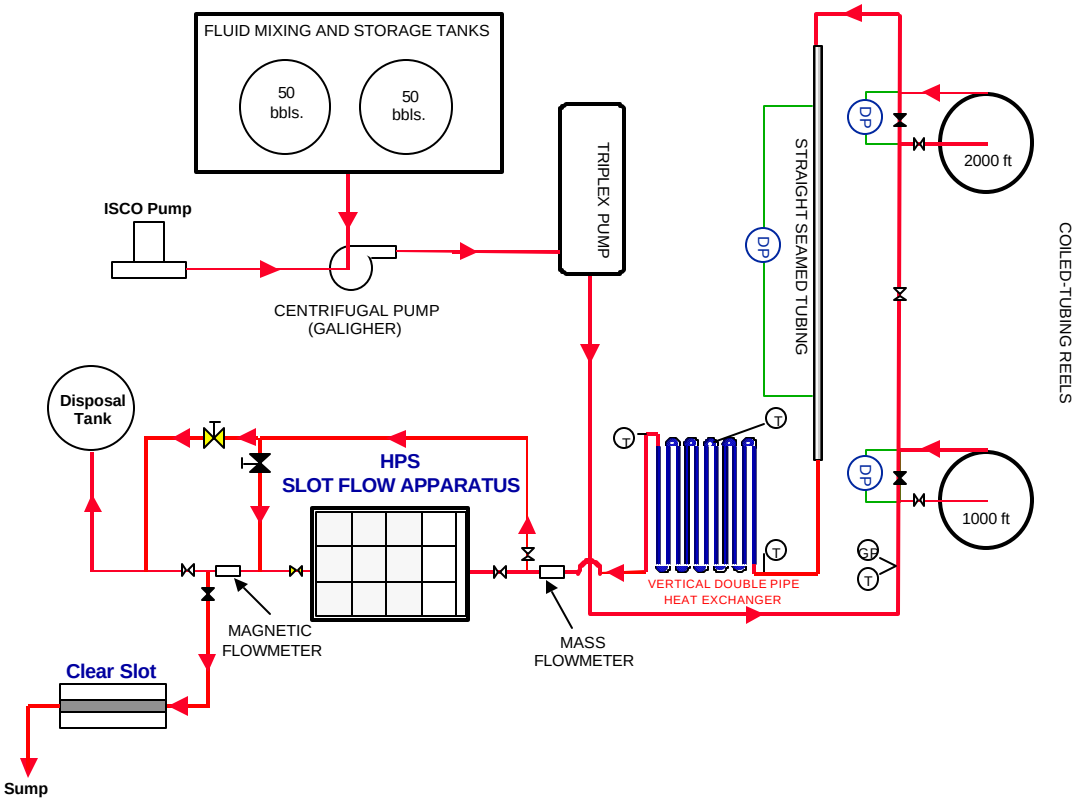

Figure 7.2.1¾ A Schematic of the Equipment Set-Up for Large Scale Testing

Results:

Borate-Crosslinked 35 lb/Mgal Guar pH 9

First the pH of the guar solution was adjusted to 9. The solution was then crosslinked with crosslinker quantities from 0 to 15 lb/Mgal.

The viscoelastic data of the borate-crosslinked guar gel at pH 9 is shown in Fig. 7.2.2. The figure shows an increase in elastic and viscous moduli with an increase in the crosslinker concentrations. This is because with an increase in the crosslinker concentration, the borate ions concentration increases, which increases the number of crosslinked sites formed in the polymer. As a result, higher *G'* and *G"* values are observed in the gels prepared at higher crosslinker concentrations.

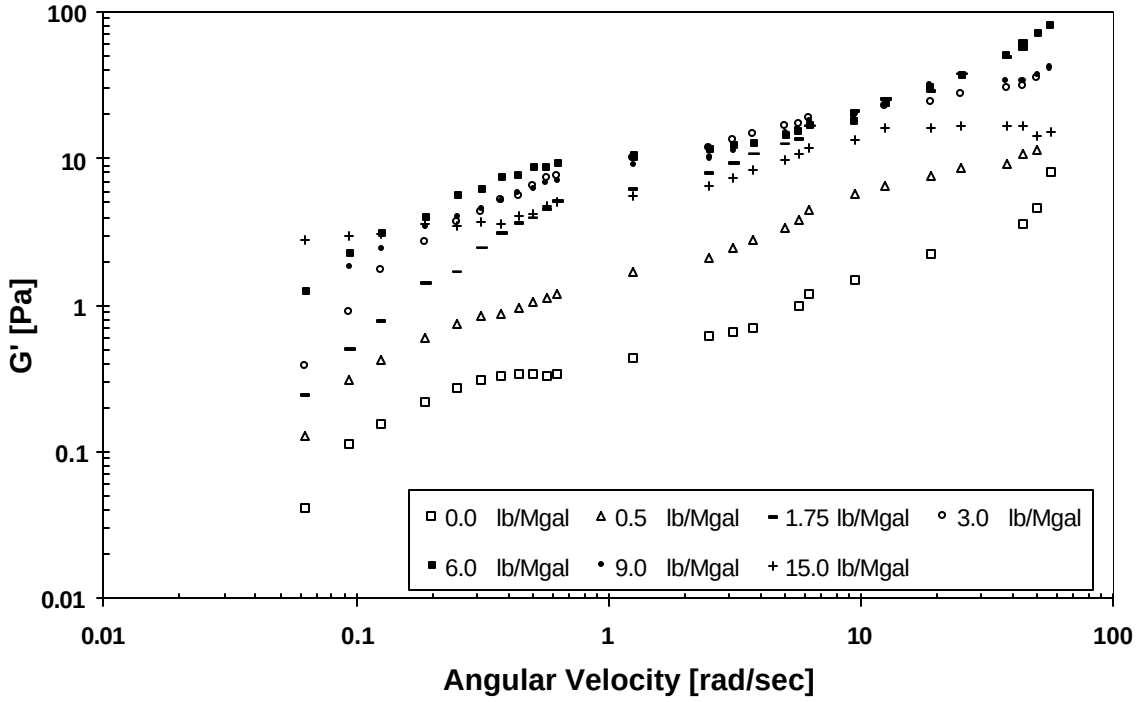

(a) Elastic Modulus Curve

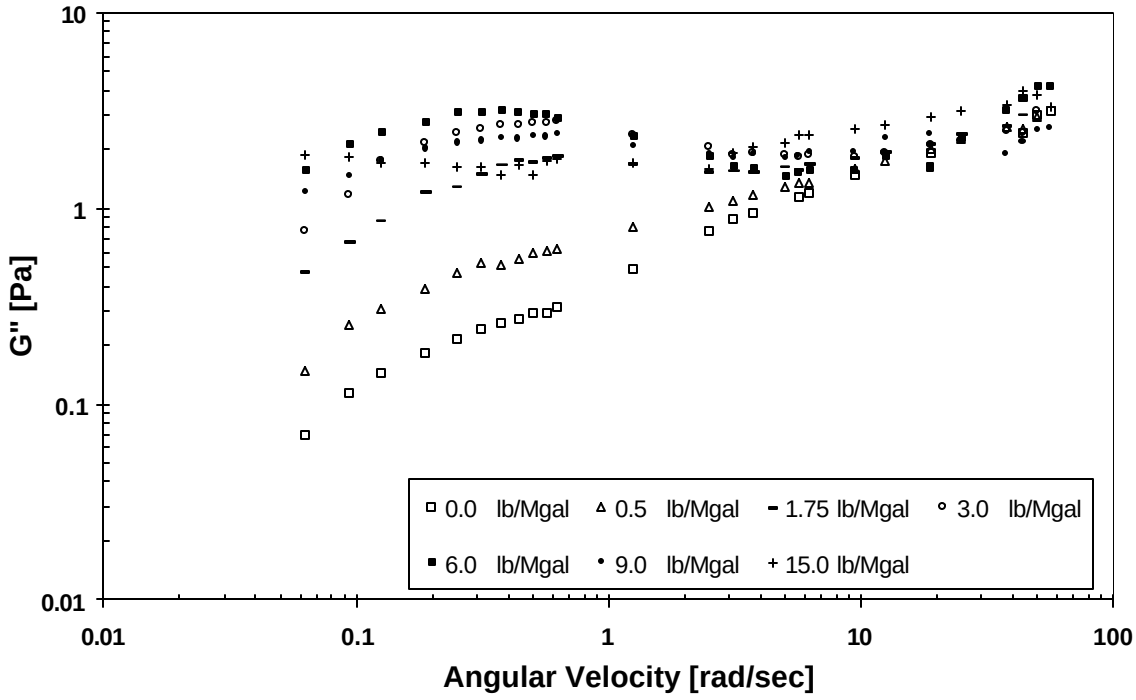

(b) Viscous Modulus Curve

Figure 7.2.2-Linear Viscoelastic Properties of Borate-Crosslinked 35 lb/Mgal Guar pH 9.0, 75 ^{o}F, prepared at different Crosslinker Concentrations

Figure 7.2.2 shows that at very low crosslinker concentrations, *G"* increases with an increase in frequency. However at and beyond 1.75 lb/Mgal crosslinker concentration, *G"* increases at low frequencies and then decreases at higher frequencies, thereby exhibiting a maximum. This maximum in the loss modulus is described by Power et al.[5] as an indication of gel point in the borate-crosslinked guar. Power used this gel point criterion to describe the proppant carrying capability of the crosslinked guar.[6] He established the relationship between the gel point and the suspension characteristics using a settling velocity criterion described by de Kruijf et al.,[9] who proposed that for settling velocities less than 5 cm/min, proppant transport is acceptable in a crosslinked fluid and for values less than 0.5 cm/min, the transport is perfect.

Settling velocities were measured under similar conditions as that used by de Kruijf et al.[9] and are shown in Fig. 7.2.3. The figure shows a decrease in settling velocities with an increase in the crosslinker concentration. It also shows that the suspension settling velocity increases as the interface moves down from the 1000 ml. mark (see inset Fig. 7.2.3), attains a maximum value in the cylinder middle, and then decreases as the interface settles into a bed height which corresponds to the sand volume in the cylinder. The initial increase in velocity is due to an increase in the sand concentration when the sand weight is redistributed in a smaller volume of the crosslinked gel. This higher sand concentration reduces the suspension capability of the gel; hence the settling velocity increases. As sand continues to settle in the cylinder, the suspension capability of the gel is influenced by another parameter, diffusion of gel molecules from the interstices of the sand particles. Since the diffusion of polymer molecules is a slower process, the sand particles settle slowly and the velocity decreases. Therefore, an increase and a decrease in the settling velocities are observed in the glass cylinder.

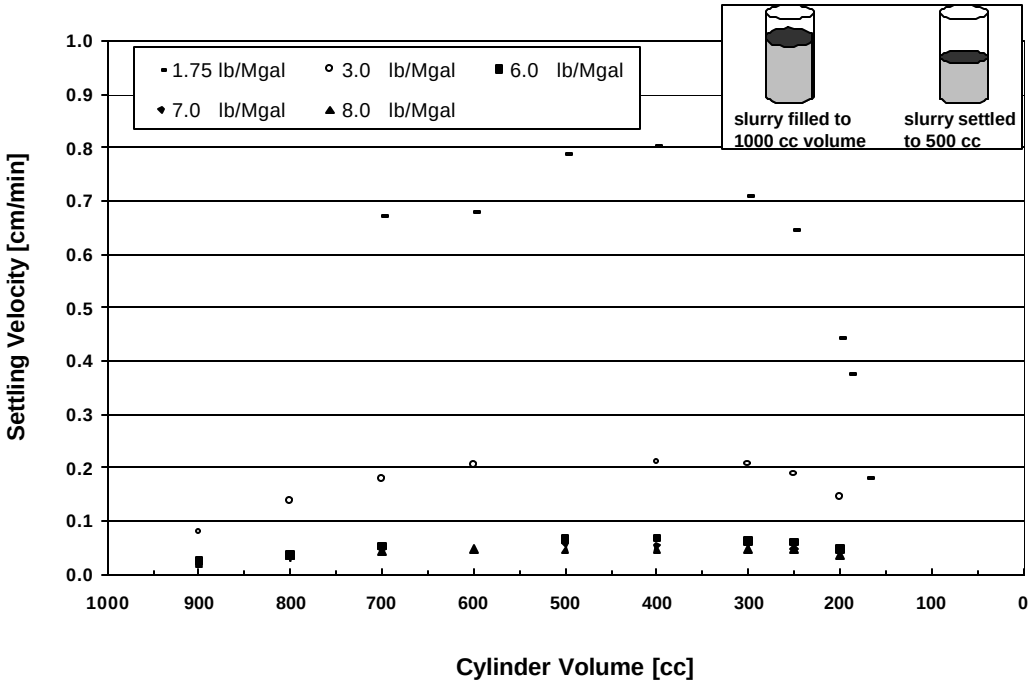

Figure 7.2.3-Settling of 2 ppg Slurry in Borate-Crosslinked 35 lb/Mgal Guar pH 9.0, 75°F prepared at different Crosslinker Concentrations

Figure 7.2.3 shows that the suspension settling velocity in the borate crosslinked gel prepared with 1.75 lb/Mgal is in the range of values described by de Kruijf et al.[9] to be acceptable for proppant transport in a fracture. Furthermore, this concentration satisfies the gel point criteria of Power et al.,[5] as it has a maximum in the loss modulus curve of Figure 7.2.2. Thus, the borate-crosslinked guar pH 9 prepared with 1.75 lb/Mgal crosslinker concentration satisfies the Power[6] and de Kruijf et al.[9] criteria and should exhibit acceptable proppant transport in a fracture. Hence, this gel was further evaluated in the slot models for its sand transport behavior.

The sand distribution in the HPS is shown in Fig. 7.2.4 when a 2 ppg slurry in the borate-crosslinked guar prepared with 1.75 lb/Mgal crosslinker is pumped through the slot model. The figure shows the image as a 33 by 33 matrix which corresponds to the number of fibers placed along the length and height of the HPS. The sand concentration is described as a combined image captured by all fibers. Figure 7.2.4 describes only two frames of the captured image, which are obtained after 5 and 20 min. of slurry flow through the HPS.

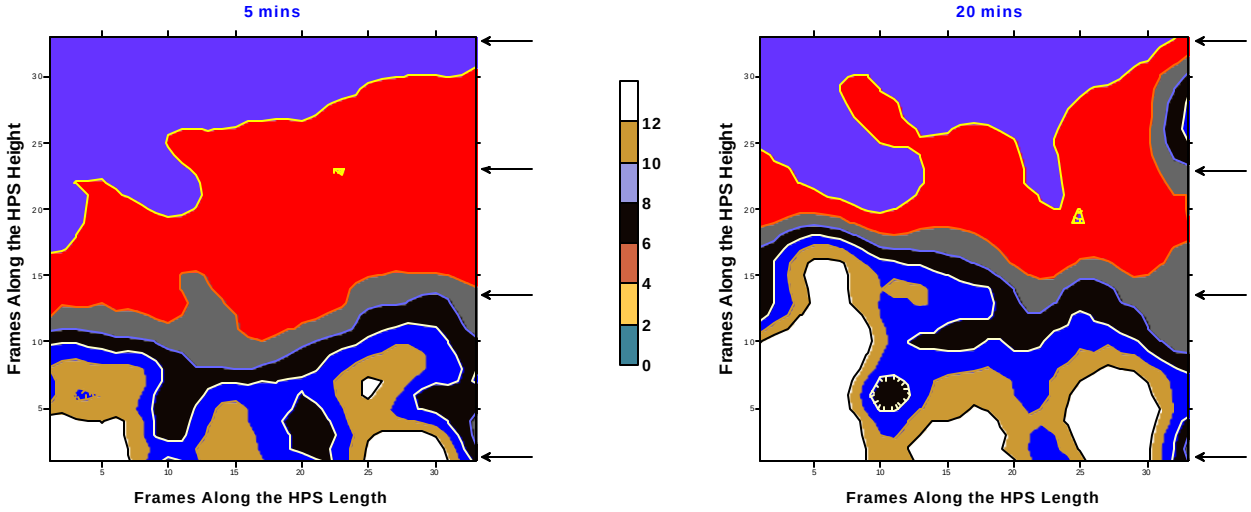

Figure 7.2.4-Sand Concentration (ppg) in the HPS after 5 and 20 mins of 2 ppg Slurry Transport with Borate-Crosslinked 35 lb/Mgal Guar pH 9.0 at 1.75 lb/Mgal, 75°F

Figure 7.2.4 shows that the gel would not be very good at suspending and transporting sand because of very high sand concentrations in the bottom-half of the HPS and very low sand concentrations at the top. Clearly, the sand particles settled during slurry flow through the HPS. The sand accumulation at the bottom means that the sand flowing out of the HPS has a lower concentration than 2 ppg. Hence there would be insufficient sand available in a real fracture, especially since a real fracture is much longer than this slot model. Now, if the proppant distribution is insufficient in the entire fracture, the productivity of the fracture will be inadequate and the stimulation treatment would be unsuccessful. This observation is made despite the fact that this gel satisfied both the gel point and the settling velocity criteria. Hence, these slot tests indicate that these two criteria are insufficient to describe the proppant transport capability of borate-guar gels.

The sand transport capability of the borate-crosslinked guar gel might be improved if a higher crosslinker concentration is used because the suspension settling velocities are lower in gels with higher crosslinker concentrations. Possibly, the higher crosslinker would also improve the gel capability to transport proppant through the fracture. Therefore a higher crosslinker concentration of 6 lb/Mgal was selected, and the new gel was evaluated in the slot model. At this concentration, the proppant distribution is shown in Fig. 7.2.5 after 5 and 20 min. of slurry flow through the HPS. This figure shows a large improvement in the suspension capability of the gel because the sand concentration is uniform in the slot, and there is no settled bed in the HPS bottom. The figure does show some clusters of higher sand concentration, a phenomenon that is frequently observed in crosslinked guar. These clusters, however, are suspended in the gel and would be easily carried away with the gel through the fracture. Thus, the 6 lb/Mgal crosslinked gel would keep the proppant suspended in the fracture and would improve the productivity of the stimulated formation.

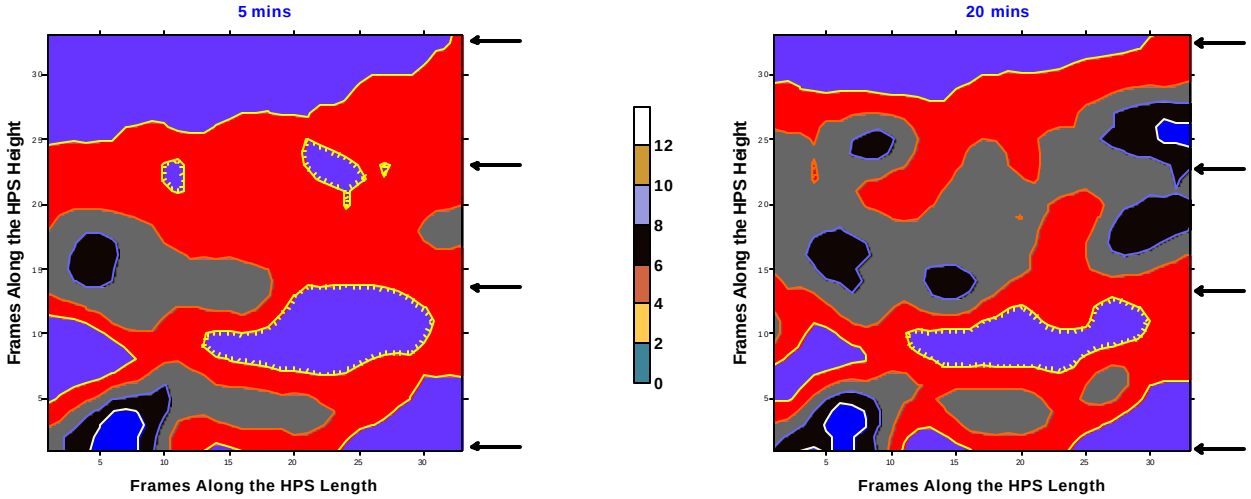

Figure 7.2.5-Sand Concentration (ppg) in the HPS after 5 and 20 mins of 2 ppg Slurry Transport with Borate-Crosslinked 35 lb/Mgal Guar pH 9.0 at 6.0 lb/Mgal, 75°F

The satisfactory proppant transport seen in Figure 7.2.5 indicates that a higher crosslink density is required to perform a satisfactory stimulation treatment with borate-crosslinked guar gel than either the Power[6] or de Kruijf[9] criterion predicts. The question remains what is the proper viscoelastic property to correlate to the proppant transport behavior.

Borate-crosslinked 35 lb/Mgal Guar pH 10

Figure 7.2.6 shows the viscoelastic properties data, and Fig. 7.2.7 describes the settling velocity in the borate-crosslinked guar prepared at pH 10 with different crosslinker concentrations.

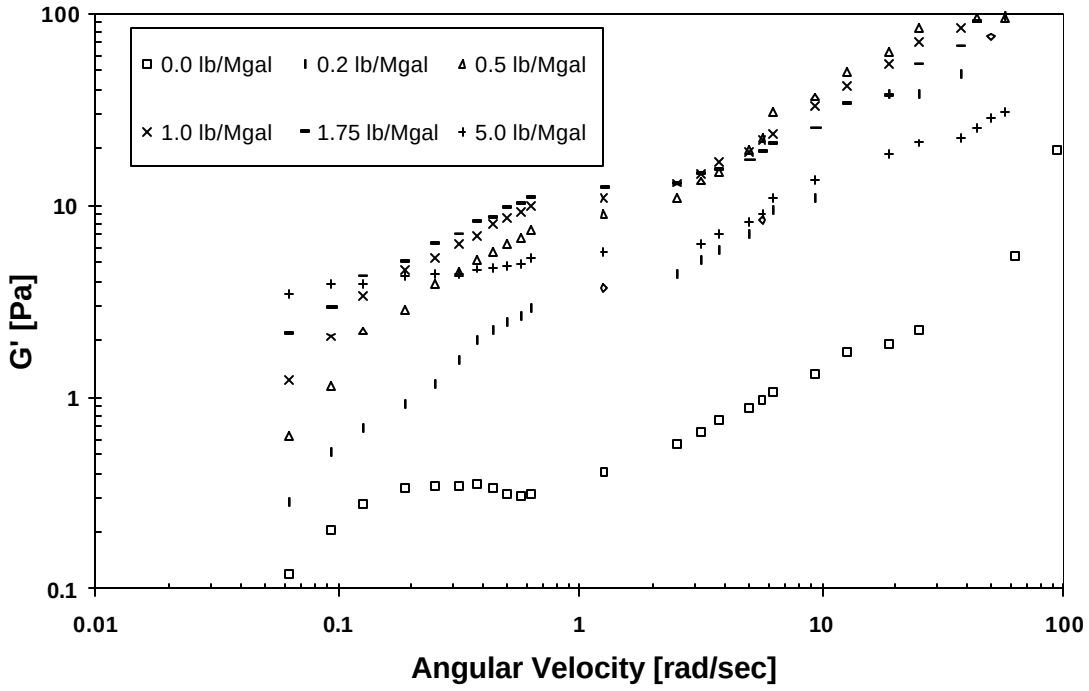

(a) Elastic Modulus Curve

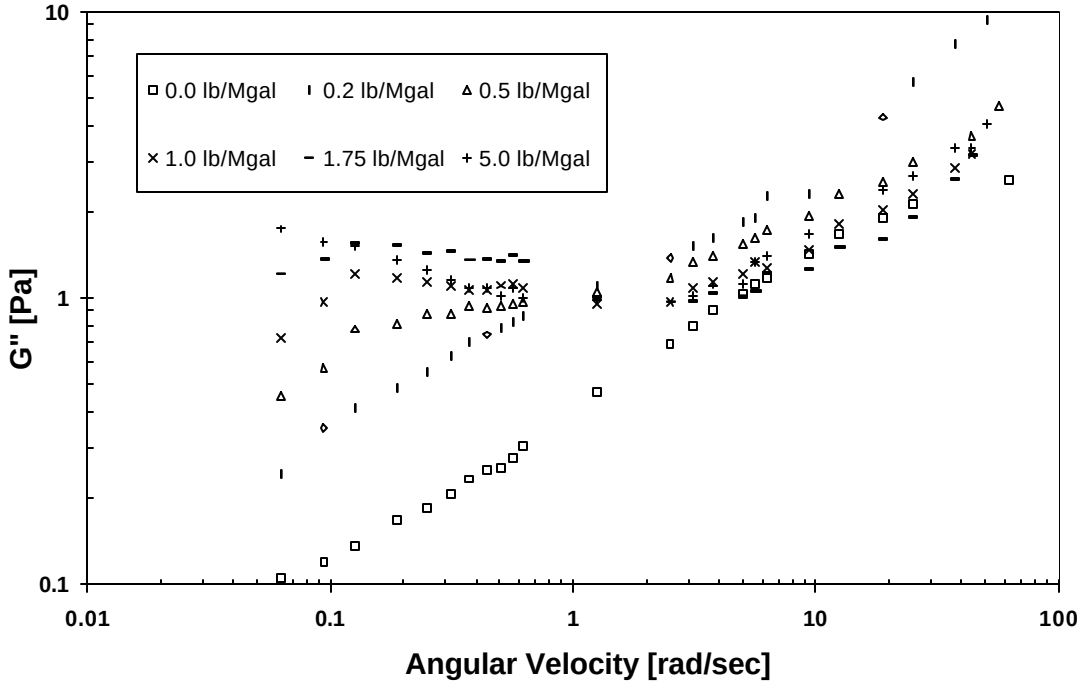

(b) Viscous Modulus Curve

Figure 7.2.6-Linear Viscoelastic Properties of Borate-Crosslinked 35 lb/Mgal Guar pH 10.0, 75 ^{o}F, prepared at different Crosslinker Concentrations

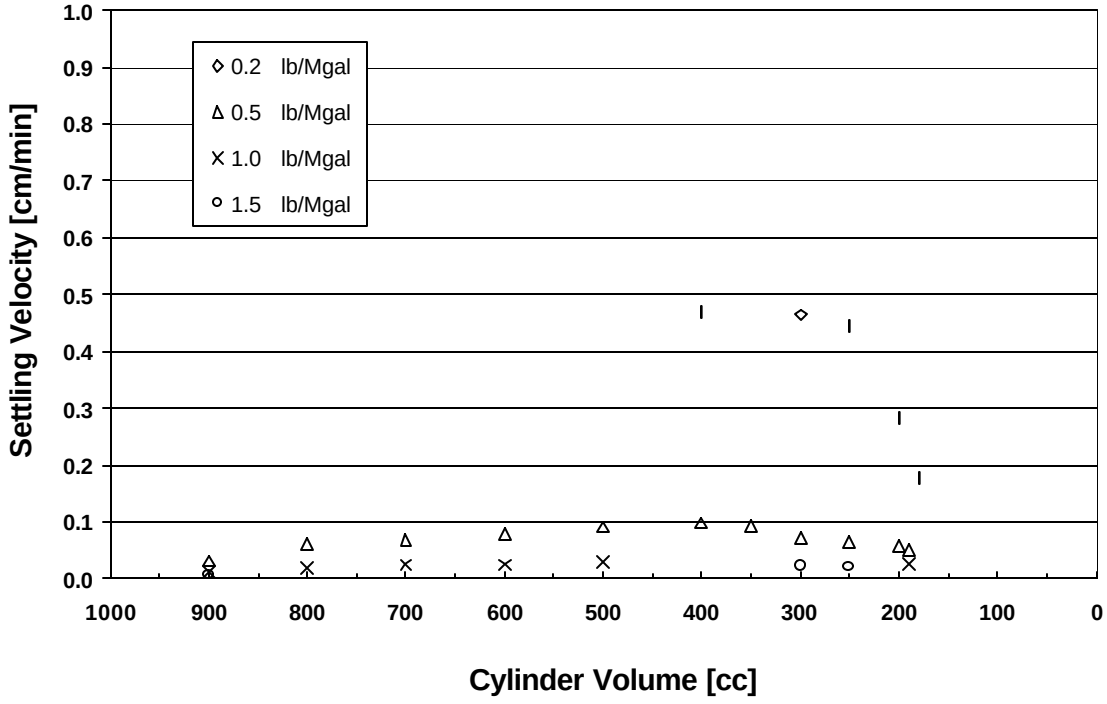

Figure 7.2.7-Settling of 2 ppg Slurry in Borate-Crosslinked 35 lb/Mgal Guar pH 10.0, 75 ^{o}F prepared in different Crosslinker Concentrations

Figure 7.2.7 shows a decrease in settling velocities of 2 ppg slurry, and Fig. 7.2.6 shows an increase in the G' and G'' values with an increase in the crosslinker concentration. These changes are similar to that seen in the gel prepared at pH 9, and are again due to an increase in the number of crosslinked sites formed in guar at higher crosslinker concentrations. Hence as the borate ions crosslink the polymer chains to establish a network structure, the gels display higher elastic and viscous moduli, and better proppant suspension capabilities.

The laboratory characterization of the different fluids prepared at pH 10 is compared to that obtained with the crosslinked guar gel prepared at pH 9 with 6 lb/Mgal crosslinker. The comparison shows that the pH 10 gel prepared with a 0.5 lb/Mgal crosslinker concentration has similar static settling velocities as those observed in the pH 9 gel. These two formulations also have similar G' values at lower frequencies, but have dissimilar G'' values. Hence, there might be satisfactory proppant transport in the pH 10 gel prepared with 0.5 lb/Mgal. To confirm this hypothesis, this gel was evaluated in the slot models for its proppant transport capabilities.

Figure 7.2.8 shows the proppant distribution in the borate-crosslinked pH 10 guar prepared at 0.5 lb/Mgal crosslinker after 5 and 15 min of 2 ppg slurry flow through the HPS. The figure shows high sand concentration in the HPS bottom after 5 min of slurry flow, but this concentration shows little height dependence after 15 min. Some high sand concentration clusters are found, but these are suspended and would maintain high permeability in the fracture. Thus, the pH 10 gel prepared with 0.5 lb/Mgal crosslinker would satisfactorily transport sand through the fracture.

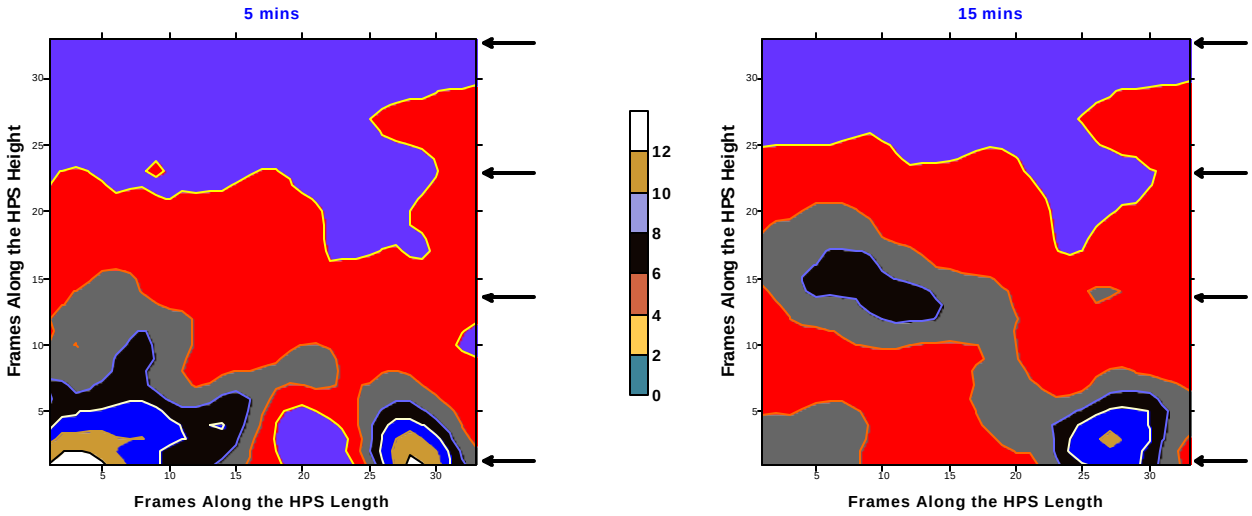

Figure 7.2.8-Sand Concentration (ppg) in the HPS after 5 and 15 mins of 2 ppg Slurry Transport with Borate-Crosslinked 35 lb/Mgal Guar pH 10.0 at 0.5 lb/Mgal, 75^{o}F

Borate-crosslinked 35 lb/Mgal Guar pH 11

A crosslinker concentration of 0.5 lb/Mgal was used to prepare crosslinked gel at pH 11. This gel was then evaluated with a different approach as the gel was tested in the clear slot first for its proppant transport behavior. The test showed that the pH 11 gel prepared with 0.5 lb/Mgal. exhibited satisfactory slurry transport, as there was good sand distribution throughout the slot without any settled bed. Then during the test, the crosslinker concentration was lowered to 0.45 lb/Mgal. and the proppant transport behavior was again observed in the clear slot. At this concentration too, the slurry was satisfactorily transported through the slot. The crosslinker concentration was then further lowered to 0.40 lb/Mgal and the gel was again evaluated in the clear slot. At this concentration however, the proppant particles began to separate from the gel, and started settling to the bottom of the slot thereby showing a diminishing capability of the 0.40 lb/Mgal gel to successfully transport proppant through the slot. This test approach showed that the crosslinker concentration of 0.45 lb/Mgal. provided a minimum crosslinker concentration above which the pH 11 gel exhibited acceptable proppant transport.

The viscoelastic data of the gel prepared at 0.45 lb/Mgal and at other crosslinker concentrations are shown in Figure 7.2.9. The viscoelastic behavior of the pH 11 gels are similar to that of the gels prepared at pH 9 and 10. The figure shows as the crosslinker concentration is increased, the elastic and viscous moduli increase showing an increasing crosslinking of the guar polymer at higher crosslinker quantity. It also shows that at a crosslinker concentration of 3 lb/Mgal, the elastic moduli are independent of the frequency. At this concentration, the gel exhibited a phase separation when the gel was kept static for 24 hrs. Harris[2] has described this phase separation as over-crosslinking or syneresis in the borate-crosslinked gel. Similar phase separation was observed in pH 10 gel at 5 lb/Mgal and in pH 9 gel at 9 lb/Mgal crosslinker concentrations.

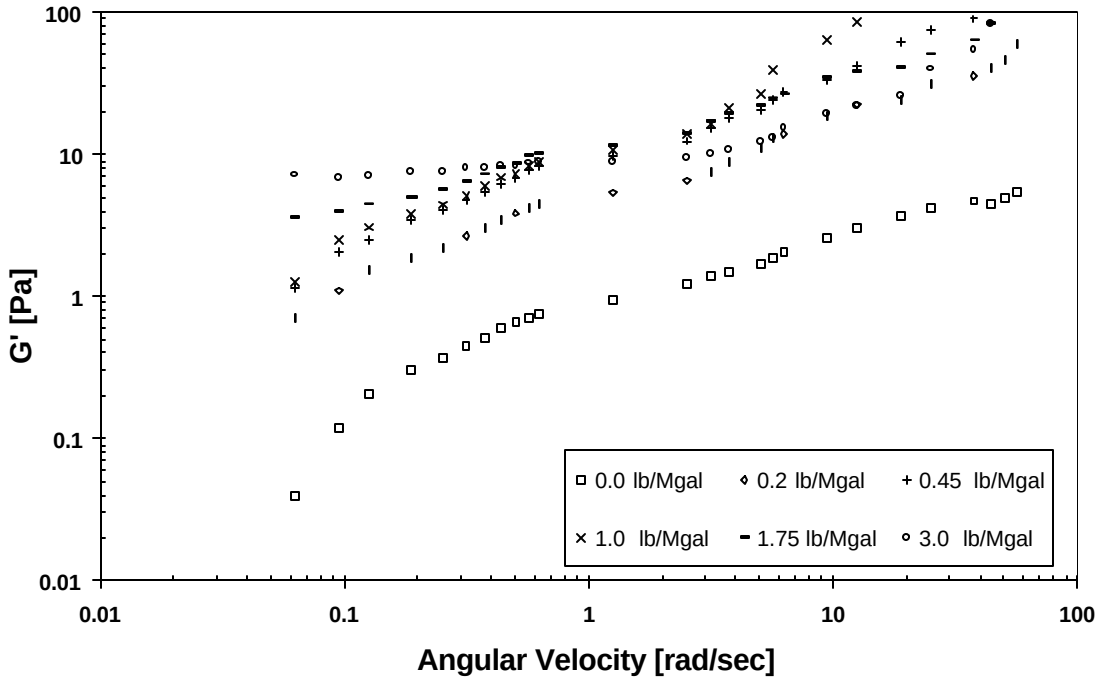

(a) Elastic Modulus Curve

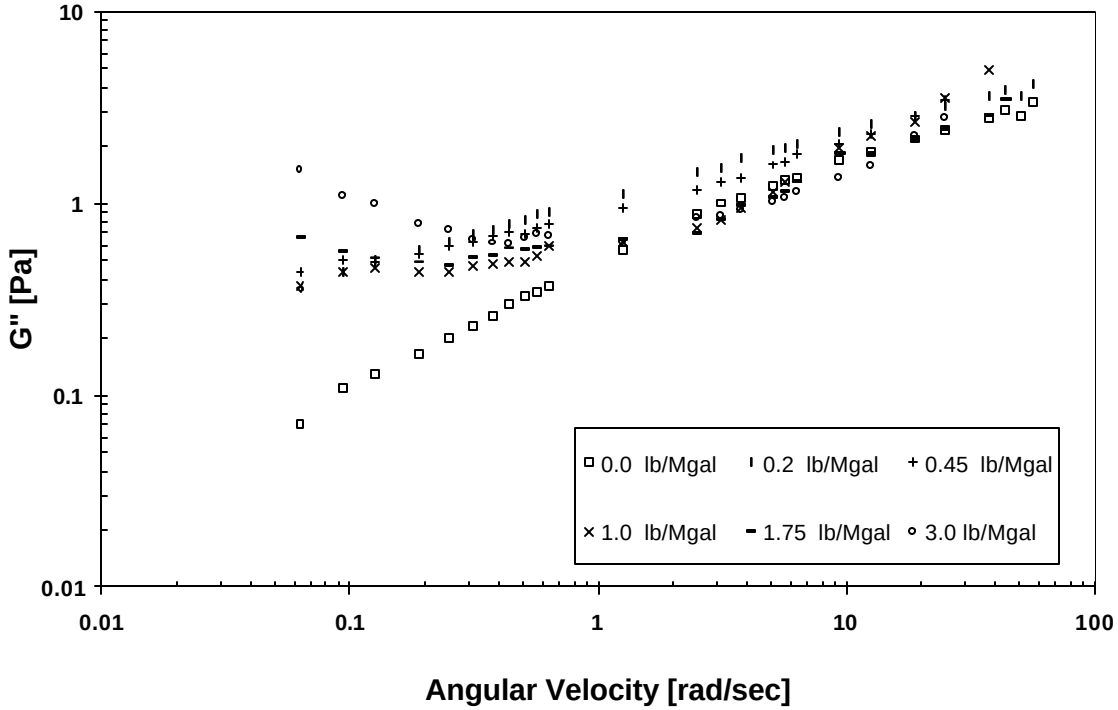

(b) Viscous Modulus Curve

Figure 7.2.9-Linear Viscoelastic Properties of Borate-Crosslinked 35 lb/Mgal Guar pH 11.0, 75 ^{o}F, prepared at different Crosslinker Concentrations

Figure 7.2.10 shows the proppant distribution in the HPS with gel prepared at pH 11 and at 0.45 lb/Mgal crosslinker concentration. The figure shows a uniform proppant distribution throughout the slot with a slightly high sand concentration in the HPS bottom.

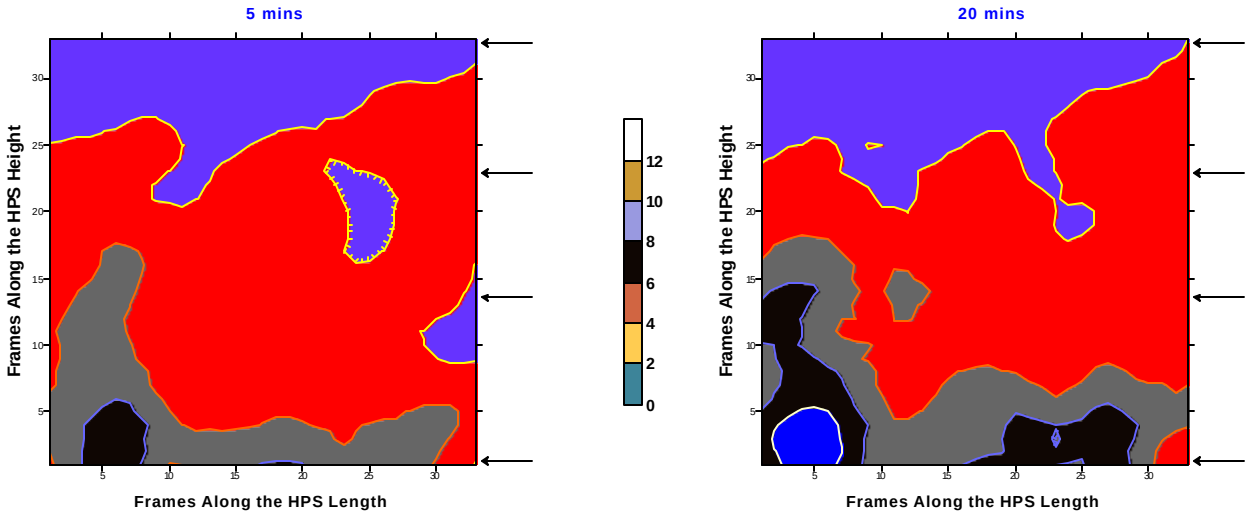

Figure 7.2.10-Sand Concentration (ppg) in the HPS after 5 and 20 mins of 2 ppg Slurry Transport with Borate-Crosslinked 35 lb/Mgal Guar pH 11.0 at 0.45 lb/Mgal, 75°F

The viscoelastic data for the gels whose proppant transport behaviors are shown earlier are combined in Fig. 7.2.11. The figure shows that the crosslinked gels which exhibit satisfactory proppant transport have similar *G'* values throughout the frequency range sampled, particularly at lower frequencies. These gels, however, have dissimilar *G"* values, and hence, have different viscosities. This difference implies that the viscosity is a poor parameter to correlate with the sand transport characteristics of a viscoelastic fluid. This result further confirms why several researchers[3,4] were unable to correlate the viscosity with particle suspension behavior. Figure 7.2.11 further shows the *G"* values of the pH 9 crosslinked gel prepared at 1.75 lb/Mgal concentration to be higher than that of the pH 10 and 11 crosslinked gels, even though its proppant transport behavior is poorer than that of the other gels, which is exactly opposite to what one should expect. On the other hand, the poor performance of the pH 9 gel at 1.75 lb/Mgal is correctly depicted in its lower *G'* values. This result further confirms that the elastic moduli better correlates the sand transport behavior of crosslinked gel.

The test results with borate-crosslinked gel indicate the suspension capabilities to be related to the entanglements. Entanglements are obtained in a crosslinked gel by crosslinking the guar chains, and can also be achieved in an uncrosslinked guar by increasing the polymer concentration. Hence if our hypothesis is correct, then one should be able to identify a critical concentration at which the uncrosslinked guar is able to transport proppant by examining its elastic moduli. A 100 lb/Mgal guar has similar elastic modulus at lower frequencies as that of the crosslinked gel as shown in Figure 7.2.11, thus it might have acceptable slurry transport behavior.

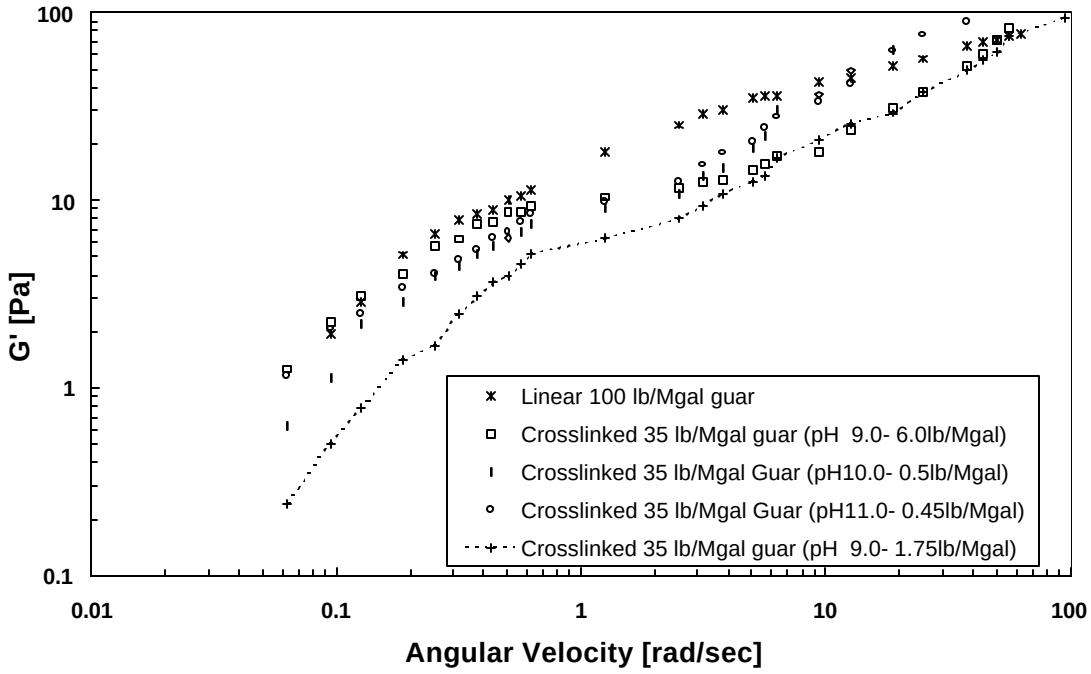

(a) Elastic Modulus Curve

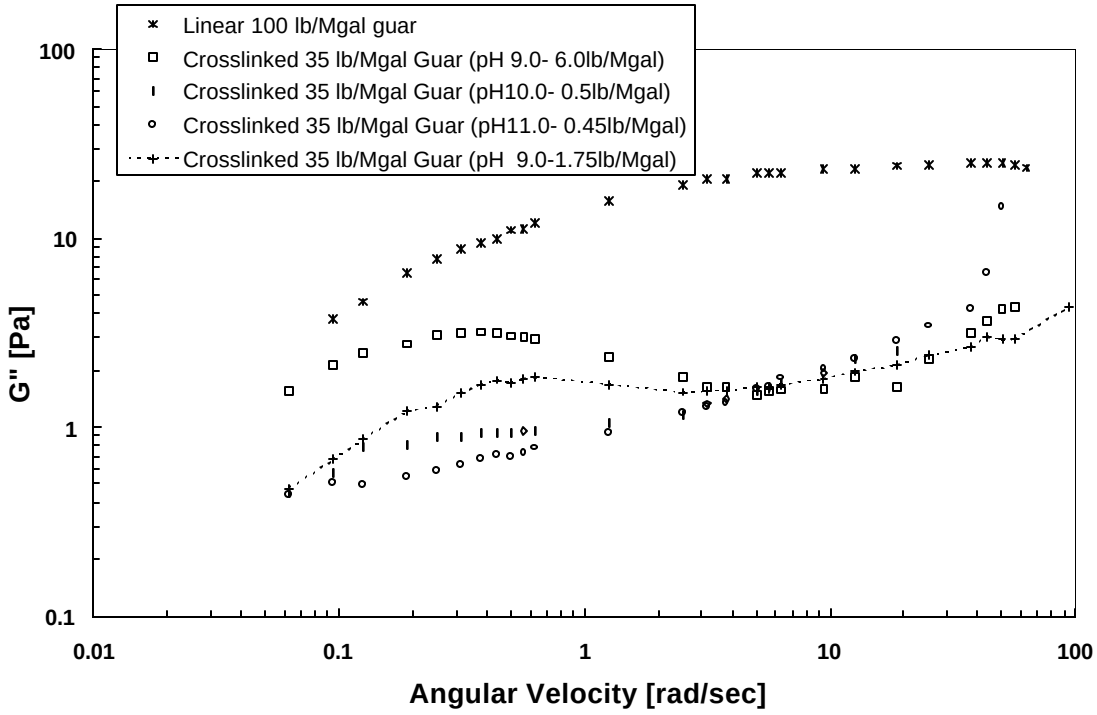

(b) Viscous Modulus Curve

Figure 7.2.11-Comparison of G' and G" values in Linear 100 lb/Mgal Guar and in Borate-Crosslinked 35 lb/Mgal guar gels prepared at Different pHs at 75 ^{o}F

The sand distribution in the HPS is shown in Figure 7.2.12 after 5 and 20 min. of flow of a 2 ppg slurry in the 100 lb/Mgal linear guar. The figure shows some settling in the HPS after 5 min., but this settled sand was carried away with the fluid as the slurry flow was continue as seen in the 20 min. image. The proppant distribution in the linear guar is similar to that seen in the crosslinked gels. Therefore, the slurry is satisfactorily transported through the slot models by the 100 lb/Mgal guar.

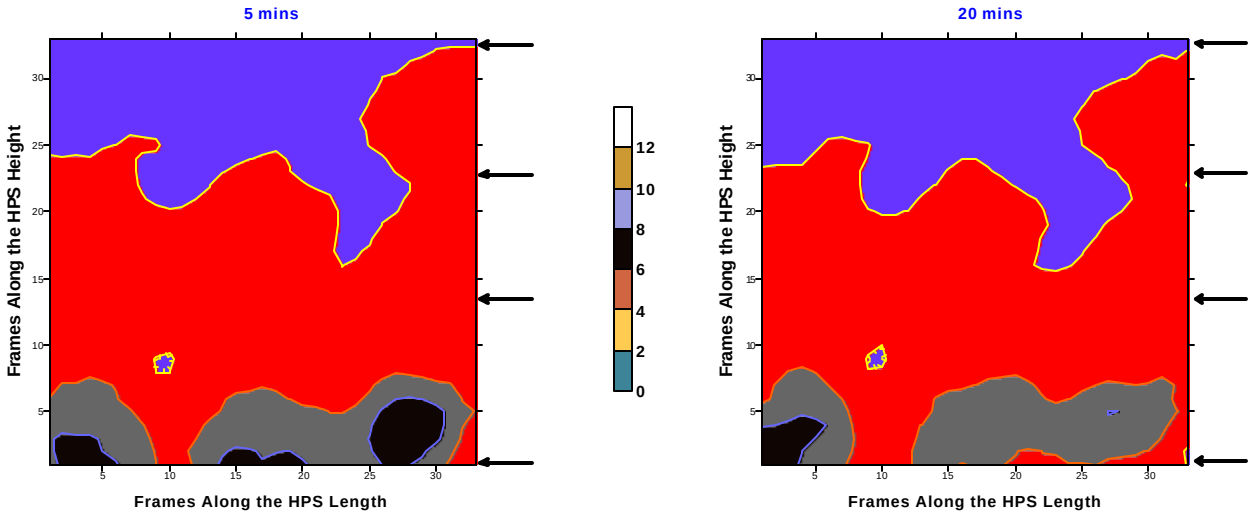

Figure 7.2.12-Sand Concentration (ppg) in the HPS after 5 and 20 mins of 2 ppg Slurry Transport with Linear 100 lb/Mgal Guar, 75°F

Figure 7.2.11 confirms that the entanglement couplings describe the proppant transport capability of a fracturing fluid. These couplings are better exhibited in the similar *G'* values of the different crosslinked gels and the uncrosslinked guar. Hence the elastic modulus provides a better method to correlate the laboratory characteristics of a fracturing fluid with its proppant transport capability.

Effect of Temperature

Since the elastic moduli correlates better with the proppant transport capability at ambient temperature, it should also correlate well at an elevated temperature. At higher temperature, however, the guar polymer degrades so a higher polymer concentration might be required to evaluate the relationship of elastic moduli and proppant transport. Hence linear 40 lb/Mgal guar solutions were prepared and their pH was adjusted to 11.5. These solutions were then crosslinked at different crosslinker concentrations to identify the crosslinker concentration that has similar elastic moduli as that of the gels which exhibited acceptable proppant transport and whose elastic moduli were shown in Fig. 7.2.11.

Figure 7.2.13 describes the viscoelastic properties of the borate-crosslinked 40 lb/Mgal guar gel prepared at pH 11.5. The figure shows an increase in elastic and viscous moduli with an increase in the crosslinker concentration. This viscoelastic behavior at 130^{o}F is similar to that seen earlier in the samples analyzed at ambient temperature. From Figure 7.2.13, the elastic moduli of the different gels were compared with that of the gels in Figure 7.2.11. This comparison showed that the moduli of the pH 11.5 gel prepared at 1 lb/Mgal is slightly lower and that at 1.25 lb/Mgal is slightly higher than that of the gels with acceptable proppant transport. Therefore, the crosslinker range from 1.0 to 1.25 lb/Mgal needs to be further evaluated in the large scale test facility for identifying the critical crosslinker concentration above which the proppant transport behavior would be satisfactory.

Borate-crosslinked 40 lb/Mgal guar gel at pH 11.5 was first evaluated in the clear slot where the crosslinker concentrations were varied from 1.25 to 1.0 lb/Mgal using ISCO pump (Fig. 7.2.1) and proppant distribution was observed. At 1.25 lb/Mgal concentration, the proppant were easily transported through the slot with no particle settling in the slot; as a result, the crosslinker rate was reduced from 1.25 to 1.1 lb/Mgal. At this lower rate also, the proppant distribution was uniform throughout the slot. As the crosslinker rate was further reduced to 1.0 lb/Mgal, the slurry flow showed non-uniformity across the slot height with slower moving slurry near the top and bottom boundaries than in the middle section of the slot height. This slow moving slurry indicates that the proppant transport capacity of the fluid had begun to decrease at 1.0 lb/Mgal. Therefore, the crosslinker concentration of 1.1 lb/Mgal is a critical value above which the proppant transport would be acceptable in a fracture.

A 2 ppg slurry was then prepared in 40 lb/Mgal guar gel crosslinked with 1.1 lb/Mgal concentration, and was pumped through the HPS. The proppant distribution in the HPS for this gel is shown in Figure 7.2.14. The figure shows that the sand concentration is uniform throughout the HPS with few high sand concentration regions. These regions being suspended in the slurry were transported with the slurry flow as seen in the image in Fig. 7.2.14 at 20 min. Thus, this formulation would perform satisfactorily in the fracture. The acceptable proppant transport through the slot, and a good comparison of elastic moduli of the gel prepared with 1.1 lb/Mgal crosslinker at 130 ^{o}F with that of the gels at ambient temperature further confirms the correlation of elastic moduli with proppant transport through a fracture.

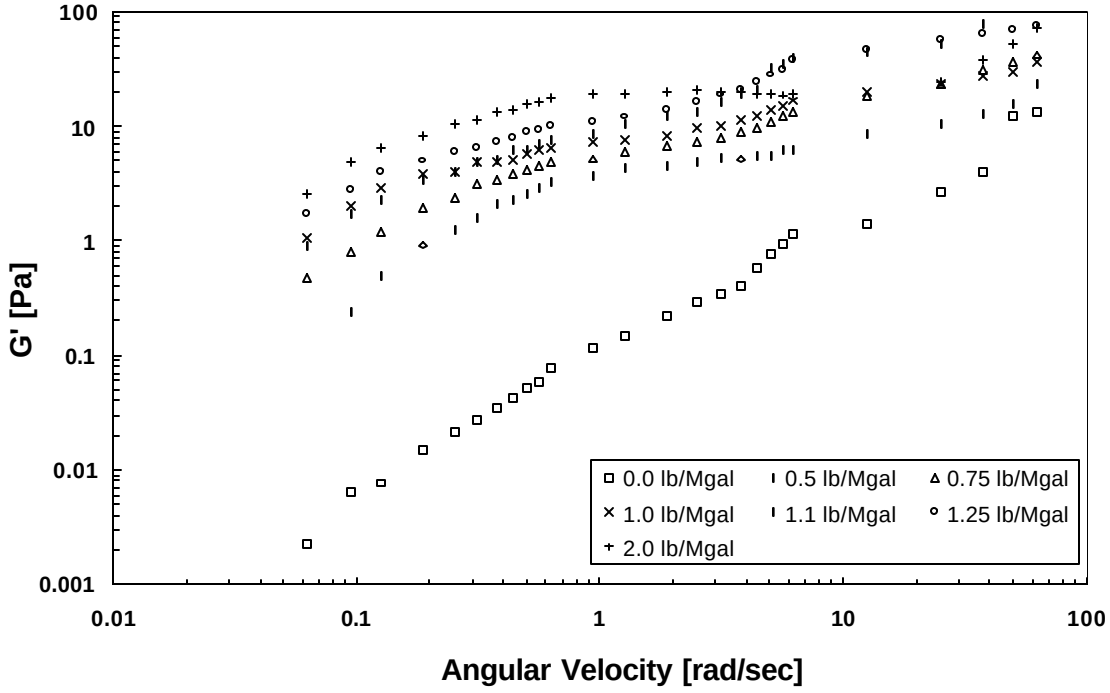

(a) Elastic Modulus Curve

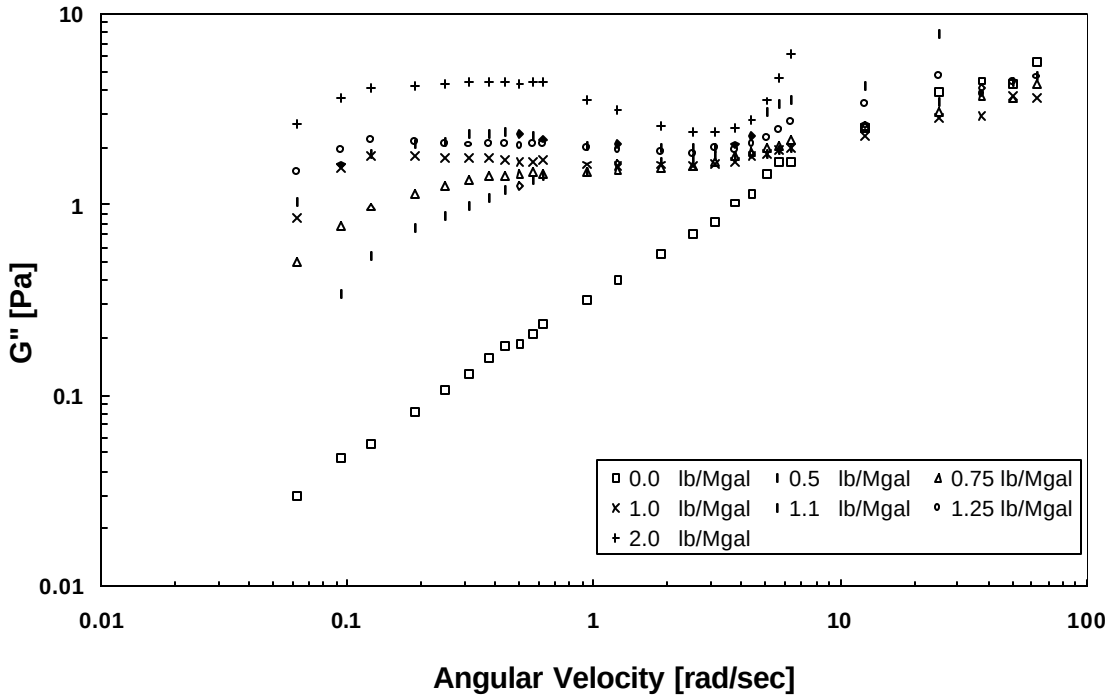

(b) Viscous Modulus Curve

Figure 7.2.13-Linear Viscoelastic Properties of Borate-Crosslinked 40 lb/Mgal Guar pH 11.5, prepared at different Crosslinker Concentrations, 130^{o}F

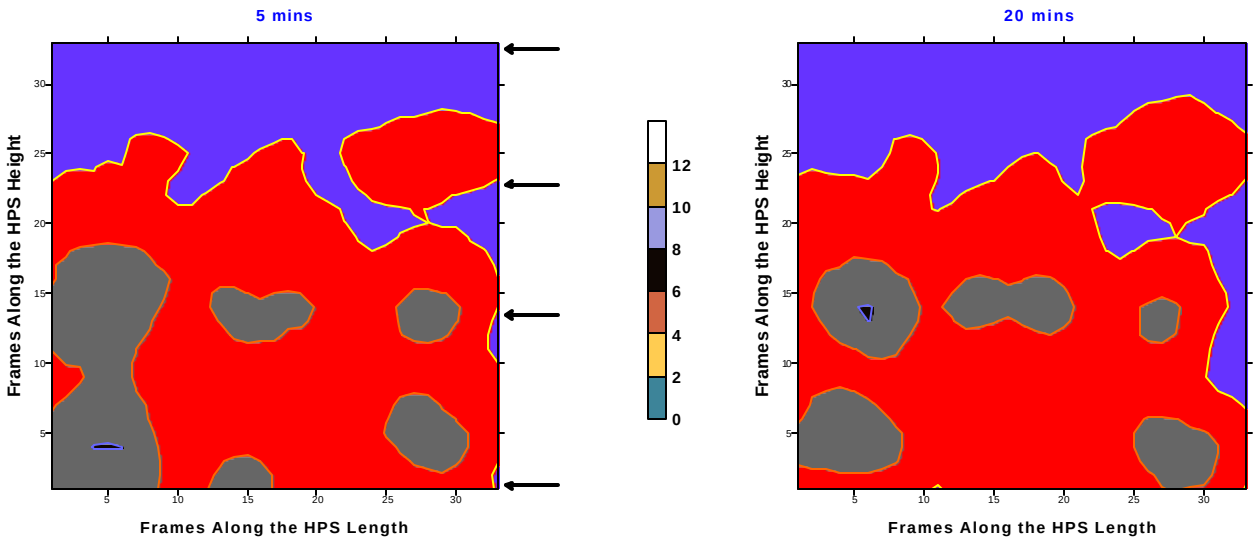

Figure 7.2.14-Sand Concentration (ppg) in the HPS after 5 and 20 mins of 2 ppg Slurry Transport with Borate-Crosslinked 40 lb/Mgal Guar pH 11.5 at 1.1 lb/Mgal, 130^{o}F

Effect of Sand Concentration:

Most fracturing treatments are performed at sand concentration varying from 2 to 10 ppg, so the fracturing fluid must be designed to transport higher concentration sand slurries. Hence the relationship between fluid rheology and its sand transport capability, which is developed from 2 ppg slurry only, should be validated with concentrated slurries. Thus, a high sand concentration of 8 ppg was selected to prepare slurries in borate-crosslinked gels at pH 9 and 10. These slurries were then studied for their proppant transport behavior in the clear slot and the HPS.

The borate-crosslinked gel was first prepared at pH 9 and crosslinked with 6 lb/Mgal concentration because this gel could satisfactorily transport 2 ppg slurry through the slots. This gel was then slurried to 8 ppg sand concentration, and its proppant transport behavior observed in the clear slot. The gel again exhibited an acceptable performance as there was no slow moving slurry in the bottom of the clear slot. Because of this satisfactory performance, the crosslinker concentration was reduced to 4 lb/Mgal to identify the critical crosslinker concentration with satisfactory proppant transport in the slot. At this crosslinker concentration, the proppant particle layers began to separate from the fluid and when the crosslinker concentration was further reduced to 3.5 lb/Mgal, the sand began to separate from the gel and settle to the bottom of the clear slot. This diminishing capability of these concentrations to transport proppant depicts their unsatisfactory performance to carry 8 ppg slurry. Therefore, the crosslinker concentration was increased to 5 lb/Mgal and slurry transport through the clear slot observed. This gel exhibited satisfactory proppant distribution throughout the clear slot showing the minimum crosslinker concentration of this formulation is 5 lb/Mgal for it to successfully transporting sand particles in fracture. Hence at this crosslinker concentration, a 8 ppg slurry was pumped through the HPS and the sand distribution obtained as shown in Figure 7.2.15. The figure shows that the sand concentration is uniform across the slot with values in a range from 8 to 12 ppg.

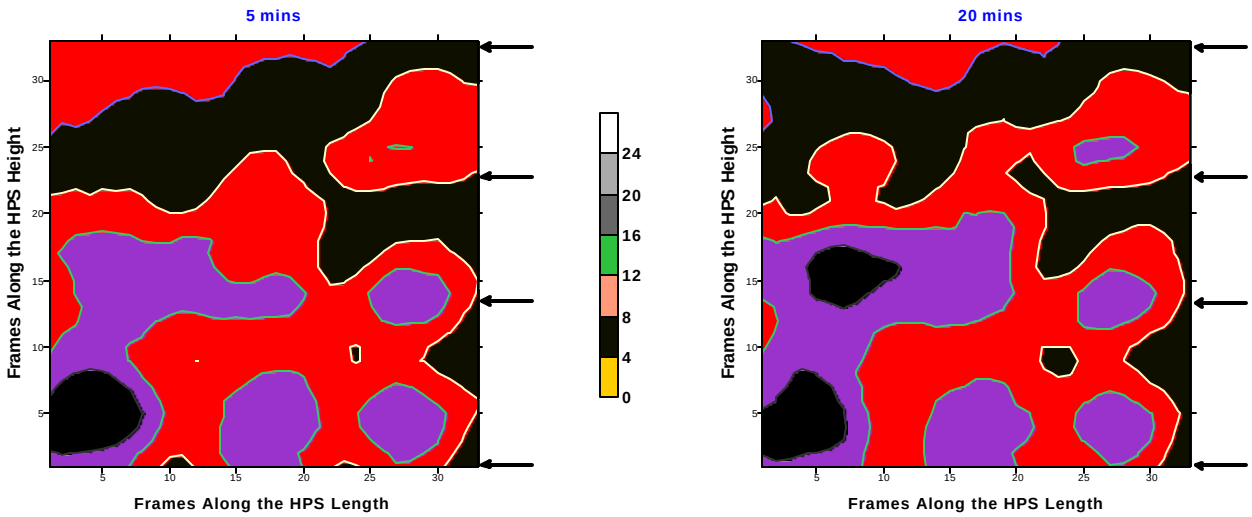

Figure 7.2.15-Sand Concentration (ppg) in the HPS after 5 and 20 mins of 8 ppg Slurry Transport with Borate-Crosslinked 35 lb/Mgal Guar pH 9.0 at 5.0 lb/Mgal, 75^{o}F

A similar 8 ppg slurry was prepared in another borate-crosslinked 35 lb/Mgal guar gel at a pH of 10. Since a crosslinker concentration of 0.5 lb/Mgal could satisfactorily transport 2 ppg slurry through the slots, it might also transport 8 ppg slurry through the slot. This gel at 0.5 lb/Mgal gel though transported the 8 ppg slurry without forming any settled sand bed in the slot, the slurry flow was non-uniform across the slot height. The slurry flow was slower at the bottom section of the slot. The slower flow region indicates that this gel has difficulty in keeping the sand under suspension. Thus, this gel with 0.5 lb/Mgal concentration is not capable of transporting high concentration sand slurry. Therefore, the crosslinker concentration was increased to 0.55 lb/Mgal and slurry transport through the clear slot was again observed. At the higher crosslinker, the slurry flow was still non-uniform with slower moving slurry in the slot bottom. At this concentration however, the regions occupied by the slowly flowing slurry were less than that in the gel prepared at 0.5 lb/Mgal. Therefore, the proppant transport behavior of the gel was improved when the crosslinker concentration was increased from 0.5 to 0.55 lb/Mgal, but it could still improve further. Thus, the crosslinker concentration was increased to 0.6 lb/Mgal and slurry transport observed through the clear slot. At 0.6 lb/Mgal concentration, the slurry transport was uniform throughout the slot indicating that this concentration can satisfactorily transport proppant through a fracture. This gel was then pumped through the HPS to obtain a digital image of the sand distribution in the slot model.

The proppant distribution in the HPS is shown in Figure 7.2.16 for the 8 ppg slurry transported by borate-crosslinked guar gel at pH 10. The figure shows an identical sand distribution as that seen in Figure 7.2.15 for pH 9 gel.

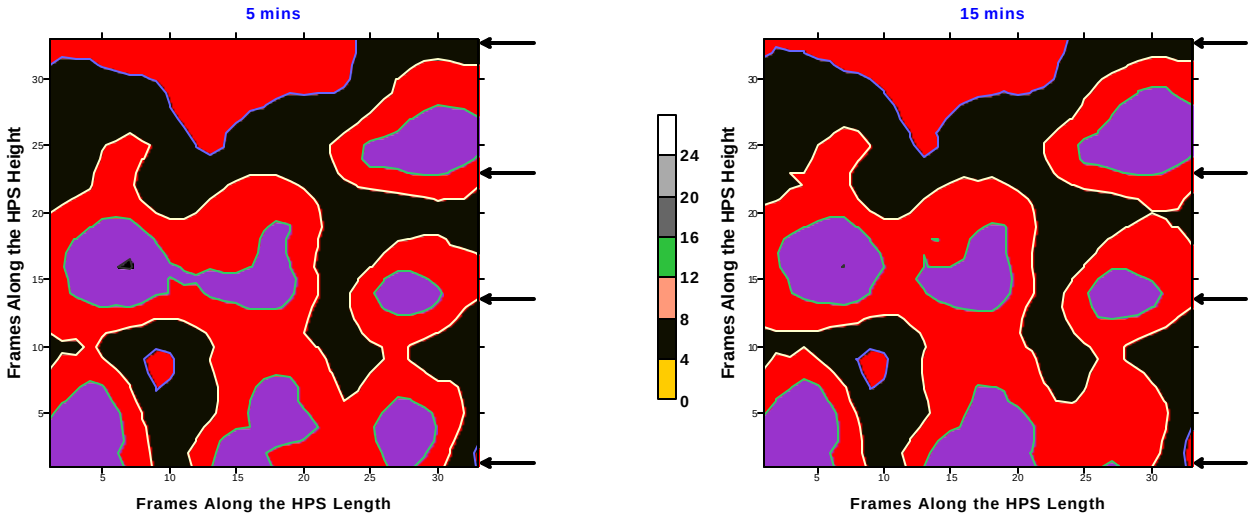

Figure 7.2.16-Sand Concentration (ppg) in the HPS after 5 and 15 mins of 8 ppg Slurry Transport with Borate-Crosslinked 35 lb/Mgal Guar pH 10.0 at 0.6 lb/Mgal, 75^{o}F

The proppant transport behavior of the borate-crosslinked guar gel prepared at pH 10 shows that a crosslinker concentration of 0.5 lb/Mgal was sufficient to transport a 2 ppg slurry whereas a higher crosslinker concentration of 0.6 lb/Mgal was required to transport the higher concentration slurry of 8 ppg. This result shows that a higher density of crosslinked sites is required to transport higher concentration slurry. The higher crosslinked density means a higher elastic moduli and a higher gel strength.

The elastic moduli of the different crosslinked gels that exhibit satisfactory proppant transport of 2 and 8 ppg sand concentrations at ambient and elevated temperatures are combined in Figure 7.2.17. The figure shows that these gels have similar elastic moduli at lower frequency regions. Furthermore, these gels are the minimum formulations required to transport proppant through a fracture and as the crosslinker concentration is increased beyond this critical value, the proppant transport capability will improve. Thus Fig. 7.2.17 describes the minimum elastic moduli required to satisfactorily transport proppant through a fracture.

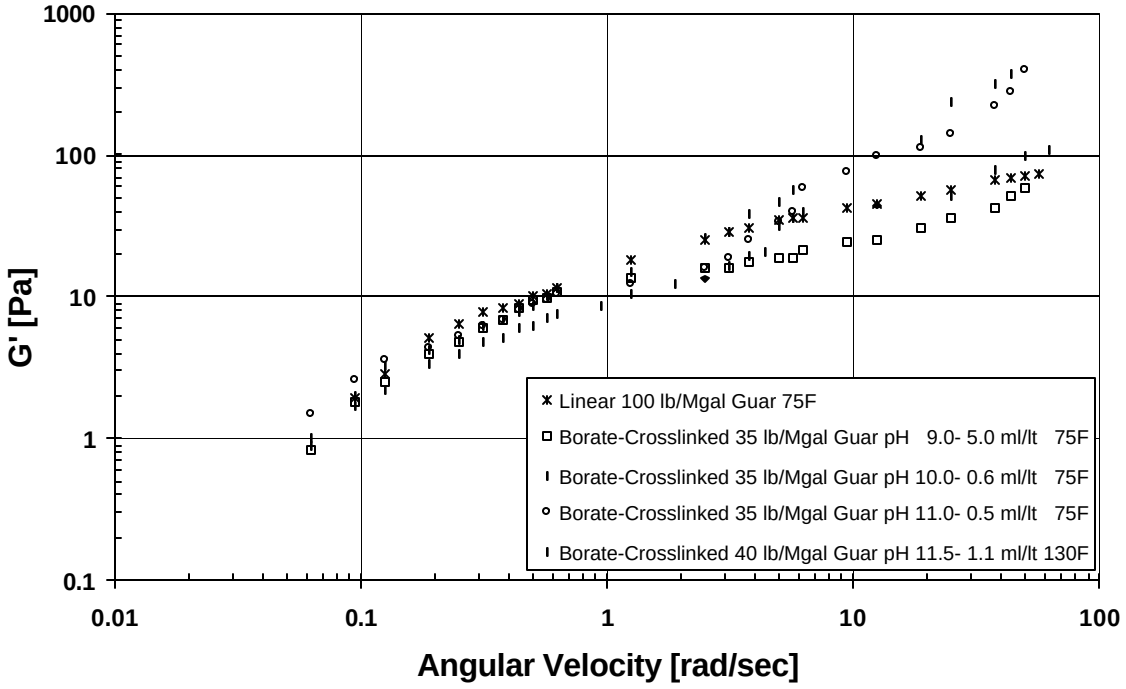

Figure 7.2.17-Comparison of Elastic Moduli of Gels with Satisfactory Proppant Transport

Implications of the Research Results:

1. The borate-crosslinked guar gel prepared at pH 9 and 1.75 lb/Mgal crosslinker concentration satisfies the gel point criteria of Power et al.[5,6] as there is a maximum in loss modulus for this concentration. This gel also satisfies the de Kruijf et al.[9] criteria for marginally acceptable proppant transport, yet Figure 7.2.4 shows that this gel does not exhibit satisfactory proppant transport through a slot model. Hence, the evaluation of these criteria with proppant transport tests imply that the two criteria available in the literature are insufficient to describe the proppant transport capability of borate-crosslinked guar gels.

2. Figure 7.2.11 shows that the crosslinked gels which exhibit satisfactory proppant transport have similar *G'* values throughout the frequency range sampled, particularly at lower frequencies. These gels, however, have dissimilar *G"* values, and hence, have different viscosities. This difference implies that the viscosity is a poor parameter to correlate with the sand transport characteristics of a viscoelastic fluid. This result further confirms why several researchers[3,4] were unable to correlate the viscosity with particle suspension behavior. The figure further shows the *G"* values of the pH 9 crosslinked gel prepared at 1.75 lb/Mgal concentration to be higher than that of the pH 10 and 11 crosslinked gels, even though its proppant transport behavior is poorer than that of the other gels, which is exactly opposite to what one should expect. On the other hand, the poor performance of the pH 9 gel at 1.75 lb/Mgal is

correctly depicted in its lower *G'* values. This result further confirms that the elastic moduli better correlates the sand transport behavior of crosslinked gel.

3. de Kruijf et al.[9] proposed a minimum elastic modulus of 2 Pa at 5 rad/sec to design a fluid that shows marginally acceptable proppant suspension. All samples shown in Fig. 7.2.17 satisfy this criterion and yet all do not exhibit acceptable proppant transport, again showing the need for a better minimum-criterion for fracturing fluid design. The figure shows that the gels with satisfactory transport have similar elastic moduli in a frequency range from 0.06 to 5 rad/sec. Thus, the elastic moduli of the gels shown in Fig. 7.2.17 describe the minimum moduli to design a fracturing fluid having satisfactory slurry transport characteristics. Hence if the minimum elastic moduli values of the crosslinked guar gels vary from approximately 1 Pa at 0.1 to 10 Pa at 1.0 rad/sec, then the fluid would exhibit satisfactory performance in a fracturing treatment.

4. The results show that the minimum crosslinker concentration for satisfactory proppant transport is a function of the sand concentration. Thus, if the slurry concentration is increased from 2 to 8 ppg, the crosslinker concentration should also be increased to improve the gel strength to successfully transport proppant through the fracture.

7.3 Proppant Transport

Objective: The purpose of the proppant transport study was three-fold: (1) to investigate factors that influence convection and encapsulation in fracturing applications, (2) to evaluate static and dynamic settling characteristics of proppants in fracturing slurries and (3) to study the fluids capability to remove fluidized layer and erode settled bed.

Introduction: Hydraulic fracturing treatment is performed to create a conductive path in the reservoir so that the well productivity is increased. The improvements in well performance depends largely on how well the proppant is transported down the wellbore and how long the proppants remain suspended in the fracturing fluid before they settle down in the fracture. A better suspension provides better placement of the proppants in front of the perforations and thus, a better fracturing stimulation.

Procedure: The proppant transport study was performed on the high pressure simulator in which fiber optics based vision system was used for the flow visualization. The encapsulation study comprised of setting the fracture to a gap width, filling the slot with water, linear gel or borate-crosslinked guar, and injecting borate-crosslinked guar slurry into the various fluids of different viscosities.

The static and dynamic characteristics were evaluated by setting the fracture to a gap width and observing settling in the shear preconditioned fracturing slurries under stationary and fluid flow conditions.

The proppant bed erosion study was performed by maintaining the simulator to required gap widths, setting different perforation configurations and pumping several fracturing fluids in a sequential pattern. A typical injection sequence through the different perforation configurations is depicted in Figure 7.3.1.

A detailed description of the procedure used to perform this study and results obtained can be found in the Annual Reports submitted to Gas Research Institute (GRI)[11-13] and in the technical papers presented at the Society of Petroleum Engineers (SPE) Conferences.[14-17]

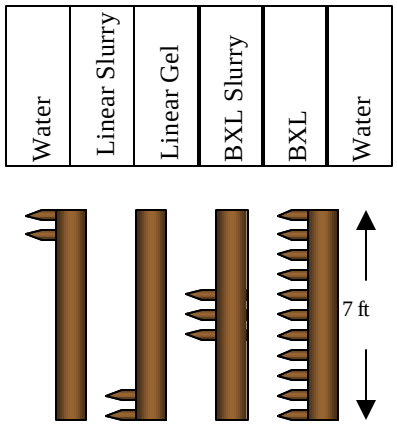

Figure 7.3.1- (Top) A Typical Sequence of Fluid Injection (Bottom) Various Perforation Configurations along the HPS Height

Results: The comprehensive investigations on encapsulation and convection showed that the encapsulation dominates particle settling in low viscous medium, but an increase in viscosity of the lower medium can prevent the encapsulation. Thus, there exists an optimum fluid viscosity that overrides density effects to form encapsulated slurry.

This influence of the viscosity is further highlighted from the reduction in settling time of the encapsulated slurry when the polymer concentration is decreased from 35 to 25 lb guar in 1000 gal of solution. In addition to the influence of the viscosity and polymer concentration, convective downward motion of the encapsulated slurry is related to fracture gap width. This effect is shown in Figure 7.3.2, which describes an exponential relationship between the convective downward motion and fracture gap width.

The study further identified that there is settling within the encapsulated slurry as shown in Figure 7.3.3, which shows the proppant concentrations in the slot in an initial period and a final phase of the experiment. The figure shows that initially, there is higher concentration in an upper portion of the cluster; but at later times, the concentration in lower portion is increased due to settling of the proppants within the cluster.

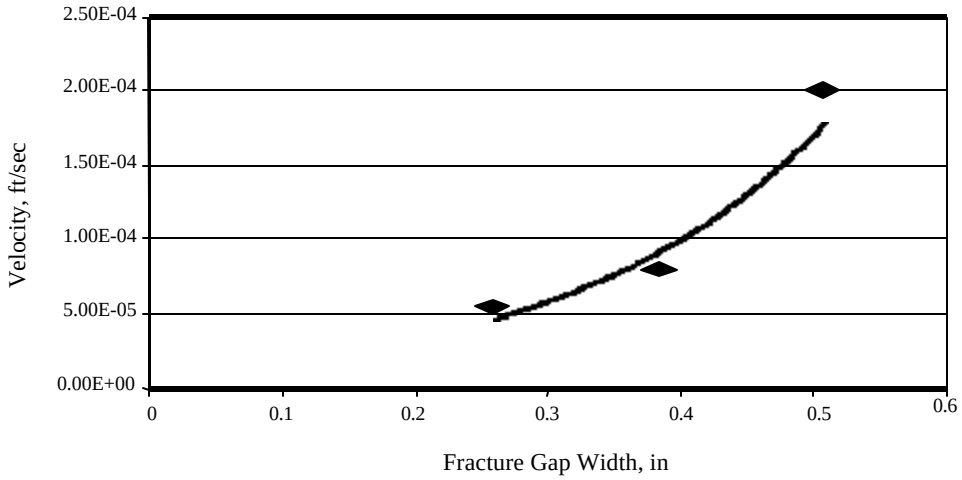

Figure 7.3.2 - Convective Downward Velocity of an Encapsulated 6 ppg Slurry into 35 lb Borate-Crosslinked at Various Fracture Widths

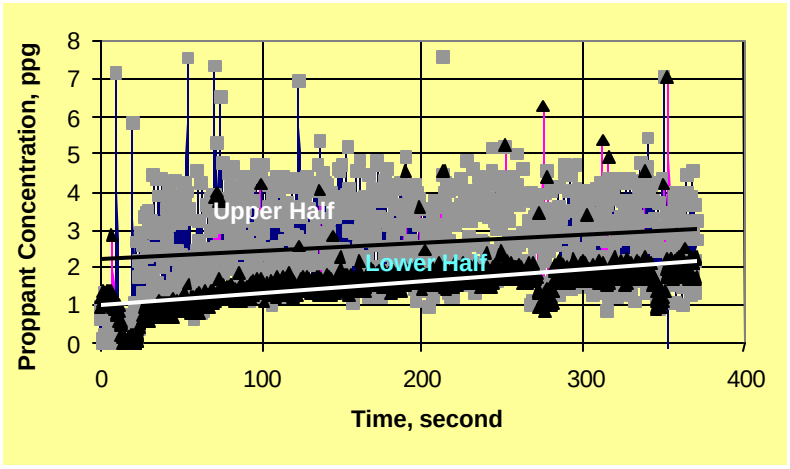

(a)

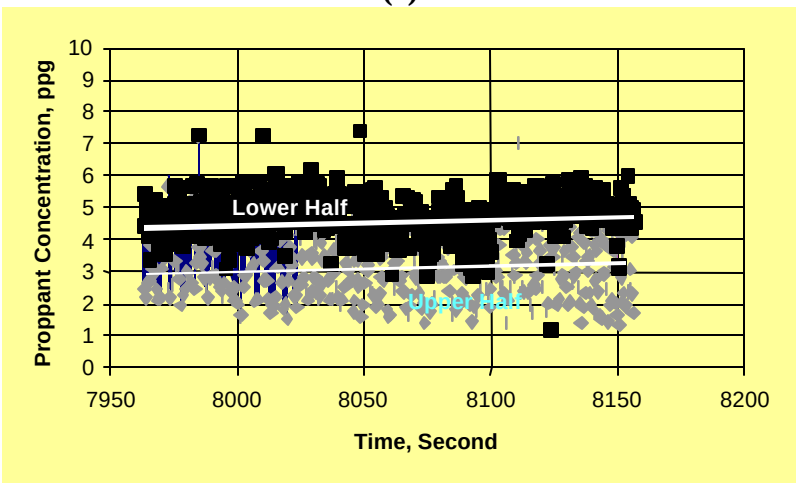

(b)

Figure 7.3.3 - Proppant Concentration within Two Halves of Encapsulated Slurry (a) During Initial 400 seconds (b) In Final 250 seconds

The static settling experiments showed a non-linear relationship between settling velocity and fluid viscosity of the fracturing fluids. A four fold increase in the fluid viscosity caused only one and half fold decrease in the settling velocity in linear HPG solutions, and a hundred fold increase resulted in almost 1000 times decrease in the settling velocity in crosslinked gels. This relationship is described in Table 7.3.1.

Fracturing Fluid	Fluid Viscosity (cp) at 5 sec^{-1}	Settling Velocity (cm/min)
Linear 40 lb/Mgal HPG	300	225
Linear 60 lb/Mgal HPG	1200	150
Borate-crosslinked 35 lb/Mgal Guar, pH 9.0	30,000	0.3

Table 7.3.1 - Relationship between Fluid Viscosity and Settling Velocity

The dynamic settling experiments showed that settling velocity increases as the shear rate is increased in a fracture because of a decrease in fluid viscosity with increase in the shear rate. The settling rates at various shear rates are shown in Figure 7.3.4 for a linear 35 lb/Mgal guar solution. For a crosslinked gel, on the other hand, rate of increment in sand concentration decreases with an increase in the shear rate. This effect of shear rate is shown in Figure 7.3.5 for a borate-crosslinked 35 lb/Mgal guar gel.

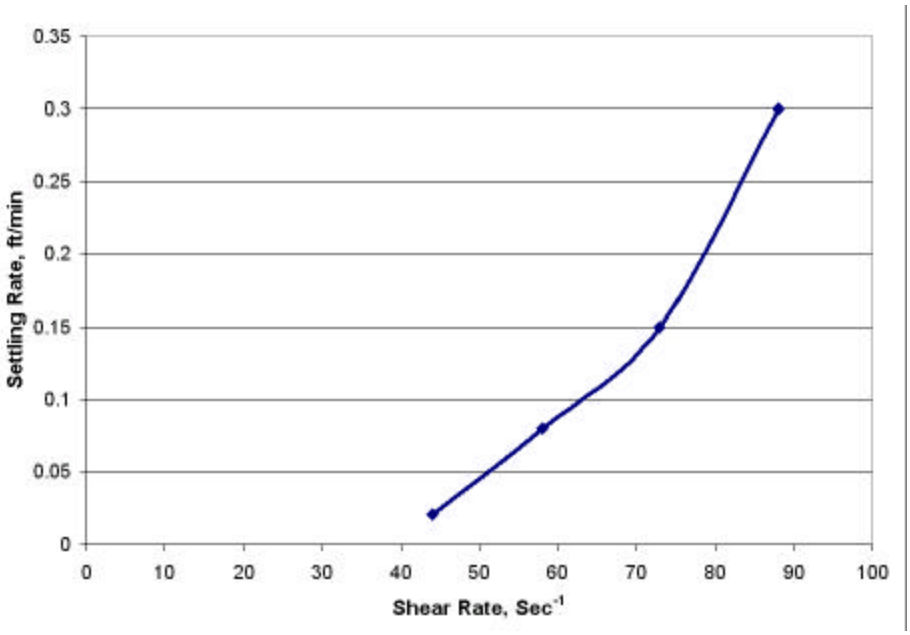

Figure 7.3.4- Settling Rate as a Function of Shear Rate for 35 lb/Mgal Guar Linear Gel

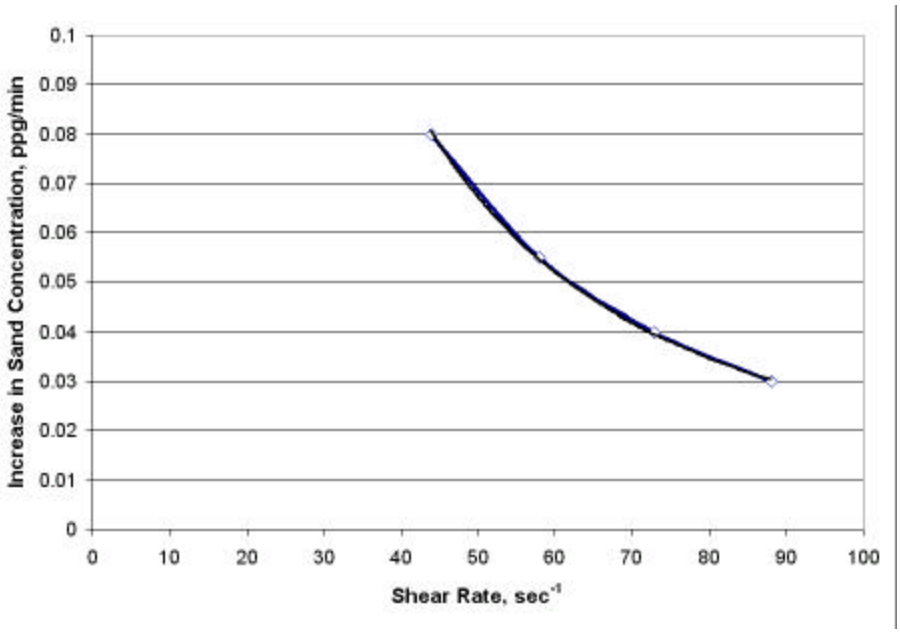

Figure 7.3.5- Proppant Settling as a Function of Shear Rate for a 7.3 ppg Slurry of Borate-Crosslinked 35 lb/Mgal Guar Gel in 0.375 in. Fracture Width

The bed erosion studies showed that the borate-crosslinked gel was able to remove particles from top of a compacted bed and transport them further down the fracture. The linear HPG gels, however, was able to remove upper layers only and was not capable of eroding the remaining compacted bed. Moreover, the linear gels exhibited a non-linear relationship between rate of erosion and fluid flush rate as shown in Figure 7.3.6.

In addition to the fluid effect, the bed erosion was affected by the perforation configuration used in the slot. The study showed that there exists a critical configuration in between the lower and middle perforations, which influences the fracturing fluid ability to transport proppant and erode the compacted bed.

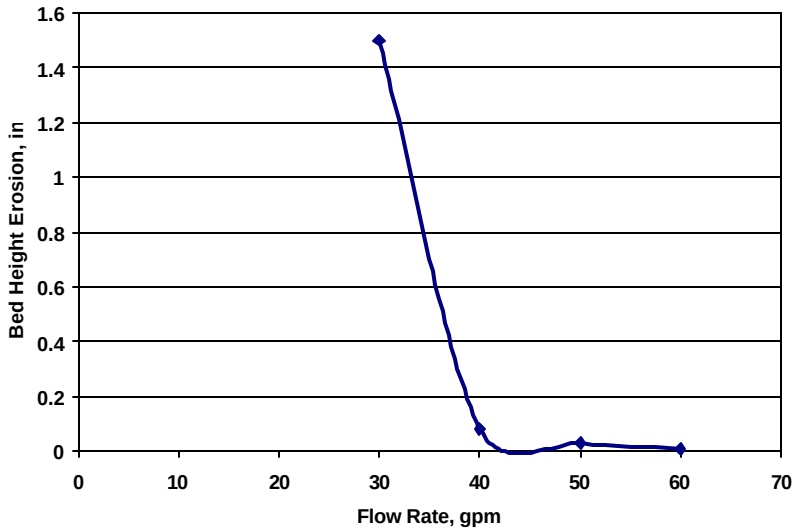

Figure 7.3.6-Relationship between Bed Erosion and Fluid Flow Rate for 40 lb/Mgal HPG

Implications of the Research Results:

1. Convection is a density driven phenomenon and in low viscosity medium it dominates proppant settling; hence, an optimum fluid viscosity exists that overrides the influence of the density to form convection.[15]

   Based on their study on Karo syrup and mineral oil, Cleary and Fonseca[18] concluded that the convection dominates proppant settling in a fracturing treatment. Their conclusion is however not supported in the results obtained at the FFCF where guar based linear and crosslinked-fracturing fluids are investigated in the HPS. The FFCF study shows that an increase in fluid viscosity, beyond an optimum value, overrides the density effects and thus prevents convective downward motion of the slurry and inhibits encapsulation. This result implies that when the high viscosity fracturing fluids are used in a well stimulation the convective phenomenon is unimportant.

2. Polymer concentration is a major factor that influences the convective downward motion of the slurry.[15]

   Clark[19] proposed a dimensionless model to identify whether the convection will be a controlling factor when a particular fracturing fluid is used. His model, however, does not include the effects of polymer concentration, which are shown to be important in the research results obtained at the FFCF. Therefore, the proposed model needs to be further evaluated to include a parameter that can more accurately describe the polymer concentration effects.

3. The FFCF study shows that crosslinked gel bed height erosion was eight times more than that by linear gel. Also, there is a threshold distance between the lower perforation and fracture bottom that greatly influences the ability of a fracturing fluid to transport or settle proppant, and to resuspend and erode the compacted bed.[16]

   The purpose of a stimulation treatment is to increase the well productivity by creating a uniform distribution of proppant pack in a fracture. To accomplish this objective, a fracturing fluid is required which can suspend and transport proppant in a fracture, and lift any settled proppant and transport them further into the fracture. These characteristics are exhibited in crosslinked fluids that were evaluated in the proppant transport study performed at the FFCF. The results show that the high viscosity crosslinked fluids not only have good proppant suspension capability, as is known to the industry, but also have better bed erosional and resuspension capacity. These two features give crosslinked guar fluids ideal characteristics to distribute proppant throughout the fracture.

4. The static settling experiments show that there is a non-linear relationship between the decrease in the settling velocity and increase in the fluid viscosity.[17] The dynamic settling experiments show that the settling rate increases when the fracture shear rate increases.[17]

   The non-linear relationship between the fluid viscosity and proppant settling implies that the viscosity is not sufficient to explain proppant suspension in a fracturing fluid and hence to predict proppant transport in the fracture. Hence,

industry should examine parameters other than the viscosity to better understand proppant carrying capabilities of the fracturing fluid.

7.4 Fluid Rheology

Objective: The purpose of the fluid rheology research was two-fold: (1) to evaluate fracturing fluid characteristics under various conditions of pH, shear history and temperature, and (2) to compare fluid behavior in laboratory and field scale characterization.

Introduction: Estimation of the fluid characteristics is crucial for success of a hydraulic fracturing treatment. A successful treatment means a wide fracture and a uniform distribution of proppant. These conditions can be created with proper selection and accurate characterization of the fracturing fluid. The impact of the fluids for the success of a fracturing treatment is exhibited in several case histories.

The knowledge of fluid characteristics is also important for computer simulations of the fracturing treatments, friction pressure loss estimations for the tubular flow and proppant transport evaluations in the fracture. Thus, the fluid behavior prediction is essential before performing stimulation in the field and during the fracturing treatments.

Procedure: The fluid rheology study comprised of preparing linear gel at different pHs, crosslinking it with boron chemicals, pre-conditioning the crosslinked gel through different shear histories, heating the gel and characterizing the fluid in the high pressure simulator. This study was performed at three fluid pHs (9, 10, and 11), four temperatures (ambient, 120, 150, 185 ^{o}F), and four shear pre-conditioning lengths (0, 1000, 3000, 5000 ft).

The comparison study was performed by simulating field scale fracturing operations in the FFCF and in the laboratories of three service companies test facilities. These companies volunteered to participate in a joint effort to understand fracturing fluid behavior. Both the FFCF and laboratories used identical chemicals, water, and fluid formulation procedure.

A detailed description of the procedure used to perform this study and results obtained from the study can be found in annual reports submitted to GRI[11-13] and technical papers presented in SPE conferences.[20-21]

Results: Prior to performing rheological characterization of fracturing fluids, measurements were made to confirm the accuracy and reproducibility of viscosities measured with the HPS slot. The result of this reproducibility test performed over seven days is shown in Figure 7.4.1. The figure shows that there is excellent agreement among measurements made on different days, verifying the reproducibility of the slot data for characterization of highly labile borate-crosslinked gels. These tests provide great confidence in the FFCF testing procedure and its capability to characterize fracturing fluids. Similar procedures were used in subsequent studies whose results are described below.

The results of the rheological characterization of borate-crosslinked guar are plotted in Figures 7.4.2 through 7.4.4 for three fluid pHs and at different shear histories and various temperatures. The figures show that the borate-crosslinked gel exhibit shear thinning as well as shear thickening behavior in the fracture shear rate range from 20 to 250 sec^{-1}. The figures also show that the fluid exhibit a shear history insensitive behavior for certain formulations. This shear history independent behavior is shown at 85, 150 and 185 ^{o}F for the borate crosslinked 35 lb/Mgal guar prepared respectively at pH 9.0, 10.0 and 11.0. Therefore, this characterization provides optimum fluid formulations for the hydraulic fracturing treatment. Moreover, the different optimized fluids have similar maximum viscosities as shown in Figure 7.4.5.

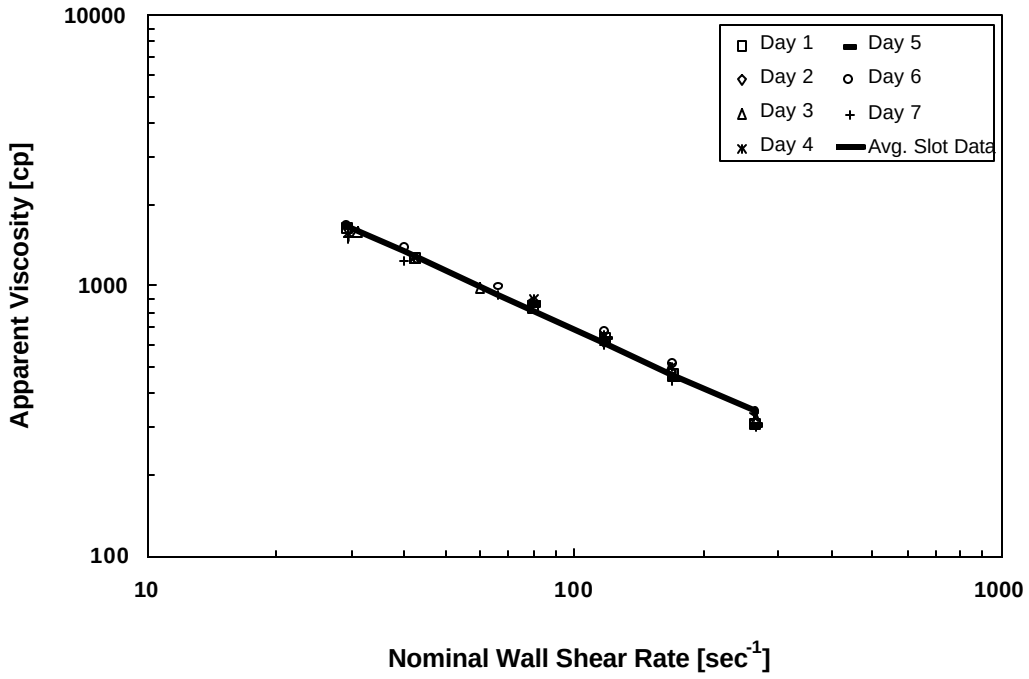

Figure 7.4.1-Rheology Characterization from Experiments Performed on Different days on Borate-Crosslinked 35 lb/Mgal Guar gel at 150^{o}F and no Shear Preconditioning

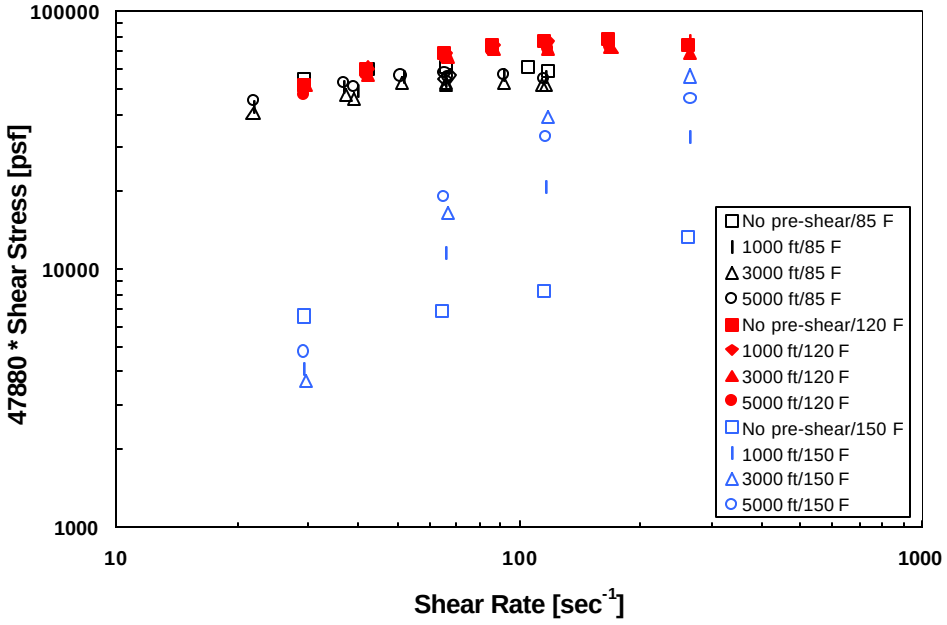

Figure 7.4.2-Rheology Data of Borate-Crosslinked 35 lb Guar/Mgal for pH 9.0 at Various Temperatures and Shear Histories

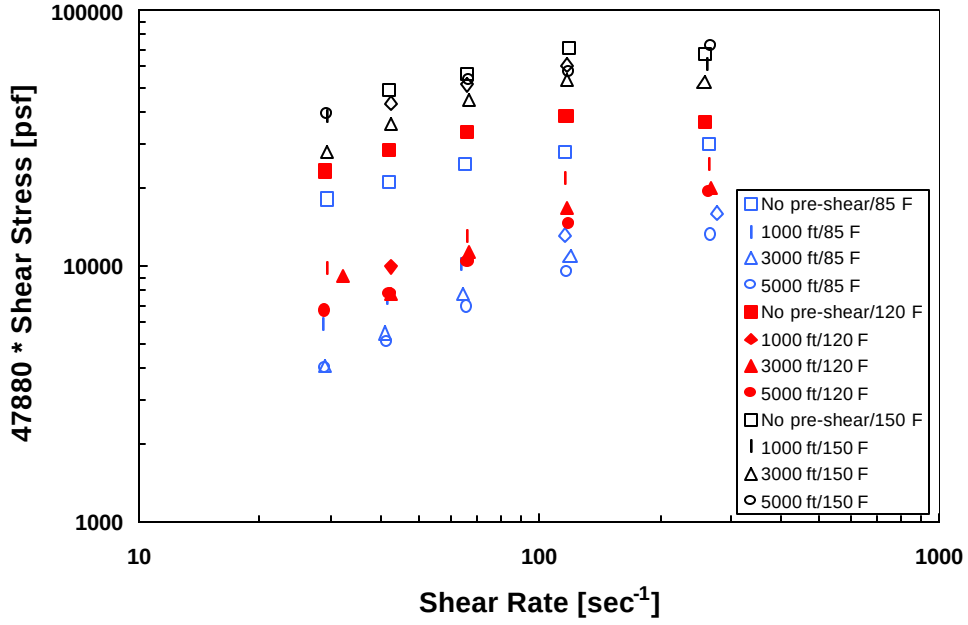

Figure 7.4.3-Rheology Data of Borate-Crosslinked 35 lb Guar/Mgal for pH 10.0 at Various Temperatures and Shear Histories

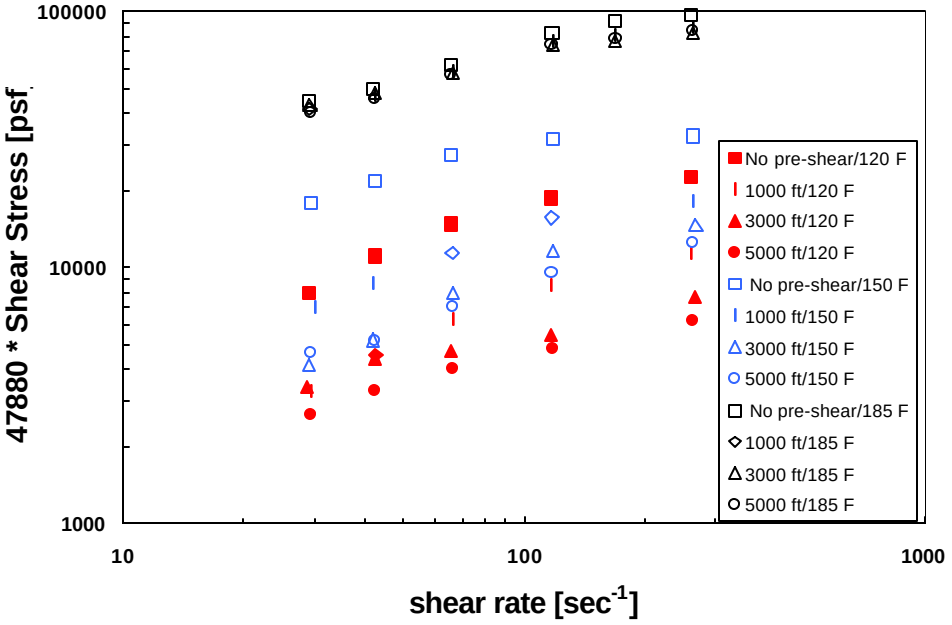

Figure 7.4.4-Rheology Data of Borate-Crosslinked 35 lb Guar/Mgal for pH 11.0 at Various Temperatures and Shear Histories

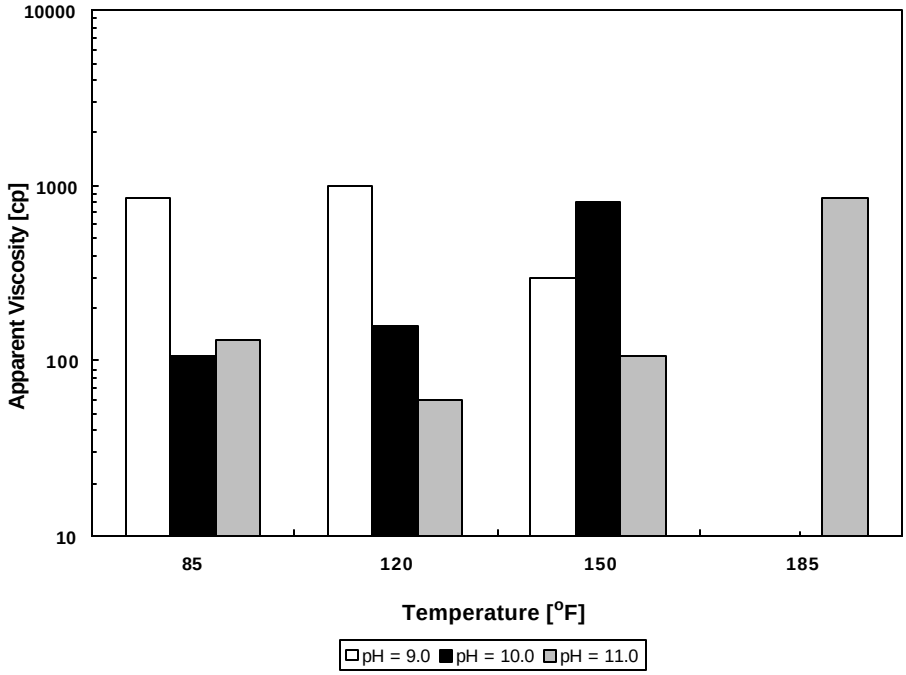

Figure 7.4.5-Apparent Viscosity at Various pHs and Temperatures for the Borate-crosslinked 35 lb/Mgal Guar gel at 65 sec^{-1} shear rate and 5 min shear history at 1400 sec^{-1}

The above gathered rheology data was used to develop a unique empirical correlation that relates nominal shear rate with apparent viscosity of borate-crosslinked 35 lb/Mgal guar as a function of wellbore shear preconditioning, reservoir temperature, and fracturing fluid pH. This correlation relates reduced apparent viscosities, μ_r, with reduced shear rates, $\dot{\gamma}_r$ as follows

$$\mu_r = K^*(\dot{\gamma}_r)^{A^* \log \dot{\gamma}_r + B} \quad \text{..... (7.4.1)}$$

where,

$$\mu_r = \frac{b_T}{a_T}\eta_{app} \quad \text{..... (7.4.2)}$$

and

$$\dot{\gamma}_r = a_T \dot{\gamma} \quad \text{..... (7.4.3)}$$

In eqns. 7.4.2 and 7.4.3, a_T and b_T are horizontal and vertical shift factors. These factors incorporate effect of temperature and shear history in the correlation as follows

$$\log a_T = \frac{-c_1(T - T_o)}{(c_2 + T - T_o)} \times \frac{1}{1 + c_3 Sn} \quad \text{..... (7.4.4)}$$

and

$$\log b_T = \frac{-d_1(T - T_o)}{(d_2 + T - T_o)} \times \frac{1}{1 + d_3 Sn} \quad \text{..... (7.4.5)}$$

In eqns. 7.4.4 and 7.4.5, *Sn*, is a dimensionless number called shearing number and it describes the shear preconditioning of the fluid in terms of energy required to pump fluid through the coiled tubing. The shearing number depends on fluid flow rate, *Q*, coiled tubing diameter, *D*, and pressure drop across the different lengths of tubing, ΔP, and fluid density, ρ, as

$$Sn = \frac{(Q\Delta p)D^4}{\rho' Q^3} \quad \text{..... (7.4.6)}$$

In eqns. 7.4.1 through 7.4.6, various constants were determined with the experimental data gathered at the FFCF. These constants are given in Tables 7.4.1 and 7.4.2 below.

pH	c_1	c_2 (^{o}F)	c_3	ESS_1	d_1	d_2 (^{o}F)	d_3	ESS_2
9	1.5	96.84	-0.00028	0.03622	-0.0689	-58.6	0.008	0.3463
10	-0.047	83.31	-0.0003	0.872	-0.434	-22	-0.00043	4.53
11	-0.036	74.50	0.0017	1.04	-1.047	-65.27	-0.000436	104

Table 7.4.1-Empirical Constants for Equations 7.4.4 and 7.4.5

pH	A	B	K	R^2
9	-0.6484	1.2405	671	0.92
10	-0.2994	0.4297	1275	0.888
11	0.2661	0.3662	1476	0.946

Table 7.4.2-Empirical Constants for Equation 7.4.1

The empirical equations are used to compare correlation calculated viscosities with the experimentally obtained values. This comparison is shown in Figure 7.4.6 for the fluid prepared at pH 9. The figure shows good agreement between the two values. Similar agreement was observed for other two fluid pHs 10 and 11.

Even though there is good agreement between empirical and experimental values, the correlation has some limitations. As the developed equations are empirical in nature, it must be used within the range of experimental measurements from which the rheology data is derived. These conditions are mentioned earlier in the procedure of the section 7.4.

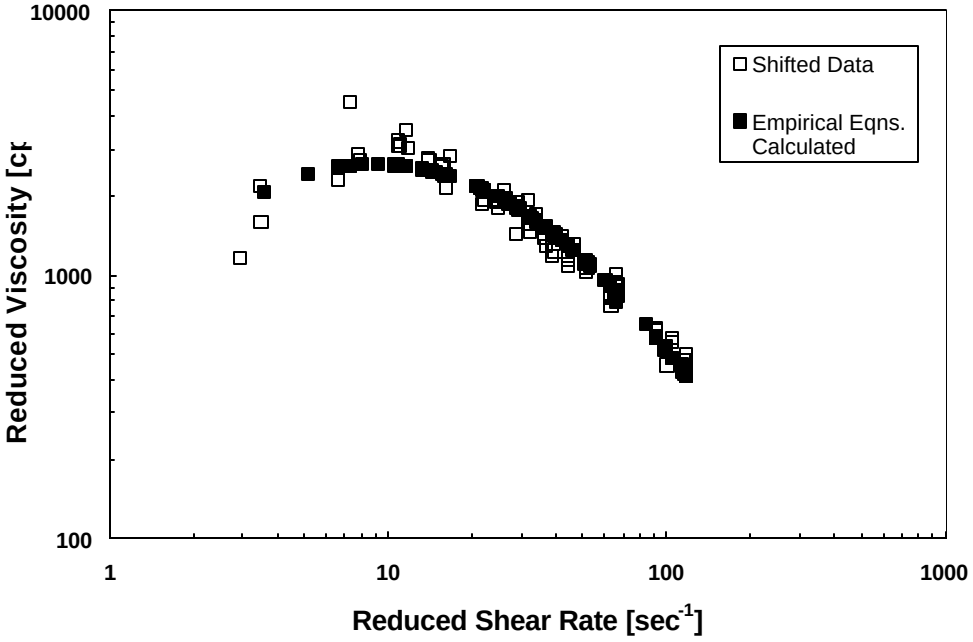

Figure 7.4.6-Comparison of Correlation Calculated Viscosities with Experimentally Obtained Values of Borate-Crosslinked 35 lb Guar/Mgal for pH 9.0

In addition to providing an empirical correlation for the fracturing fluids, the rheological characterization performed at the FFCF was compared with the laboratory measurements made at three service companies. This comparison is shown in Table 7.4.3. The table shows that laboratory measured viscosities are closer to that of the fluid subjected to zero shear history in the FFCF field scale fracture simulator. The laboratory viscosities, however, are very much different from values obtained for fluid subjected to shear conditioning representative of the wellbore.

FFCF Slot		**Company A**		**Company B**	**Company C**		**FFCF Laboratory**
Shear History	Slot	R1B5	R1B1	R1B5	R1B5x	R1B5x	R1B5x
No Shearing	689	588	553	1037	655	913	706
3000 ft	532	-	-	-	-	-	-

Table 7.4.3-Comparisons of Field and Laboratory Scale Characterization of Borate-Crosslinked 35 lb/Mgal guar viscosity (cp @ 100 sec^{-1}) at 150 ^{o}F

Implications of the Research Results:

1. The master curves provide fluid viscosity over a wide range of fracture shear rates without actually measuring the data over the entire range. Thus, the curves provide a unique approach to save time and to reduce costs of the rheology measurements.

   The master curves developed in this study will also help to address the question as to whether a fluid has sufficient viscosity after it is pumped through the wellbore, or what fluid formulation provides the required viscosity in the fracture. Often the industry compares the laboratory-measured rheology with viscosity-shear rate criteria developed by them through their experience from the numerous fracturing treatments. A similar comparison can be made between the industry-developed criteria and the master curve-calculated viscosities of several formulations. This comparison can tell which fluid formulation satisfies the criterion so that proper fluid formulation can be selected for a particular fracturing treatment. Thus, several fluid formulations can be evaluated with the help of the master curves.

   For example in a fracturing treatment, the tubing diameter and length are known from the well configuration; the friction pressure drop in the tubing is also readily available and so is the reservoir temperature. This information can be used to calculate shift factors from the empirical equations and to determine the fluid viscosities using the master curves provided in this paper. Moreover, the developed empirical correlation can be incorporated into fracturing software to readily and reliably calculate fluid viscosity in the fracture.

2. The comparison of the fluid rheological characterization between the laboratory and field scale measurements at the FFCF showed that the viscometers provide viscosity

values closer to those measured with the HPS under the no pre-shear condition. The results, however, also showed that the viscometer values differ considerably from the HPS viscosities measured after shear conditioning through 3000 ft length of the coiled tubing.[21] This result implies that the crosslinked fluid may exhibit ideal fluid properties under laboratory conditions, but under actual field conditions its behavior may be completely different.[20] Hence the borate crosslinked fluid rheology must be determined under conditions that closely simulate pumping environment through the wellbore and therefore, the laboratory characterization must incorporate shear history simulations prior to the viscometric measurements.

Sometimes, however, it is difficult to incorporate shear history simulation in the laboratory measurements, an inexpensive alternate method could be to use the empirical correlation developed at the FFCF[22] as this correlation incorporates the effect of shear history on the viscosity. For example in a fracturing treatment, the wellbore tubing diameter and length are known from the well configuration; the friction pressure drop in the tubing is also readily available and so is the reservoir temperature. This information can be used to calculate shift factors from the empirical equations and to determine fluid viscosities using the master curves provided in the study. The viscosities calculated using the correlation would thus include tubing shear history and would more accurately correspond to the fluid behavior in a fracture.

7.5 LDV Study

Objectives: The objective of the study is (1) to explore the potential and capabilities of the assembled slot flow loop for measuring point velocities and thus velocity profiles of the fluids of interest, (2) to observe plug flow phenomena and experimentally determine corresponding threshold flowrates, and (3) to determine experimental velocity profiles of proppant-laden fluids and comparison with a theoretically developed velocity profiles.

Introduction: In the recent past, the application of LDV systems upon slot experiments has yielded a great deal of information regarding the valuable parameters related to fracturing fluids. The LDV systems have shown great promise for the slot/fracture simulation experiments and the advantages include:

- Flow type determination, that is, whether the flow in fracture is uniform and laminar or turbulent.
- Velocity profile determination. This provides fracturing fluid rheologist a better idea about the condition of the fracturing fluid at various points in the flow due to entrance effects and/or settling of concentrations.
- Realistic modeling / simulations of fractures and flow situations.
- Proppant-settling phenomena investigation (in both dynamic and static flow situations) over a variety of fluid and proppant concentrations.
- Velocity profile determination for drilling and completion fluids.

Even though LDV has proved itself a valuable technique for fluid applications, it does have a major drawback. This major drawback lies in its high sensitivity to small details related to both procedural and experimental setup. However, it should be noted that most of the burden for LDV accuracy falls upon the experimenter who must construct a precise experimental setup and follow a detailed procedure with full attention to all the precautions.

Since LDV application upon fluid systems is relatively new and requires sophisticated electronic tools, there have been only a few studies conducted, and the data or information gathered is not enough to explore the full potential and application of LDV systems. The work at hand is an attempt to explore the potential and capabilities of an LDV based slot system for important design parameters related to fractures and fracturing fluids.

Procedure: In simple terms, the integrated translational motion scale was used to move the LDV probe (inwards and outwards), and the total gap is traversed by measuring point velocities at incremental distances across the slot gap. The gap can be traversed by either traversing the gap from the front wall to the back wall (i.e. front traversing) or the other way round (i.e. back traversing). In either case it is crucial to coincide the two laser beams perfectly, otherwise, the point velocities measured would not represent the actual location. Typically, an error in beam coincidence is indicated in terms of horizontal shift of experimental profile with respect to the theoretical velocity profile. Similarly, if the flow rate is not measured correctly, the experimental velocity profile shows lateral shift with respect to the theoretical velocity profile. Fig. 7.5.1 shows graphical representation of the procedure used for point velocity determination.

Results:

1. <u>Location Experiments</u>

A series of experiments was performed at different locations on the slot, namely A, B, C, D, and E, using the various concentration of 40 lbm/Mgal HPG fluid (Fig. 7.5.2). Using the correlation for the entrance length of non-Newtonian fluids in turbulent flow, an entrance length of 7.0 inch was calculated. Since all the selected locations were two or more feet beyond the entrance, it was thus established that the LDV measurements at these locations would not be affected by the entrance effects.

Experimental velocity profile acquired at point 'A' for 40 lbm/Mgal HPG showed an average correction factor (Correction Factor = Theoretical/ Experimental) of 1.30 when compared to the theoretically developed velocity profile. Similarly, experimental velocity profiles were acquired at locations B, C and D for the same fluid and the correction factors thus obtained at these locations are presented in Table 7.5.1.

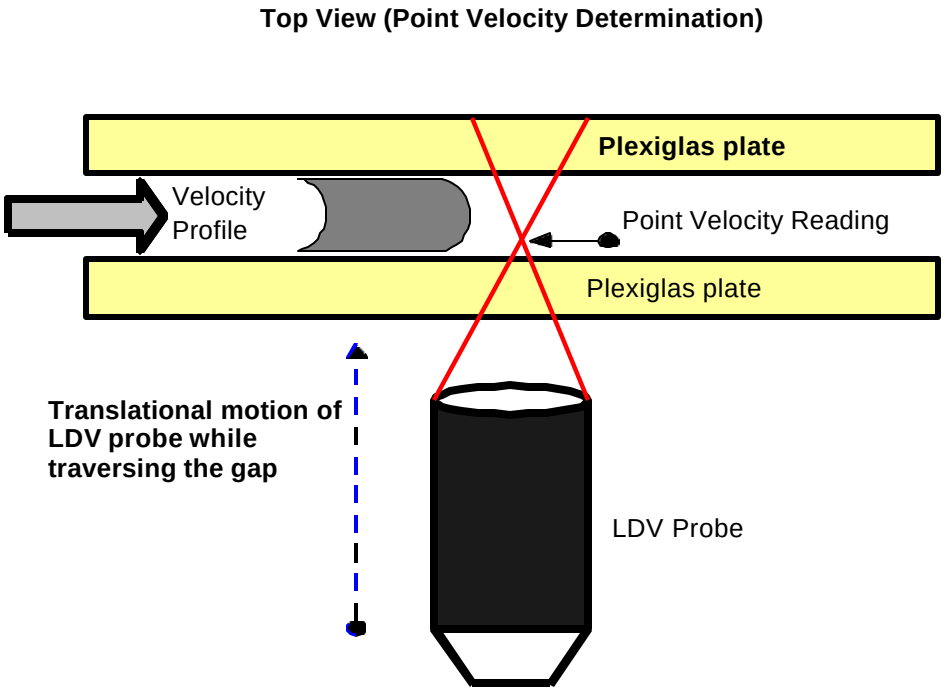

Figure 7.5.1-Velocity Profiling by LDV

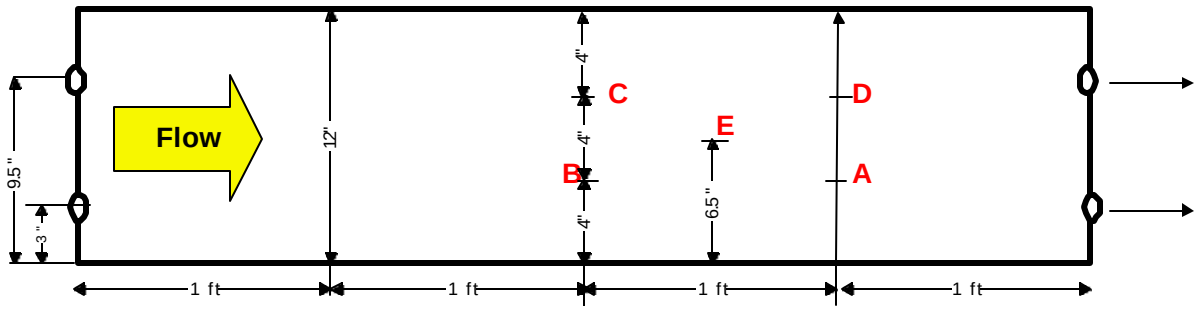

Figure 7.5.2-LDV Reading Locations

Table 7.5.1 - The Theoretical/Experimental ratios at Various Locations

Location	Theo./Exp.
A	1.28
B	1.45
C	1.33
D	1.37
E	1.00

Different concentrations of HPG were tested at location E to cover wider range of "*n*". The results showed good agreement between the theoretical and experimental velocity profiles. A Newtonian fluid (corn syrup) was also tried at location E to confirm whether the above-mentioned agreement is valid for other fluid models.

An interesting phenomenon observed during location experiments is the varied gap size at different locations. The gap size at E is 10.0 mm and at locations A, B, C, and D it is between 8.0-9.0 mm. This is a unique application in which LDV was used to determine actual gap size distribution of the slot. In order to measure the gap sizes at other locations, two holes were drilled into the midsection near the inlet, and gap size was manually measured to be 11.6 mm. The slot, thus have a highly variable size distribution. Figure 7.3.3 shows the gap size distribution of the slot. Table 7.5.2 shows the test matrix of the location experiments performed during this study.

Table: 7.5.2 - Location Experiments

no.	Fluid	lb/Mgal	n	K (eq.cp)	N_{Re}	q (gpm)	Vel-ft/sec
1	Guar-HPG	40	0.41	1200	13.7	3.84	0.29
2	Guar-HPG	40	0.42	1300	10.4	3.46	0.26
3	Guar-HPG	40	0.43	1300	9.9	3.40	0.25
4	Guar-HPG	40	0.42	1300	9.0	3.17	0.24
5	Guar-HPG	40	0.46	1300	11.5	4.08	0.30
6	Guar-HPG	60	0.33	3201	5.0	2.72	0.20
7	Guar-HPG	70	0.30	3460	3.4	2.80	0.21
8	Guar-HPG	80	0.15	19065	1.0	1.75	0.13
9	Corn Syrup	x	0.99	x	9.0	2.28	0.17

Note: ' x ' implies data were not acquired.

By trial and error, an area was established which when used in the theoretical velocity profile equations all the profiles matched at all the locations. The results obtained at location E for 40 lbm/Mgal HPG is shown in Fig. 7.5.4.

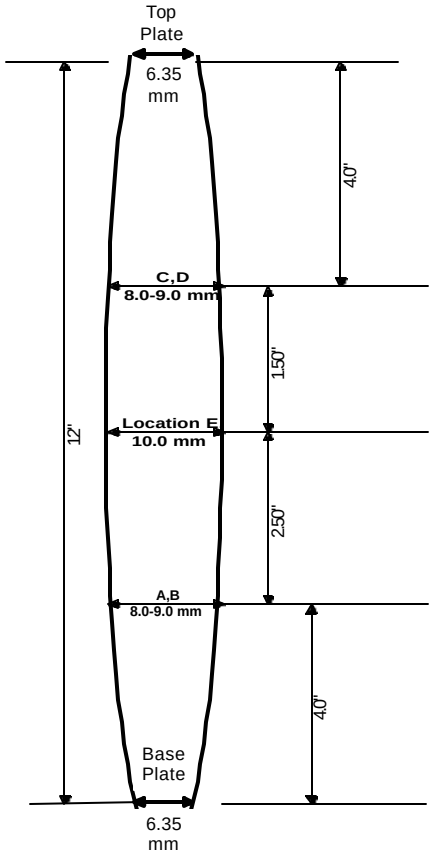

Figure 7.5.3 -Gap Size Distribution of Slot

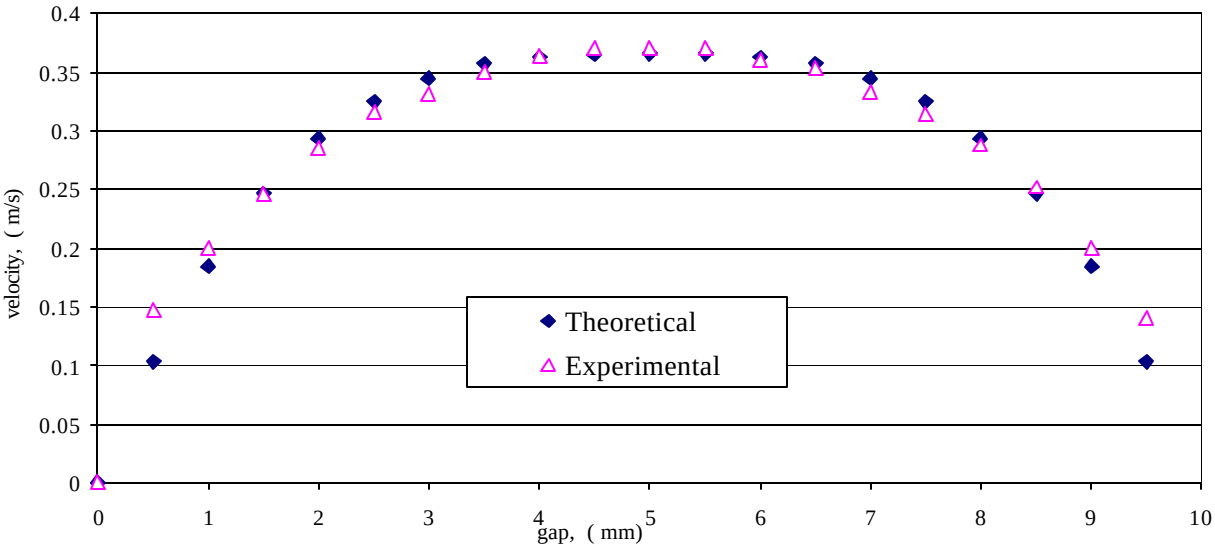

Figure 7.5.4 - Location E, 40 lbm/Mgal HPG, *q* = 4.08 gpm, *n* = 0.464

2. Multirate Experiments

Multirate experiments were conducted to investigate the so-called "plug flow" phenomenon, which is observed when the flow rate does not generate enough shear stress to exceed the yield stress of the flowing fluid. The velocity profile of the fluid having complete plug is totally flat and there is no significant curvature in the otherwise parabolic shape.

First multi-rate experiment was conducted with 40 lbm/Mgal Xanthan fluid at the flow rates of 3.17, 2.28, 1.60, and 0.60 gpm. When the data were analyzed and velocity profiles were plotted, complete plug flow was observed to be started at some flow rate between 1.60 gpm and 0.60 gpm (Fig. 7.5.5).

It can be seen in Fig. 7.5.5 that the shape of the velocity profiles changed from the highest flow rate to lowest flow rate, that is, the size of top plateau or the plug region is decreasing with the increasing flow rates.

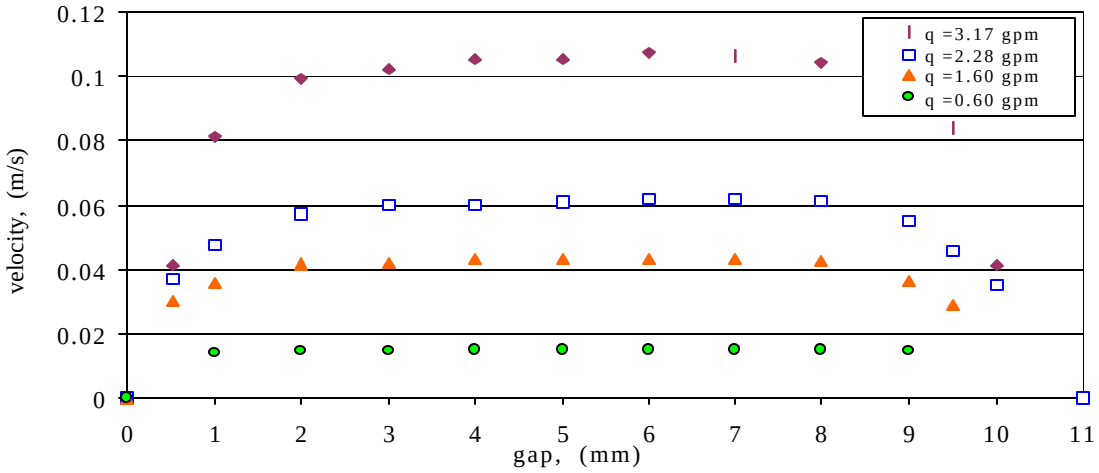

Figure 7.5.5- First Multirate Experiment Showing Plug Flow at 0.6 gpm

A second multirate experiment (3.0, 1.30 and 1.05 gpm) was performed with the identical fluid (40 lbm/Mgal Xanthan), focussing on the lower flow rate range to determine the flow rate at which the fluid starts flowing with a complete plug flow. The analysis of the second multirate experiment exhibited complete plug flow at the flow rate of 1.05 gpm as shown in Fig. 7.5.6.

There seems to be insignificant difference between the two profiles (Fig. 7.5.6) obtained at 1.30 gpm and 1.05 gpm. However, when the velocity profiles for 1.30 gpm and 1.05 gpm were plotted on a separate chart, the plug phenomenon at the lower flow rate 1.05 gpm seemed to be more pronounced (Fig. 7.5.7).

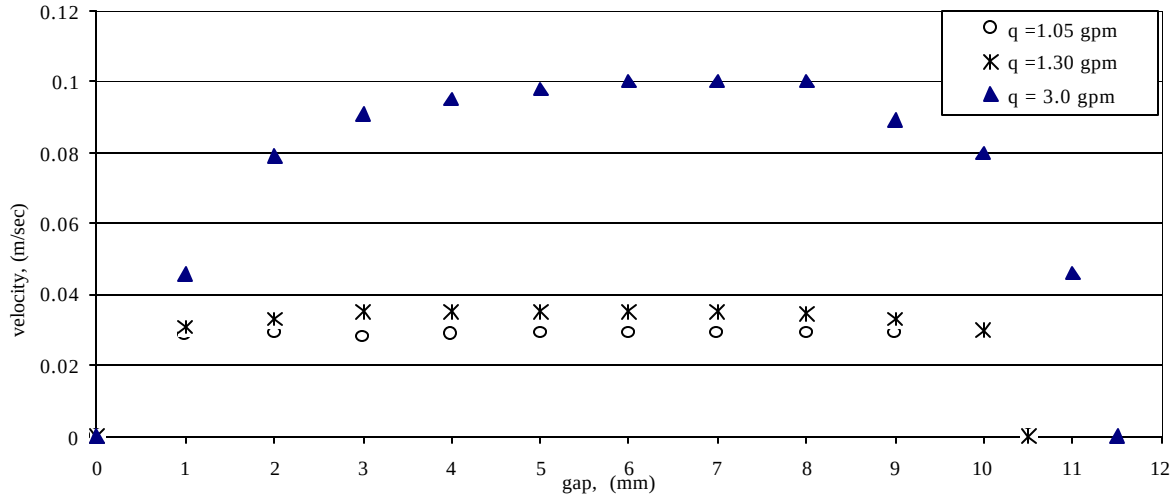

Figure 7.5.6 - Second Multirate Experiment 40 lbm/Mgal Xanthan, *n*=0.33

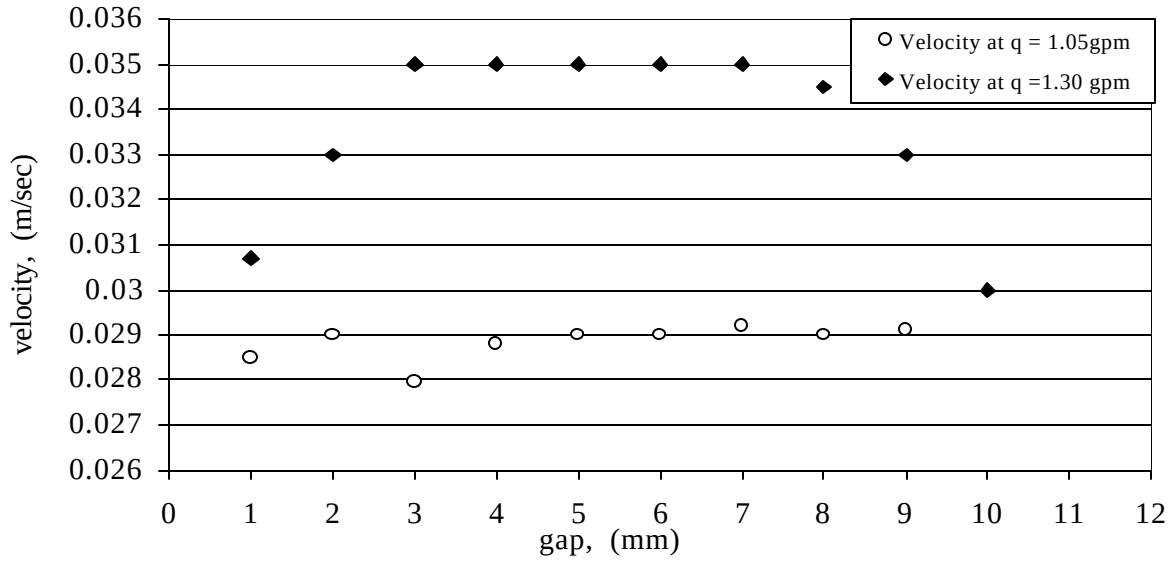

Figure 7.5.7 - Comparison Between the Two Flow Rates 1.30 and 1.05 gpm

Thus, LDV technique was successfully used to experimentally establish a threshold flow rate at which the fluid just started flowing with a complete plug. Knowing this threshold flow rate is an important parameter as it could be used for:

- Determining the highest flow rate that can be afforded to keep the fluid in the plug flow condition so that the fluid can efficiently carry or transport cuttings with its flow.
- Designing the fluids for special applications like cementing and fluid displacements.
- Planning the flow rates schedule for different petroleum engineering operations involving fluids.

3. Experiment with Proppant-Laden Fluid

The LDV-based system was also applied upon proppant-laden fluids to test its applicability to complex fluids. These experiments were intended to address the fluids that are rheologically too complex to be explained by any available rheological model.

The initial experimental plan was to increase the proppant concentration from 1 ppg to higher concentrations systematically and measure the velocity profiles at each concentration. When 1ppg experiment (1 lbm of 20/40-mesh sand per 1 gal 50 lbm/Mgal Xanthan) was carried out at the flow rate of 3.0 gpm, high settling rate was observed. The pump pressure could not be increased further because the slot had already started leaking. Though the leak was not intense it indicated that the joints and connections are not designed for higher flow rates.

The velocity profile of first proppant concentration (1 pound 20/40 mesh sand per 1 gal of 50 lbm/Mgal Xanthan) at flow rate of 3.0 gpm was completed successfully and is shown in Fig. 7.5.8. The pump pressure (rpm) was increased in an attempt to slow down the settling and 2-ppg experiment was run immediately, but the increased rpm did not help and settling continued until the experiment had to be stopped. However about 65 % of the gap was still covered as plotted in Fig. 7.5.9.

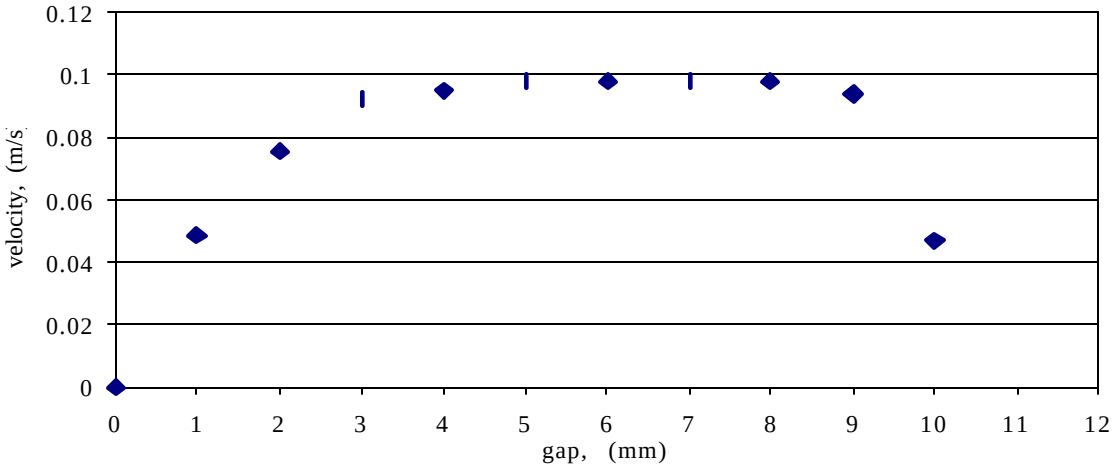

Figure 7.5.8 - LDV Application for Proppant-Laden Fluid (1 ppg) at 3.0 gpm

Currently, the flow loop system has plastic pipes and flexible hose connections, which is a very weak setup for this kind of proppant-laden fluid experiments. Technically speaking, the system has worked successfully with the proppant-laden fluids but the limitation imposed was the pressure rating of the slot which forbade the necessary higher flow rates required to prevent settling in the slot gap. The solution to this problem, however, does not call for major changes in the setup. Metal plate reinforcement on the slot structure and rigid pipe connections may be used as a viable solution to this problem.

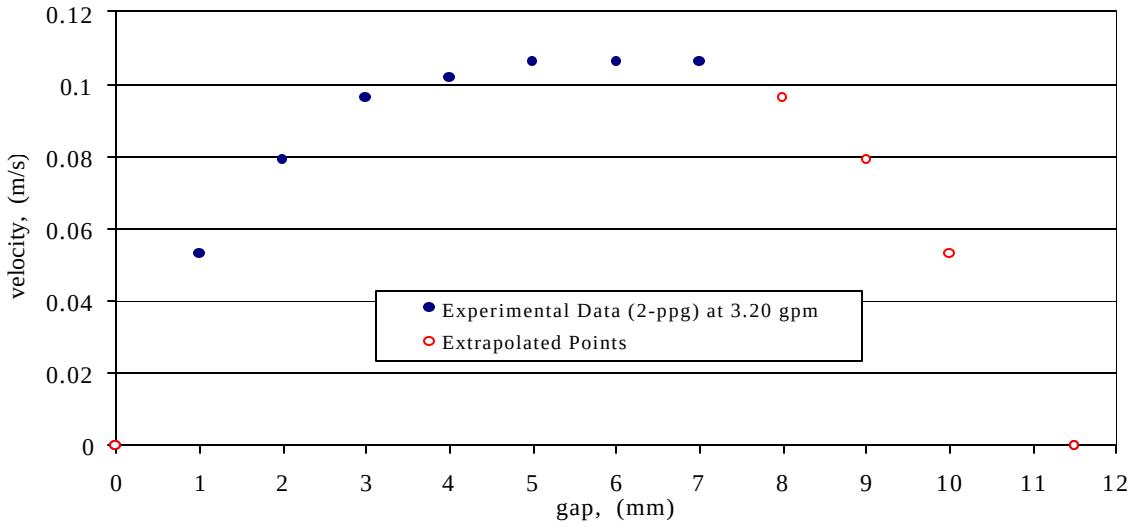

Figure 7.5.9 - LDV Application for Proppant-Laden Fluid (2 ppg) at *q* =3.20 gpm

Thus, following conclusions could be drawn from the study. During this LDV work, the shape of the slot gap size was identified to be an oval rather than a rectangle. Multirate experiments with Xanthan (a yield fluid) helped determine a threshold flow rate at which the phenomenon of plug flow begins. The setup was applied upon the proppant-laden fluids and experimental velocity profile was acquired for 1-ppg sand concentration. The existing setup was found to be unsuitable (because of its low pressure rating) for the higher proppant concentrations.

Implications of the Results: The current experimental work offers many possibilities for future adventures in the LDV applications upon slot experiments. For example, the following applications may be realized using this type of experimental setup.

1. The LDV technique could be applied to identify the actual gap size distributions (or gap uniformity) in the transparent or semi-transparent flow loops.

2. Entrance length may be easily determined for any fluid by measuring the velocity profiles along the length of plexiglas slot. One may also replace slot with the plexiglas pipe to determine the entrance length of a pipe. Since LDV can be used to indicate the entrance effects, so it could be used to design "adjustments" to the inlet and exit of the slot to improve flow uniformity. For example, one may measure entrance length after incorporating certain design adjustments and reach a design at which the entrance length is minimum.

3. Uniformity of velocity profile of a proppant-laden fluid is a qualitative indicator of successful design because such a fluid can deliver proppant deeper into the formation while fracturing. Manipulating the parameters related to either the proppant or gel can improve velocity profiles and hence can help design the best proppant-gel combination for the fracturing job.

7.6 Foam Fluid Rheology

Objective: The objective of the Foam Fluid study was to determine the effects of foam quality, temperature, and gelling agent concentration on foam viscosity and develop empirical correlations to predict foam viscosity as a function of foam quality and temperature.

Introduction: The use of foamed fluids in the petroleum industry has been widely recognized. Foams have been in use for applications such as a fracturing, stimulation, completion, and drilling due to their very unique properties. The properties are - high viscosity, low liquid content, low fluid loss, high carrying capacity, low hydrostatic head, low pressure loss due to friction, quick fluid recovery and good clean up performance, low formation damage, and no reduction of fracture conductivity due to fluid ingredients. When foam reaches the pit or tank it can be broken rapidly, so only the liquids comprising the foam solution and contaminants must be handled. Inspite of their importance, relatively little has been studied about foams. This task is made even more difficult because of the presence of the gas phase whose properties change with temperature and pressure.

Procedure: The foam loop at the WCTC was used for the rheological characterization of foam fluids. A brief description of this flow loop and a schematic is provided in Chapter 4. For this investigation, the liquid phase was prepared by mixing powdered xanthan/Guar and water. Then a foaming agent was added and mixed. The liquid phase was then mixed with a gas phase (nitrogen). Different gelling agent concentrations 20, 30, and 40 lb/Mgal of water were used. A 0.5% (vol.) of the foaming agent concentration was used for all the tests carried out. This is the recommended concentration for the test conditions used, as previously found at WCTC. For Xanthan foam, a ½ inch outside diameter (0.43 in ID) pipe was used for all the tests. In case of Guar, two pipe sizes- 1/2 and 3/8 in were used. Experiments were carried out at ambient temperature as well as at temperatures ranging from 75 to 200°F.

An average absolute pressure of 1000 psia was used for all the tests. This level of absolute pressure allowed the assumption that foam quality is constant and homogeneous inside the loop. Although this is not absolutely true, this assumption is necessary for data analysis purposes and does not lead to significant errors given the shortness of the loop. The test matrix for Xanthan foam is shown in Table 7.6.1.
Table 7.6.2 shows that a total of two aqueous foams and four gelled foams were tested. The foams were generated with nitrogen as the gas phase and Howcosuds® or Sodium Dodecyl Sulfate (SDS) as the foaming agent. The liquid phase was either water or guar polymer solutions. All tests were performed at 1000 psi and ambient temperature conditions.

Table 7.6.1: Test Matrix for Xanthan

No.	Gel (lb/Mgal)	Temperature (^{o}F)					
		75	100	125	150	175	200
1	20 lb Xanthan	x	'x	x	x	x	x
2	30 lb Xanthan	x	'x	x	x	x	x
3	40 lb Xanthan	x	x	x	x	x	x
4	40 lb PHPA	x	-	-	-	x	-

Table 7.6.2 Typical Test Matrix for Guar Foam Rheology Study

Test Number	Foam Type	Liquid Phase	Foaming Agent
Test 1	Aqueous	Water	0.5% (vol.) Howcosuds
Test 2	Aqueous	Water	1.0% (vol.) Howcosuds
Test 3	Gelled	0.5% (wt.) Guar	0.5% (vol.) Howcosuds
Test 4	Gelled	0.5% (wt.) Guar	0.25% (wt.) S.D.S.
Test 5	Gelled	1.0% (wt.) Guar	0.5% (wt.) S.D.S.
Test 6	Gelled	0.5% (wt.) Guar	0.125% (wt.) S.D.S.

A similar procedure was followed for Guar foam at 20, 40, 60, lb/Mgal gel concentration and qualities ranging from 0 to 80 %. Rheograms were then developed for Xanthan and Guar foams and comparisons made between Guar, Xanthan and PHPA foams. Effects of quality, temperature, gelling agent concentration on viscosity were studied.

Results: Foam fluids exhibit non-Newtonian behavior in which the foam viscosity decreases with increasing shear rate. Rheograms for the foam fluids are shown in Figure 7.6.1. The figure describes the apparent viscosity of foams as a function of their quality. The foam quality is the most important parameter for foam rheology. The figure shows that for a given shear rate, the foam viscosity increases with increase in the foam quality.

In addition to the gas phase fraction, liquid phase composition also affects the foam viscosity. The effect of change in liquid from water to a viscous guar solution is shown in Figure 7.6.2. The figure shows that an increase in liquid viscosity results in an increase in the foam viscosity. The figure also shows that the foam viscosity increases for an increase in the guar concentration. On the other hand, an increase in foaming agent concentration did not have any effect on the foam viscosity. A change in foaming agent concentration from 0.125 to 0.25 does not exhibit any change in viscosity as shown in Figure 7.6.3. The data in this figure are drawn for foams having similar quality and same liquid phase.

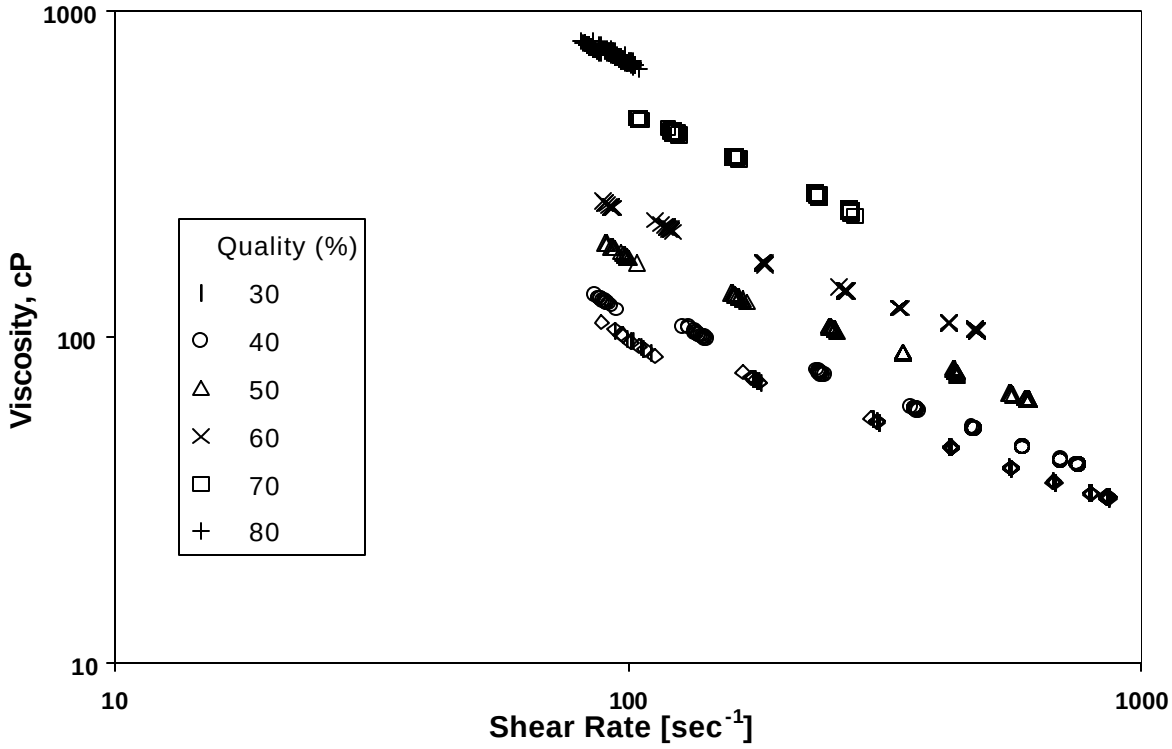

Figure 7.6.1 Effect of Quality on Apparent Viscosity of 0.5% (wt.) Guar Foam Prepared Using 0.5% (vol.) HowcosudsÒ

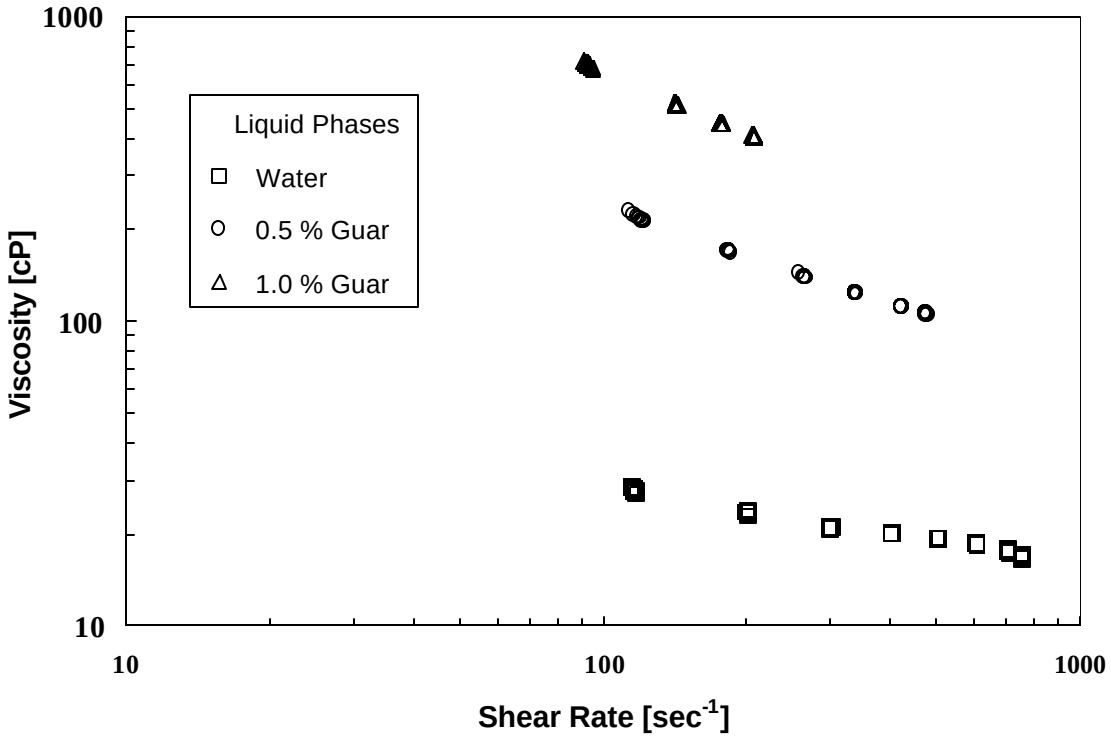

Figure 7.6.2 Effect of Liquid Phase Composition on Viscosity of a 60% Quality Foam

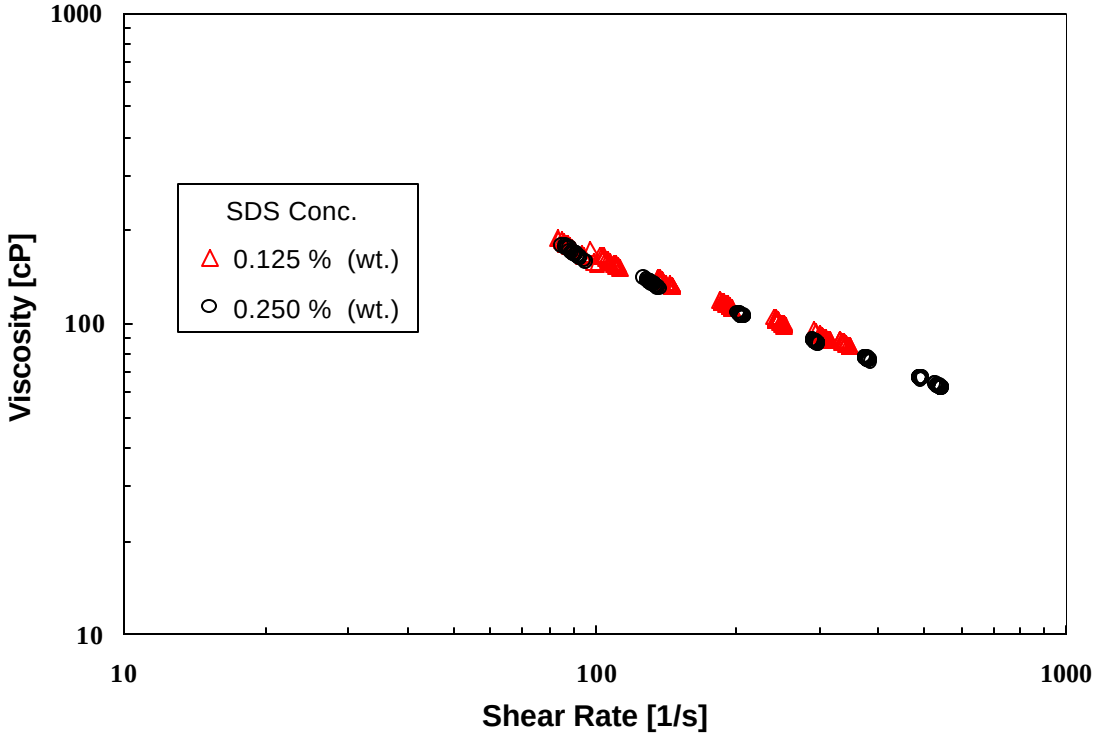

Figure 7.6.3-Effect of Foamer Concentration on Viscosity of 0.5% (wt.) Guar Foam of 50% Quality

Correlations such as the one shown in Fig. 7.6.4 and 7.6.5 were developed for Xanthan foam

Using the model parameters from this study, apparent viscosity was calculated at a shear rate of 511 s^{-1} using Eq. 7.6.1. By dividing the flow behavior index of the foam with the flow behavior index at 75 ^{o}F, a value close to 1 was obtained. For subsequent analysis, the flow behavior index for the foam was taken as that of the gel and with the previously calculated viscosity, the foam consistency index was calculated.

By dividing the foam consistency index with that of the liquid gel, a relative value was obtained. Figures 7.6.4 and 7.6.5 show the relationship of the relative consistency index and yield stress as a function of quality at different temperatures. The relative consistency index and the yield stress increased gradually at low qualities, then rose exponentially as the quality increased beyond 60%. The data was a bit scattered at 80% quality for the high temperature experiments. The following correlations were obtained.

$$\frac{K_F}{K_L} = e^{(1.556Q_a + 2.813Q_a^2)} \quad \text{.....} \quad (7.6.1)$$

$$t_o = 0.013e^{3.5Q_a} \quad \text{.....} \quad (7.6.2)$$

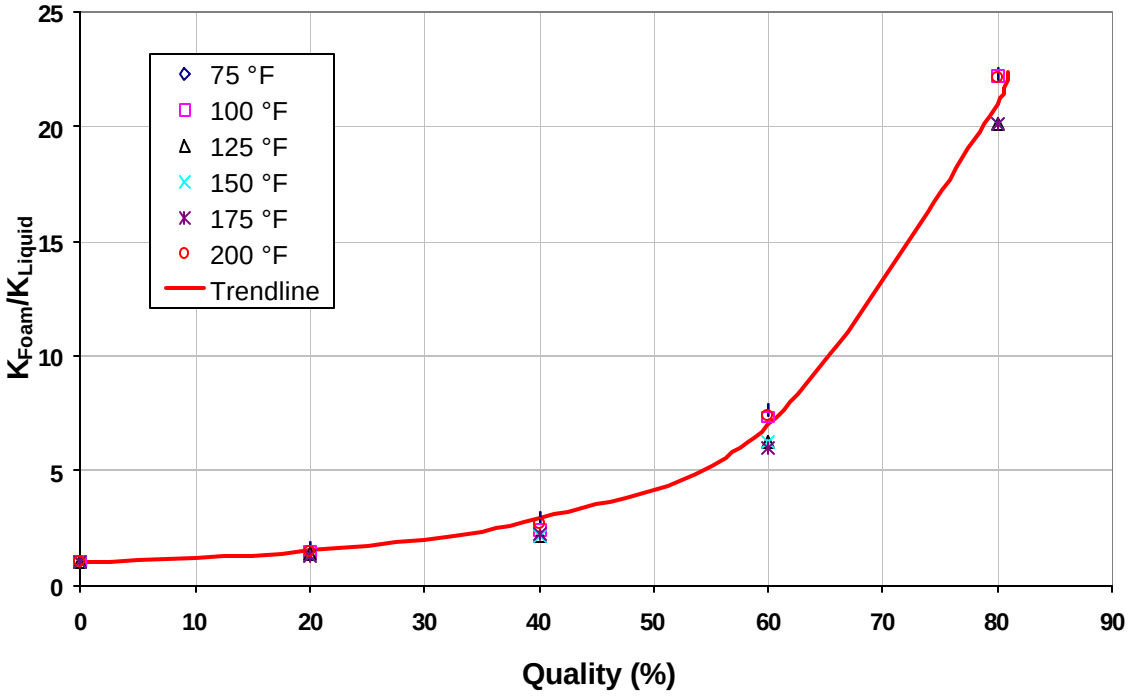

Figure 7.6.4-Relative Consistency Index for 20 lb/Mgal Xanthan Foam

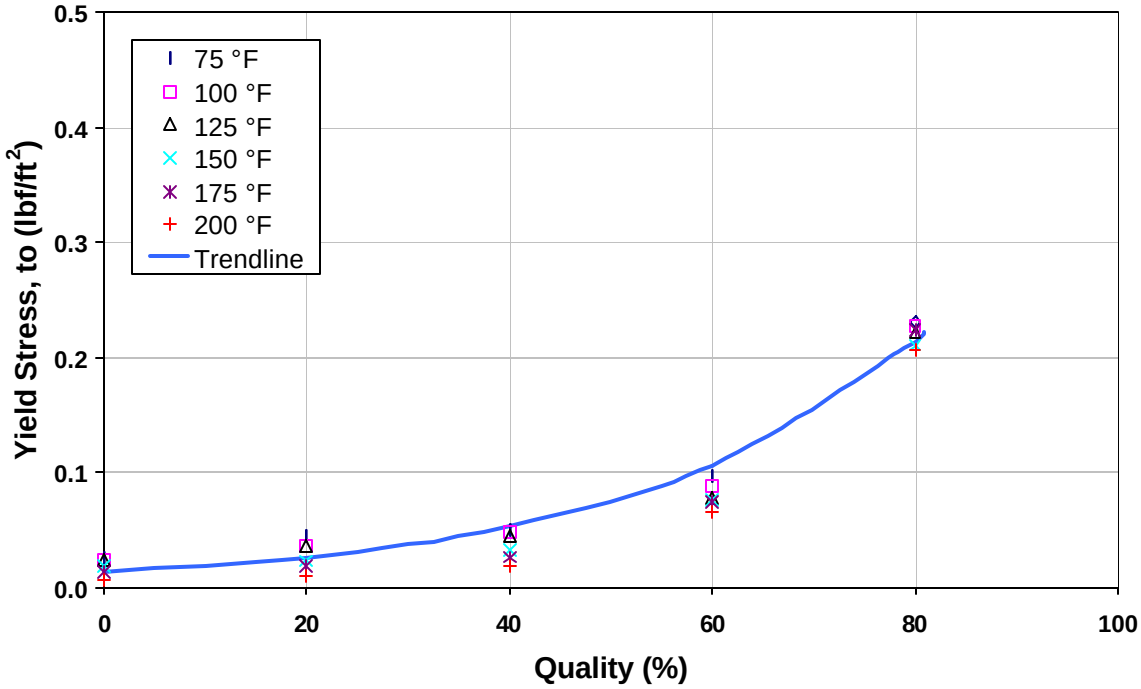

Figure 7.6.5-Yield Stress as a Function of Quality for 20 lb/Mgal Xanthan Foam

Similar correlations were developed for Guar foam. The ratio of the foam consistency index to the liquid phase flow consistency index can be approximated by the following equations for 20 lb/Mgal and 40 lb/Mgal guar gels respectively,

$$\frac{K_f}{K_L} = e^{\left(0.5168Q_a + 4.1224Q_a^2\right)} \quad \text{.....} \quad (7.6.3)$$

$$\frac{K_f}{K_L} = e^{\left(0.01182Q_a + 2.9396Q_a^2\right)} \quad \text{.....} \quad (7.6.4)$$

Trends similar to those in Xanthan were observed in case of Guar. A comparison was made between Xanthan, Guar and PHPA foam. As an illustration, a comparison between Xanthan and Guar foams is shown in Fig 7.6.6.

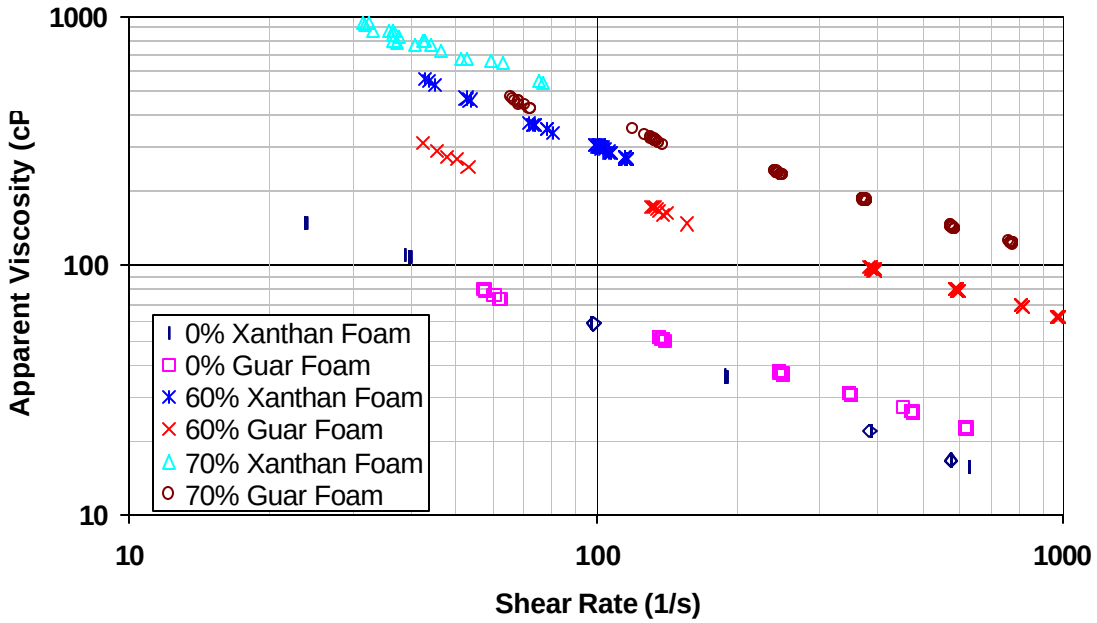

Figure 7.6.6 Apparent Viscosity Comparison for 40 lb/Mgal Xanthan Foam and 40 lb/Mgal Guar Foam at 100 ^{0}F

Implications of the Research Results:

1. The foam viscosity increases with an increase in the foam quality. This result implies that a higher fraction of gas in the foam can be used to generate a viscous fluid. As high viscosity is useful to successfully transport proppant in a fracture, the higher quality foams are better choice to perform a fracturing treatment and stimulate a well. Similarly high viscosity is required to transport wellbore cuttings during a drilling operation; thus the higher quality foam is a better choice for a drilling fluid.

   The higher quality foam contains a lower fraction of the liquid in the foam. It means that a smaller amount of liquid will leak off into the formation when high quality foams are used in either a drilling operation or a fracturing treatment. The low leak off implies that the damage to the surrounding formation is minimal, and therefore the cost for remedial treatment is low.

   The low liquid content in the foam also reduces the damage to a proppant in a fracture. Hence fracture conductivity is maintained high when stimulation treatments are performed with foam based fracturing fluid.

2. The foam viscosity increases with an increase in the liquid polymer concentration. Moreover the polymers have higher viscosity and exhibit lower friction loss than that of water. Therefore, polymers enhance the capabilities of foams. This result implies that polymer-based foams have more advantages over aqueous foams, and they provide an economical method to perform a stimulation treatment or a drilling operation.

3. Comparison of xanthan, guar, HPG, and PHPA foams show that each system has its own properties (constants used in the correlations), although the general behavior of the rheograms is basically the same.

7.7 Heat Transfer

Objective: The purpose of the heat transfer study was to understand heat transfer characteristics of the fracturing fluids and generate heat transfer coefficients of the linear, crosslinked and sand-laden fracturing fluids.

Introduction: Temperature of the fracturing fluids changes from ambient conditions on the surface in tanks to reservoir temperature in the subsurface in fracture. This change in temperature causes change in fluid characteristics, which affects the fluid performance in a treatment. The change in characteristics depends on the capability of the fluid to absorb heat, which is a function of the heat transfer coefficient of the fluid.

Very few studies are reported in the literature that evaluate heat transfer data of the fracturing fluid. Due to lack of the accurate data, fracturing simulators substitute heat transfer coefficient of water for the fracturing fluids. These numbers, however, are an order of magnitude different from that of the real fluids. Therefore, erroneous estimates are made of the fluid characteristics and as a result, fracturing treatments are improperly designed.

A 500 ft long double pipe heat exchanger, available at the FFCF, was used to generate valuable heat transfer data of several fracturing fluids.[23-24]

Procedure: The test procedure comprised of pumping fracturing fluids through inner pipe of the double pipe heat exchanger and heating fluid with hot water flowing in the annulus. The fluid was preconditioned through various lengths of the coiled tubing so that effects of shear history are included in the heat transfer study. The heat transfer coefficients were determined by measuring fluid temperature at four points along the length of the heat exchanger. The coefficients were measured for several fluids. These fluids included water, linear guar and HPG solutions, borate-crosslinked guar gels and crosslinked guar slurry.

Results: The overall heat transfer coefficient of the water is 200 Btu/hr ^{o}F ft^{2}. The heat transfer coefficients of the linear guar and HPG, however, are less than that of the water. These coefficients increase with increase in fluid flow rate through the heat exchanger as shown in Figure 7.7.1. The figure shows that there is not much difference in the coefficients of the guar and HPG polymer solutions.

The fluid rheology study, in the previous section, showed that the fluid behavior of the borate-crosslinked guar is a strong function of shear history, fluid pH and temperature. Therefore, the heat transfer characteristics of these fluids must also be dependent on the same parameters. This is confirmed from the evaluation of the heat transfer coefficients of these fluids as shown in Figure 7.7.2. The figure is drawn for a relative coefficient which is the ratio of heat transfer coefficient of the fracturing fluid to

that of the water. The figure shows that the fluid prepared at pH 9 has the highest heat transfer coefficient and its value decreases with an increase in the shear history through the coiled tubing. The figure also shows that the heat transfer coefficient of the crosslinked gel is less than one half of the water value. Similarly, the heat transfer coefficient of the sand-laden crosslinked fluid is less than that of the water as shown in Figure 7.7.3. But this slurry coefficient is much closer to the water value than that of the clean fluid. The figure shows that the coefficient of the sand slurry is more than that of the clean fluid.

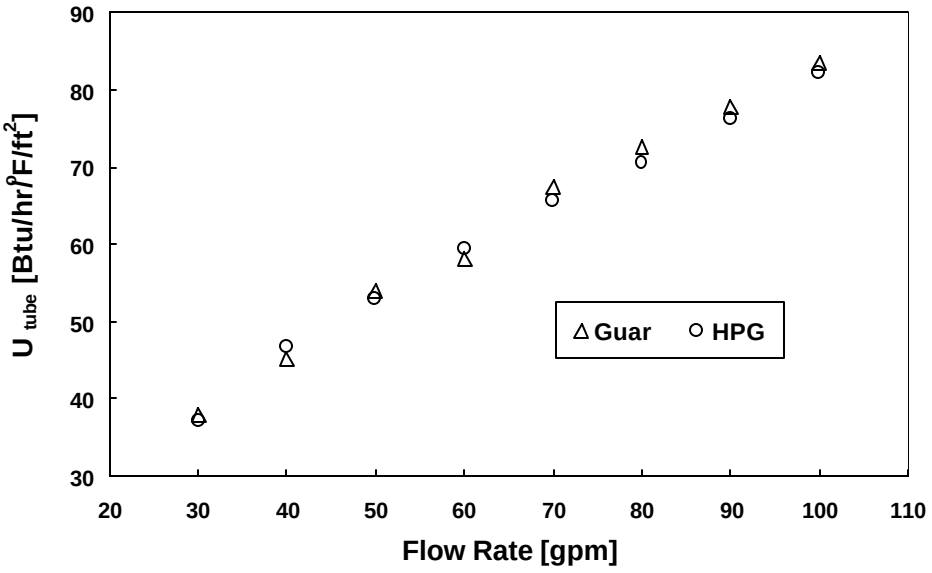

Figure 7.7.1-Heat Transfer Coefficients of 35 lb/Mgal Guar and HPG at Several Flow Rates

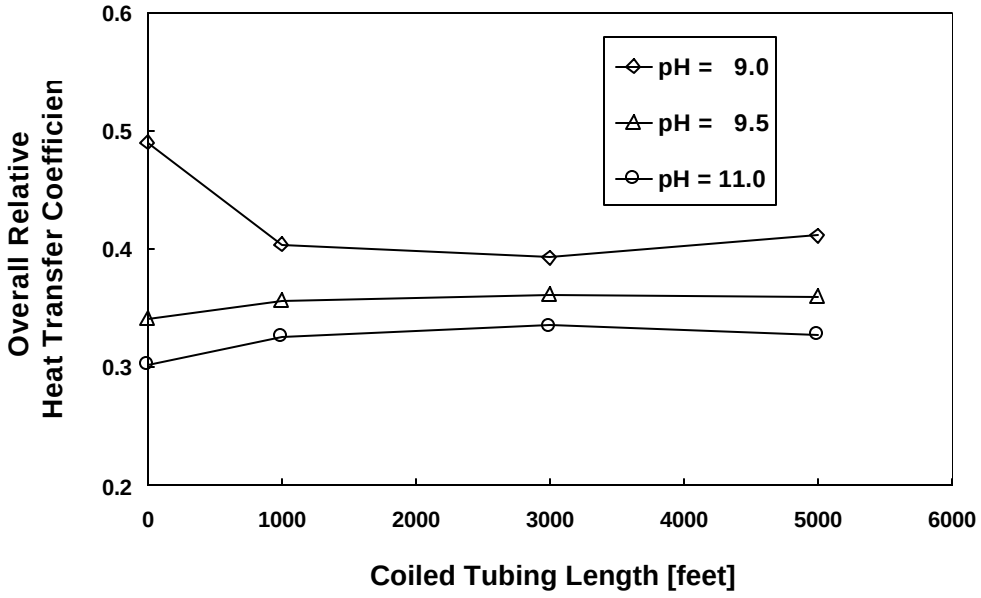

Figure 7.7.2-Heat Transfer Coefficients of Borate-Crosslinked 35 lb/Mgal Guar

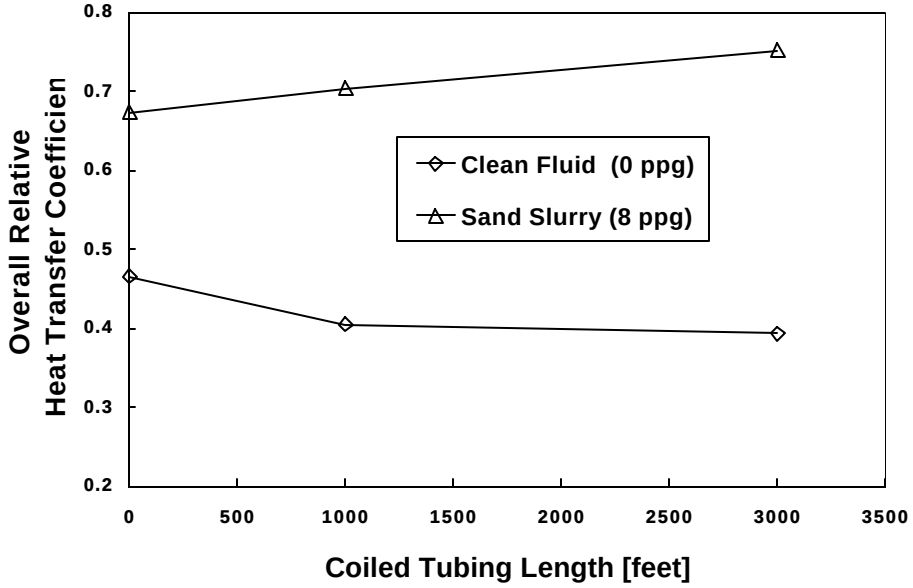

Figure 7.7.3-Heat Transfer Coefficients of Borate-Crosslinked 35 lb/Mgal Guar, pH 10.0

Implications of the Research Results:

1. The heat transfer coefficients of the linear guar and HPG solutions, and crosslinked gels are lower than that of the water.[24] The lower coefficient means that the heat transfer characteristics of fracturing fluids are poorer than that of water. Therefore these fluids will heat up at slower rate when they are pumped through the fracture and they will attain reservoir temperatures at longer times than if water is pumped through the fracture. The slower heat up rate means that the fracturing fluids will retain their characteristic viscosities in the fracture for a longer period before the reservoir conditions begin to affect the fluid behavior at higher temperatures. This prolonged stability of the fluid suggests that the fracturing fluids may perform better under real downhole conditions than what is predicted from the current industry practice of substituting the heat transfer coefficient of water for the fracturing fluids.

2. On the other hand, the heat transfer coefficient of the guar slurry is similar to that of the water.[21] This similarity means that the heat transfer characteristics of the fracturing slurry can be satisfactorily estimated from that for the water. Therefore, the current practice of predicting the slurry heat transfer characteristics with water can be successfully continued without compromising the fluid performance under real conditions.

7.8 Proppant Flowback

Objective: The purpose of the proppant flowback study was to determine minimum cleanup rate before proppant flowback begins and evaluate the effects of various fracturing and reservoir parameters on the critical flow rates.

Introduction: After a fracturing treatment, reservoir is flowed back to remove any fracturing fluid left in the proppant pack and thus, cleanup the fracture. The flowback is performed by opening well through surface chokes, whose size is slowly increased so that most of the fluid is recovered and well begins to flow reservoir fluids at a stimulated rate. A controlled flowback is important to recover the maximum quantity of fracturing polymer in minimum time and without any flowback of proppants. Any flowback of the proppant is undesirable because sand removed from the propped area reduces total propped height and fracture length, causing a loss in fracture conductivity. Therefore, the present study was performed to identify flow rates that will allow proppant-free fracture cleanup.

Procedure: The proppant flowback rates were evaluated in the slot, which provides a unique 9400 inch^2 of the fracture wall area. The fluid was pumped into the slot set to a fracture gap width and filled with sand. The sand pack was subjected to an orthogonal applied pressure to simulate closure stress on the fracture. The flowback tests were

performed at two fracture gap widths, 0.16 and 0.40 inch, two proppant size, 20/40 and 12/20 mesh sand, and four closure stresses, 0, 200, 500 and 1000 psi.

A detailed description of the procedure used to perform this study can be found in GRI annual reports[12,13] and SPE technical paper.[25]

Results: The results of the investigation showed that stability of the proppant pack is a strong function of the reservoir and fracturing parameters. The minimum flow rates for initiation of proppant flowback are shown in Figure 7.8.1. It shows that the pack destabilizes at lower water flowback rates as the closure stress is increased from zero to 1000 psi. On the other hand, the pack produces proppant at higher flow rates as the sand size is increased. The pack, however, destabilizes at lower water flowback rates when the fracture gap width is increased.

The increase in the closure stress also results in increase in the cumulative proppant production. This effect is shown in Figure 7.8.2 on a proppant pack prepared with a 20/40 mesh sand. The figure shows that up to 40 minutes of flowback, the total sand production is maximum for 1000 psi closure and 0.4 inch gap width. It also shows that in just 120 mins, 30% of the packed sand is produced. The proppant distributions in the fracture after 40 and 120 mins of flowback are shown in Figure 7.8.3. The figure displays digitized images of the tests recorded on the video. It describes sand free areas inside white ovals.

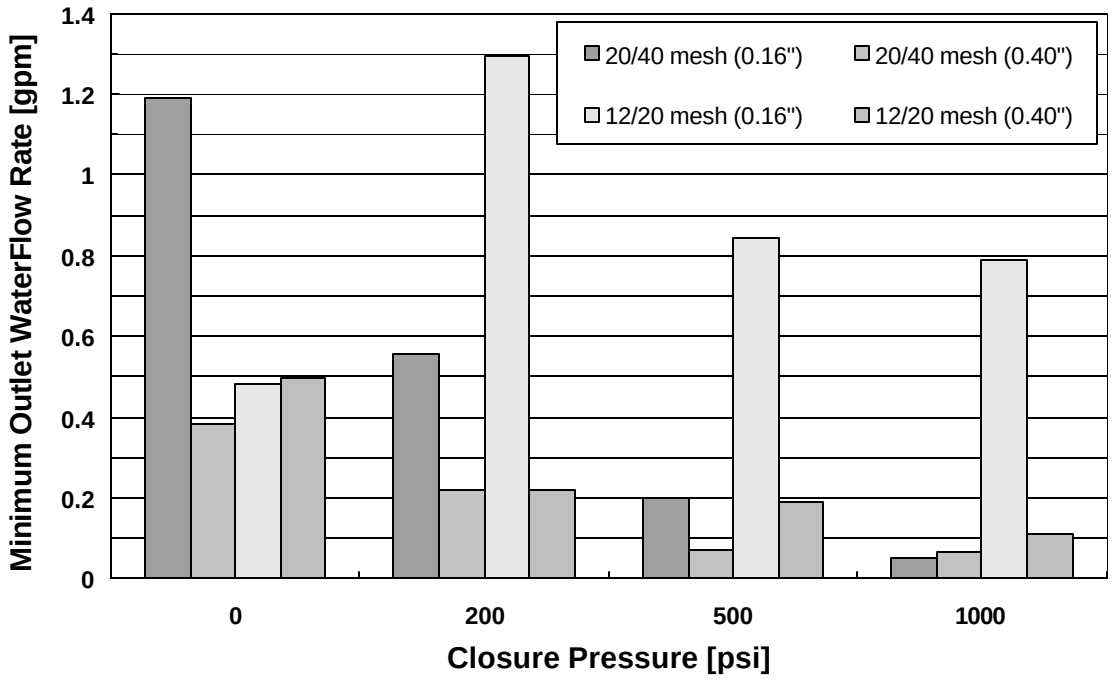

Figure 7.8.1- Proppant Flowback Initiation/ Pack Stability Tests through Fracture Gap Widths of 0.16 and 0.40 inch

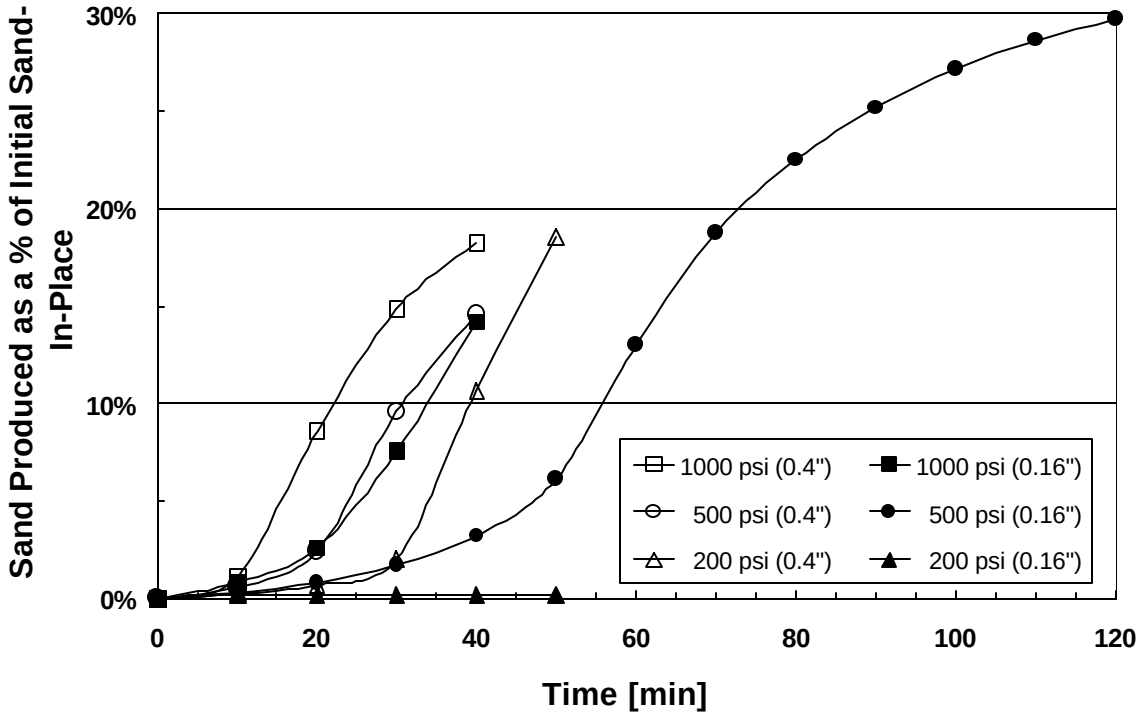

Figure 7.8.2¾ Percentage of 20/40 mesh Sand Produced for 0.5 gpm Inlet Water Flow Rate through Sand Pack of 0.16 and 0.40 inch Gap Widths

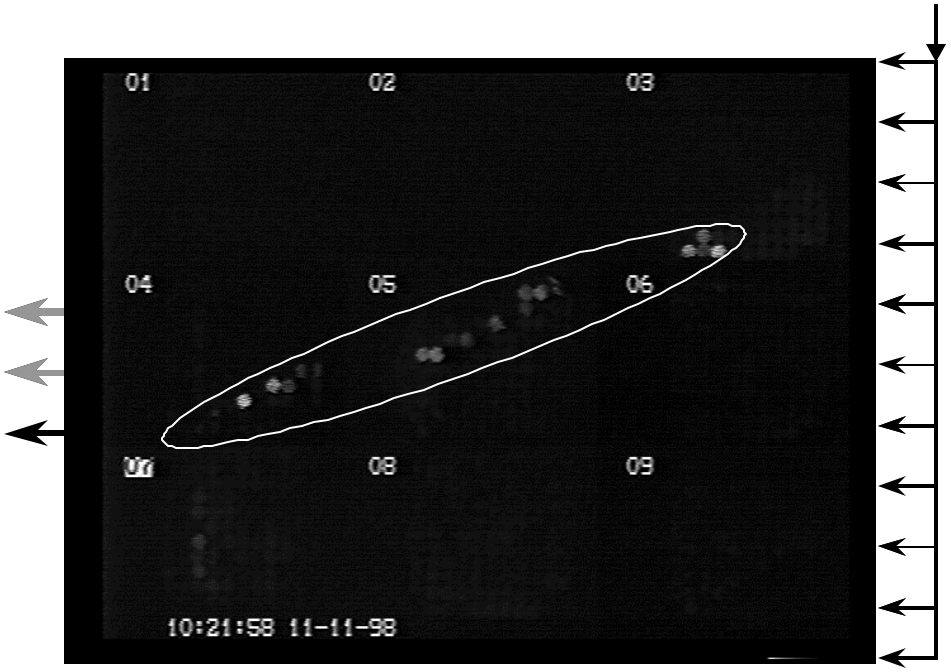

Figure 7.8.3(a) ¾ Proppant Distribution after 40 minutes of Flowing Back Water at a Rate of 0.5 gpm through a Fracture Width of 0.16" Maintained under a Closure Pressure of 500 psi

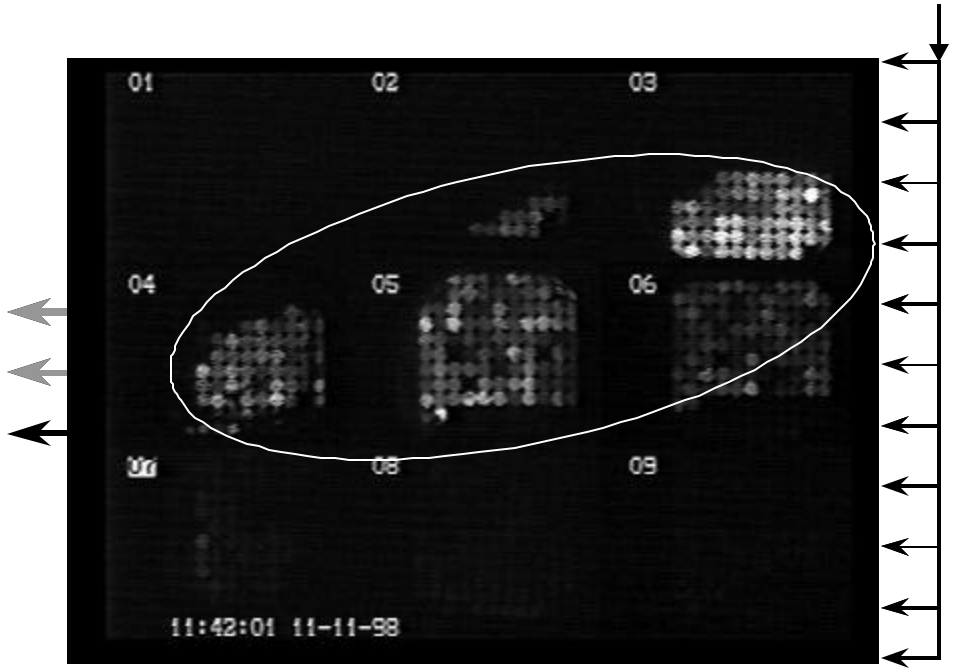

Figure 7.8.3(b) ¾ Proppant Distribution after 120 minutes of Flowing Back Water at a Rate of 0.5 gpm through a Fracture Width of 0.16" Maintained under a Closure of 500 psi

Implications of the Research Results:

1. The results show that the critical flowrate is a function of proppant size, fracture width and closure stress. This means that the stability of the propped fracture is strongly dependent on the stimulation parameters and reservoir conditions.

   The FFCF study shows that there is a critical flow rate beyond which the sand will be produced from the propped fracture; below this rate, there is negligible sand production.[25] This result disproves Stein's[26] conclusion that the unconsolidated sand would flowback at any flow rate.

2. The FFCF results show that the critical flow rate decreases when the closure stress is increased. This result is a unique observation made in the proppant flowback study at the FFCF as the relationship between the flowrate and closure stress was not considered in previous studies.

   Since the closure stress affects the pack stability, there are practical implications of the results. It implies that if a low closure is maintained during flowback operation, the fracture cleanup can be performed at higher rates than those being currently used in the industry. Higher rates mean that the fracture cleanup time can be reduced and costs for flowback operation can be decreased.

3. The results show that the critical flow rate decreases as the ratio of the gap width (w) to particle diameter (d_p) is increased from 3.2 to 16.0, and the relationship

between the pack stability and w/d_p ratio is dependent on the closure pressure. This result implies that the proppant pack could be stable at higher w/d_p ratios than the three to six range values if the closure pressure is low. This may be a possible reason why there is no proppant flowback observed in field when the fracture widths are more than those predicted by the six times the proppant diameter.

Previous numerical and experimental investigations of the flowback phenomena concluded that a proppant pack is stable when the range of the ratio of the fracture width to proppant diameter is between the values from three to six.[27-29] But these studies did not observe that these ratios are dependent on the cleanup flow rates; on the other hand, the FFCF results[25] show that the proppant flowback can occur within the recommended ratios, albeit at higher fluid rates as compared to the rates for the higher ratios.

4. The FFCF study shows that upto 30% of the sand placed in a fracture can be produced in just two hour. This result has great implications on the well productivity. When this result is compared to the stimulation ratios obtained at different percentages of the filled fracture, it is observed that the well productivity decreased from 10.5 in a fully propped fracture to only 1.2 in the 70% filled fracture.[30] This huge decrease in the stimulation ratio means that all potential benefits of the hydraulic fracturing treatment can be lost due to proppant flowback from a fracture.

7.9 Dynamic Fluid Loss

Objective: Dynamic fluid loss experiments were performed to achieve the following objectives: (1) to compare large surface area experiments performed in the HPS with those obtained in the laboratory, (2) to explore mechanistic differences between fluid loss behavior of polymer solutions and crosslinked gels, (3) to investigate and document differences between gel fluid loss behavior on low and high permeability media, and (4) to investigate dynamic fluid loss behavior on natural fractures.

Introduction: Quantifying the rate at which fluid is lost to permeable fracture faces is important for the design and execution of successful hydraulic fracturing treatments. Fluid lost to the porous rock matrix during a treatment increases the overall fluid volume needed to achieve specific fracture dimensions. Fluid efficiency has been used as a measure of fluid loss control and is defined as the ratio of fracture volume to fluid volume pumped. Based on this definition it is easy to demonstrate that an increase in fluid efficiency from 50 to 90% will decrease the fluid volume needed to create a specific fracture geometry by over 40%. Therefore, the potential benefit that can be derived from a greater understanding of fluid loss control mechanisms is significant.

Procedure: Prior to performing a dynamic fluid-loss test, the facing permeability to water was determined. The HPS slot was pressurized to approximately 200 psi with

water. The fluid collection port was opened and a stabilized flow was attained. Slot pressure, stabilized flow rate, and facing surface area were used in Darcy's Law to calculate permeability. This process also served the dual purpose of water saturating the facing permeability prior to the dynamic fluid loss test. After the water permeability test, the fluid leak-off valve was closed. Polymer solution was then circulated through the slot and back to the 100 bbl storage tank with a high pressure pump. Circulation through the 0.5-inch wide slot at 45 gpm provided a shear rate of 50 sec^{-1}. While circulating fluid through the slot, system pressure was elevated with a throttling valve to the desired level. When system pressure, flow rate, and gap width were all set at the desired values, flow was diverted from the storage tank to the disposal tank. The fluid leak-off valve was then opened to begin fluid collection for the test. During crosslinked gel tests, crosslinker addition was started when the flow was diverted to the disposal tank. Crosslinker was added continuously to the eye of the centrifugal pump supplying fluid to the high-pressure pump. System pressure was reduced and flow through the HPS stopped when approximately 10 bbls of fluid remained in the storage tank. The fluid loss valve remained open during and after test termination. The HPS was opened to observe and sample any filter cake buildup on the facings. The procedure used with fractured media was identical to that just described for polymer solutions and gels, except the facings used contained closed hairline fractures. Samples of the permeable facing material were evaluated in scaled laboratory experiments for comparison to the results obtained from the HPS.

A detailed description of the equipment and procedures used in the laboratory experiments are described in GRI annual reports[11,23,24] and a SPE technical paper.[31]

Results: Wall-building fluid-loss coefficients (C_w), determined from scaled experiments in the laboratory, compared favorably with coefficients measured over the large surface area of an HPS facing. However, spurt-loss values measured in the laboratory were generally larger than those measured in the HPS. Edge effects and other artifacts would more easily influence fluid-loss experiments performed on the small surface areas found in laboratory experiments. Large surface-area experiments, such as those available with the HPS may be required to provide realistic spurt-loss values. Table 7.9.1 provides a comparison of laboratory fluid-loss results with those obtained from the HPS.

A resin-sand composite was developed as a synthetic permeable media for HPS facings. Dynamic fluid loss tests performed in the HPS with these facings and in the laboratory with samples from these facings failed to produce a filter-cake. Although a filter-cake was not obtained, fluid loss control was observed to follow a wall-building response. As a result of these observations, natural rock facings were developed for the HPS. Dynamic fluid loss experiments performed with natural rock facings produced the first evidence of filter-cake formation in the HPS. However, fluid loss control did not appear to be any better than that observed on synthetic rock. The coarse texture of the natural rock facing was postulated to be a contributing factor to the formation of filter-cake. To test this hypothesis, the glossy surface of the mold-cast synthetic rock facing was lightly sand blasted before subjecting it to a dynamic fluid-loss test. Surprisingly, a filter-cake did form on the artificially roughened surface. However, gel fluid loss control was essentially the same with and without filter-cake, and therefore some other factor appeared to be responsible for providing the observed fluid loss control. Formation of an

internal filter-cake was postulated to be the controlling factor and experiments were designed to test this hypothesis. Figures 7.9.1 and 7.9.2 show the results of an experiment in which filter-cake from a first fluid loss test (Stage 1) was physically removed prior to beginning a second fluid loss test on the same media (Stage 2). Several minutes were required for the fluid loss to reach a limiting value during Stage 1. Following a brief spurt loss period associated with re-pressurization of the test cell at the beginning of Stage 2, fluid loss rate returned quickly to the same level experienced at the end of Stage 1. Since fluid loss control was attained quickly during Stage 2 in the absence of a filter-cake, the extended period required for development of limiting fluid loss control behavior during Stage 1 was probably associated with building an internal filter-cake. An internal filter-cake was already present at the beginning of Stage 2 and therefore very little time was required for the fluid loss to reach a limiting condition.

Sample	**Source**	**Permeability md**	**C_w ft/min$^{1/2}$**	**Spurt Loss gal/ft^2**
Borate-crosslinked 3- lb/Mgal Guar	HPS	1.350	0.000409	0.1350
	HPS	1.590	0.000138	0.0480
	LAB	1.250	0.000500	1.2200
Titanium crosslinked 60 lb/Mgal HPG	HPS	2.546	0.000148	0.0812
	HPS	2.575	0.000179	0.0277
	HPS	7.926	0.000231	0.0579
	LAB	5.330	0.000300	0.1800
60 lb/Mgal HPG + 50 lb/Mgal Silica Flour	HPS	4.160	0.000408	0.0655
	LAB	2.560	0.000300	0.0950
60 lb/Mgal HPG + 25 lb/Mgal Silica Flour	HPS	7.728	0.000593	0.1610
	LAB	5.530	0.000800	0.0850
Titanium-crosslinked 40 lb/Mgal HPG	HPS	4.4742	0.000094	0.0924
	HPS	4.976	0.000275	0.0937
	LAB	2.300	0.000400	0.2550
Zirconium-crosslinked 40 lb/Mgal CMHPG	HPS	5.844	0.000128	0.0827
	LAB	5.070	0.000300	0.0200

Table 7.9.1-Comparison of HPS Data with Laboratory Data

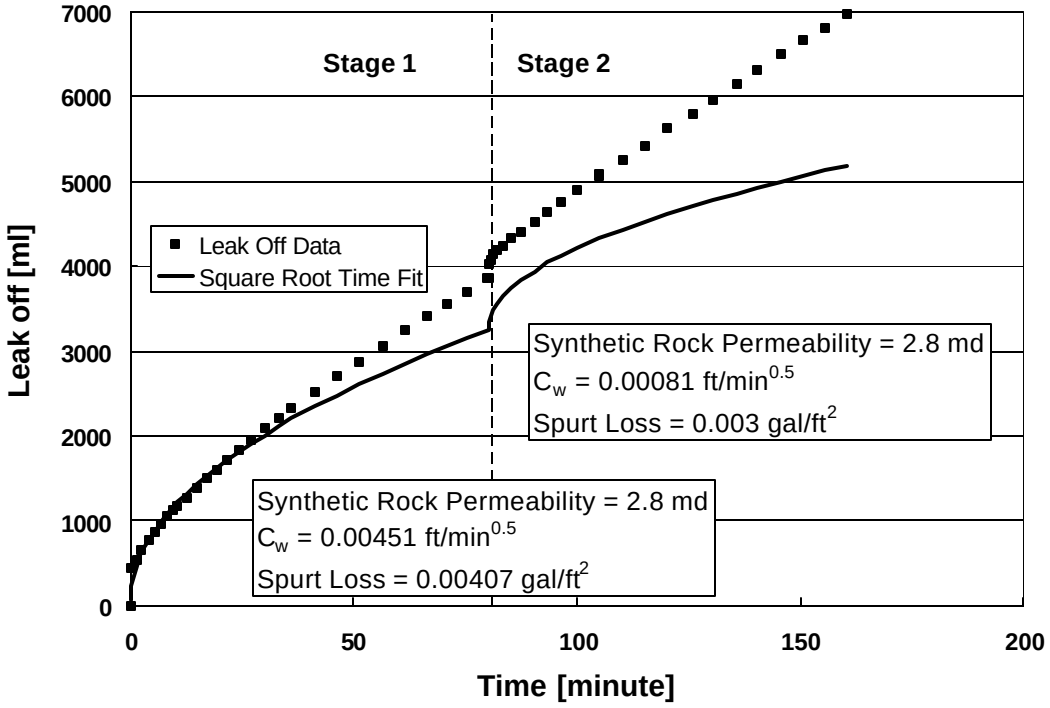

Figure 7.9.1-Dynamic Fluid-Loss Test with Borate-Crosslinked 35 lb/Mgal Guar

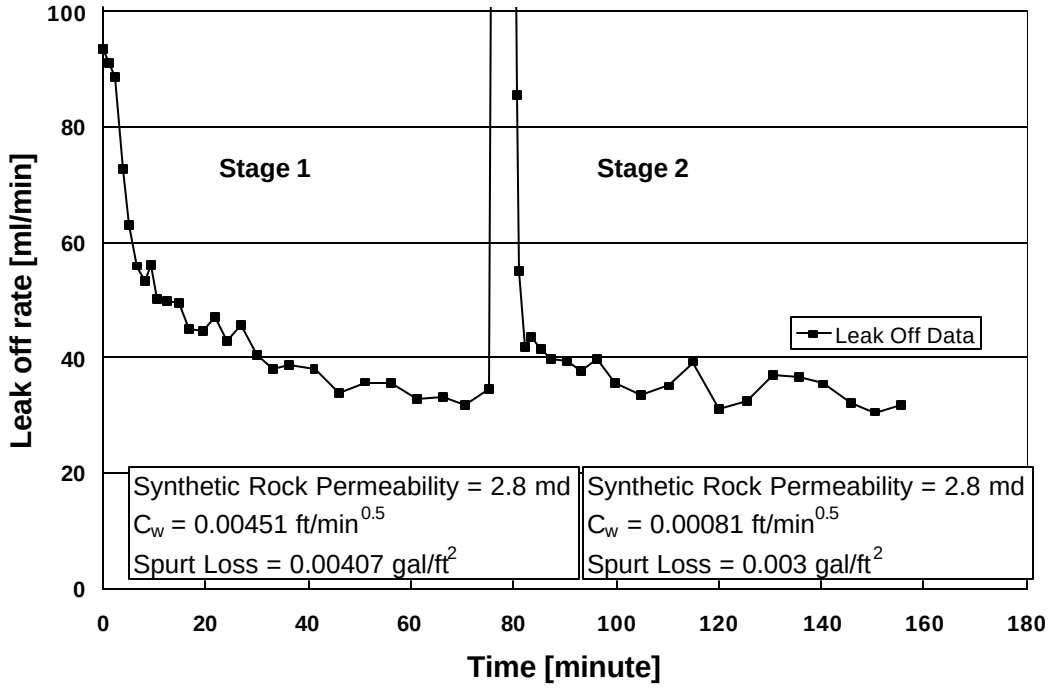

Figure 7.9.2-Leakoff Rate during Dynamic Fluid-loss Tests with Borate-Crosslinked 35 lb/Mgal Guar

In high-permeability media, crosslinked gels follow square-root-time behavior for an extended time period. However, in low-permeability media, gel fluid loss deviates from square-root-of-time behavior at some point and reaches limiting or linear behavior. The point at which deviation from square-root-of-time behavior occurs decreases as the permeability decreases. Polymer solutions generally follow square-root-of-time behavior on all but very low permeability media. Therefore, crosslinked gels are typically more efficient than polymer solutions at early times because they control spurt loss better. However, at longer times, polymer solutions become more efficient because they continue to follow square-root-of-time behavior while gels develop linear or limiting fluid-loss behavior. This behavior is illustrated by the fluid loss behavior shown graphically in Figs.7.9.3 and 7.9.4 for a polymer solution and gel respectively. At the end of the 80-minute test period, both show a cumulative fluid loss of approximately 3000 ml and therefore both exhibit the same fluid efficiency at this point in time. However, the polymer solution leak-off rate has diminished to 8 ml/min and could decrease even more if the cumulative fluid-loss volume continues to follow a square-root-of-time relationship. In contrast, the crosslinked gel leak-off rate continues at the limiting rate of 30 ml/min, which was established approximately 20 minutes into the test. Based on these leak-off rates, the polymer solution will become more efficient than the gel beyond 80 minutes. Therefore, fluid loss efficiency provided by a polymer solution may become substantially better than a gel when injection times are long. Under these circumstances, a polymer solution may be selected as the treating fluid because less fluid volume would be required. Another obvious application of these findings would be to implement a two-fluid treatment schedule. A crosslinked gel would be used during the pad to open the fracture and control spurt-loss and would be followed by a polymer solution to control fluid loss and transport proppant.

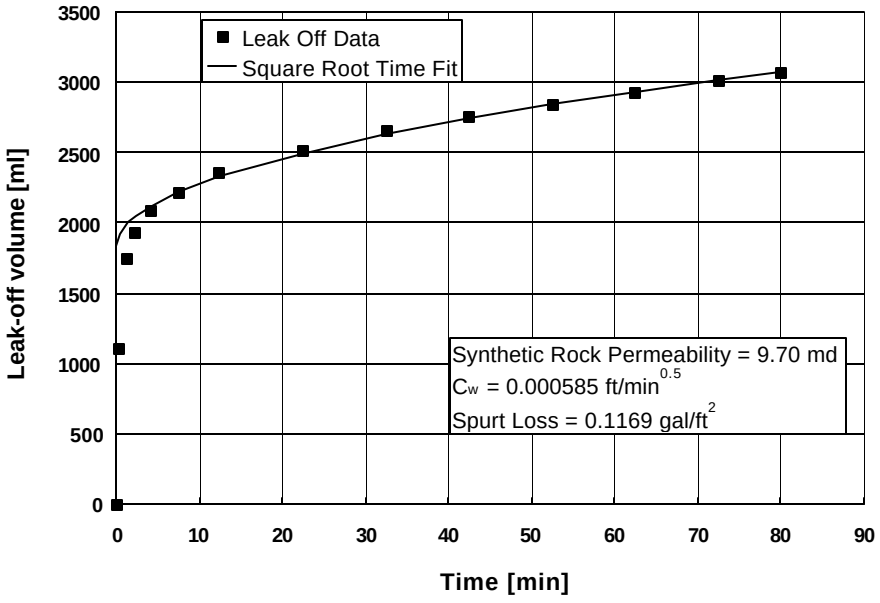

Figure 7.9.3-Dynamic Fluid-Loss Test with 60 lb/Mgal HPG + 25 lb/Mgal Si (Synthetic Rock)

Neither the viscosity of a crosslinked gel nor filter-cake formation was sufficient to control leak-off through naturally fractured media. Solids in combination with a viscous gel were needed to control the leak-off through naturally fractured Berea sandstone. It was necessary to optimize both particle size and concentration to control leak-off through this media.

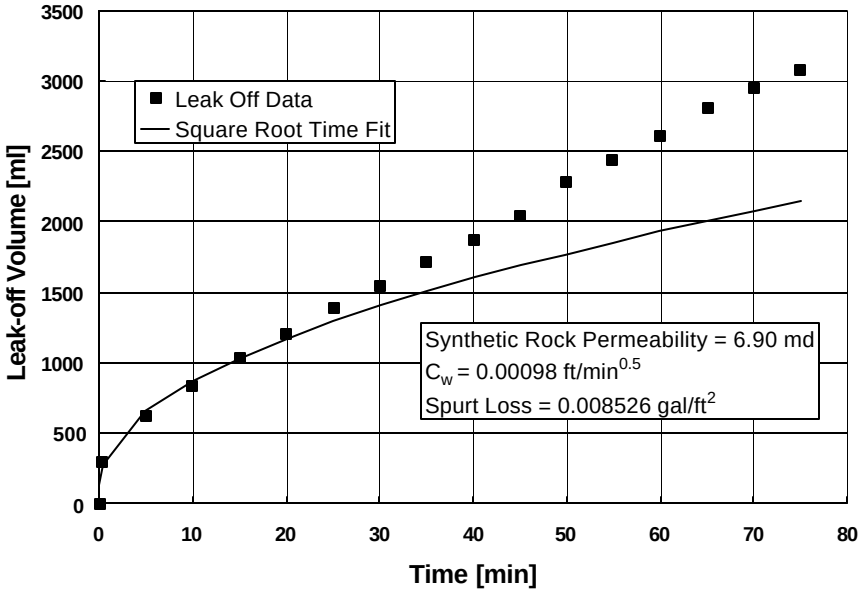

Figure 7.9.4-Dynamic Fluid-Loss Test with Borate-Crosslinked 35 lb/Mgal Guar

Implications of the Research Results:

1. Spurt loss values measured in the laboratory cell were generally larger than those measured using the HPS at the FFCF.[31] This result implies that the use of uncorrected spurt-loss values obtained from conventional laboratory testing could lead to over-design of fracturing treatments in terms of fluid volume requirements. In the case of large differences in spurt-loss values, several thousand gallons of fracturing fluid could potentially be pumped unnecessarily. With the recognition of this problem, the industry should develop a method for correcting spurt-loss values obtained from conventional testing. Large surface-area experiments, such as those available with the HPS, will be required to provide the spurt-loss values needed for development of such corrections.

2. The gel fluid loss control was essentially the same with and without filter-cake as internal filter-cake was the controlling factor. These results are considered to be evidence that a filter-cake is not a requirement for fluid loss control in all instances. The primary fluid loss control mechanism with crosslinked gels appears to be pore-plugging. The major implication of these findings is the discovery that the industry has been too focused on filter-cake formation and its contribution to fluid loss control. A paradigm shift is needed to allow the industry to focus on the concept of pore-plugging or an "internal filter-cake" as a source of fluid loss control.

3. Neither the viscosity of a crosslinked gel nor filter cake formation was sufficient to control leak-off through naturally fractured media. Solids in combination with a viscous gel were needed to control the leak-off through naturally fractured Berea sandstone. The implication of these findings is that a gel containing a broad spectrum of particle sizes will be needed to control fluid loss to natural fractures. In the absence of experience with a particular naturally fractured formation, mixtures of 100 mesh sand and silica flour should be incorporated into a gelled prepad or pad fluid to control leak-off.

7.10 Perforation Pressure Loss

Objective: Perforation pressure loss data were to be acquired with various fluids and slurries using the simulated wellbore/fracture entry available on the HPS. These perforation pressure loss data were to be analyzed and correlations developed to describe this important property of fracturing fluids and slurries. An additional objective was to develop a correlation that describes the dynamic change in the coefficient of discharge produced by slurry erosion.

Introduction: An accurate estimate of perforation pressure loss is needed when performing a limited entry treatment, treating near the maximum allowable surface pressure, and when attempting to perform either real-time or post-treatment fracturing pressure analysis. Limited entry is a method for simultaneously treating multiple zones having different fracture gradients. Application of this technique requires *a priori* estimates of perforation pressure loss to determine the number of perforations needed in each zone. However, perforation pressure loss is a dynamic property that changes continually as the result of erosion produced by abrasive sand slurries. Predicting the dynamic change in discharge coefficient caused by erosion is crucial to achieving the desired zonal injection profiles and hence to the success of a limited entry treatment. An accurate determination of perforation pressure loss also is essential for reliable treating pressure analysis. A large perforation pressure loss that is not anticipated during a treatment may lead to erroneous conclusions about fracture growth when analyzing real-time pressure data. Calculated bottom-hole treating pressures must also be corrected for perforation pressure loss effects to provide a reliable estimate of fracture geometry from history-match analysis.

Procedure: The experimental procedure for each fluid type differs depending on the factors investigated. For most clean polymer solutions, the low-pressure equipment setup (described in Chapter 3) was used. When testing crosslinked gels, the high-pressure equipment (described in Chapter 3) was used to investigate the effect of shear history on perforation pressure loss. For sand slurries, experiments were conducted using low-pressure equipment to investigate factors effecting the perforation pressure loss in the absence of erosion. Investigation of erosion effects, on the other hand, was carried out with the high-pressure equipment because large volumes of slurry are needed. The following sections discuss in detail the procedure used with each fluid type.

Polymer Solutions. Approximately 1000 gallons of polymer solution was mixed and circulated through the HPS using stainless steel perforations of sizes 0.25″, 0.375″, and 0.5″. Each test used two perforations of the same size installed on 16″ spacing. Perforation pressure loss data were acquired at several different flow rates with a differential pressure transducer. The test procedure was repeated for each perforation size.

Crosslinked Gels. Approximately 100 bbls of polymer solution were prepared in a mixing tank and then fed to the high-pressure triplex pump using a centrifugal pump. The clean fluid was circulated through the HPS until a steady flow rate of 60 gpm was attained. Directing the polymer solution in a single pass, crosslinker was added at the suction of the centrifugal pump using two computer-controlled metering pumps. The crosslinking gel was pumped into the HPS through two stainless steel perforations of the same size. Perforation sizes of either 0.25″, 0.375″, or 0.5″ were installed on 16″ spacing in each test. Perforation pressure loss data were acquired at various flow rates so that the differential pressure across the perforations remained less than 500 psi. Bypassing a portion of the flow around the HPS provided variable flow rates through the slot. By following this procedure, the crosslinking rate was kept constant and uniform rheological properties for the crosslinked fluid were achieved.

To investigate the effect of shear history, the discharge of the triplex pump was diverted through the desired coiled tubing length, without interruption to the flow, by properly placed valves. The sheared fluid exited from the coiled tubing into the HPS. Perforation pressure loss data were acquired at various flow rates so that the differential pressure across perforations remained less than 100 psi. Variable flow rates through the slot are attained by bypassing a portion of the flow around the HPS as before. Once again this procedure insured uniform rheological properties for the crosslinked fluid.

Sand Slurries. The low-pressure equipment was used to investigate the influence of perforation size, proppant size, and proppant concentration on perforation pressure loss in the absence of erosion. Approximately 200 gallons of polymer solution were mixed with various amounts of 20/40-mesh sand to prepare slurries with sand concentrations of 0 to10 ppg. Four perforations, of the same size (0.375″ or 0.5″), were installed in the HPS on 8″ spacing. Differential pressure was measured as a function of flow rate for each perforation size. The same procedure was followed with slurries prepared by mixing polymer solution with 12/20-mesh sand. Flow rates in these tests were minimized to avoid erosion effects.

The investigation of erosion required the high flow rates and large slurry volumes that could only be supplied by the high-pressure equipment. Sand slurries were prepared in the mixing tank at the desired concentration and pumped into the HPS through two 0.375″ steel-cement composite perforations on 16″ spacing. The pressure drop across the perforations was measured as a function of time at two different flow rates (2 and 3 bbl/min) using a differential pressure transducer.

Results: Currently, the industry is using a sharp-edged orifice equation to estimate the pressure drop across the perforation. This equation includes a kinetic energy correction factor, commonly known as the “coefficient of discharge,” which is used in calculating

the perforation pressure loss (psi) as follows:

$$\Delta p_{perf} = \frac{0.2369\,\rho}{d_{perf}^4 C_d^2}\left(\frac{Q'}{N}\right)^2 \quad \text{..... (7.10.1)}$$

Although the coefficient of discharge depends on fluid type and restriction (orifice) size, it is common practice to assume a fixed value for all fluids and perforation sizes. However, recent studies have shown that the coefficient of discharge can vary significantly with fluid viscosity and perforation size.[21,22] Thus, a rough estimate for the coefficient of discharge can introduce a serious error in the predicted perforation pressure loss. For instance, an error of 10 % in the coefficient of discharge will result in a 25% error in the predicted pressure loss across the perforations. Correlations have been developed to provide reliable estimates of the coefficient of discharge for polymer solutions and for both transition metal (titanium) and borate crosslinked gels. The following coefficient-of-discharge correlations have been developed:

HPG Solutions:

$$C_d = \left(1 - e^{\frac{-2.2 d_{perf}}{m_a^{0.1}}}\right)^{0.4}, \; r^2 = 0.886 \quad \text{..... (7.10.2)}$$

Titanium-Crosslinked HPG Gels:

$$C_d = \left(1 - e^{\frac{-1.76}{(m_a \cdot d_{perf})^{0.25}}}\right)^{0.6}, \; r^2 = 0.962 \quad \text{..... (7.10.3)}$$

Borate-Crosslinked HPG Gels:

$$C_d = \left(1 - e^{\frac{-3.79 d_{perf}^{0.32}}{m_a^{0.25}}}\right)^{0.6} \quad \text{..... (7.10.4)}$$

Eqs. 7.10.2 to 7.10.4 can be used in conjunction with Eq. 7.10.1 to calculate the pressure loss across perforations with the specified fluids. In addition, the correlation developed with HPG polymer solutions has also been shown to be applicable to guar gum solutions. The borate-crosslinked gel correlation applies to formulations prepared at optimum pH. Under these conditions, the coefficient-of-discharge varies little with shear history. In Eqs. 7.10.2 to 7.10.4 the discharge coefficient is correlated with apparent viscosity (cP) of the polymer solution at 511 sec^{-1} shear rate and perforation diameter (in.). The apparent viscosity m_a, (511 sec^{-1}) of the linear polymer solution is defined as:

$$m_a = 47880 \times k \times (511)^{(n-1)} \quad \text{..... (7.10.5)}$$

In addition to being influenced by carrier fluid viscosity and perforation diameter, the coefficient-of-discharge for sand slurries is also influenced by proppant concentration and size. Experiments show that perforation pressure loss increases with increased sand concentration (Figure 7.10.1) while the coefficient-of-discharge decreases. This behavior becomes less significant as sand size increases. Moreover, pressure loss for 20/40 mesh sand slurries is higher than 12/20 mesh sand slurries (Figure 7.10.2). This difference in perforation pressure loss between the two sand size slurries is due to the fact that a 12/20 mesh sand slurry is less viscous than a 20/40 mesh sand slurry at the same concentration. Figure 7.28 shows the discharge coefficient plotted versus cumulative mass of sand pumped at two different rates. After an initial rapid rise, the discharge coefficient at both pump rates was observed to increase monotonically with increasing quantity of sand pumped. The composite perforations did not have any significant weight reduction and the only evidence of erosion during these tests was a rounding of the entrance. Figure 7.10.3 also shows that a larger discharge coefficient was obtained at the higher injection rate. This implies that the dynamic change in the discharge coefficient caused by erosion is a function of pump rate as well as the cumulative mass of sand pumped. The dynamic change in discharge coefficient is therefore a function of cumulative kinetic energy passing through a perforation. Since slurry kinetic energy is proportional to density, the dynamic change in discharge coefficient is also expected to vary with sand concentration. To estimate perforation pressure loss for slurries, a relationship must be developed which describes the dynamic change in discharge coefficient as a function of pump rate, sand concentration, and cumulative mass of sand pumped.

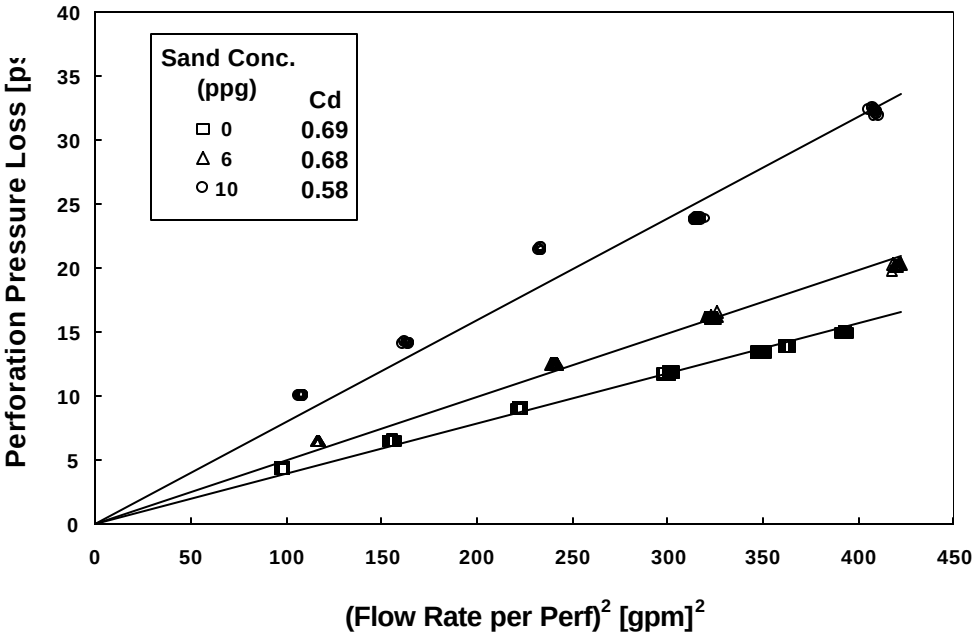

Figure 7.10.1-60 lb HPG + 20/40 Mesh Sand; 0.5 in. Perforation Diameter

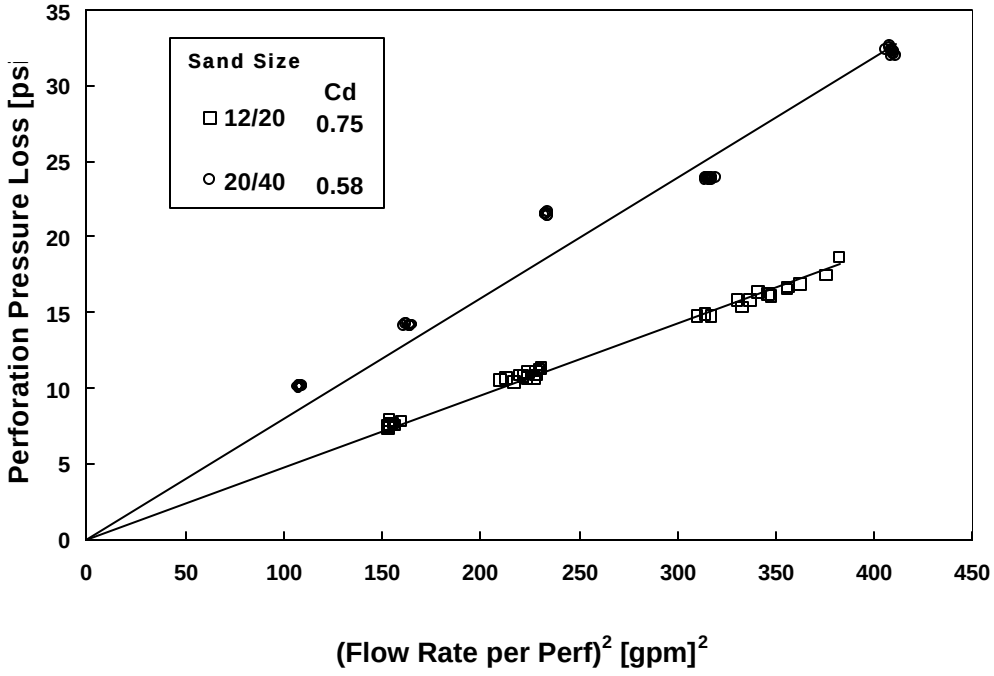

Figure 7.10.2-60 lb HPG +10 ppg Sand; 0.5 in. Perforation Diameter

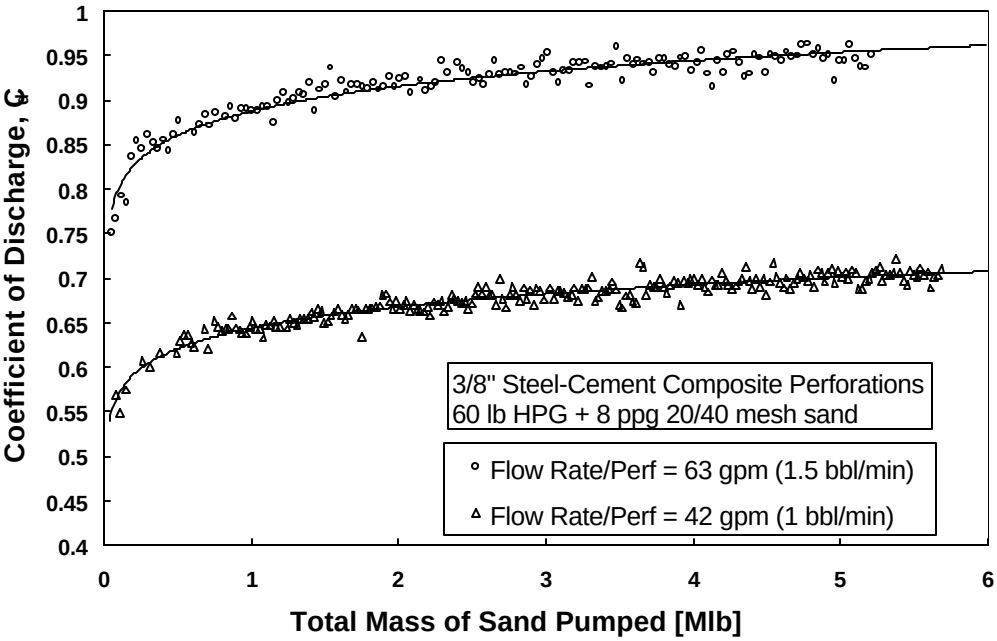

Figure 7.10.3-60 lb HPG + 20/40 mesh Sand

Using data obtained with a 20/40-mesh sand slurry and the dimensional analysis described in El-Rabba et al.,[32] the following correlation was developed:

$$C_d = \left\{ \left(1 - e^{\frac{-2.2 d_{perf}}{m_a^{0.1}}} \right)^{0.8} + A \Pi_3^B \right\}^{\frac{1}{2}} \quad \text{..... (7.10.6)}$$

where:

$$\left.\begin{aligned} A &= \frac{13.34 \left(\Pi_2 \right)^{5.48} e^{-8.7 \Pi_2}}{13.20 \left(\Pi_2 \right)^{5.48} + 38 \times 10^{-5}} \\ B &= 0.4 - 993 \left(0.5 - \Pi_2 \right)^{3.82} e^{-12.6 \left(0.5 - \Pi_2 \right)} \\ \Pi_2 &= \frac{D \rho Q'}{m_a d_{perf}} \le 0.5 \\ \Pi_3 &= \frac{\rho Q'^2 t}{m_a d_{perf}^4} \end{aligned}\right| \quad \text{..... (7.10.7)}$$

The coefficient of discharge calculated from Eq. 7.10.6 can be used in conjunction with Eq. 7.10.1 to estimate the perforation pressure loss for slurries.

In Figure 7.10.4, the coefficient of discharge calculated from the perforation pressure loss data, acquired from the erosion tests with 20/40 mesh sand slurry, are plotted versus the cumulative mass of sand pumped. It can be seen that the correlation fits the experimental data well and appropriately accommodates the field practice of pumping different sand concentrations in different stages. Thus, for limited-entry treatments, this correlation can be used during the design stage to select the sand concentration that would produce minimum erosion. Furthermore, this correlation can be used to determine the required increase in flow rate to compensate for the drop in perforation pressure loss due to erosion.

Limited experimental results with 12/20-mesh sand indicates that the dynamic change in discharge coefficient can also be a function of sand size in addition to the parameters included in Eqs. 7.10.6 and 7.10.7. Discharge coefficients and the observed erosion of the composite perforations (Figure 7.10.5) indicate that slurries prepared with larger sand sizes produce more erosion. In other words, the erosion process is dependent on the proppant size as well as the cumulative mass of sand pumped and the flow rate. The reason for this behavior is that for the same sand concentration slurries prepared with a large sand size contain fewer particles. Thus, a lesser quantity of kinetic energy is lost due to friction and collision between sand particles while a larger portion contributes to the erosion process.

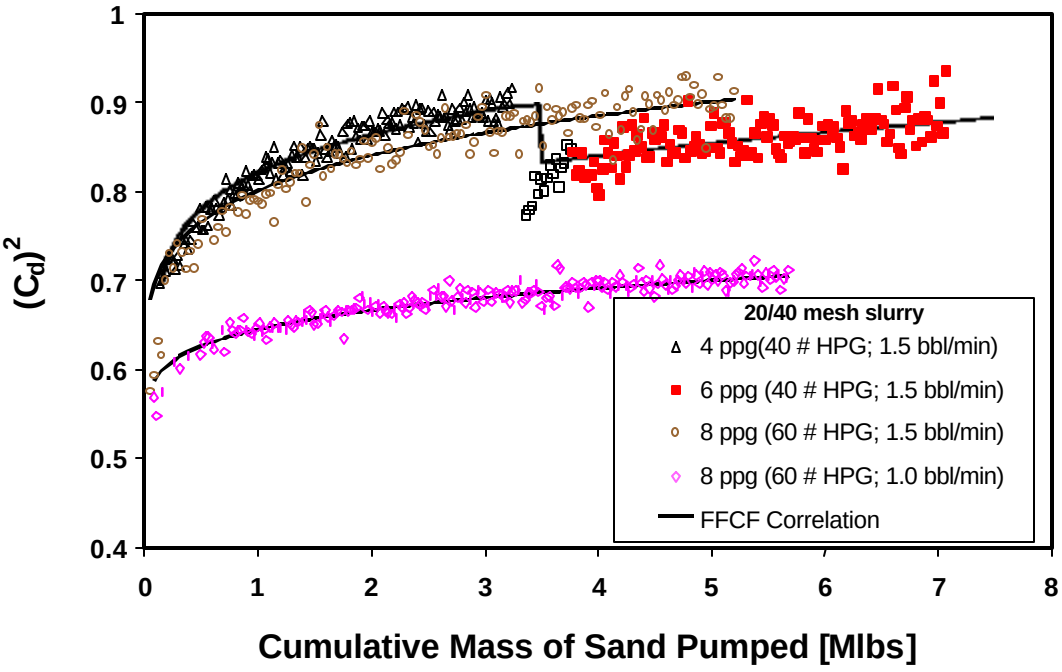

Figure 7.10.4-Empirical Model Fit of Experimental Data

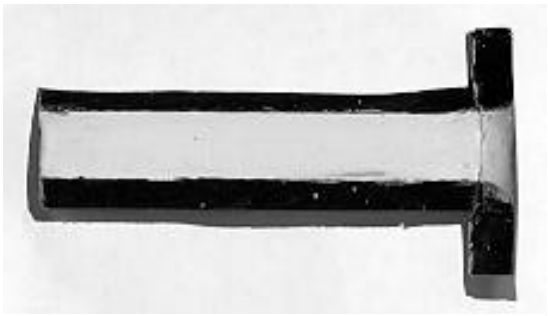

Composite Perforation
40 lb HPG + 20/40 mesh Sand

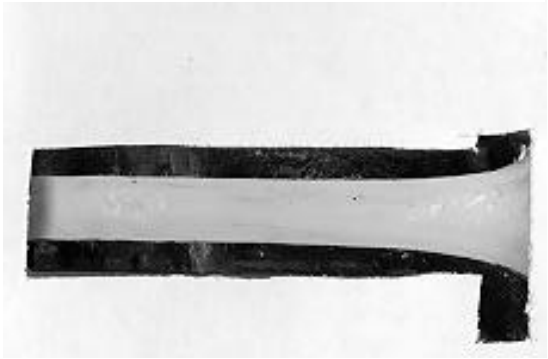

Stainless Steel Perforation
Borate-crosslinked 35 lb Guar + 12/20 mesh Sand

Figure 7.10.5-Cross-section of the Perforation After the Test

Presently, this correlation does not account for slurries of different proppant size. Yet, the effect of proppant size on perforation pressure loss for slurries can be significant. The dimensional analysis approach used to develop these correlations can be extended to incorporate the effect of proppant size. In addition, the correlation presented in this study is for linear polymer solution slurries only. Crosslinked gel slurries may behave differently from linear polymer solution slurries because of differences in viscous forces exerted on the sand particles. Particles in crosslinked gel slurries might migrate towards the center of the flow stream because of the viscoelastic nature of these fluids, and thus, the erosional effects may be reduced. Further experiments are needed to investigate these effects.

Nonetheless, the developed correlations should prove to be useful for the design of many currently used fracturing treatments that utilize the fluids tested in this study.

7.11 Tubular Friction Loss

Objective: Tubular pressure loss and flow rate data were to be collected and correlated to provide a method for estimating the frictional pressure loss of turbulent, non-Newtonian flows in coiled tubing. Frictional pressure loss in coiled tubing was to be determined for fluids such as water, guar gum solutions, hydroxypropyl guar (HPG) solutions, and borate-crosslinked gels. The influence of coiled tubing curvature and seam on the friction loss of these fluids was also to be investigated.

Introduction: Since coiled tubing is gaining in popularity for a number of applications in the petroleum industry, it is important that an accurate means of predicting friction loss be made available. Flow through coiled tubing is uniquely different from that in straight pipe because of the secondary flow pattern induced by the imbalance between the forces acting across the radius of the pipe. This secondary flow pattern is composed of counter-rotating vortices commonly called Dean vortices. The effect of this secondary flow pattern is to increase the frictional pressure loss above that which would be produced in straight pipe. Turbulent flow of Newtonian fluids in curved pipe has been the subject of numerous prior investigations, while similar investigations with non-Newtonian fluids have been scarce. The goal of the current investigation is to provide additional knowledge on turbulent flow of non-Newtonian fluids in curved pipe.

Procedure: The equipment used for this investigation consisted of one 1000-ft and two 2000-ft coiled tubing reels that can be arranged to provide lengths of 1000 ft, 2000 ft, 3000 ft, 4000 ft, and 5000 ft, respectively. Furthermore, the coiled tubing reels could be bypassed altogether if desired. In this way, test fluids could be sheared for various lengths of time, at a desired nominal shear rate. The nominal shear rate selected for crosslinked fluid testing was 1400 sec^{-1} at 60 gpm. The residence time at this shear rate is approximately 1 minute per 1000 ft of coiled tubing. The system also includes straight sections of seamed and seamless tubing with the same nominal diameter (1 1/2 in.) located downstream of the coiled tubing reels. The inside diameter of the seamless tubing and the hydraulic diameter of the seamed tubing were determined (from volumetric measurements) to be approximately 1.1817 in. and 1.1752 in., respectively.

During any test only one of these sections was used. Straight sections were used in a comparative study to determine the influence of tubing seam on frictional pressure loss. Coiled tubing was used to study the influence of pipe curvature on frictional pressure loss and to provide shear pre-conditioning for crosslinked gels.

Fluids investigated include water, polymer solutions (guar gum and hydroxypropyl guar), and borate-crosslinked gels. Borate-crosslinked gels were prepared from guar gum and hydroxypropyl guar solutions under conditions typically encountered in stimulation operations. These crosslinked fluids were evaluated at typical pH values of 9, 10, and 11. Test fluids cover a wide range of rheological types and exhibit strong drag-reducing characteristics. The polymer solutions and gels exhibit non-Newtonian behavior of the Power-law type. The crosslinked structure of a gel gives viscoelastic characteristics to the fluid. The Yield Power-law model best approximates the flow behavior of these structured fluids. However, for the range of shear rates considered, assuming Power-law behavior provides an adequate approximation. The *n* and *k* values were obtained from measurements made with a Fann model 35 rheometer.

Polymer solutions were prepared in 100 bbl batches. These fluids were pumped at the desired flow rate through the test apparatus using a triplex pump boosted with a centrifugal pump. During tests with gels, crosslinker was added through the eye of the centrifugal pump to achieve optimum mixing. Crosslinker was added at a rate proportional to the tubing flow rate to provide concentrations of 0.05% and 0.15% (by weight) in the guar gum and HPG polymer gels, respectively. At 60 gpm the crosslinker addition rate was 398 ml/min. and 1192 ml/min for guar and HPG solutions, respectively. Crosslinker was added using two syringe pumps in tandem. Additional details about fluid mixing and pumping equipment are found in Chapter 3.

Results: Results of the experimental investigation are summarized graphically in Figures 7.11.1 through 7.11.12.[33] Data obtained with water will be discussed first, followed by those obtained for the stimulation fluids.

Water. Friction factor versus Reynolds number data are presented in Figure 7.11.1 for straight sections of seamed and seamless tubing, for a range of Reynolds number varying from 1.3×10^5 to 3.2×10^5 (turbulent flow). Computed smooth pipe results based on the following Prandtl's equation are also plotted for comparison

$$\frac{1}{\sqrt{f}} = 2\log\left(N_{Re}\sqrt{f}\right) - 0.8 \quad \text{..... (7.11.1)}$$

Notice that the seamless tubing exhibits friction factor values that are higher than those for the smooth pipe, which is an indication that some roughness is present in the seamless tubing. This is not very surprising. On the other hand, the results shown for the seamed tubing are rather interesting. Indeed, two features are noteworthy. First, the friction factor for the seamed tubing is lower than that for the seamless tubing, with the difference increasing with increasing Reynolds number (as much as 9% for the highest Reynolds number value considered). Second, the seamed tubing yields results that are very close to the smooth pipe results, which would seem to suggest that it does not have any roughness. While this may or may not be the case, its lower friction factor compared to

that of the seamless tubing is more likely due to the presence of the seam. Indeed, instead of acting as an added roughness, the seam alters the turbulence spectrum by damping the high turbulence frequencies and thus, causing a decrease in the turbulent frictional pressure drop. The seam and the roughness have opposing effects on the friction factor. This in turn suggests that some roughness must be present in the seamed tubing used in this study. Otherwise, the friction factor values would be lower than those of a smooth pipe. These experimental results suggest that friction factor for seamed tubing relates to that of the seamless tubing by an expression of the form:

$$f_{seamed} = 1.667\left(N_{Re}^{-0.049}\right) f_{seamless} \text{ .....} \quad (7.11.2)$$

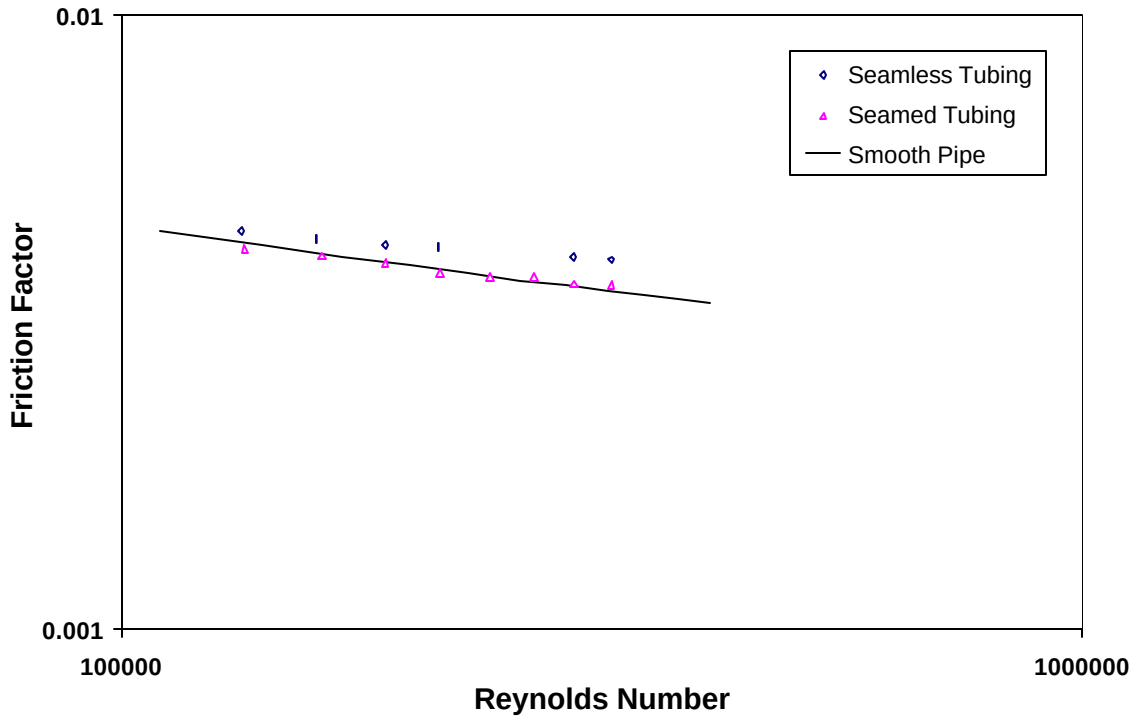

Figure 7.11.1-Friction Factor for Water Flowing in Straight Sections of Seamed and Seamless Tubing

The effect of tubing curvature on the frictional pressure loss of water is illustrated in Figure 7.11.2 which compares coiled tubing results to results from a straight section of seamed tubing. This comparison indicates that coiled tubing curvature has a significant effect on frictional pressure loss. Friction loss for coiled tubing is much higher than for seamed tubing. The relative increase in friction factor, due to curvature, increases with increasing Reynolds number, from 31% to 44% as shown in Figure 7.11.2. Relationships between frictional pressure loss in coiled tubing and straight pipe sections were derived and are of the form:

$$f_{CT} = 0.6\left(N_{Re_G}^{0.068}\right) f_{seamed} \quad \text{..... (7.11.3)}$$

and

$$f_{CT} = 1.017\left(N_{Re_G}^{0.019}\right) f_{seamless} \quad \text{..... (7.11.4)}$$

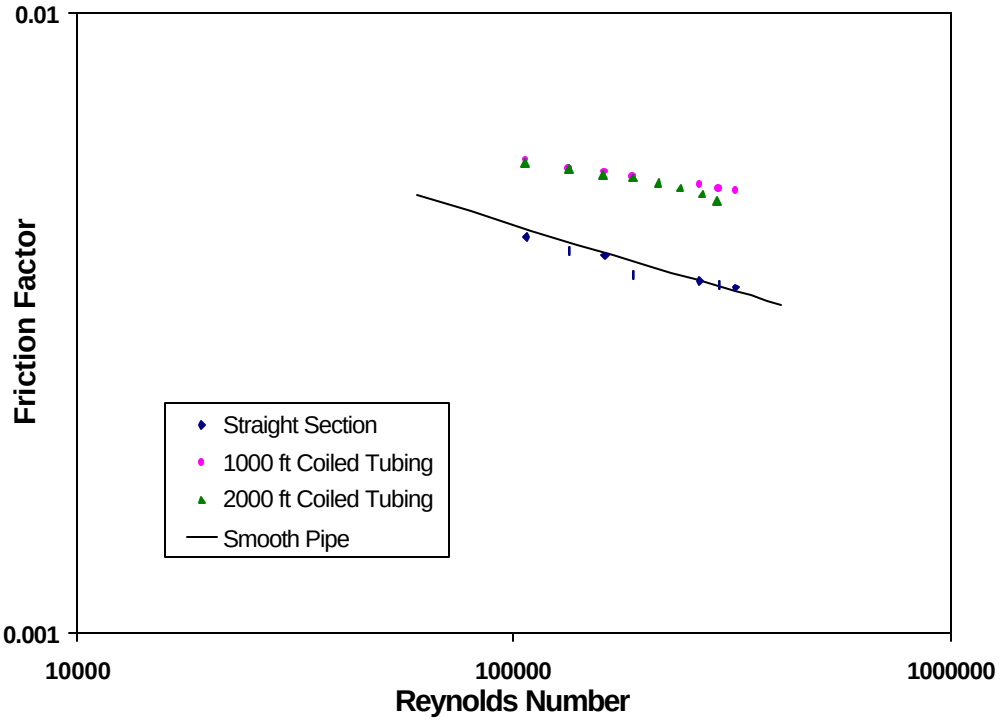

Figure 7.11.2-Friction Factor for Water Flowing in CT and in a straight Section of Seamed Tubing

Results obtained for 1000-ft and 2000-ft lengths of coiled tubing, as shown in Figure 7.11.2, suggest that the number of turns on the reel has no effect on the frictional pressure loss. However, the reader should be cautioned that the average reel diameters for the 1000-ft and the 2000-ft coils are not significantly different, resulting in approximately the same value for the ratio of tubing ID to reel diameter.

35 lb Guar Gum/Mgal Polymer Solution. Results obtained for a 35 lb guar/Mgal polymer solution (n = 0.53, k = 0.0112 psf sec^n) are presented graphically in Figure 7.11.3. Laminar and smooth pipe flow results are also plotted for comparison. It can be observed that friction factor values for the polymer solution are much lower than those obtained with water. In the range of Reynolds number considered, drag reduction varying from 29% to 78% is obtained with the polymer solution. As expected, curvature of the coiled tubing has a significant effect on frictional pressure loss. Indeed, it can be observed that friction factor values with coiled tubing are higher than with straight sections. Interestingly, unlike water, tubing seam does not seem to have an effect on the

friction factor of this polymer solution. Since, as stated earlier, the seam tends to suppress the high turbulence frequencies. These results suggest that, for the drag-reducing fluid under investigation, the turbulence spectrum is composed mainly of low - turbulence frequencies, on which the tubing seam has no effect. Examination of the experimental data suggest that coiled tubing friction factor is related to straight pipe friction factor by the following relationship:

$$f_{CT} = 0.747\left(N_{Re_G}^{0.015}\right) f_{SP} \quad \text{..... (7.11.5)}$$

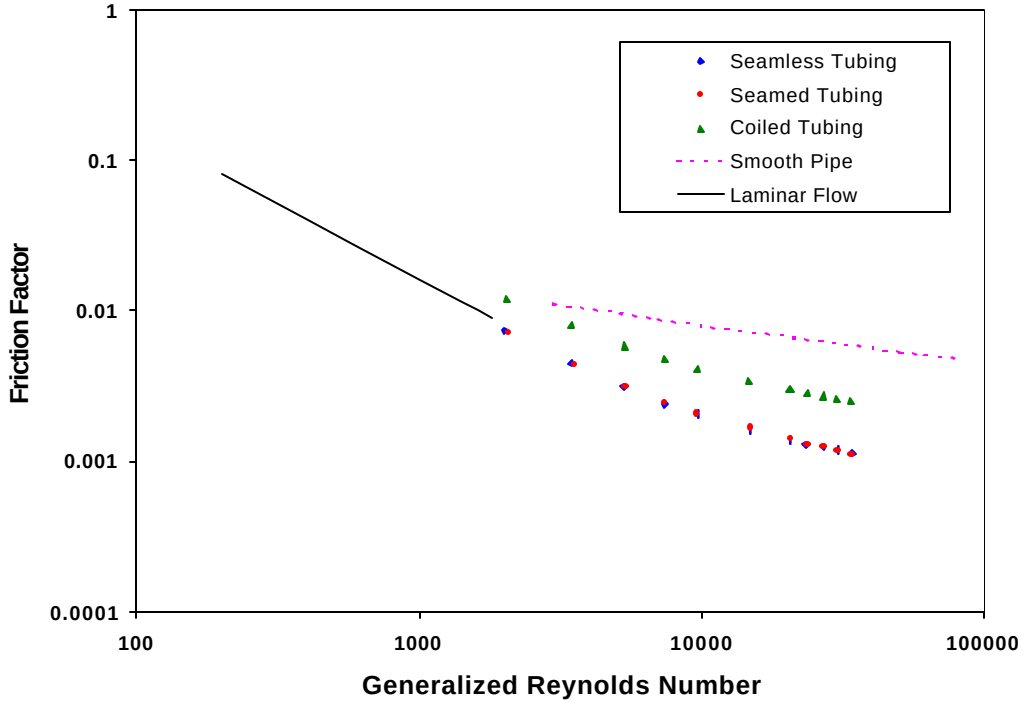

Figure 7.11.3-Friction Factor for Linear 35 lb guar/1000 gal Solution

40 lb HPG/Mgal Polymer Solution. Figure 7.11.4 summarizes results obtained for a 40 lb HPG/Mgal polymer solution (n = 0.42, k = 0.034 psf sec^n). Again, the same observations made earlier for the guar gum solution can also be made for the HPG solution. It is noteworthy that these results indicate that HPG has better drag-reducing properties than the guar gum solution. However, this could be due to the higher concentration of HPG (40 lb/Mgal) as compared to the previous case involving guar. Again, as for the case with guar, the following equation relating coiled tubing friction factor to that in straight pipe was derived based on the experimental results:

$$f_{CT} = 0.596\left(N_{Re_G}^{0.135}\right) f_{SP} \quad \text{..... (7.11.6)}$$

It must be emphasized that the effect of coil (reel) diameter is not taken into account. In principle, the correlations should be expressed in terms of the Dean number instead of the Reynolds number. Unfortunately, only one reel diameter was available during the course of this investigation. These correlations are unique to the specific fluid system under investigation and should be used with caution.

In the case of crosslinked gels, no equation was derived relating straight and curved tubing because straight and coiled tubing sections have vastly different lengths. Consequently, it is impossible to distinguish between the effects of curvature and those associated with shear history. These shortcomings as well as that discussed earlier in connection with the Dean number are to be addressed in the future.

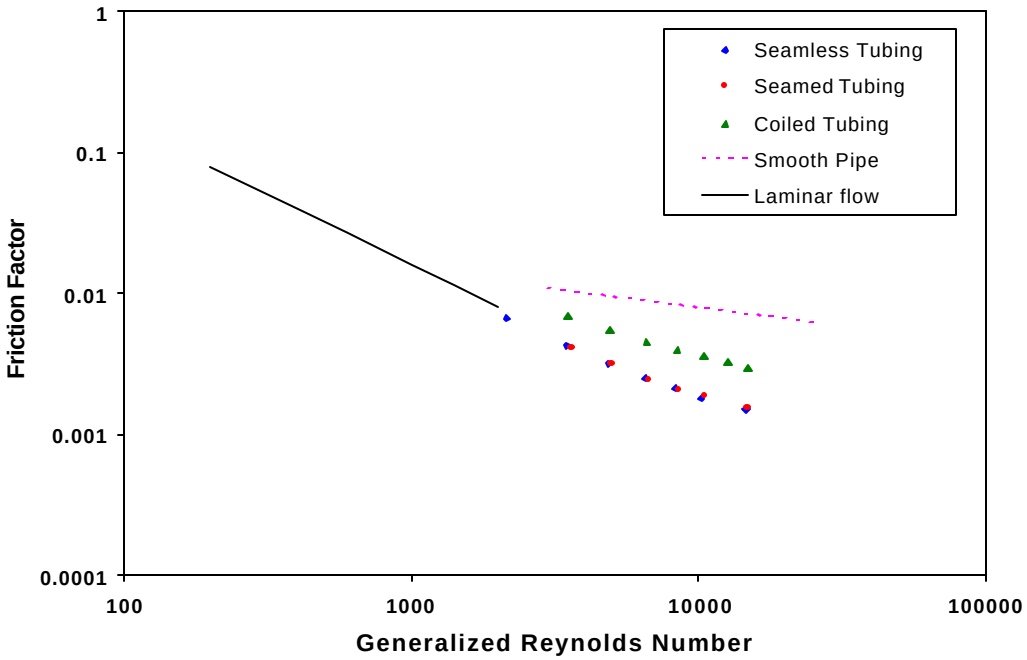

Figure 7.11.4-Friction Factor for Linear 40 lb HPG/1000 gal Solution

Borate-Crosslinked 35 lb Guar Gum/Mgal Polymer Gel. Pressure loss measurements in straight seamed and seamless tubing sections are shown in Figures 7.11.5 through 7.11.7 for borate-crosslinked 35 lb guar/Mgal gels prepared at pH values of 9,10, and 11, respectively. These figures illustrate the effects of pH, shear history, and the presence of a seam. At pH=9 pressure drop decreases continuously with increasing shear history, as expected. On the other hand, for pH=10 and pH=11 the frictional pressure drop first decreases to a minimum value, corresponding to a shear history of 1 minute, then starts increasing with increasing shear history. This behavior is probably related to the different mechanisms active when a borate-crosslinked gel flows through tubing.

Crosslink bonds form initially, break as the result of shearing, and then reform through a process of rehealing. All of these mechanisms are active and dependent on flowing conditions such as temperature and shear rate. The continual decrease in pressure loss with increased shear history at pH=9 can be hypothesized to be the result of crosslink bonds being destroyed more rapidly than they can reheal. This results in a decrease in the viscosity of the fluid and thus, in the pressure drop. This same behavior is observed at pH=10 and pH=11 for shear histories less than or equal to 1 minute. However, for longer shear histories the combined rate of new crosslinked bond formation and the rehealing of broken bonds becomes higher than the rate at which the crosslinked bonds are destroyed by shearing. This results in the presence of a local minimum in the viscosity versus shear history curve and, thus, in the pressure drop versus shear history curve. Interestingly, the effect of the seam on the pressure drop is significant only for pH=9 and short shear histories.

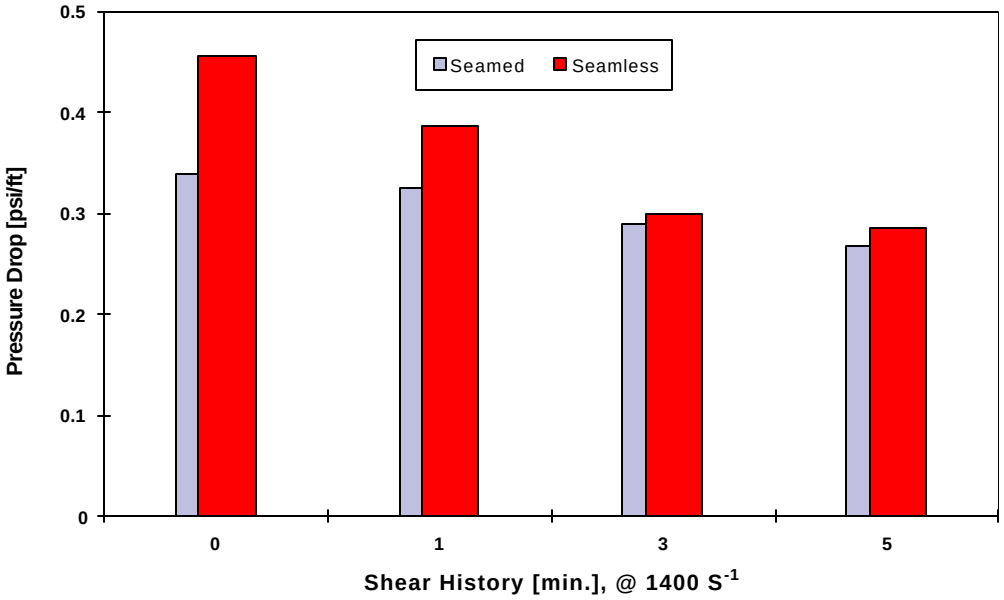

Figure 7.11.5-Pressure Drop in Seamed and Seamless Tubing for Borate-Crosslinked 35 lb guar/1000 gal gel, at pH 9.0 and Flow Rate 60 gal/min

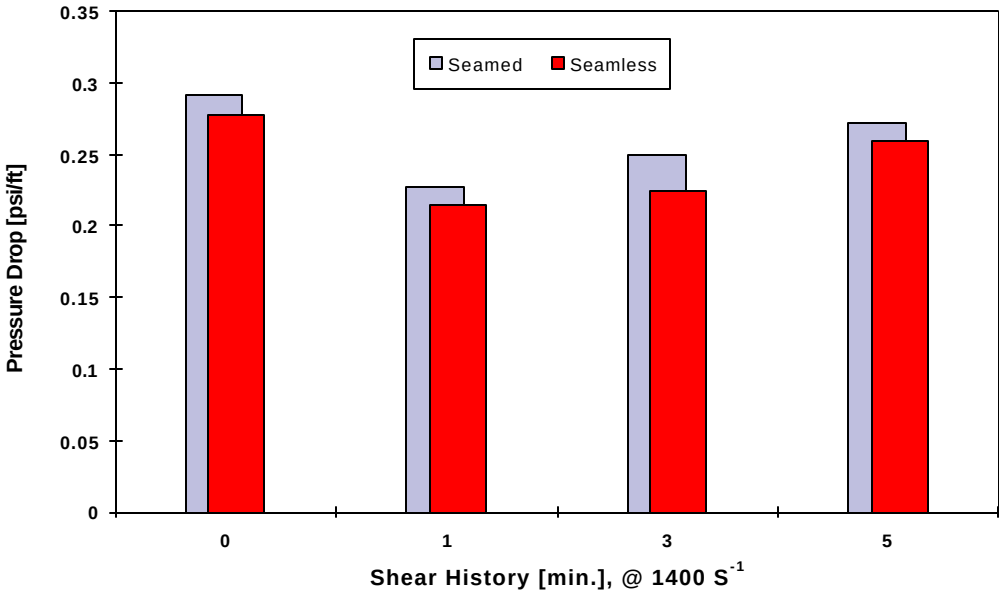

Figure 7.11.6-Pressure Drop in Seamed and Seamless Tubing for Borate-Crosslinked 35 lb guar/1000 gal gel, at pH 10.0 and Flow Rate 60 gal/min

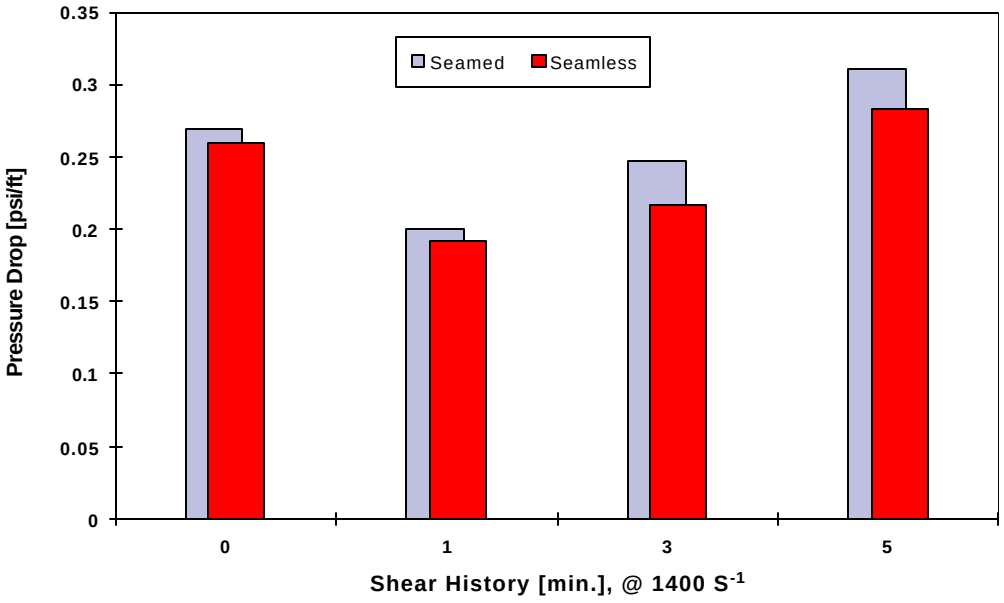

Figure 7.11.7-Pressure Drop in Seamed and Seamless Tubing for Borate-Crosslinked 35 lb guar/1000 gal gel, at pH 11.0 and Flow Rate 60 gal/min

The effect of pH and coiled tubing length on pressure loss is illustrated graphically in Figure 7.11.8. As expected, crosslinking increases the pressure gradient. Moreover, increasing the pH results in lower values for the pressure gradient. The change in pressure gradient with length of tubing at constant pH is insignificant. At first this may seem inconsistent with the earlier claim regarding the effect of shear history on the pressure drop in straight tubing sections. However, while the use of the term shear history may be descriptive for a short straight section located at the exit of the preconditioning loop, it is not as meaningful in the case of fluid flowing in a long section of coiled tubing. Fluid exiting a long section of coiled tubing has experienced the maximum degree of preconditioning while fluid just entering the coil has experienced the least. Thus, measurements taken across a long section of coiled tubing are not specific to a particular shear history, but represent a broad spectrum of shear histories.

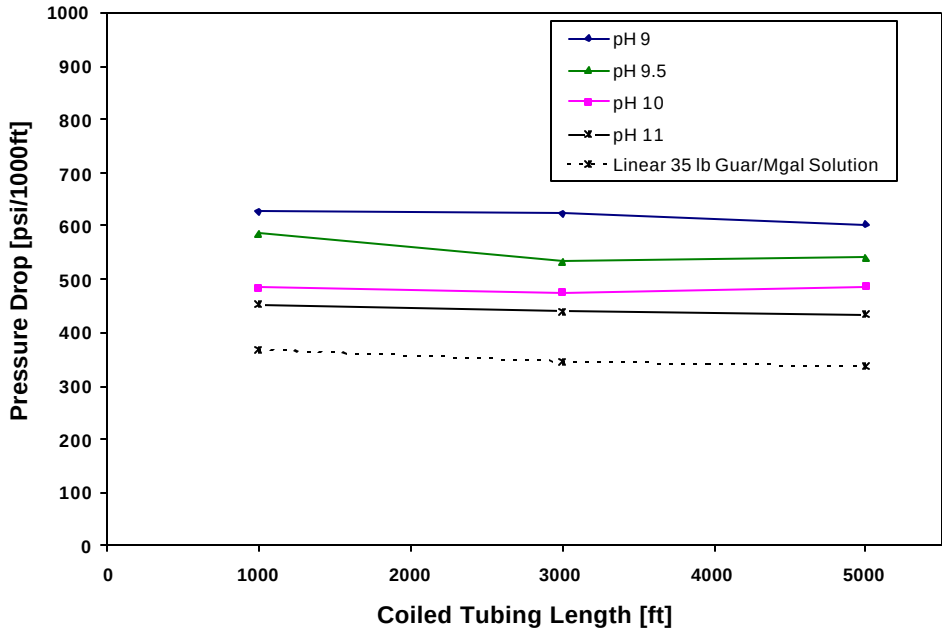

Figure 7.11.8-Pressure Drop in CT for Borate-Crosslinked 35 lb guar/1000 gal Gel

Borate-Crosslinked 35 lb HPG/Mgal Gel. Pressure loss measurements in straight seamed and seamless tubing sections are shown in Figures 7.11.9 through 7.11.11 for borate-crosslinked 35 lb HPG/Mgal gels prepared at pH values of 9,10, and 11, respectively. These figures illustrate the effects of pH, shear history, and the presence of a seam. Unlike the results for borate-crosslinked guar, the pressure drop in the straight tubing sections is a decreasing function of shear history for all pH values considered. These results suggest that the rate at which crosslinked bonds are destroyed by shearing is higher than the rate at which new bonds are being formed. The viscosity of the fluid and thus, the pressure drop, is a decreasing function of shear history. Interestingly, as with borate-crosslinked guar, the tubing seam seems to decrease the pressure drop only at pH=9 and in the absence of shear history for the current case.

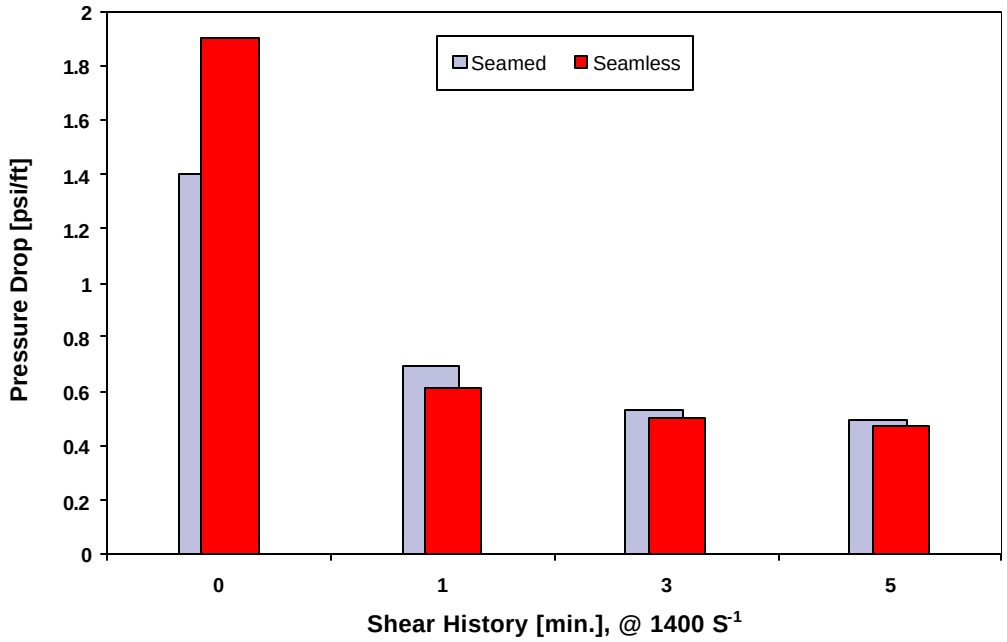

Figure 7.11.9-Pressure Drop in Seamed and Seamless Tubing for Borate-Crosslinked 35 lb HPG/1000 gal gel, at pH 9.0 and Flow Rate 60 gal/min

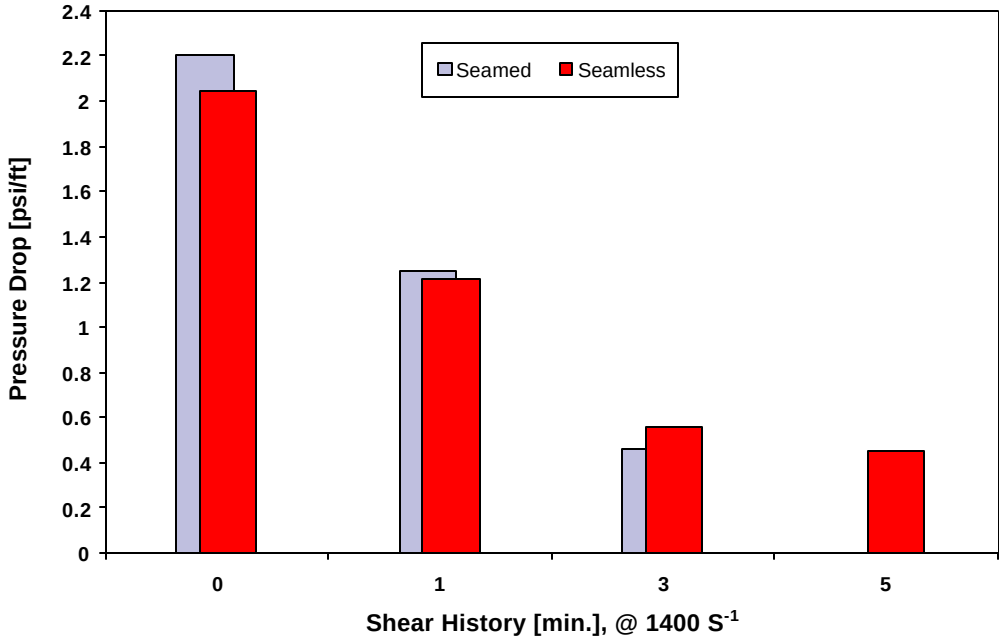

Figure 7.11.10-Pressure Drop in Seamed and Seamless Tubing for Borate-Crosslinked 35 lb HPG/1000 gal gel, at pH 10.0 and Flow Rate 60 gal/min

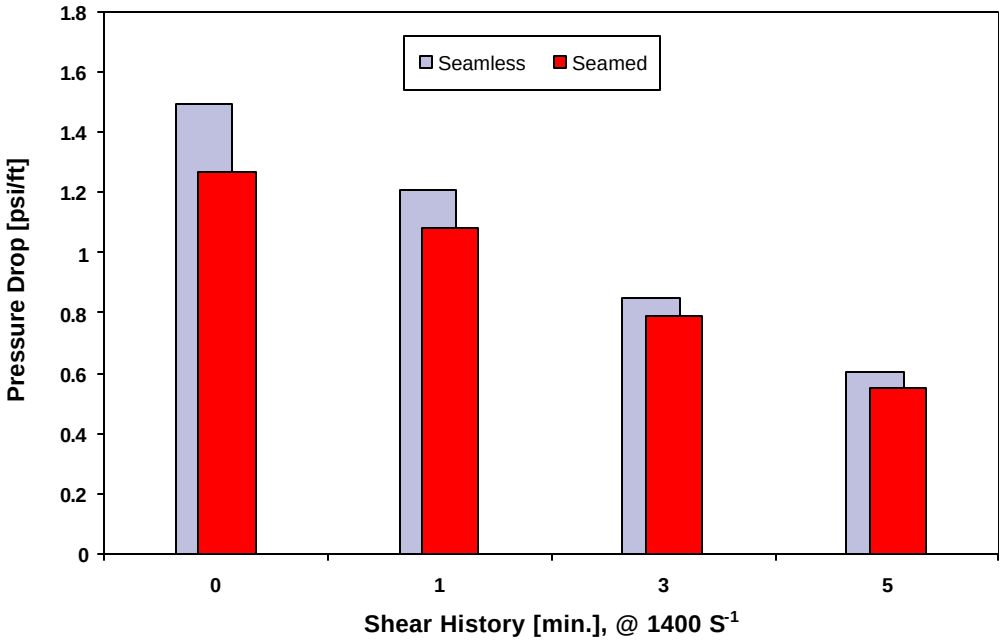

Figure 7.11.11-Pressure Drop in Seamed and Seamless Tubing for Borate-Crosslinked 35 lb HPG/1000 gal gel, at pH 11.0 and Flow Rate 60 gal/min

Pressure drop results measured in coiled tubing of various lengths are shown in Figure 7.11.12. Unlike for borate-crosslinked guar, the dependence of the pressure gradient on the length of coiled tubing across which it is measured is strikingly strong. The pressure gradient first decreases sharply and then seems to approach a limiting asymptote. However, this could actually be a local minimum in the curve of pressure drop versus coiled tubing length. Observations made earlier with borate-crosslinked guar certainly tend to support this claim, which can only be verified with additional coiled tubing length.

Frictional pressure loss measurements with borate-crosslinked 35 lb guar/Mgal and 35 lb HPG/Mgal gels are compared in Table 7.11.1 for injection through 1000-ft and 3000-ft lengths of coiled tubing at 60 gpm (1400 sec^{-1}). Two observations can be made. First, HPG pressure losses are significantly higher than those for guar at all pH values and for all coiled tubing lengths. Second, the pressure drop is lower for flow through 3000 ft of coiled tubing with both gels and at all pH values. The longer shearing time in the 3000-ft coil tends to partially destroy the crosslink network responsible for the higher frictional pressure losses observed in the 1000-ft coil.

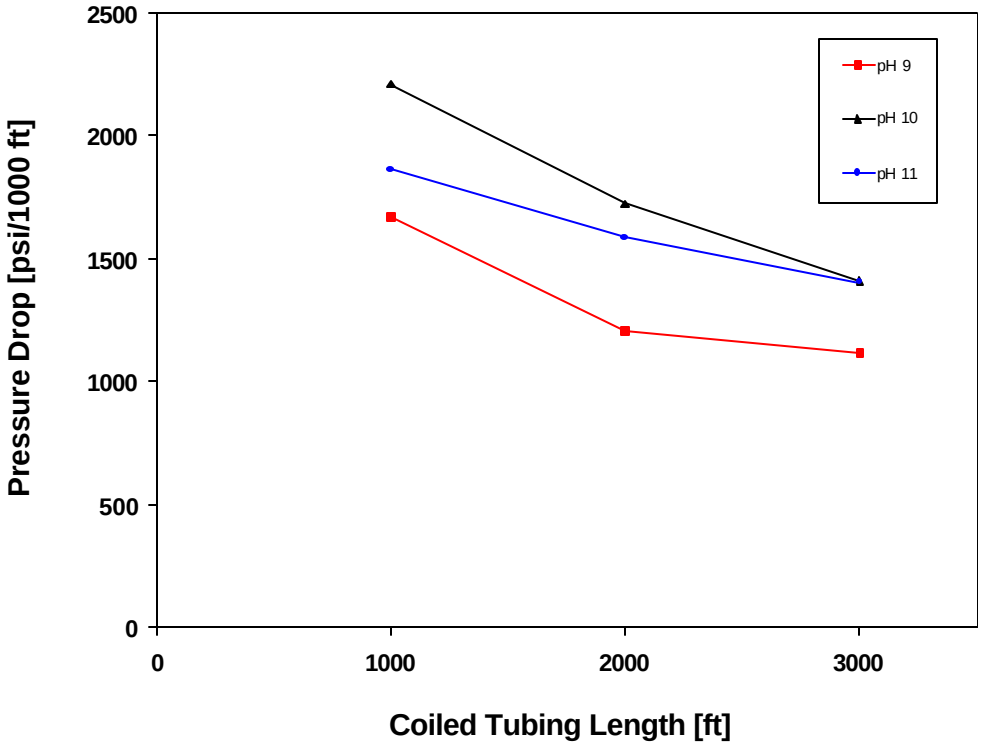

Figure 7.11.12-Pressure Drop in CT for Borate-Crosslinked 35 lb HPG/1000 gal Gel

		Pressure Drop (psi/1000 ft)		
CT Length (ft)	pH	Borate-Crosslinked 35 lb Guar/1000 gal	Borate-Crosslinked 35 lb HPG/1000 gal	Difference (%)
1000	9.0	626	1668	166
	10.0	484	2206	356
	11.0	453	1861	311
3000	9.0	623	1113	79
	10.0	475	1407	196
	11.0	439	1403	220

Table 7.11.1-Comparison of Pressure Losses of Borate-Crosslinked Guar and HPG

7.12 References

1. Gidley, J.L., Holditch, S.A., Nierode, D.E., and Veatch, R.W.: *Recent Advances in Hydraulic Fracturing, SPE Monograph Vol. 12,* (1989).
2. Harris, P.C.: "Chemistry and Rheology of Borate-Crosslinked Fluids at Temperatures to 300^{o}F," *JPT* (March 1993) 264-269.
3. Hannah, R.R., and Harrington, L.J.: "Measurement of Dynamic Proppant Fall Rates in Fracturing Gels Using a Concentric Cylinder Tester," *JPT* (May 1981) 909-913.
4. Clark, P.E., and Quadir, J.A.: "Proppant Transport in Hydraulic Fractures: A Critical Review of Particle Settling Velocity Equations," paper SPE 9866 presented at the 1981 SPE/DOE Low Permeability Symposium, Denver, Colorado, 27-29 May.
5. Power, D.J., Rodd, A.B., Paterson, L., and Boger, D.V.: "Gel Transition Studies on Nonideal Polymer Networks using Small Amplitude Oscillatory Rheometry," *J. Rheol.* (1998) **42**, No. 5, 1021-1037.
6. Power, D.J.: "Rheological Characterization of Hydraulic Fracturing Fluids," Ph.D. Dissertation, University of Melbourne, 1997.
7. Winter, H.H., and Chambon, F.: "Analysis of Linear Viscoelasticity of a Crosslinking Polymer at the Gel Point," *J. Rheol.* (1986) **30**, No. 2, 367-382.
8. Acharya, A.: "Viscoelasticity of Crosslinked Fracturing Fluids and Proppant Transport," paper SPE 15937 presented at the 1986 SPE Eastern Regional Meeting, Columbus, Ohio, 12-14 November.
9. de Kruijf, A.S., Roodhart, L.P., and Davies, D.R.: "Relation Between Chemistry and Flow Mechanics of Borate-Crosslinked Fracturing Fluids," *SPEPF* (August 1993) **8**, No. 3, 165-170.
10. Jin, L., and Penny, G.S.: "Dimensionless Methods for the Study of Particle Settling in Non-Newtonian Fluids," *JPT* (March 1995) 223-228.
11. "Fracturing Fluid Characterization Facility (FFCF)," Annual Report, GRI-97/0050, December 1996.
12. "Fracturing Fluid Characterization Facility (FFCF)," Annual Report, GRI-98/0235, December 1997.
13. "Fracturing Fluid Characterization Facility (FFCF)," Annual Report, GRI-99/0128, December 1998.
14. Hejjo, H., Fagan, J. E., and Shah, S. N.: "Flow Visualization Technique for Investigation of Hydraulic Fracturing," paper SPE 38579 presented at the 1997 SPE Annual technical Conference and Exhibition, San Antonio, Oct. 5-8.
15. Shah, S. N., and Asadi, M.: "Convection/Encapsulation in Hydraulic Fracturing," paper SPE 39961 presented at the 1998 SPE Rocky Mountain Regional/Low Permeability Reservoirs Symposium and Exhibition, Denver, Apr. 5-8.
16. Shah, S. N., and Asadi, M., and Lord, D. L.: "Proppant Transport Characterization of Hydraulic Fracturing Fluids using a High Pressure Simulator Integrated with a Fiber Optic/LED Vision System," paper SPE 49040 presented at the 1998 SPE Annual Technical Conference and Exhibition, New Orleans, Sept. 27-30.
17. Asadi, M., Shah, S. N., and Lord, D. L.: "Static/Dynamic Settling of Proppant in Non-Newtonian Hydraulic Fracturing Fluids," paper SPE 52217 presented at the 1999 SPE Mid-Continent Operations Symposium, Ok City, Mar. 28-31.
18. Cleary, M. P., and Fonseca, A.: "Proppant Convection and Encapsulation in

Hydraulic Fracturing: Practical Implications of Computer and Laboratory Simulations," paper SPE 24825 presented at the 1992 SPE Annual Technical Conference and Exhibition, Washington D.C., Oct. 4-7.
19. Clark, P. E., and Zhu, Q.: "Convective Transport of Propping Agents During Hydraulic Fracturing," paper SPE 37358 presented at the 1996 SPE Eastern Regional Meeting, Columbus, Oct. 23-25.
20. Shah, S. N., Lord, D. L., and Rao, B. N.: "Borate-Crosslinked Fluid Rheology Under Various pH, Temperature, and Shear History Conditions," paper SPE 37487 presented at the 1997 SPE Production Operations Symposium, Oklahoma City, 9-11 March.
21. Goel, Naval, Willingham, J. D., Shah, S. N., and Lord, D. L.: "A Comparative Study of Borate-Crosslinked Gel Rheology Using Laboratory and Field Scale Fracturing Simulations," paper SPE 38618 presented at the 1997 SPE Annual Technical Conference and Exhibition, San Antonio, 5-8 October.
22. Goel, Naval, Shah, S. N., and Asadi, M.: "A New Empirical Correlation to Predict Apparent Viscosity of Borate-Crosslinked Guar Gel in Hydraulic Fractures," paper SPE 39816 presented at the 1998 SPE Permian Basin Oil and Gas Recovery Conference, Midland, 25-27 March.
23. "Fracturing Fluid Characterization Facility (FFCF)," Annual Report, GRI-95/0091, December 1994.
24. "Fracturing Fluid Characterization Facility (FFCF)," Annual Report, GRI-96/0145, December 1995.
25. Goel, Naval, and Shah, S. N.: "Experimental Investigation of Proppant Flowback Phenomena Using a Large Scale Fracturing Simulator," paper SPE 56880 presented at the 1999 SPE Annual Technical Conference and Exhibition, Houston, 3-6 October.
26. Stein, N.: "Calculate Drawdown that will Cause Sand Production," *World Oil* (Apr. 1988) 48-49.
27. Romero, J., and Feraud, J. P.: "Stability of Proppant Pack Reinforced with Fiber for Proppant Flowback Control," paper SPE 31093 presented at the 1996 SPE Formation Damage Control Symposium, Lafayette, Feb. 14-15.
28. Milton-Tayler, D., Stephenson, C., and Asgian, M. I.: "Factors Affecting the Stability of Proppant in Propped Fractures: Results of a Laboratory Study," paper SPE 24821 presented at the 1992 SPE Annual Technical Conference and Exhibition, Washington D.C., Oct. 4-7.
29. Asgian, M. I., Cundall, P. A., and Brady, B. H. G.: "The Mechanical Stability of Propped Hydraulic Fractures: A Numerical Study," paper SPE 28510 presented at the 1994 SPE Annual Technical Conference and Exhibition, New Orleans, Sept. 25-28.
30. Raymond, L. R., and Binder, Jr., G. G.: "Productivity of Wells in Vertically Fractured Damaged Formations," *JPT* (Jan. 1967) 120-130.
31. Lord, D. L., Vinod, P. S., Shah, S. N., and Bishop, M. L.: "An Investigation of Fluid Leakoff Phenomena by Use of a High-Pressure Simulator," *SPEPF* (Nov. 1998) 250.
32. El-Rabba, A. M., Shah, S. N., and Lord, D. L.: "New Perforation Pressure-Loss Correlations for Limited-Entry Fracturing Treatments," *SPEPF* **14**(1) (Feb. 1999) 63.
33. Azouz, I., Shah, S. N., Vinod, P. S.: "Experimental Investigation of Frictional Pressure Losses in Coiled Tubing," *SPEPF* (May 1998) 91.

7.13 Nomenclature

A	=	constant
a_T	=	horizontal shift factor, dimensionless
$a_{Tcalculated}$	=	calculated horizontal shift factor, dimensionless
B	=	constant
b_T	=	vertical shift factor, dimensionless
$b_{Tcalculated}$	=	calculated vertical shift factor, dimensionless
C	=	constant
c_1, d_1	=	constants, dimensionless
c_2, d_2	=	constants, T, $^oK/^oF$
c_3, d_3	=	constants, dimensionless
C_d	=	perforation coefficient of discharge, dimensionless
d	=	diameter of coiled tubing, L, in.
D	=	diameter of coiled tubing, L, m
d_{perf}	=	initial perforation diameter, L, in.
ESS_1	=	error terms, dimensionless, $ESS_1 = \Sigma(a_{T_i} - a_{T_{calculated_i}})^2$
ESS_2	=	error terms, dimensionless, $ESS_2 = \Sigma(b_{T_i} - b_{T_{calculated_i}})^2$
f	=	friction factor, dimensionless
f_{CT}	=	friction factor for flow in coiled tubing, dimensionless
f_{seamed}	=	friction factor for flow in seamed tube , dimensionless
$f_{seamless}$	=	friction factor for flow in seamless tube, dimensionless
$f_{straightpipe}$	=	friction factor for flow in straight pipe, dimensionless
G'	=	Elastic Modulus
G''	=	Viscous Modulus
k	=	consistency index, dimensionless, M/LT^{2-n}, psf sec^n
K_F	=	consistency index for foam
K_L	=	consistency index for liquid
l	=	length between pressure ports, L, ft
N	=	number of perforations, dimensionless
n	=	power law index, dimensionless
N_{Re}	=	Reynolds number, dimensionless
N_{ReG}	=	Generalized Reynolds number, dimensionless
q	=	volumetric flow rate
Q	=	volumetric flow rate, L^3/t, m^3/sec
Q'	=	flow rate, L^3/T, bbl/min
Q_a	=	foam quality
Sn	=	shearing number, dimensionless
T	=	temperature, T, $^oK/^oF$
t	=	total pumping time, T, min.
T_o	=	reference temperature, T, $^oK/^oF$
$\boldsymbol{p}$	=	dimensionless numbers
$\boldsymbol{r}$	=	fluid density, M/L^3, lb/gal
$\boldsymbol{r}'$	=	density, m/L^3, kg/m^3

μ_{app}	=	apparent viscosity of the fluid, m/Lt, cP
Δp	=	pressure drop across coiled tubing, m/Lt^2, N/m^2
τ_r	=	reduced wall shear stress, m/Lt^2, psf
γ_r	=	reduced nominal shear rate, 1/t, sec^{-1}
γ	=	nominal shear rate, 1/t, sec^{-1}
μ_r	=	reduced apparent viscosity of the fluid, m/Lt, cP
τ_o	=	yield shear stress
τ_w	=	wall shear stress, m/Lt^2, psf
$\Delta\rho$	=	slurry density-clean fluid density, M/L^3, lb/gal

Chapter 8 COILED TUBING CONSORTIUM

8.1 Introduction

Coiled Tubing (CT) has gained increased importance in the petroleum industry and there has been interest expressed in the characterization of fluids in reeled tubing. Therefore, the Coiled Tubing Consortium (CTC) was established in July 1997 for the purpose of investigating the flow phenomena of drilling and completion fluids in coiled tubing. Since its establishment, the CTC has successfully accomplished all its goals of the first stage of research. Now, the CTC has entered the second stage of research with expanded research areas. This chapter briefly presents the CTC research capabilities and accomplishments.

8.2 The Mission of Coiled Tubing Consortium

Phase I: The Mission of the Coiled Tubing Consortium is to develop a database and correlations for determining the frictional losses and rheology of non-Newtonian fluids and foams representing popular drilling, completion, and stimulation fluids pumped through reeled and straight portions of coiled tubing strings as well as concentric and eccentric annuli.
Phase II: The research objective of the second phase of the Coiled Tubing Consortium is to investigate the coiled tubing hydraulics for drilling, wellbore cleanout/cuttings removal, and stimulation employing drilling, completion, and stimulation fluids.

8.3 Membership

The present members of the CTC includes the companies listed below:

- BJ SERVICES
- BP AMOCO
- BAKER
- DOWELL-SCHLUMBERGER
- HALLIBURTON-BAROID
- KELCO
- QUALITY TUBING
- SONATRACH
- PHILLIPS PETROLEUM

8.4 Experimental Setup and Procedure

Figure 8.1 shows the experimental apparatus used in this study. Two 50 bbl tanks are used for fluid mixing and storage and a Galigher centrifugal pump is used to feed a

Triplex plunger pump. There are seven reels of coiled tubing segments: one 1000 ft reel and one 2000 ft reel of 2 3/8 in. nominal tubing, one 1000 ft reel and two 2000 ft reels of 1 1/2 in. nominal tubing and one 500 ft reel and one 1000 ft reel of 1 in. nominal tubing. Each of the tubing sizes is accompanied by two straightened sections of coiled tubing of the same size, 30 ft in length where differential pressure is measured across 20 ft of the length. Two 30-ft annular test strings with 2 3/8-in. pipe inside 3 1/2 in. with differential pressure measurements across 20 ft are also used. One annular test string is concentric while the other is eccentric. Honeywell differential pressure transducers are used for the measurement of differential pressure across the straightened segments, the annular test strings and the reeled tubing strings. A Micromotion flow meter is used to record the flow rate, temperature and density of the fluids under investigation.

The procedure followed in testing involved proper fluid preparation as the various fluids studied required specific mixing procedures for each one. The first tubing size used for each test was the 2 3/8-in. tubing. The fluid was first pumped through both reels followed by the longest reel alone and lastly the shortest reel alone. After the fluid was prepared, water was pumped through the system as a system calibration check to insure accuracy during operation. The fluid was then pumped through the system, and when the system was filled, it was closed in for recirculation of the fluid. The fluid was pumped at various flow rates up to either the maximum flow rate available from the Triplex, or reaching the maximum system pressure of 5000 psi. This same sequence of events was followed for the 1 1/2 in. coiled tubing and the 1-in. coiled tubing as well.

Fluid mixing tank samples were taken before the test was run followed by on-line sampling during circulation before each segment of the test followed by a final sample at the end of the test. In this way, any changes in fluid viscosity due to heating or degradation were taken into account.

The data of interest gathered from the data acquisition system include:

- Flow rates
- Differential pressures over coiled tubing segments,
- Differential pressures over straight tubing sections
- Differential pressures over annular tubing sections.
- Fluid density
- Fluid temperatures at various locations along the flow loop

These data items have been used as the basis for the frictional loss analysis. Fluid samples taken from the on-line sampling port were used for rheological evaluation by both a model 35 Fann viscometer and a Bohlin viscometer. The Bohlin viscometer provides measurements at elevated temperature.

The data gathered from the flow tests and viscometer measurements were first cleaned to get rid of noises and outliers. Then, the relationship between friction factor and generalized Reynolds number was examined. Previous friction factor correlations were tried to see their ability of predicting the friction loss in coiled tubing for the fluids investigated. Finally, new correlations were developed for coiled tubing as well as straight tubing.

8.5 Laboratory Rheology

The objective of laboratory study is to understand the flow behavior of fluids under various shear rate and temperature conditions. Knowledge of fluid rheology is essential to estimate the frictional pressure losses in pipes. Generally, drilling and completion fluids are not Newtonian fluids, i.e., their viscosities are not constant, but changing with shear rate.

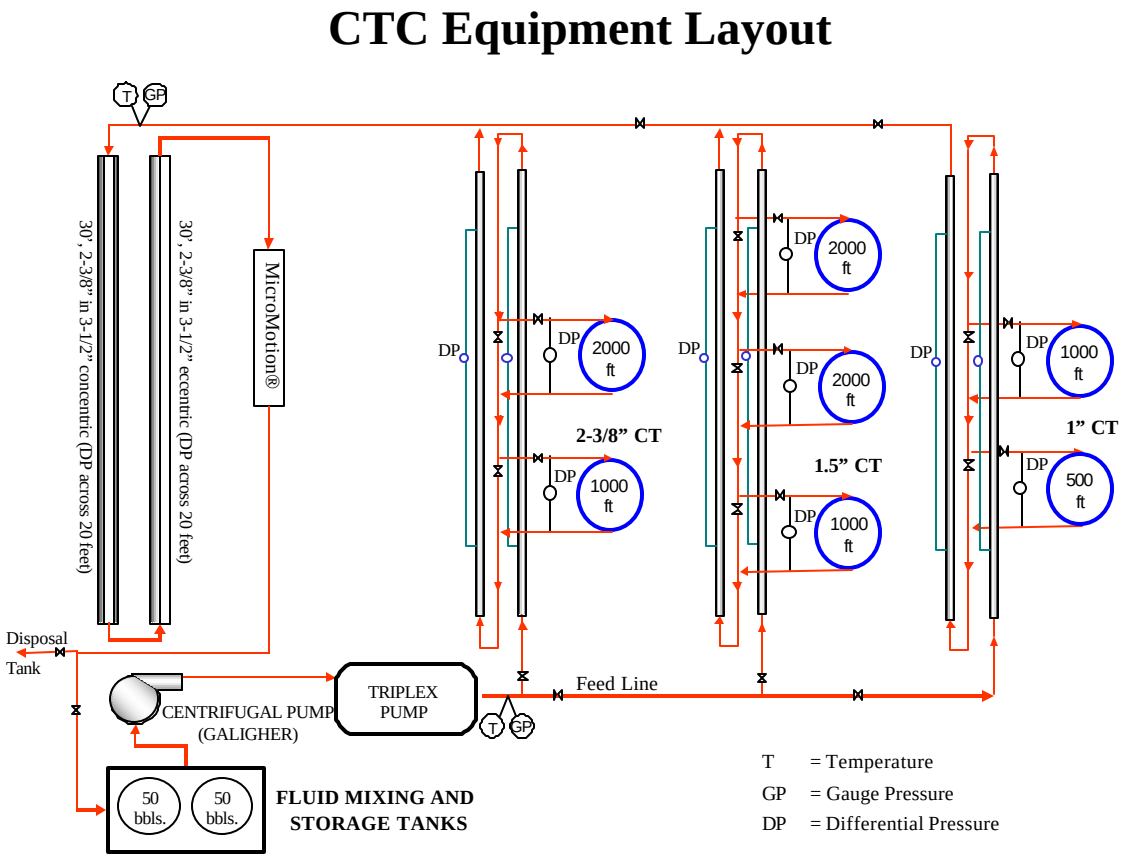

Figure 8.1 Schematic of Coiled Tubing Test Facility

Therefore, more complex rheological models are needed to characterize these fluids. The CTC laboratory rheology study involves testing the rheological properties with both model 35 Fann viscometer and Bohlin viscometer.

Test with Model 35 Fann Viscometer

The model 35 Fann viscometer is essentially a concentric cylinder rotary viscometer. The main elements of the viscometer include an outer cup and an inner cylinder or bob. The outer cup rotates concentrically around the bob which is suspended from a torsion wire. A dial affixed to the wire and a fixed pointer enable the angle through which the wire has

turned to be measured. The fluid sample in the narrow gap between the bob and cup undergoes shear when the cup rotates. The shear stress (τ_w) can be estimated from the dial reading and a conversion factor for a given spring number. The shear rate ($\dot{g}_w$) can be calculated from the RPM (revolutions per minute) of the cup and a conversion factor which depends on the instrument dimensions. Proper rheological models and their parameters can then be established based on the rheograms of shear stress versus shear rate. There are six RPMs with model 35 Fann viscometer: 3, 6, 100, 200, 300, and 600 which correspond to a shear rate range of 5 to 1021 sec^{-1}. And only tests at ambient temperatures can be run with Fann viscometer. For higher temperature test, we need to use Bohlin viscometer.

Tests with Bohlin Rheometer

Bohlin CS50 rheometer is essentially a controlled stress, rotary viscometer. Its test cell has more geometries: bob and cup, cone and plate, and parallel plates, etc. More importantly, the High Pressure Cell (HPC) enables measurements at elevated temperatures. The test control and data recording are computerized. The results of shear stress and shear rate as well as viscosities are given in a format of data file. The data can then be analyzed to rheologically characterize the fluid. During this study, the shear rate range is 0.01 to 800 sec^{-1}. The temperature range is 75 to 250 °F. It is found that most of the fluids investigated can be described by power law model in the range of shear rate that would most probably be encountered in practical applications. The correlations between power law parameters and temperature were also developed.

8.6 Accomplishments of CTC - Phase I

By May 1999, the CTC had accomplished successfully all its goals set by the CTC members. All the research results had been reported to the member companies on the CTC annual meeting, May 27, 1999, Houston, TX and other semi-annual and annual meetings. The following is a brief summary of the first stage accomplishments.

8.6.1 Experimental Work

The experimental work of the CTC in the first phase includes two parts: coiled tubing flow loop tests and laboratory rheology tests. Test procedures have been discussed previously. According to the test matrix agreed upon by the CTC members, extensive flow tests and laboratory rheology tests were conducted. The fluid systems investigated are shown in the following tables:

Table 8.1 Fluid Systems – Linear gels

Type	Concentration	Temperature Range
HEC	10, 20, 40 lb/Mgal	75 – 250 °F
Xanthan	10, 20, 40 lb/Mgal	75 – 250 °F
PHPA	20, 40 lb/Mgal	75 – 250 °F
Guar	20, 30, 40 lb/Mgal	75 – 250 °F
Foams	Water (40-80% quality) 20, 30, 40 lb/Mgal Guar (30-80% quality)	75 °F 100 – 175 °F

Table 8.2 Fluid Systems-Drilling Fluids

Type	Additives
8 lb/bbl Bentonite + Fresh Water	1 lb/bbl MMH
8 lb/bbl Bentonite + Fresh Water	1 lb/bbl Starch
2 lb/bbl Xanthan + Fresh Water	1 /lb/bbl Starch
1 lb/bbl Xanthan + Fresh Water	3% vol. Rev Dust

In each experiment, the fluid was prepared according to the formulation and preparation instructions of that fluid. Then, the fluid was pumped through the largest tubing loop, i.e., the 2-3/8" CT loop at various flow rates. Differential pressures across various CT segments, straight sections as well as annular sections were gathered. Other data such as fluid density and temperature were also recorded. After the test on 2-3/8" tubing was finished, the flow was switched to 1-1/2" tubing and 1" tubing loops. Similar data were gathered for 1-1/2" and 1" tubing loop.

The fluid sample taken from the on-line sampling port was split into two parts: one part was tested using model 35 Fann viscometer, the other part was tested using Bohlin viscometer. The test results with Fann viscometer helped in fluid quality control as well as providing rheological parameters at ambient temperature. When the fluid sample was tested on Bohlin viscometer, the temperature was set at 75, 100, 125, 150, 175, 200, 225, and 250 °F. At each temperature, the shear rate was varied from 0.01 to 800 sec-1. The shear sequence (shear sweep) was set as shearing from low shear rate to high shear rate. After finishing the sweeps at each temperature, the system was heated up to a higher temperature and shear sweep was repeated until the test at the final temperature was finished.

8.6.2 Data Analysis and Development of New Correlations

During the data analysis of each test, the raw data recorded by the data acquisition system was first cleaned to delete the transitional data, noises, and any outliers. Generalized Reynolds number and friction factor were calculated from flow rate, various pressure drops, tubing geometry, and viscosities from Fann viscometer. Correlations from literature, such as Mccann and Islas [1], Mashelkar and Devarajan[2], and Screenivasan and Strykowski[3] were tried to compare with the experimental data. For straight tubing data, correlations from literature were also investigated. These included Shah[4], Drew[5], and Dodge and Metzner[6] correlations. Based on these comparisons, new correlations were developed for both reeled coiled tubing and straightened coiled tubing respectively. For polymer solutions, the Fanning friction factor as a function of Reynolds number could be described by the following general equation:

$$\sqrt{f} = a + \frac{b}{\sqrt{N_{Reg}^{c}}} \quad \text{.....} \quad (8.1)$$

where f = Fanning friction factor

N_{Reg} = generalized Reynolds number

a, b, c = constants which are correlated with the tubing diameter, the curvature ratio (the ratio of tubing diameter to reel diameter) as well as apparent viscosity

For drilling mud, data analysis indicated that a relationship between the friction factor and Reynolds number as:

$$f^{2} = a + \frac{b}{N_{Reg}^{2}} \quad \text{.....} \quad (8.2)$$

where a, b are correlated with tubing diameter and curvature ratio of the coiled tubing reel.

The analysis of laboratory rheology data indicated that most of the fluids investigated can be characterized by power law model over wide ranges of shear rate and at various temperatures except for the very low and very high shear rate regions where they exhibited upper and lower Newtonian regions. The power law parameters of each fluid at various polymer concentrations and various temperatures were calculated. It was found that these parameters could be correlated well with temperature. Correlations of power law parameters as function of temperature were thus developed.

8.6.3 Deliverables

- Correlations to determine frictional losses in CT, straight sections of CT, as well as concentric and eccentric annuli for linear gels and drilling fluids
- Comparison of experimental data from CT, straight sections of CT, as well as concentric and eccentric annuli with literature

- Correlations for determining the alteration in rheological properties of linear gels and drilling fluids
- Flow loop for testing and evaluating foam fluids for their rheological behavior
- Rheology data of the aqueous and guar-gelled foams
- Correlations for estimating rheological parameters for the aqueous and guar-gelled foam fluids
- Cleaned raw data from CT flow tests and laboratory rheology tests, that forms the basis of various correlations. Data provided in Excel workbook format on 3.5 in. Diskette.
- Semi-annual and annual reports

8.7 Accomplishments of CTC - Phase II

The CTC Phase II kickoff meeting was held on July 20, 1999 when new research areas had been proposed. According to the meeting, the first six months have been primarily devoted to verify the newly developed friction pressure loss correlations.

8.7.1 Evaluation of CTC Correlations Using Real Drilling Fluids

Two real drill-in fluids were provided by M-I Drilling and Baroid for the flow tests. It was expected that the data from these real drilling fluids could provide an independent check for the accuracy and performance of the CTC correlations.

M-I Fluids:

Table 8.3 shows the formulations of M-I fluids. The base gel is Xanthan polymer solution. The xanthan concentration was about 69 lb/Mgal to achieve a yield point of 30 $lb_f/100ft^2$. Lubricants (Lubetex) at concentrations of 1% and 3% (vol.) were added to the base gel to test the effect of friction reduction. Following the addition of lubricants, Rev Dust at concentrations of 0.5%, 1%, and 2% (vol.) were mixed into the fluid to simulate the effect of drilling solids. During and after each addition of additives, we kept high rate circulation and allowed adequate mixing. For each fluid formulation, we ran the flow test. Therefore, altogether 6 flow tests were conducted with M-I fluids.

Baroid Fluids:

Table 8.4 shows the formulations of Baroid fluids. The base gel is again Xanthan polymer solution. The xanthan concentration was about 53 lb/Mgal to achieve a yield point of 24 $lb_f/100ft^2$. Encapsulator (ClaySeal) at concentrations of 4 lb/bbl was first added to the base gel. Then, Lubricant 1 (LUBETEX) and Lubricant 2 (DRIL-N-SLIDE) were added. Finally, Rev Dust was mixed into the fluid to simulate the drilling solids content. Similarly, six tests were run with the base gel and subsequent additives.

No.	Formulation	Legend
1	Base Gel: Xanthan (YP: 30 $lb_f/100ft^2$)	MI 1
2	Xanthan + 1% Lubricant	MI 2
3	Xanthan + 3% Lubricant	MI 3
4	Xanthan + 3% Lubricant + 0.5% RevDust	MI 4
5	Xanthan + 3% Lubricant + 1% RevDust	MI 5
6	Xanthan + 3% Lubricant + 2% RevDust	MI 6

Table 8.3 Formulations of M-I Fluid

No.	Formulation	Legend
1	Base Gel: Xanthan (YP: 24 $lb_f/100ft^2$)	B 1
2	Xanthan + 4 lb/bbl Encapsulator	B 2
3	Xanthan + 4 lb/bbl Encapsulator +1.5% Lubricant 1	B 3
4	Xanthan + 4 lb/bbl Encapsulator +1.5% Lubricant 1 + 0.5% Lubricant 2	B 4
5	Xanthan + 4 lb/bbl Encapsulator +1.5% Lubricant 1 + 0.5% Lubricant 2 + 12 lb/bbl RevDust	B 5
6	Xanthan + 4 lb/bbl Encapsulator +1.5%Lubricant 1 + 0.5%Lubricant 2 + 18 lb/bbl RevDust	B 6

Table 8.4 Formulations of Baroid Fluids

Test Procedure

The 1-1/2" coiled tubing flow loop was used for all the tests. Before flowing base gel into flow loop, water was flushed through the system to ensure the flow loop was cleaned. Then, the base gel was pumped at various rates, and data were collected. Before and after the flow test of each fluid, fluid samples were collected and their rheological properties were measured using model 35 Fann viscometer. The flow rates were: 30, 40, 50, 60, 80, 100, 120, 140 gpm, and up to the highest rate possible. Upon completing each test, the fluid was circulated at high rate and additive was mixed into the system. Fluid was

circulated until the additive was uniformly dispersed and well-mixed. The flow test was then conducted. The above procedure was repeated for all the additives.

New flow data were gathered using the WCTC CT test facility. Meanwhile, rheological data were gathered using Bohlin and Fann model 35 viscometers. The data analysis of the friction loss data and rheological data have been completed. The analysis results showed that the friction loss correlations developed by the WCTC could adequately predict the friction pressure losses for the real drilling fluids. The test data and data analysis results have been reported to the CTC member companies.

Results and Discussions

a) The experimental results of friction factor as a function of Reynolds number were compared with the predictions by the CTC correlations developed previously. It was found that the CTC correlation for coiled tubing predicts the friction factor of the base gels quite well for both M-I and Baroid fluids. Even better agreement was obtained at high Reynolds numbers.
b) At low Reynolds numbers, the correlation overestimates the friction factor. But, the biggest deviation is less than 11% for M-I base gel and Baroid base gel.
c) For both M-I and Baroid fluids, as the fluids became more complex (due to addition of lubricants and solids), the correlation is not working as well. Since the CTC correlation was developed based on data of clean fluids, some deviation from the experimental values is not surprising. In fact, even for the complex formulations, the biggest deviation is still less than 18% for M-I fluids and 23% for Baroid fluids. As more data for such complex fluids are gathered, the correlation can then be modified accordingly.
d) *The Effect of Lubricants on Friction Pressure*. As indicated in Tables 8.3 and 8.4, in both M-I and Baroid fluids, lubricants were added to reduce fiction pressure. Results showed that as 1% and 3% (vol.) lubricants were added to the M-I base gel, the friction pressure was reduced significantly. Similarly, as the encapsulator, 1.5% lubricant, and 0.5% lubricant were added sequentially to the Baroid base gel, friction pressure was also reduced.
e) *Effect of Drilling Solids on Friction Pressure*. In order to study the effect of drilling solids on the flow resistance of drilling fluids in tubulars, Rev Dust was added to the drilling fluids to simulate the drilling solids. Experimental results showed that at low concentrations of Rev Dust (such as 0.5% and 1%), the increase in friction pressure due to drilling solids is not significant, especially after lubricants were added. But, at high Rev dust concentration (2%), the increase of friction pressure became important.

8.7.2 Enhancement of Coiled Tubing Test Facility

In order to meet the growing interest and requirements from the CTC member companies, efforts have been made to enhance the capabilities of the coiled tubing test facility. These efforts involve purchasing, construction, and installation of additional equipments.

- One reel of 2-3/8” CT and one reel of 1-1/2” CT, each having length of 200 ft, were obtained to build the longer straight test sections.

- One new reel of 1-3/4" CT, single-wrapped on 72" core and one new reel of 2-3/8" CT, single-wrapped on a 72" core were also obtained. The purpose of obtaining these new reels is to provide more necessary data on the effect of CT diameter and curvature ratio.

8.7.3 Research Report and Publications

- A semi-annual research report was completed and sent to the CTC members. This report includes all the flow test data and laboratory rheology data, experiment details, and results of data interpretation and analysis.
- Based on the CTC work and with the permission of the CTC members, three papers were published in SPE meetings and two more papers have been submitted for publication.
- Three master theses were completed based on part of the CTC research project.

8.8 Future Research Plans

8.8.1 Research Plan for the Next Six months

At the July 20, 1999 CTC meeting in Norman, OK, the CTC members agreed upon the following research areas for the second half of the first year of Phase II research plan. First, construct a loop with longer straight tubing section and conduct flow tests on these straight sections. The objective is to acquire more accurate data and to evaluate the straight tubing friction loss correlations. The second task is to install two new CT reels and build four annular sections. The aim of constructing these additional components is to study the effect of CT geometry (tubing diameter and tubing diameter to reel diameter ratio) and annulus geometry (equivalent diameters and eccentricity) on the friction loss. Two new CT reels and four annular sections will be constructed and installed. The third task that was proposed at the last meeting is to evaluate the CTC correlations using the field Pressure While Drilling (PWD) data. Some PWD data have already been obtained. In the next six months, further efforts will be made to acquire all necessary PWD data and then the analysis of these data will be completed.

8.8.2 Research Topics for the Second Year of CTC Phase II

- *Drag Reduction of Solids-Laden Fluids*: the aim is to gather friction loss data of solids-laden fluids in CT and straight sections and to develop correlations to predict friction loss values for solids-laden drilling fluids.
- *Wellbore Cleanout*: wellbore cleanout constitutes the majority of the CT operations (>60% CT activities). Experimental study will include solids transport in vertical, inclined, and horizontal annulus when employing CT for cleanout jobs. Meanwhile, mathematical models and computer programs will be established to simulate the complete wellbore cleanout process. The programs will help to improve the design of solids cleanout operations.

- *Foam Friction Pressure Loss*: The objectives include: a) to gather experimental data of foam fluid rheology and friction losses and b) to develop empirical correlations to predict friction pressure losses of foam fluids and empirical correlations to predict foam fluid rheology
- *CT Fracturing*: to gather experimental data of frictional losses of fracturing fluids in coiled tubing, straight tubing, and annuli, and develop correlations for CT fracturing applications.
- *Field Data Comparison/Confirmation of the CTC correlations*
- *Others*: Some CTC members also expressed interests in the following research areas:
  - friction loss study for e-line/CT annulus
  - Performance evaluation of mud motors
  - Friction loss study of tapered strings
  - Friction loss study of hydraulic line/CT annulus
  - Composite coiled tubing

Nomenclature

a, b, c = empirical constants in Eq. (8.1) and Eq. (8.2)
f = Fanning friction factor
N_{Reg} = generalized Reynolds number
τ_w = shear stress at wall
$\dot{g}_w$ = shear rate at wall

References

1. McCann, R.C. and Islas, C.G.: "Frictional Pressure Loss During Turbulent Flow in Coiled Tubing," paper SPE 36345, presented at the SPE/ICoTA North American Coiled Tubing Roundtable, Montgomery, TX, Feb. 26-28, 1996.
2. Mashelkar, R.A. and Devarajan, G.V.: "Secondary Flow of Non-Newtonian Fluids: part III – Turbulent Flow of Visco-Inelastic Fluids in Coiled Tubes," *Trans. Inst. Chem. Engrs*., Vol. 55, 1977, pp29-37.
3. Screenivasan, K.R. and Strykowski, P.J.: "Stabilization Effect in Flow Through Helically Coiled Pipes," *Experiments in Fluids*, Vol. 1, 1983, pp31-36.
4. Shah, S. N.: "Correlations Predict Friction pressures of Fracturing Gels," *Oil and Gas Journal*, January 16, 1984, pp.92-98.
5. Drew, T.B., Koo, E.C. and McAdams, W.H.: "The Friction factors for Clean Round Pipes," Trans. *AIChE*, Vol. 28, 56, 1932.
6. Dodge, D. and Metzner, A.: "Turbulent Flow of Non-Newtonian System," *AIChE Journal* Vol. 5 (1959), 189.

Chapter 9 TECHNOLOGY DISSEMINATION

9.1 Introduction

The purpose of technology dissemination is to translate the research results at the FFCF into practical nuggets of information that will directly benefit the industry. As often the case, the current level of technical knowledge with the service companies and operators does not translate to the field. One of the main reasons for this technology gap between the research and field personnel is the limitations in scaling down the field conditions to the laboratory. The FFCF simulates to the maximum degree practical, all conditions experienced by a fracturing fluid from its simple condition on the surface to harsh environment while flowing down the wellbore, through perforations, its injection into the fracture, and leakage into the rock matrix. Since this hurdle has been overcome in the technology transfer chain, the impediments to the technology adoption are shifted to providing the results in an *end-user-understandable* form.

Promotional tours and advertising of this research initiative were targeted to the technical service departments of the producers and service companies. The FFCF utilized the resources of the Department of Energy (DOE), Gas Research Institute (GRI), the Sarkeys Energy Center, and the School of Petroleum and Geological Engineering at the University of Oklahoma (OU) in spreading the word about the facility. The campaign included the exhibition of a prototype of the High Pressure Simulator (HPS) in the booths of OU and GRI at various trade shows, distributing publications and brochures detailing the capabilities and services available.

In this chapter, Technology Dissemination activities conducted at the FFCF are provided in some detail. These efforts include, technical papers and publications, trade shows, Masters theses and Doctoral dissertations, articles in trade journals, FFCF WEB site and industry in-house presentations. These efforts have also resulted in third-party testing, establishment of a Proppant Flowback Consortium and a Coiled Tubing Consortium. These activities are provided in greater detail in the following sections.

9.2 Technology Dissemination

Following are the approaches taken by the FFCF to effectively disseminating the research findings to the industry:

1. Technical publications/presentations
2. Master thesis and Doctoral dissertations
3. Brochures
4. Technical Articles
5. Reports
6. Patents
7. Benefits to the industry
8. Other means of transferring research findings

9.2.1 Technical Publications/Presentations

A plan was developed to publish and present the FFCF research findings in the form of extended abstracts, technical papers, and technical presentations at various conferences. Following is a list of papers prepared and presented by the FFCF team.

- "A Model for Flow in the Fractured Porous Media Based on Cellular-automation," A. Rodriquez, D. Lin and J. C. Roegiers, Proceedings of the ISRM International Symposium EUROROCK '93.

- "A Low Deborah Number Model for a Viscoelastic Flow Driven Along a Channel by Suction at Porous Walls," D. Lin and R. Evans, American Society of Mechanical Engineering 1993 Winter Annual Meeting, New Orleans.

- "A Study of Squeezing Flow in Fracture Channel," D. Lin and J. C. Roegiers, Proceedings of the 34th U.S. Symposium on Rock Mechanics, 1993.

- "Application of Advanced Computational Technology to Fracturing Fluid Characterization Facility," D. Lin and J. C. Roegiers, Proceedings of International Symposium on Computer Methods in Rock Mechanics (ISCMRM '93).

- "The Use of Laser Doppler Velocimetry (LDV) for the Measurement of Fracturing Fluid Flow in the FFCF Simulator," R. B. Mears, J. J. Sluss, Jr., J. E. Fagan and R. K. Menon, SPE 26619, 68th Annual Technical Conference and Exhibition of the Society of Petroleum Engineers, Houston, TX, October 3-6, 1993.

- "Description of a Large, High-Pressure Slot flow Apparatus for Characterizing Fracturing Fluids," R. G. Rein, Jr., D. L. Lord, and S. N. Shah, SPE 26524, 68th Annual Technical Conference and Exhibition of the Society of Petroleum Engineers, Houston, TX, October 3-6, 1993.

- "Fracturing Fluid Characterization Facility," R. D. Evans, Fuels Technology Contractors Review Meeting, Morgantown, WV, November 16-18, 1993.

- "Simulation of Non-Newtonian Inelastic Two-dimensional Slot Flow," J. C. Roegiers and D. Lin, SPE 27014, SPE III Latin America and Caribbean Petroleum Engineering Conference, Buenos Aires, Argentina, April 27-29, 1994.

- "Analysis of Leakoff in Laminar Flow Through a Porous Fracture Channel," J. C. Roegiers and D. Lin, SPE 27008, SPE III Latin America and Caribbean Petroleum Engineering Conference, Buenos Aires, Argentina, April 27-29, 1994.

- "Chebyshev Spectral Collocation Method for Leakoff in Hydraulic Fracturing," S. Marisela, D. Lin and J. C. Roegiers, Eighth International Conference on Computer Methods and Advances in Geomechanics, West Virginia, 1994.

- "Poisson Bracket Formulation for Proppant Transport in Hydraulic Fracturing," D. Lin, J. C. Roegiers, and A. A. Rodriguez, Eighth International Conference on Computer Methods and Advances in Geomechanics, West Virginia, 1994.

- "Shearing Motion of Dense Proppant Material in Hydraulic Fracturing," D. Lin and J. C. Roegiers, 1st NARMS, The University of Texas at Austin, (ed. P. P. Nelson & S. E. Laubach), pp. 201-208, June 1994.

- "Fuzzy Logic Controls Pressure in Fracturing Fluid Characterization Facility," V. P. Rivera and L.M. Farabee, SPE 28239, 1994 SPE Petroleum Computer Conference, Dallas, TX, July 31-August 3.

- "Study of Perforation Friction Pressure Employing a Large-Scale Fracturing Flow Simulator," D. L. Lord, S. N. Shah, R. G. Rein, Jr., J. T. Lawson, III, SPE 28508, 1994 SPE Annual Technical Conference and Exhibition, New Orleans, LA, September 25-28.

- "Study of Perforation Friction Pressure Employing a Large-Scale Fracturing Flow Simulator," D. L. Lord, S. N. Shah, R. G. Rein, Jr., J. T. Lawson, III, SPE Paper No. 28508, "Peer Reviewed"

- "Tests Confirm Operational Status of a Large-Slot Flow Apparatus for Characterizing Fracturing Fluids," S. N. Shah and D. L. Lord, SPE 29499, Production Operations Symposium, Oklahoma City, OK, April 2-4, 1995.

- "Fracturing Fluid Characterization Facility (FFCF): Recent Advances," S. N. Shah, Natural Gas RD&D Contractors Review Meeting, Baton Rouge, LA, April 4-6, 1995.

- "An Investigation of Fluid Leakoff Phenomena Employing a High-Pressure Simulator," D. L. Lord, P. S. Vinod, S. N. Shah, and M. L. Bishop, SPE 30496, 1995 SPE Annual Technical Conference and Exhibition, Dallas, TX, October 22-25.

- "The Determination of Dynamic Proppant Concentration Field in Slot Flow in the FFCF," R. Beason and J. Fagan, SPE 30515, 1995 SPE Annual Technical Conference and Exhibition, Dallas, TX, October 22-25.

- "New Insights on Hydraulic Fracturing from the Fracturing Fluid Characterization Facility," L. R. Brand, S. N. Shah, and D. L. Lord, 1995 International Gas Research Conference, Cannes, France, November 6-9.

- "Discussion of Experimental and Numerical Modeling of Convective Proppant Transport," by F. Civan, S.N. Shah, and P.S. Vinod, JPT, vol. 47, No. 11, November 1995.

- "Experimental Investigation of Heat Transfer Characteristics of Guar-Based Polymer Solutions and Gels," Paper 26K, I. Azouz, P. S. Vinod, S. N. Shah, T. Lear, and D. L. Lord, 1996 AIChE National Heat Transfer Conference, Houston, TX, August 3-6.

- "Experimental Investigation of Frictional Pressure Losses in Coiled Tubing," I. Azouz, S. N. Shah, P. S. Vinod, and D. L. Lord, SPE 37328, 1996 SPE Eastern Regional Meeting, Columbus, OH, October 23-25.

- "Rheological Characterization of Hydraulic Fracturing Fluids Using a Large, High Pressure Slot Flow Apparatus," N. Goel, B. N. Rao, R. Subramanian, S. N. Shah, and D. L. Lord, Society of Rheology, Houston, TX, February 16-20, 1997.

- "Borate-Crosslinked Fluid Rheology Under Various pH, Temperature and Shear History Conditions," S. N. Shah, D. L. Lord, and B. N. Rao, SPE 37487, 1997 SPE Production Operations Symposium, Oklahoma City, OK, March 9-11.

- "Impairment of Producibility Due to Fracturing Fluid Leakoff in Oil Reservoirs," B. Gadiyar, A. Gupta, and S.N. Shah, SPE 37491, 1997 SPE Production Operations Symposium, Oklahoma City, OK, March 9-11.

- "Fracturing Fluid Characterization: State-of-the-art Facility and Advanced Technology," S. N. Shah and M. Asadi, DOE's Natural Gas Conference, Houston, TX, March 24-27, 1997.

- "New Perforation Pressure Loss Correlations for Fracturing Fluids and Slurries," A. M. ElRabaa, S. N. Shah, and D.L. Lord, SPE 38373, 1997 SPE Rocky Mountain Regional Meeting, Casper, WY, May 18-21.

- "Effects of Coiled Tubing Shear History on the Rheological and Hydraulic Properties of Fracturing Fluids," S. N. Shah and R. Subramanian, SPE 38421, 2nd North American Coiled Tubing Roundtable, Montgomery, TX, April 1-3, 1997.

- "Dimensionless Correlations for Predicting the Filtration of Fracturing Fluids from Fracture Faces," A. Gupta, B. R. Gadiyar, and S. N. Shah, American Filtration and Separations Society Summer Technical Conference and Expo, Lafayette, LA, July 15-16, 1997.

- "Characterization of Polymer Solutions and Crosslinked Gels at Downhole Conditions Using an Advanced High Pressure Simulator," S. N. Shah and M. Asadi, 3rd International Conference on Reservoir Conformance Profile Control, Water & Gas Shut Off, Houston, TX, August 6-8, 1997.

- "An Investigation of Fluid Leakoff Phenomena Employing a High-Pressure Simulator," D. L. Lord, P. S. Vinod, S. N. Shah, and M. L. Bishop, SPE Production & Facilities, November 1998.

- "A New Empirical Correlation to Predict Apparent Viscosity of Borate-Crosslinked Guar Gel in Hydraulic Fractures," N. Goel, M. Asadi, and S. N. Shah, SPE Paper No. 39816, Proceedings of the 1998 SPE Permian Basin Oil and Gas Recovery Conference, Midland, TX.

- "Convection/Encapsulation in Hydraulic Fracturing," M. Asadi, and S. N. Shah, SPE Paper No. 39961, Proceedings of the 1998 SPE Rocky Mountain Regional/Low-Permeability Reservoirs Symposium and Exhibition, Denver, CO.

- "Proppant Transport Characterization of Hydraulic Fracturing Fluids using a High Pressure Simulator Integrated with a Fiber Optic/LED Vision System," S. N. Shah, M. Asadi, and D. L. Lord, SPE Paper No. 49040, Proceedings of the 1998 SPE Annual Technical Conference and Exhibition, New Orleans, LA

- "Experimental Investigation of Frictional Pressure Losses in Coiled Tubing," I. A. Azouz, P. S. Vinod, D. L. Lord, and S. N. Shah, SPE Production & Facilities, May 1998.

- "Advances in Hydraulic Fracturing Fluid Characterization using a Field Scale High Pressure Simulator," A. Berkat A., and S. N. Shah, Proceedings of 3rd Journees Scientifiques Et Techniques, Alger, Algeria.

- El-Rabba, A.M., Shah, S.N., and Lord, D.L.: "New Perforation Pressure-Loss Correlations for Limited-Entry Fracturing Treatments," SPE Production and Facilities, 14(1) (February 1999) 63.

- Asadi, M., Shah, S.N., and Lord, D.L.: "Static/Dynamic Settling of Proppant in Non-Newtonian Hydraulic Fracturing Fluids" paper SPE 52217 presented at the 1999 SPE Mid-Continent Operations Symposium, March 28-31.

- Goel, N. and Shah, S.N.: "Experimental Investigation of Proppant Flowback Phenomena Using a Large Scale Fracturing Simulator" paper SPE 56880 presented at the 1999 SPE Annual Technical Conference and Exhibition, Houston, October 4-6.

- Goel, N. and Shah, S.N.: "Experimental Investigation of Proppant Flowback Phenomena using a Large Scale Fracturing Simulator" Highlighted in JPT (March 2000) 32.

- Bonilla, L.F. and Shah, S.N.: "Experimental Investigation on the Rheology of Foams" paper SPE 59752 presented at the 2000 SPE/CERI Gas Technology Symposium, Calgary, April 3-5.

- Medjani, B. and Shah, S.N.: "A New Approach for Predicting Frictional Pressure Losses of Non-Newtonian Fluids in Coiled Tubing" paper SPE 60319 presented at the 2000 SPE Rocky Mountain Regional/Low Permeability Reservoirs Symposium, Denver, March 12-15.

- Willingham, J.D. and Shah, S.N.: "Friction Pressures of Newtonian and Non-Newtonian Fluids in Straight and Reeled Coiled Tubing" paper SPE 60719 presented at the 2000 SPE/ICoTA Coiled Tubing Roundtable, Houston, April 5-6.

- Silva, M.A. and Shah, S.N.: " Friction Pressure Correlations of Newtonian and Non-Newtonian Fluids Through Concentric and Eccentric Annuli" paper SPE 60720 presented at the 2000 SPE/ICoTA Coiled Tubing Roundtable, Houston, April 5-6.

- Goel, N., Shah, S.N., and Asadi, M.: "New Empirical Correlation to Predict Apparent Viscosity of Borate-Crosslinked Guar Gel in Hydraulic Fractures," SPE Production and Facilities, (May 2000) 90.

- Cho, H. and Shah, S.N.: "A Three-Layer Modeling for Cuttings Transport in Coiled Tubing Horizontal Drilling," paper SPE 63269 presented at the 2000 SPE Annual Technical Conference and Exhibition, Dallas, October 1-4.

- Cho, H. and Shah, S.N.: "A Three-Segment Hydraulic Model for Cuttings Transport in Horizontal and Deviated Well," paper SPE 65488 presented at the 2000 SPE/CIM International Conference on Horizontal Well Technology, Calgary, November 6-8.

9.2.2 MS Theses and Ph.D. Dissertations

A number of graduate students from the University of Oklahoma were involved in conducting research in various areas of hydraulic fracturing at the FFCF. As a result, a number of Masters theses and Doctoral dissertations have been completed. The research findings were transferred to both industry and university communities by one of the means of transformation described in previous sections. In addition, a copy of published theses/dissertations was available through the University of Oklahoma Libraries. Listed below is a complete list of Graduate students that have taken part in this project and have written or working on their Thesis/Dissertation.

Completed:

Al El Rabaa – Masters, 1997

Brian Mears - Masters, 1993

Chee (Thomas) Liu - Masters, 1993

Doug Lonsinger - Masters, 1994

Farooq Tareen – Masters, 1999

Hazem Hejjo - Masters, 1993

Hazem Hejjo – Ph.D., 1999

John Hassell - Masters, 1992

John Lawson - Masters, 1994

John Zhao - Ph.D., 1994

K.A. Jaganatha - Masters, 1993

K.D. Thakore - Masters, 1992

Kevin Bjornen - Masters, 1994

Kok Tan - Masters, 1993

Linda Guan - Masters, 1993

Luis Bonilla – Masters, 1999

Mahadev A. – Masters, 1998

Moises Silva – Masters, 1999

Ronnie Beason - Masters, 1992

Sonja Lear - Masters, 1994

Tommy Lear - Masters, 1996

Tony Howl - Masters, 1995

Victor Abyad - Masters, 1993

Abu Sani – Masters, 1999

Brahim Medjani – Masters, 1999

Ridha Ouezzani – Masters, 1999

Naeem Saddiqui - Masters, 2000

Ivan Gil - Masters, 2000

Sonja Wilkinson - Ph.D., 2000

Stewart Mills - Masters, 1999

In Process:

Brian Mears - Ph.D.

Naval Goel - Ph.D.

Hyun Cho- Ph.D.

Ameet Raichur- Masters

Ramaswami Subramanian - Ph.D.

Ronnie Beason - Ph.D.

Yunxu Zhou – Ph.D.

Sudhakar Khade - Masters

9.2.3 Technical Brochures

A number of brochures were published for the FFCF. These were published jointly between GRI, DOE and the University of Oklahoma during the course of the project. Listed below is a list of the Technical Brochures that were published for Industry use.

- GRI Tech Profile, "New Facility Aids in Fracture Fluid Study."
- GRI Fact Sheet, "Fracturing Fluid Characterization Facility (FFCF)."
- DOE Office of Fossil Natural Gas Research Energy Project Facts, "The Fracturing Fluid Characterization Facility at the University of Oklahoma."
- The University of Oklahoma Fracturing Fluid Characterization Facility, "FFCF and Its Capabilities."
- The University of Oklahoma Fracturing Fluid Characterization Facility, "FFCF Perforation Pressure Loss Correlation."

9.2.4 Technical Articles

A number of technical articles were also published in an attempt to disseminate the new technology generated by the project. Listed below are the articles published.

- "OU Researcher Looking to Free Gas Resources," *The Sunday Oklahoman*, October 6, 1991, p. 1-C.

- "Concept and Objectives of the Fracturing Fluid Characterization Facility (FFCF)," *GRI In Focus - Tight Gas Sands*, vol. 7, no. 3, December 1991.

- "The Fracturing Fluids Characterization Facility," *ISRM News Journal*, by Robert G. Rein, Jr., vol. 2, no. 1, p. 7 (and cover photo), Spring 1994.

- "Fracturing Fluid Characterization Facility (FFCF) Improves Design and Control of Fracturing Treatments, *GRI Wellsight*, vol. 2, no. 3, p. 3, September 1994.

- "Research Facility Gets New Leader, New Look," *The University of Oklahoma Sarkeys Energy Center News*, vol. 2, no.1, Fall 1994.

- "Fracturing Fluid Characterization Facility," *GRI Natural Gas Supply Product Reference Guide*, p. 19, Spring 1995.

- "FFCF - A *Benchmark* for Characterizing Fracturing Fluids," *GRID*, vol. 19, no. 2, Summer 1996.

- "Fracturing Fluids and Their Impact are Focus of Test Facility and GRI Short Course," *GRI Wellsight*, vol. 4, no. 3, September 1996.

- "Frac simulator available for industry applications," *Oil and Gas Journal*, vol. 95, no. 29, July 21, 1997.

- "Well Construction Technology Center, University of Oklahoma," *Reel Reporter*, vol. 5, no. 1, March 2000.

9.2.5 GRI Topical, Internal Reports and Technical Summaries

Listed below are a list of Internal Reports, Topical Reports and GRI Technical Summaries published during the duration of DOE's participation in the FFCF project.

- "Evaluative Report of Three Schematic Alternatives for the Fracturing Fluid Characterization Facility," by Mark Caldwell.

- "An Architectural Program for the Fracturing Fluid Characterization Facility," by Eren Erdener.

- Internal Report 91-01, "Gas Research Institute Fracturing Fluid Characterization Facility Conceptual Plan," compiled by J. C. Roegiers, February 1991.

- Internal Report 91-02, "Feasibility of Using Geosynthetics as a Facing Material in the FFCF Simulator," compiled by D. J. Cruickshank, May 1991.

- Internal Report 91-03, “Review of Hele-Shaw Models and Their Applications,” by D. J. Cruickshank, August 1991.

- Internal Report 91-04, “Preliminary Facility Program for the FFCF,” by Eren Erdener, May 1991.

- Internal Report 91-05, “Critical Review of Rheological Models Applicable to Description of Hydraulic Fracturing Fluids,” by S. N. Shah, May 1991.

- Internal Report 91-06, “Oklahoma University Fracturing Fluid Characterization Facility (FFCF) Simulator Functional Requirements,” by Fred Tsuchiya, May 20, 1991.

- Internal Report 91-07, “FFCF Project Data Acquisition and Control System Selection,” compiled by J. E. Fagan, May 1991.

- Internal Report 91-08, “Some Remarks on Numerical Simulation of Non-Newtonian Flow,” by D. Lin, March 30, 1991.

- Internal Report 91-09, “Important Capabilities of the Planned Fracturing Fluids Characterization Facility,” by D. L. Lord and R. Rein, June 1991.

- Internal Report 91-10, “Need and Description for the FFCF Prototype,” by D. Ballew, J. Bushey, and K. Mellegard, June 1991.

- Internal Report 91-11, “Approach to Uncertainty Analyses for FFCF Test Results,” compiled by K. Mellegard, September 27, 1991.

- GRI Topical Report November 1991, “Gas Research Institute Fracturing Fluid Characterization Facility Conceptual Plan,” GRI-91/0349, prepared by the University of Oklahoma, November 1991.

- GRI Topical Report January 1990-December 1991, “Rheology of Fracturing Fluid Slurries,” by R. K. Prud’homme, GRI-93/0444, January 1992.

- GRI Topical Report January 1991-November 1991, “Fracturing Fluid Characterization Facility Simulator Functional Requirements,” GRI-91/0348, prepared by the University of Oklahoma, March 1992.

- “Strength and Stability Analyses of Retaining Structure Models for the Fracturing Fluid Characterization Facility (FFCF),” by K. D. Thakore and A. G. Striz, May 1992.

- GRI Topical Report, “Review of Technical Issues Pertaining to the Fracturing Fluid Characterization Facility (FFCF), GRI-91/0350, October 1992.

- Topical Report RSI-0450, "Heat-Transfer Simulations of the Fracturing Fluid Characterization Facility Prototype," by J. D. Osnes, October 1992.

- "Annual Report for August 1991-July 1992 Fracturing Fluid Characterization Facility (FFCF)," GRI-93/0134, December 1992.

- Internal Report 92-03, "An Experimental Investigation of Jet Penetration into a Slot," by J. T. Lawson and R. G. Rein, Jr., December 1992.

- Internal Report 93-02, "Rheology of HPG Solutions According to Giesekus's Model (Linear and nonlinear viscoelastic behavior)," by A. L. Diek, March 1993.

- FFCF Quality Assurance Procedures (Draft), April 27, 1993.

- Business Plan for the Fracturing Fluid Characterization Facility (FFCF), prepared by the University of Oklahoma, October 1, 1993.

- Topical Report RSI-0483, "Probabilistic Uncertainty Analyses for Fracturing Fluid Quantities Using Approximate Methods: High-Pressure Fracture Simulator (HPFS)," by T. W. Pfeifle, October 1993.

- "Annual Report for January 1993-December 1993 Fracturing Fluid Characterization Facility (FFCF)," GRI-94/0065, December 1993.

- "Research and Development Plan for the Fracturing Fluid Characterization Facility (FFCF)," prepared by the University of Oklahoma, May 1994.

- GRI Topical Report, "Functional Capabilities of the High Pressure Simulator for Fracturing Fluid Characterization," by P. S. Vinod, GRI-94/0438, December 1994.

- "Annual Report for January 1994-December 1994 Fracturing Fluid Characterization Facility (FFCF)," GRI-95/0091, December 1994.

- "Annual Report for January 1995-December 1995 Fracturing Fluid Characterization Facility (FFCF)," GRI 96/0145.

- GRI Technical Summary "New Correlations for Perforation Pressure Loss" by The University of Oklahoma, GRI-96/0208, October 1996.

- "Annual Report for January 1996-December 1996 Fracturing Fluid Characterization Facility (FFCF)," GRI –97/0050.

- "Annual Report for January 1997-December 1997 Fracturing Fluid Characterization Facility (FFCF)," GRI –98/0235.

- "Annual Report for January 1998-December 1998 Fracturing Fluid Characterization Facility (FFCF)," GRI –99/0128.

- "Annual Report for January 1999-December 1999 Fracturing Fluid Characterization Facility (FFCF)," GRI-00/.

- "Final Report for January 1991-September 1998 Fracturing Fluid Characterization Facility (FFCF)," GRI –99/0126.

9.2.6 Patents

Listed below are the patents awarded for the unique research accomplished at the Fracturing Fluid Characterization Facility (FFCF). Below is the abstract for the patents issued and a description of how each pertains to the original abstract.

> *A system for characterizing the pressure, temperature, movement and flow patterns of a fluid under high pressure within a test cell. The test cell is lined internally with adjustable rock facings. Pressure is measured within the cell using a device employing pressure-distortable optical fibers. Fluid velocity, flow direction, and filter-cake buildup are measured with laser Doppler velocimetry. The flow pattern of the fluid is viewed using corresponding arrays of transmitting and receiving optical fibers. Temperature of the fluid is estimated using a combination of thermal sensors. The pressure, velocity, viewing and temperature systems are integral to the rock facings of the test cell.*

1. U.S. Patent Number 5,249,864 issued October 5, 1993, "System for Characterizing Temperature of Fluids," John E. Fagan and Ronnie B. Beason.

   System for characterizing temperature of Fluids

2. U.S. Patent Number 5,271,675 issued December 21, 1993, "System for Characterizing Pressure, Movement, Temperature and Flow Pattern of Fluids," John E. Fagan; James J. Sluss, Jr.; John W. Hassell; R. Brian Mears; Ronnie B. Beason; Sonja R. Wilkinson; Tommy Lear; Kok S. Tan.

   System for characterizing pressure, movement, temperature and flow patterns of fluids

3. U.S. Patent Number 5,272,333 issued December 21, 1993, "System for Characterizing Pressure, Movement, and Temperature of Fluids," John E. Fagan; James J. Sluss, Jr.;

John W. Hassell; R. Brian Mears; Ronnie B. Beason; Sonja R. Wilkinson; Tommy Lear.

System for characterizing pressure, movement, and temperature of fluids

4. U.S. Patent Number 5,324,956 issued June 28, 1994, "System for Characterizing Movement and Temperature of Fluids," John E. Fagan; James J. Sluss, Jr.; John W. Hassell; R. Brian Mears; Ronnie B. Beason.

   System for characterizing movement and temperature of fluids

5. U.S. Patent Number 5,326,969 issued July 5, 1994, "System for Characterizing Flow Pattern and Pressure of a Fluid," John E. Fagan; James J. Sluss, Jr.; John W. Hassell; R. Brian Mears; Ronnie B. Beason; Sonja R. Wilkinson; Tommy Lear; Kok S. Tan.

   System for characterizing flow pattern and pressure of a fluid

6. U.S. Patent Number 5,488,224 issued January 30, 1996, "System for Characterizing Flow Pattern, Pressure and Movement of a Fluid," John E. Fagan; James J. Sluss, Jr.; John W. Hassell; R. Brian Mears; Ronnie B. Beason; Sonja R. Wilkinson; Tommy Lear; Kok S. Tan.

   System for characterizing flow pattern, pressure and movement of a fluid

9.2.7 Benefits to the Industry

The following section describes the benefits that the industry has gained from the work that was performed at the Fracturing Fluid Characterization Facility in the areas of proppant transport, heat transfer, proppant flowback, rheology and perforation pressure loss. These implications are discussed in further detail in the previous sections.

Proppant Transport

- Convection is a density driven phenomenon and in low viscosity medium it dominates proppant settling; hence, an optimum fluid viscosity exists that overrides the influence of the density to form convection. This result implies that when the high viscosity fracturing fluids are used in a well stimulation the convective phenomenon is unimportant.

- The FFCF study shows that crosslinked gel bed height erosion was eight times more than that by linear gel. The results show that the high viscosity crosslinked fluids not only have good proppant suspension capability, as is known to the industry, but also have better bed erosional and resuspension capacity. These two features give crosslinked guar fluids ideal characteristics to distribute proppant throughout the fracture.

- Static settling experiments show that there is a non-linear relationship between the decrease in the settling and increase in the fluid viscosity. Hence, industry should examine parameters other than the viscosity to better understand proppant carrying capabilities of the fracturing fluid.

Heat Transfer

- The heat transfer coefficients of the linear guar and HPG solutions, and crosslinked gels are lower than that of water. This suggest that the fracturing fluids may perform better under real downhole conditions than what is predicted from the current industry practice of substituting the heat transfer coefficient of water for the fracturing fluids. On the other hand, the heat transfer coefficient of the guar slurry is similar to that of the water. Therefore, the current practice of predicting the slurry heat transfer characteristics with water can be successfully continued without compromising the fluid performance under real conditions.

Proppant Flowback

- Results show that the critical flowrate is a function of proppant size, fracture width and closure stress. This means that the stability of the propped fracture is strongly dependent on the stimulation parameters and reservoir conditions. The significance of these results show that a huge decrease in stimulation ratio means that all potential benefits of the hydraulic fracturing treatment can be lost due to proppant flowback produced from the fracturing treatment.

Foam Rheology

- Foam viscosity increases with an increase in the foam quality. This implies that a higher fraction of gas in the foam can be used to generate a viscous fluid. The low liquid content in the foam reduces the damage to a proppant in the fracture. Hence, fracture conductivity is maintained when stimulation treatments are performed with foam based fracturing fluid.

Dynamic Fluid Loss

- Spurt loss values measured in the laboratory cell were generally larger than those measured using the HPS at the FFCF. In the case of large differences in spurt loss values, several thousand gallons of fracturing fluid could potentially be pumped unnecessarily. Large surface-area experiments, such as those available with the HPS, will be required to provide the spurt loss values needed for development of such corrections.

- Filter-cake is not a requirement for fluid loss control in all instances. The primary fluid loss control mechanism with crosslinked gels appears to be pore-plugging. A

paradigm shift is needed to allow the industry to focus on the concept of pore-plugging or an "internal filter-cake" as a source of fluid loss control.

- Neither the viscosity of a crosslinked gel nor filter cake formation was sufficient to control leak-off through naturally fractured media. In the absence of experience with a particular naturally fractured formation, mixtures of 100 mesh sand and silica flour should be incorporated into a gelled prepad or pad fluid to control leak-off.

Fluid Rheology

- The rheology study provided a unique empirical correlation that relates the nominal shear rate with the apparent viscosity of borate-crosslinked guar fluid. The industry can use the correlation to simultaneously evaluate several fluid formulations and select optimum formulation for a given fracturing treatment, thereby, saving time and reducing costs for rheologically characterizing fluids.

Perforation Pressure Loss

- A new perforation pressure loss correlation was developed which accounted for the rheological characterics of fracturing fluids. The developed correlation will provide significant benefits by improving the design of limited entry treatments and in fracturing pressure analysis. The correlation was developed in such a way that made it easily incorporated into hydraulic fracturing simulators such as Frac Pro and others commonly used by the industry.

9.2.8 Other Means of Disseminating Technology

The following section describes the other methods of transferring technology that was used by the FFCF team.

1. Industry In-House Presentations
2. Trade Shows
3. FFCF WEB site
4. Annual Reports

Industry in-house presentations have played a large role in Technology Transfer. The semi-annual and annual meetings for the Coiled Tubing Consortium (CTC) resulted in having several companies' personnel visit our facility. This resulted in several third-party tests being conducted during 1998 and 1999.

Another way of disseminating research results and our capabilities is through Industry Trade Shows. Our philosophy is that the more personal contacts that can be made the better our research results and capabilities can be utilized. We also attend the Coiled Tubing Roundtable annually which, has been very productive as far as understanding industry needs in this area, recruiting new members to the Coiled Tubing Consortium, and also utilization of the facility for further research.

Annual Reports have been submitted to GRI & DOE from 1991-1998. All of the Research activities have been documented in these reports. GRI & DOE and The University of Oklahoma have all of the published reports on file for industry reference.

In September 1997, the FFCF staff met with Schafer and Associates regarding establishing a FFCF WEB site on the Internet. Consequently, a contract to design a WEB site was awarded. In March of 1998 the WEB site was made fully operational and is now providing the industry the latest research findings, activities and consortium news. Our staff is currently maintaining the WEB page at the FFCF. The FFCF name has since been changed to Well Construction Technology Center (WCTC) and so the World Wide Web address is www.ou.edu/wctc.

Chapter 10 COMMERCIALIZATION OF FFCF

10.1 Introduction

The Fracturing Fluid Characterization Facility (FFCF) has been in existence since 1991. It was established with funding from Gas Research Institute (GRI), U.S. Department of Energy (DOE), University of Oklahoma (OU), and co-funding from Halliburton Energy Services, MTS Systems Corporation, and RE/SPEC, Inc. The objective of the facility was to provide the oil and gas industry with a better understanding of the behavior of fracturing fluids and their proppant transport capabilities under downhole conditions.

The objectives and goals set forth to date for the research and development plan have been accomplished and results are well documented in the FFCF Annual Reports submitted to GRI and DOE. As a natural extension of the original FFCF research project, a joint-industry consortia, Coiled Tubing Consortium Consortium has been established through the Completion Engineering Association, CEA-93. Furthermore, aggressive efforts have been made to acquire client testing projects and other government grants.

The FFCF is now available to industry for characterizing and understanding the behavior of complex fluid systems. It is the desire of the University to have this facility self-sustained by the year 2000. Therefore, a comprehensive feasibility study of the FFCF was required in which the University assessed the current status and determined if it is feasible for the FFCF to be a self-sufficient research entity by the year 2000.

This chapter outlines different steps taken by OU to make the FFCF self-sufficient by the year 2000.

10.2 Formation of OU FFCF Commercialization Committee

The University of Oklahoma formed a commercialization committee and considered conducting a feasibility study for the FFCF. The committee and feasibility study is discussed in the following sections.

Prior to initiating the commercialization process, the very first step was to form a committee at the University of Oklahoma. A committee was formed and it consisted of the Vice President, Research and Administration, Dean, College of Engineering, Director, School of Petroleum & Geological Engineering, and Director, Fracturing Fluid Characterization Facility. The committee headed by the FFCF Director was responsible for developing and directing the commercialization activities of the FFCF. The FFCF commercialization committee was also responsible for developing and executing a market search in order to determine the necessary path towards commercialization. This market search was to be performed within the oil and gas industry as well as other industries outside the petroleum industry that might utilize the capabilities of the FFCF. Furthermore, the OU FFCF committee was also charged with the development of a commercialization strategy based on the results of the market search.

10.3 Feasibility Study for the FFCF

The commercialization committee developed a "Scope of Work" (SOW) for the feasibility study of the FFCF as a University research unit. The SOW for the feasibility study included an inventory of existing resources, assessment of current FFCF resources, analysis of commercial markets open to FFCF, and recommendations for the future of the FFCF.

The committee identified the following three competent and well recognized consultants to conduct the feasibility study. These consultants are:

Mr. P. R. (Bob) Sprehe – Performance Engineered Drilling Systems, Inc.
Mr. A. Richard Sinclair – Well Stimulation, Inc.
Ms. Aneta S. Newton – Phoenix Processes, Inc.

These consultants were selected based on their diverse educational background and experience, OU would benefit the most if these consultants were asked to conduct studies in different markets. In order to identify additional consultants the committee had also contacted Mr. Brian Gahan, FFCF Project Manager, GRI and Mr. Bill Lawson, DOE. The committee was to recommend the number of consultants to be used once the additional names became available. As soon as the decision of a team of consultants had been made, the budget for the feasibility study was to be prepared.

At this point, OU was anticipating significant changes in its administration. The College of Engineering was naming a new Dean and the School of Petroleum & Geological Engineering (PGE) was naming a new Director. Therefore, the decision of the feasibility study was deferred until both appointments were finalized. Once, both the Dean of College of Engineering and the Director of PGE were appointed, the decision was made not to hire external consultants to do the feasibility study as described in the SOW but, instead, develop the commercialization strategies within OU. It was decided to increase the market share for FFCF by staying within the oil and gas industry and expanding the capabilities to include other areas besides stimulation and coiled tubing and not actively pursuing other industries.

10.4 Name Change of the Facility

As the research and technology transfer efforts of the Fracturing Fluid Characterization Facility have expanded into other areas of the petroleum industry, the FFCF was renamed Well Construction Technology Center (WCTC) to encompass the broad spectrum of the petroleum industry. With this change, the FFCF Project becomes part of the Well Construction Technology Center. Similarly, the current joint-industry Coiled Tubing Consortium becomes part of the WCTC. Similarly, there will be additional projects within the WCTC dealing with other areas. For the purpose of commercialization it is imperative that WCTC expands the capabilities in other oil and gas industry related areas, e.g. drilling, completions, and production.

10.5 Plans for Expansion and Acquisition of Equipment for Extended Capabilities

It is the plan of WCTC to expand its present capacity so that the facility can provide the necessary research and engineering services. Plans have been made to acquire additional equipment for extended capabilities of mixing and pumping various types of fluids used for stimulation and drilling operations. Furthermore, to expand the capacity into the drilling area, the acquisition of the BP/Amoco Catoosa Facility was seriously considered. After careful analysis it was determined by WCTC that it was not in the best interest of the University at the present time.

Recently, BP/Amoco has donated the drilling rig and fluid mechanics laboratory in Bldg. 4 of Amoco facility in Tulsa to WCTC. This facility will be utilized for testing bits and to conduct drilling related research. Furthermore, the University of Oklahoma recently signed a Memorandum of Understanding (MOU) with Sandia National Laboratories to perform joint research projects to help increase oil, gas, and geothermal energy production.

10.6 Client Testing

The FFCF has been actively seeking innovative ways to make the industry aware of the capabilities of this unique facility. The staff of the FFCF tries to keep themselves in tune to the immediate and future needs of the petroleum industry. We try to accomplish this by attending trade shows, personal contacts, industry presentations and keeping ourselves abreast of any proposals that we could submit to different agencies. In this time of down sizing and mergers in the petroleum industry, we look upon this as an opportunity to absorb some of the research needs of the industry. As internal R&D personnel is at a all time low, facilities like the FFCF will play a critical role in continuing the needed research through industry J.I.P.'s or propriety projects.

Tests Performed. Several tests for clients have been performed in the areas of fluid rheology, coiled tubing applications and foam fluid rheology. A brief listing of these tests is presented below.

- Fluid Rheology and Proppant Transport
  - Petroleum Research and Consulting Services, Tulsa, Oklahoma
  - Halliburton Energy Services, Duncan, Oklahoma
  - Dowell Schlumberger, Sugarland, Texas
  - Mobil Exploration and Production, Dallas, Texas
- Fluid Rheology
  - Baker Hughes INTEQ, Houston, Texas
  - Halliburton Energy Services, Duncan, Oklahoma
  - Dowell Schlumberger, Sugarland, Texas
  - Mobil Exploration and Production, Dallas, Texas
  - Applied Geodynamics, Steamboat Springs, Colorado

- Coiled Tubing Applications
  - Baker Hughes INTEQ, Houston, Texas
  - Mobil Exploration and Production, Dallas, Texas
- Foam Fluid Rheology
  - Applied Geodynamics, Steamboat Springs, Colorado
  - Halliburton Energy Services, Duncan, Oklahoma

These tests brought very encouraging response from the customers. The clients expressed their satisfaction with the services provided by the facility. As a result, more client-testing is anticipated in the future.

Proposals Submitted. In addition to the above-mentioned tests, proposals are submitted to various agencies in order that we may capitalize upon our unique capabilities.

- Plugging Abandoned Wells
  - Submitted to Oklahoma Center for the Advancement of Science and Technology (OCAST)
- Foam Fluid Rheology
  - Submitted to National Science Foundation, jointly with applied Geodynamics, Steamboat Springs, Colorado
- Drilling
  - Performance Engineering Drilling Systems, Covington, Louisiana
- Perforating
  - Hi Tech Fluids, Boerne, Texas
- Crosslinked Slurry Rheology
  - Pre-application to the U.S. Department of Energy

10.6.1 Future Efforts

Present tests and proposals have not been limited to the petroleum industry. It should be noted that the facility has performed tests for the mining industry as part of an SBIR proposal in 1998. Also, in 1999 we have submitted another joint SBIR proposal with Applied Geodynamics in Steamboat Springs, Colorado. This research will be used for Extra-Terrestrial excavation for a future NASA project.

Even though the research capabilities of the FFCF are centered around the petroleum industry, we must continually seek out other avenues for opportunities to benefit our clients and ourselves.

10.7 Other Commercialization Activities

As part of FFCF commercialization, several other activities were also performed. Technical presentations were made to several companies at their locations and during their visits at the FFCF. An update on the Proppant Flowback Consortium (PFC) and Coiled Tubing Consortium (CTC) were presented at the annual meeting of the

Completion Engineers Association and the CTC members. To disseminate the knowledge gained, technical papers were presented at the annual and regional Society of Petroleum Engineers conferences. To increase the visibility within and outside the oil and gas industry, the FFCF World Wide Web Internet site was developed and made available.

Appendix A
FINAL REPORT FROM MTS REGARDING THE FRACTURING FLUID CHARACTERIZATION FACILITY

A.1 Overall Project Objective

MTS Systems Corporation is known as a supplier of high performance systems for testing and manufacturing. As part of the Fracturing Fluid Characterization Facility (FFCF) Project team, MTS was charged with supplying the mechanical and electronic hardware which allows fracturing fluid researchers to understand the dynamics of fracturing fluids and proppants in a large scale, controlled laboratory environment.
As a first step in meeting the long term goal of a large scale test system, MTS worked on the definition, design, fabrication, checkout, testing, and delivery of the Prototype Hardware.
In the long term, a Full Scale System was preliminarily designed on the experience gained from the Prototype Hardware, though no hardware was built.

A.2 Summary of Work

1. Work performed involved the development of the Functional Requirements for the Prototype Hardware, initiation of the Conceptual Design, support of the Project at Contractor, TAG, and PAG meetings.
2. The major accomplishment was the development of the Functional Requirements, design, assembly, test, and installation of the Prototype Hardware.
3. The major conclusion was developing a consensus between the contractors, OU, GRI, and the advisory groups that the Functional Requirements reflected the overall goals of the Prototype Hardware.
4. Definition and design of a full scale Low Pressure Simulator.

A.3 Specific Objectives

The specific objective was to deliver the Prototype Hardware to Oklahoma University within the established budget. Overall, MTS achieved this through delivery of the Prototype Hardware to the FFCF Laboratory in July 1992. The budget was also met at the delivery date.

A.4 Work Performed

1. MTS supported the FFCF Program Simulator Team (OU, MTS, Halliburton, RE/SPEC). The MTS developed simulator encompassed the servo-controlled platens for simulated crack motion. Key areas where MTS interacted with other Program Team members included:

a) Halliburton – Fracturing fluid handling and interface of the MTS hardware to pumping equipment.
b) RE/SPEC – Operational procedures, task planning, and test techniques.
c) OU – Interface of MTS hardware to sensors, data acquisition, simulated rock, laboratory, and host controller. Analysis of fracturing fluid rheology and its effect on simulator design. Structural analysis of the simulator.

2. MTS planned the following overall design tasks:
   a) Develop (and finalize) Functional Requirements
   b) Develop Conceptual Design
   c) Finalize Detail Design
   d) Procure and Fabricate Parts
   e) Assemble and Test Prototype at MTS
   f) Install at FFCF, Oklahoma University

This work was executed in parallel with the activities by the other project teams. Interaction with them was identified as a critical component to an effective Prototype design.

3. The first year deliverable was planned as a Prototype System to help determine and evaluate the Full-Scale Simulator design issues. The Prototype was sized at approximately, 10 ft high, 11 ft long, and 10 ft in width. The size of the simulated crack was approximately 18 times greater in square footage than the previously envisioned Prototype (January 1991).
4. MTS supported the interfacing of the Prototype simulator hardware (MTS supplied Mechanical and Electrical Hardware) with the Oklahoma University and Halliburton supplied hardware. (OU – simulated rock, sensors for measurement of fluid characteristics, data acquisition, and user interface; Halliburton – fracturing fluid pumping and conditioning hardware).
5. MTS supported the installation and interfacing of the MTS supplied hardware with the other subsystems in the FFCF. It was planned that MTS would have a mechanical engineer, electrical engineer, and a checkout technician on site to support the installation and interfacing tasks.
6. MTS supported RE/SPEC in the development and analysis of activity plans for systems testing and scientific investigation of fracturing fluid mechanics, as well as the development of facility plans and operational techniques for the OU – FFCF Laboratory.
7. MTS supported FFCF researchers (OU, Halliburton, RE/SPEC) during the development of experiments for fracture fluid testing. Technical assistance in the aspects of the MTS supplied Prototype system was proposed. Training of the FFCF researchers in the operation of the Mechanical and Electrical hardware was planned.
8. MTS provided modifications, enhancements, or repairs to the Prototype as required or as requested by OU. It was anticipated that fieldwork performed after installation and discussions with FFCF researchers would result in the installation of these changes at the FFCF. MTS proposed a mechanical engineer, electrical engineer, and a checkout technician be made available to support the installation and interfacing Tasks.
9. MTS provided project management for the control of the project efforts at MTS. This included monthly reports, cost control, materials control, and other support as required by OU.

10. MTS supported OU in the development of cost estimates, project plans, proposals, and technical analyses of the Full Scale Simulator. Develop functional requirements for the Full Scale Simulator. Develop specifications for the Full Scale Simulator.
11. MTS attended FFCF Project, Technical Advisory, and Project Advisory Meetings as required.

In general, MTS completed all activities discussed above. Some work is continuing as support to the installed Prototype Hardware. Additional comments are given below.

1. MTS continues to interact with OU, Halliburton, and RE/SPEC as required.
2. The Prototype Hardware was delivered and installed in July 1992. The final size of the Prototype had increased the scope of the design effort in the following task areas:
   - Larger size of the mechanical system requiring more structural design.
   - Increased temperature resulting in a more complex seal design.
   - Increased number of control channels (from 4 to 12) increasing cross coupling complexity in the controller and software development.
   - Evolution of the sensor system with the fiber optics integrated in the facings requiring more detailed design interaction between MTS and OU. Also the addition of high-pressure windows for the LDV system.
   - Overall size of the Prototype increased the number of parts and volume of hardware to build it.
4. MTS continues to support the installation and interfacing of the MTS supplied hardware with the other subsystems in the FFCF.
5. MTS has trained OU researchers in the operation of the Mechanical and Electrical hardware as planned.
6. Repair of the actuators and modifications to the software were made in September 1992.
7. MTS gathered information on the Full Scale Functional Requirements to support OU in the development of cost estimates, project plans, proposals, and technical analyses of the Full Scale Simulator. Specifications for the Full Scale Simulator. Specifications for the Full Scale Simulator were generated.
8. MTS provided mechanical support during the facility move to its current location.
9. MTS sent a new application controller program, which featured an additional control mode.
10. MTS sent an Apple / Macintosh utility to investigate the Macintosh operating system the year 2000 readiness.

A.5 Delivery of the Prototype Hardware

In addition to the on time and on budget delivery of the Prototype Hardware, a significant achievement was the development of the square seals for the platen system.

A.6 Low Pressure System

MTS used the information gathered from the design and development of the Prototype Hardware to design the Low Pressure System (LPS). MTS focused efforts toward the following activities:

1. Develop the functional requirements and mechanical / hydraulic design specifications for the much larger LPS.
2. Develop a plan for securing qualified vendors to fabricate the major mechanical components of the LPS.

The goal of the LPS was to provide a laboratory-based system to study fracturing fluids in a large scale, Low Pressure physical model. Three key phenomena's to be studied were fluid behavior, fluid leakoff, and proppant transport.
Considerable effort was expended in developing the functional requirements for the LPS since the design included a much larger apparatus. The Low Pressure System was never constructed based on many financial and commercial issues.

Appendix B
FINAL SUBCONTRACTOR REPORT FROM HALLIBURTON ENERGY SERVICES

B.1 Overall Project Objective

Halliburton Energy Services (HES) is known worldwide as a leading supplier of oilfield products and services. For this reason, HES (then known as Halliburton Services) was selected to participate as a member of the Fracturing Fluid Characterization Facility (FFCF) Project team. HES was awarded Subcontract No.1991-12 by the University of Oklahoma to delineate its project responsibilities. HES was charged with providing consultation services, chemicals and materials for formulating fluids, and equipment for fluid mixing, pumping, and conditioning. These services, materials and equipment were to be provided in support of a large-scale test facility dedicated to quantifying the behavior of fracturing fluids and slurries under conditions approximating those found in field operations.

As an initial step in meeting the long-term objectives of the project, HES worked with the University of Oklahoma (OU) and the other subcontractors to prepare the successful bid submitted to GRI. HES collaborated with OU and the subcontractors to develop the Functional Requirements for the high-pressure fracture simulator (HPS) and to define measurements needed to characterize the behavior of fracturing fluids.

Since project inception, HES has provided assistance to help the FFCF become a facility that is recognized world wide as a center of excellence for fluid property characterization.

B.2 Scope of Activities

HES provided valuable insight concerning industry practices during formulation of the bid proposal and during the project feasibility study conducted in the first year.

HES worked with other project team members (MTS, OU, and RE/SPEC) to develop the Functional Requirements for the high-pressure fracture simulator (HPS). Laboratory assistance was provided during formulation and evaluation of simulated fracture surfaces (facings) to be used in the HPS.

Fluid mixing, handling, and pumping equipment were made available to the facility through a lease agreement. A high-pressure throttling valve and a heat exchanger for fluid preconditioning were made available to the facility through an amortized purchase plan. These latter equipment items were custom designed for use at the facility.

Chemicals and proppant for fluid and slurry formulation were made available to the facility at cost. Equipment maintenance and other supplies (hoses, connectors, etc.) were also made available to the facility at cost.

Engineering and operations personnel were provided on a cost sharing basis to assist with the execution of testing designed to meet the requirements set forth in the various verification and research plans.

Engineering assistance with the analysis of data was also provided until the facility could become fully staffed.

HES played a major role in technology transfer by assisting with preparation and presentation of technical papers, preparation of technical bulletins, contributions to annual reports to GRI, preparation and presentation of short course materials, and the preparation and presentation of research results to Technical and Project Advisory Groups.

B.3 Work Performed

Activities tabulated in this section are not to be construed as an exhaustive list of the work performed by Halliburton Energy Services (HES). Activity descriptions that follow simply show the depth to which HES was involved and committed to the success of this project. As of September 30, 1998, HES had provided $1,278,650.00 in co-funding to the project.

HES worked with other project team members to develop the Functional Requirements for the prototype simulator and other proposed successor simulators. Since successor simulators were not fabricated, the prototype was placed in service as the High Pressure Simulator (HPS). Industry thoughts and ideas concerning fracture geometry were conveyed to the team during the development of a simulator design. Guidance was provided concerning any compromises that would be required. Pressure, temperature, and other design considerations were also addressed using the experience base offered by HES.

HES worked with RE/SPEC, OU Environmental Safety Services, Oklahoma State Department of Health, and the City of Norman to gain approval for the disposal of effluent from broken crosslinked fracturing fluids and slurries into the sanitary sewer system.

During the project feasibility study, a critical review of rheological models being used in the petroleum industry was undertaken by the rheology team composed of members from OU and HES. As expected, the power-law model was found to be the most widely used for fluids without yield stress. The three-parameter Ellis model was used to some extent for these same fluids when attempting to cover a wide shear rate range. For fluids exhibiting a yield stress, the two-parameter Bingham plastic model and three-parameter Herschel-Bulkley model were both used frequently by the industry.

Mathematical expressions were developed which permit calculation of the uncertainty in derived rheological parameters such as shear rate, shear stress, and apparent viscosity. These expressions permit sensitivity studies to be performed to determine the accuracy needed in measurement of flow rate, pressure loss, and fracture width.

Polyethylene glycol (Polyol or Carbowax 8000) and corn syrup solutions were evaluated in HES Duncan to determine which would be the most suitable as a Newtonian calibration fluid for the HPS. Corn syrup solutions were selected because they provided the highest viscosity at 180 F without creating handling and disposal problems at ambient conditions.

A feasibility study was made to determine the possibility of investigating foamed fracturing fluids at the facility. Using phase diagrams, CO_2 foams created under field like conditions were shown to undergo an approximate six-fold expansion while being heated

to 250 F at simulator operating pressures. The resulting low-density CO_2 foam would not be representative of those being applied in the field. Expansion of N_2 foams was shown to be less severe, but their evaluation would still be limited to the 1200 psi working pressure of the HPS.

Assistance was provided with definition and selection of instrumentation (pressure transducers, temperature probes, flow meters, and densiometers) for the characterization of fracturing fluid and slurry behavior in the HPS. Additionally, guidance was provided during the selection of laboratory rheometers for the bench top characterization of fluid behavior.

LDV (Laser Doppler Velocimetry) technology was evaluated in Duncan at the Rheology Lab using a transparent slot model. A caliper was modified to measure the actual width during testing. Fluids and slurries evaluated were a 40 lb/Mgal guar solution, 40 lb/Mgal crosslinked gel, and a 40 lb/Mgal crosslinked gel slurry containing various sand concentrations up to 10 lb/gal. A core wafer was also set in place on one side of the slot to evaluate the possibility of filter-cake thickness measurement with the LDV.

An extensive effort was made with assistance from HES to determine the viability of cement facings for use in the HPS. Fluid loss experiments performed in Duncan with core wafers uncovered a problem with the bonding of fiber optics to the cement matrix. It was necessary to bond fiber optics within the facings to have a functional vision system. Application of a resin coating to the embedded fibers was found to be a solution to this problem. Cement facings were found to possess an extremely low and time-dependent permeability and were therefore abandoned in favor of a resin-sand composite material. At a later time, assistance was also provided in locating a source of natural rock for use as facing material in fluid loss tests.

A quartz pressure transducer and operating software were leased to OU on a short-term basis. This device was used as a pressure reference during the development of a fiber optic pressure transducer. A test fixture for mounting and evaluating the device was also developed and supplied to the team by HES.

Pilot-plant scale equipment were leased to the facility for fluid/slurry mixing, handling and pumping during low-pressure testing. Field-scale fluid/slurry mixing, handling, and pumping equipment were renovated and leased to the facility for high-pressure testing. On May 1, 1999, previously leased equipment were donated to the University.

Experiments were performed in Duncan to determine if neutron particles could be used to detect the presence of sand and borate-crosslinked gel filter cake sandwiched between two 5-inch thick steel slabs. The technique appeared to be feasible, but would require a much stronger neutron source to minimize the exposure time required.

A throttling valve was designed and fabricated for use as either a flow splitter or a backpressure regulator. Valve operation and slurry erosion resistance were evaluated by Halliburton in Duncan prior to delivery to the facility. The valve has been used routinely to maintain 1000 psi pressure within the HPS slot during dynamic fluid loss tests.

A flow system was developed for measuring the simultaneous fluid leak-off from multiple facings. Flow meters in this system were selected based on the expectation that the filtrate would be low viscosity. Unfortunately, during the first evaluation of this

apparatus, the filtrate was very viscous and plugged the flow meters. The apparatus remains available if another attempt is made to address fluid loss on this scale.

Dynamic fluid loss in the HPS was modeled to determine if it would be possible to detect an increase in polymer concentration over the length of the HPS. Modeling based on steady-state behavior indicated that a significant build-up in polymer concentration should be observed with a 40 lb/Mgal polymer solution flowing at 10 sec^{-1} through a ¼-inch gap width.

Dynamic fluid loss experiments were performed in the laboratory using samples of the HPS facing material. Fluid loss parameters obtained from these small surface area samples were compared to those obtained from the large surface area facings found in the HPS. Wall-building coefficients from the HES laboratory experiments were found to be similar to those determined using the HPS facings. However, spurt-loss values from the laboratory experiments were found to be generally larger.

HES worked with its coiled tubing supplier, Quality Tubing Inc., to obtain a donation of 5000-ft of 1 ½-inch tubing for the facility. The tubing was supplied on two 2000-ft reels and one 1000-ft reel. The tubing serves as a wellbore simulator and provides shear history conditioning for fluids and slurries evaluated in the HPS.

A vertical, concentric-pipe, heat exchanger was fabricated and evaluated in Duncan prior to moving it to the test facility on the OU North Campus. The heat exchanger serves as a formation simulator that elevates the temperature of test fluids and slurries prior to their evaluation in the HPS. Heat transfer properties of fracturing fluids and slurries have also been investigated using data collected during operation of the exchanger.

Recommendations were made concerning a method for converting the vision system to a device for determining the spatial proppant concentration profile in the HPS. The instrumentation team subsequently adopted these recommendations and a method for determining proppant concentration was developed based on digital image processing.

A proposal was made for using variations in platen hydraulic pressure as a means for determining the normal stress exerted by viscoelastic crosslinked fracturing gels. It was proposed that these measurements could and should be collaborated with the normal stress measuring capabilities of the Bohlin rheometer.

HES engineering and operations personnel were directly responsible for the design and execution of literally hundreds of tests performed at the facility during its first few years of operation. However, with increased staffing and training, the facility has gradually become self-sufficient and currently requires very little, if any, direct assistance from HES.

HES personnel participated in the preparation and presentation of an industry short course entitled “Impact of Fracturing Fluids on Stimulation Design.” This short course was co-sponsored by GRI and OIPA and had 84 participants.

HES authors have collaborated in the preparation and /or presentation of 14 technical papers and/or publications on behalf of the FFCF. HES personnel participated routinely in the preparation and presentation of research results to TAG and PAG Advisory Groups. HES has routinely contributed to Monthly and Annual Reports to GRI. HES has also made a substantial contribution to the Final Project Report to GRI.